

Application of Design Synthesis Technology in Architectural Practice



Peter S. Park

Department of Civil and Structural Engineering
School of Architecture
University of Sheffield

A thesis submitted for the degree of

Doctor of Philosophy

January 2013

Declaration of Authorship

I, Peter Seong-Uk Park, declare that this thesis and the work presented in the thesis are entirely my own, unless stated or acknowledged to the contrary.

Signed:

Date:

Abstract

The use of computational tools and techniques has opened up new possibilities in architectural form generation. In parallel there have also been developments in structural engineering analysis and design methods, with the primary focuses being on accurate modelling of material behaviour and structural stability, and on ensuring economy.

Having accepted that form and structure are mutually concomitant, something that is particularly important when considering freeform architecture, there are two distinct design approaches: (i) shape-driven architectural forms and adoption of creative integrated post-rationalisation for a predefined freeform, and (ii) form-structure integration from conception, manifested by a growing number of methods for use at various stages in the design process.

In this regard, a truss layout optimisation technique is proposed as a versatile design tool. This has a potential role in both these approaches to form generation at the conceptual design stage. A series of design studies are employed for this purpose, and generated forms are discussed. Additionally, further form generation possibilities are explored, using an extended version of the aforementioned technique. As a representative example, ‘tensegrity’ forms are studied in greater detail. The generated forms are extensively tested using a commercial structural analysis package, in order to verify the correctness of the conclusions drawn.

To my parents, who never told me off for being curious.

Acknowledgements

I am most indebted to my parents, who have continued to provide unconditional support throughout my studies.

My supervisors, Dr Matthew Gilbert, Dr Andrew Tyas and Prof. Olga Popovic Larsen, are thanked for their advice, guidance and patience, without which this thesis would not have been possible.

I would also like to express my gratitude to those¹ who have befriended me in the most eventful period of my life so far.

Also acknowledged are the University of Sheffield, the Worldwide Universities Network (WUN), the Leche Trust, and the British Council for their financial assistance at various stages of my studies.

Finally, I thank God for this, more-or-less, life, in which ordinary things have happened in the usual, surprisingly extraordinary, fashion.

¹ including, but not limited to: A Babiker, RF Carvalho, SK Choi, M Cheeseman, SJ Gimbert, MW Jones, IS Kim, KY Koo, CW Kwon, KAL, H Hutchings-Georgiou, HJ Lee, JH Lee, FK Leung, R Newman, K-U Park, TJ Pritchard, M Taib, and E Yoon.

Contents

Declaration of Authorship	i
Abstract	ii
Acknowledgements	iv
Nomenclature	xvi
1 Introduction	1
1.1 Research Overview	1
1.2 Scope of Research	4
1.3 Aims	5
1.4 Methodology	7
1.5 Structure of the Thesis	8
I Literature Review	11
2 Computer-aided Architectural Design and Form-generation	14
2.1 Computer-aided Design Approaches	14
2.2 Shape-driven Form-generation Techniques	16
2.2.1 Pattern Generation - Nature Imitation	17
2.2.2 Pattern Generation - Abstraction	19
2.2.3 Discretisation over Predefined Surface Form	25
2.3 Integrated Design	26
2.3.1 Computational Form-finding: from continuous to discrete .	27
2.3.2 Optimisation-driven approaches	33

2.4	Summarising Remarks	36
3	Structural Optimisation	39
3.1	Mathematical Optimisation: Terminology	40
3.1.1	Objective Function	40
3.1.2	Variables	41
3.1.3	Constraints	42
3.1.4	Feasible Set and Global Optimum	43
3.1.5	Convexity and Local Optima	43
3.2	Types of Structural Optimisation	44
3.2.1	Topology Optimisation	45
3.2.2	Size Optimisation	45
3.2.3	Geometry Optimisation	46
3.2.4	Shape Optimisation	47
3.2.5	Material Optimisation	47
3.2.6	Layout Optimisation	47
3.3	Types of Solution Methodologies	52
3.3.1	Mathematical Programming: Linear and Nonlinear Programming	52
3.3.2	Homogenisation	55
3.3.3	Evolutionary Structural Optimisation	56
3.3.4	Genetic Algorithms	57
3.3.5	Dynamic Programming	58
3.3.6	Simulated Annealing and Particle Swarm Optimisation	59
3.3.7	Tabu Search and Ant Colony Optimisation	60
3.4	Chapter Conclusion	61
3.4.1	Justification for Use of Linear Programming: linear vs non-linear approaches	61
3.4.2	Justification for Use of Layout Truss Optimisation	61
3.4.3	Limitations of LP plastic layout optimisation	62
3.4.4	Concluding remarks	65

4 Tensegrity	67
4.1 Introduction	67
4.2 ‘Invention’ of Tensegrity	68
4.3 Definitions	71
4.4 Recent Development in Tensegrity Research in Engineering	74
4.5 Classification of Regular Tensegrity	75
4.5.1 Spherical Cells	75
4.5.2 Star Cell Type	77
4.5.3 Assemblies	78
4.6 Form-finding and Control of Tensegrity	78
4.6.1 Experimental Form-finding based on Polyhedral Geometries	79
4.6.2 Numerical Approaches	80
4.7 Automatic Generation of Tensegrity	87
4.8 Concluding Remarks	90
II Generation of Conceptual Form of Conventional Structural Configuration	92
Preface	93
5 Potential Use of Structural Layout Optimisation at the Conceptual Design Stage	95
5.1 Introduction	96
5.2 Form-generation Methods in Context	97
5.2.1 Background	97
5.2.2 Division between the ‘Visual’ and ‘Technical’ Elements of Design	98
5.2.3 Inter-relationship between Form and Structure	101
5.2.4 A Critical Appraisal of the Role of Computers in the Design Process	102
5.2.5 The Computer as a Truly Integrative Design Tool	105
5.3 3D Design Examples	108
5.3.1 Thinking Pods	108
5.3.2 Exhibition Space	111

5.3.3	Pharaonic Village Project	117
5.3.4	Canopy for Roof Terrace in Multi-storey Building	118
5.3.5	Roof Vault	124
5.4	2D usage Design Examples	127
5.4.1	Bicycle Canopy	127
5.4.2	Façade Design	129
5.4.3	Window Frame Design	131
5.5	Discussion	133
5.6	Conclusions	137
Postscript		138
5.6.1	Graphical User Interface	138
 III Generation of Conceptual Form of an Unconventional Structural Configuration: Tensegrity		 141
Preface to Chapter 6		142
 6 Obtaining More Practical Solutions using Mixed Integer Linear Programming		 144
6.1	Abstract	144
6.2	Introduction	145
6.3	Formulation	148
6.3.1	Introduction of Binary Variables	148
6.4	Effects of Integer Constraints	150
6.4.1	3 x 3 Grid Example	150
6.4.2	5 x 3 Truss	155
6.4.3	5 x 3 Michell Cantilever	157
6.5	Parametric Studies	158
6.5.1	N_{UB} and Total Volume in Final Structure	159
6.5.2	Effects of Reduction Factor on CPU time	159
6.5.3	Effects of Desired Number of Members on CPU time	163
6.6	Discussion and Conclusions	169
Preface Chapter 7		172

7	Layout Optimisation of Tensegrity Structures	174
7.1	Abstract	174
7.2	Introduction	175
7.3	MILP Formulation for Tensegrity Structures	177
7.3.1	Background	177
7.3.2	Plastic LP Layout Optimisation Formulation	178
7.3.3	Introduction of Binary Variables	178
7.4	Michell Structure Problems	179
7.4.1	Central Point Load between Pin and Pin/Roller Supports .	180
7.4.2	Central Point Load between Pin and Pin Supports	184
7.5	Effects of material properties: tensile and compressive strengths .	186
7.6	Tensegrity Columns	190
7.6.1	Tensegrity ‘Stayed Column’	190
7.6.2	Investigation of Structure and Internal Loads	192
7.6.3	Load-bearing Capacity of Tensegrity ‘Stayed Column’ . . .	197
7.6.4	Tensegrity ‘XIX’ Column	202
7.6.5	Tensegrity ‘XIIX’ Column	210
7.7	Other Tensegrity-type Structures	220
7.8	Discussion	223
7.9	Conclusions	224
	Postscript	227
IV	Discussion, Contributions, Conclusions and Recommendations for Future Work	228
	Preface to Part IV	229
8	Discussion of Research Findings	230
9	Contributions and Recommendations for Future Work	239
9.1	Contributions	239
9.2	Recommendations for Future Work	241
9.2.1	Form-generation and Integrated Design Approach	241
9.2.2	Structural Optimisation	242

9.2.3 Tensegrity	243
References	244
A Structural Layout Optimization	267
A.1 Description of structural layout optimization process	267
A.2 Linear programming (LP) structural layout optimization formulation	268
A.3 Mixed integer linear programming (MILP) structural layout optimization formulation	268
A.4 Transmissible Load	269
B MILP zero area members	270
B.0.1 3 x 3 Grid Example	270
B.0.2 5 x 3 Truss	270
B.0.3 5 x 3 Michell Cantilever	270
C MatLab code for MILP	275
D Further Explanation of Effect of Additional Constraints on Optimality	280
E Comparisons between Tensegrity and Corresponding LP structures	283
E.0.4 Tensegrity ‘XIIX’ Column	283

List of Figures

1.1	Diagram for scope of research	6
2.1	Cellular Automata. Mani Rastogi, 1994	18
2.2	Lindenmayer system-generated free form	19
2.3	Beijing National Aquatics Center	20
2.4	Zaha Hadid Architects, Kartal-Pendik Masterplan, Istanbul, Turkey, 2006	22
2.5	Metropol Parasol, Seville.	22
2.6	Centre Pompidou, Metz, France.	23
2.7	Antonio Gaudi's Sagrada Familia	27
2.8	Heinz Isler's inverted hanging cloth cast form.	28
2.9	Sun Valleys, EXPO Axis Shanghai.	29
2.10	Smithsonian Institution, Foster + Partners and Buro Happold.	30
2.11	Hexagonal freeform shell with six supports.	31
2.12	Trada plywood shell by Ramboll Computational Design	31
2.13	Freeform Masonry Shell	32
2.14	The Hylomorphic Project in the central court of the Schindler House	34
2.15	Underground Station Roof Structure, Piazza Garibaldi, Naples	35
2.16	Optimised loft slab [1]. Source: [1]	36
3.1	Classification of optimisation	42
3.2	Global and local optima	43
3.3	Non-convex and convex optimisation	44
3.4	Topology optimisation	45
3.5	Size optimisation	46

LIST OF FIGURES

3.6	Geometry optimisation	46
3.7	Ground structure	49
3.8	Different types of constraints	53
3.9	Instability of a node within a compression chain	63
4.1	Class 1 shell tensegrity	73
4.2	Tensegrity:‘Simplex’ configuration in isometric and plan views . .	76
4.3	Zigzag tensegrity	77
4.4	Three Star cell tensegrity configurations	78
4.5	General polygon-based tensegrity	81
4.6	Simple tensegrity prism	83
4.7	Initial and optimised tensegrity beam design, showing deformation under load	88
4.8	Initial and optimised tensegrity beam design, showing deformation under load	90
5.1	Garibaldi Exhibition Centre, Grimshaw-Architects, Milan 2006 . .	99
5.2	Brian Boyer non-structurally initiated	99
5.3	Guggenheim Museum Bilbao, Gehry & Partners	100
5.4	Ambiguity in definitions of ‘form’ vs. ‘structure’.	102
5.5	Ambiguity between ‘form’ and ‘structure’	103
5.6	Example structures generated using layout optimisation	107
5.7	Conceptual design of thinking pods: manually derived.	109
5.8	Conceptual design of thinking pods: obtained using structural lay- out optimisation.	110
5.9	Conceptual design of exhibition dome: design domain expressed as 3D masses	112
5.10	Conceptual design of exhibition dome: further division of design domain for 2D plane structures	113
5.11	Conceptual design of exhibition dome: assembly	113
5.12	Conceptual design of exhibition dome: optimised catenary arches	114
5.13	Conceptual design of exhibition dome: optimised catenary arches	115
5.14	Conceptual design of glass pyramid, obtained using structural lay- out optimisation.	117

LIST OF FIGURES

5.15	Conceptual design of glass pyramid obtained using structural layout optimisation - initial detailed solution: (a) side view; (b) plan view; (c) internal view.	119
5.16	Conceptual design of glass pyramid obtained using structural layout optimisation - subsequent simplified solution: (a) side view; (b) plan view; (c) internal view.	119
5.17	Original canopy for roof terrace: in context of the main building framing elements	121
5.18	New canopy for roof terrace: in context of the main building framing elements	122
5.19	New canopy for roof terrace: front view.	123
5.20	New canopy for roof terrace: side view.	123
5.21	Roof vault design - a quarter model in a discretised, near catenary shape.	124
5.22	Roof vault design: top view in parallel projection	125
5.23	Roof vault design: elevation view in parallel projection	125
5.24	Roof vault design: isometric view.	126
5.25	2D original optimised structure with two fixed pinned supports: green arrows represent applied forces, tensile members are denoted in red and compressive members in blue.	127
5.26	Bike canopy: 2D planar optimisation and replication approach	128
5.27	2D original optimised structure for Façade design	129
5.28	Façade design: 2D planar optimisation and replication example	130
5.29	Design domain and loads for window frame with nodal density target number of 100	132
5.30	Window frame patterns, optimised for given loads, differing in their nodal density	133
5.31	The Dutch Maritime Museum: courtyard roof form-structure [2]. Design: Ney and Partners	134
5.32	Hanging chain models	135
5.33	Hanging net models	136
5.34	‘Metamorphosis from a cube to a distorted cuboidal shape along a horizontal axis with reinforcement	139

LIST OF FIGURES

5.35 ‘Metamorphosis’ from a cube to a rotated cuboidal shape about a vertical axis with reinforcement	139
5.36 ‘Metamorphosis’: a modification process of a truss structure.	140
6.1 Potential members in ground structure and the load. $L = 1, F = 3.00$	151
6.2 Optimised structure without integer constraints - solid red lines represent compression members, and Dashed blue lines, tension members	152
6.3 Optimised structures with integer constraints	153
6.4 Optimised structures with integer constraints and zero area members	154
6.5 Optimised structure with integer constraints, $R=2$	155
6.6 Potential members in ground structure and the load. $F = 3.00$	156
6.7 Optimised structure without integer constraints - solid red lines represent compression members, and dashed blue lines, tension members	156
6.8 Potential members in ground structure and the load. $F = 3.00$	157
6.9 Optimised structure without integer constraints - solid red lines represent compression members, and dashed blue lines, tension members	157
6.10 Identical volume with 3 members and 5 members in the final structures	162
6.11 Effects of R and N_{UB} on CPU time: 3 x 3 grid	165
6.12 Effects of R and N_{UB} on CPU time: 5 x 3 Half Wheel - $R=1$	166
6.13 Effects of R and N_{UB} on CPU time: 5 x 3 Half Wheel	167
6.14 Effects of R and N_{UB} on CPU time: 5 x 3 Michell Cantilever Truss	168
7.1 Design domain with supports and a central load; $L=1, F_y=-1$	181
7.2 Optimised structure: close to Michell’s theoretical optimum ‘half-wheel’ structure; final volume=3.14784, 0.2% heavier than the exact analytical solution of π	181
7.3 Volume convergence between MILP tensegrity and LP for pin and pin/roller support case	184
7.4 Design domain with supports and a central load; $L=1, F_y=-1$	185

LIST OF FIGURES

7.5	Optimised structure, close to Michell’s true optimum ‘half wheel’ structure; final volume=2.57762, 0.2% heavier than the exact analytical solution of $\frac{\pi/+2}{2}$	185
7.6	Volume convergence between MILP tensegrity and LP for pin and pin support case	187
7.7	2D tensegrity type structure, modified with additional tensile members	193
7.8	A physical model of 2D tensegrity structure, based on MILP automatically generated structures in Fig. 8.1	194
7.9	Internal member forces, based on SACS analysis; (a) compressive forces; (b) tensile forces	195
7.10	Dimensions of tensegrity column	197
7.11	One-bar ‘structure’: internal member force and utilisation ratio, U_c based on SACS analysis	199
7.12	Tensegrity ‘XIX’ column with additional members	205
7.13	LP structure corresponding to Tensegrity ‘XIX’ Column	205
7.14	LP structure (corresponding to ‘XIX’): internal member forces and utilisation ratios, U_c	207
7.15	LP structure: internal member forces and utilisation ratios, U_c	209
7.16	Tensegrity ‘XIIX’ column with additional members	213
7.17	LP Structure corresponding to Tensegrity ‘XIIX’ column	213
7.18	LP structure: internal member forces and utilisation ratios, U_c	215
7.19	MILP-derived ‘XIIX’ tensegrity structure: internal member forces and utilisation ratios, U_c	217
7.20	LP structure: internal member forces and utilisation ratios, U_c	218
7.21	MILP structure: internal member forces and utilisation ratios, U_c	219
7.22	Cross-sectional area vs Compressive capacity, for CHS sections available in UK; (a)1m, (b)5m, (c)10m. Source:[3]	225
8.1	2D tensegrity type structure with conjectured additional tensile members	236
8.2	Physical models of 2D tensegrity structure, based on MILP automatically generated structures in Fig. 8.1	238

LIST OF FIGURES

A.1	Illustration of Transmissible Load	269
B.1	3 x 3 Grid - optimized structures with integer constraints and zero area members	271
B.2	5 x 3 Truss - optimized structures with integer constraints and zero area members	272
B.3	5 x 3 Truss - optimized structures with integer constraints and zero area members	273
B.4	5 x 3 Michell Cantilever - optimized structure with integer constraints and zero area member	274
D.1	Original solution domain: enclosed by three constraints	281
D.2	Introduction of additional constraints	282
E.1	Tensegrity ‘XIIX’ column with additional members	287
E.2	LP Structure corresponding to Tensegrity ‘XIIX’ column	288
E.3	LP structure: internal member forces and utilisation ratios, U_c	290
E.4	MILP-derived ‘XIIX’ tensegrity structure: internal member forces and utilisation ratios, U_c	292
E.5	LP structure: internal member forces and utilisation ratios, U_c	294
E.6	MILP structure: internal member forces and utilisation ratios, U_c	295

Chapter 1

Introduction

1.1 Research Overview

In the latter half of the 19th century, Viollet-le-Duc described the state of French architecture as being “*plagued with the regressive Neoclassical architecture*”, such that the only original works in architecture belonged to engineers. He criticised the architects of his time for their obsession with the aesthetics of classical forms, and for their lack of interest in newly introduced materials and construction techniques. He also asserted that academic training should cease to focus wholly on the aesthetic side of architecture and instead should also seek to address the technological concerns of engineers [4].

This polemic, although referring to the state of architectural practice of over a century ago, could also be considered to be relevant to the computer-aided architectural design practice of the recent past, since the possibilities of freeform (e.g. via the use of relevant techniques such as NURB¹-derived forms or parametric modelling techniques) have been made available, in which the focus was on visual expression, shape-driven geometric pattern generation and sculptural quality of form. Indeed, whilst being inspiring methods of satisfying aesthetic criteria in design, many of the computer-aided form-generation methods of this period did little to take into consideration the complex physical behaviours of the forms,

¹Non-Uniform Rational B-spline.

nor did they attempt to model structural aspects realistically. It is not untrue to say that the scope for application of computer technology beyond geometric manipulation was being overlooked to a large extent, although separate tools were employed to render digitally generated forms structurally possible, thereby partially compensating for their initial lack of adequate structural justification.

Concurrently, there has been extensive development of engineering design and analysis methods, such as the Finite Element Method (FEM) and computational analysis methods and both linear and nonlinear optimisation techniques, primarily concerned with accurate modelling of material behaviour, structural stability and economy (and to a lesser extent in relation to this thesis, Computer Numerical Control (CNC) fabricators in manufacturing). In particular relation to the presented thesis, structural optimisation is a technique which makes use of appropriate physical laws in order to automatically synthesise structurally efficient forms. It is a process in which form-generation and analysis are effectively integrated. A number of computational tools for structural optimisation exist. One such tool is the structural layout optimisation software being developed at the University of Sheffield. However, such tools have hitherto been developed without taking aesthetic design considerations into account.

Perhaps due to the aforementioned trend of envisioning form ahead of a supporting structural solution, on the one hand it posed much greater engineering (and manufacturing) design challenges, and hence required advancement of post-rationalised design solutions, whilst on the other hand, it served as a beneficial catalyst for the advent of a new breed of integrative design solutions, whether reflected in the organisational structure of multidisciplinary teams and design processes, and/or in design methodologies and technologies.

Presently, in the field of building form design, and particularly in the subcategory of form-generation, having learnt that form and structure are inseparable, especially considering the aforementioned freeform type, there are a variety of post-rationalising methods which integratively respond to shape-driven architectural form design, and also there are a growing number of methods which attempt

to integrate at various stages of design, form and structure, some of which have also been developed and realised in built form. Respectively, these are (i) methods which use discretisation of initial form (e.g. grid-shell design), which is a practical structural design response for a given predefined form (either freeform or ‘form-found surface’), which imposes little on the initially conceived external envelope and thus allows much of the freedom frequently desired by architects for roofs etc., and (ii) methods which derive form from resultant material response to gravitational force, such as form-finding techniques.

Additionally, there are methods which employ discrete (static) structural optimisation as a definitive source of form generation, a significant differentiating feature being that response of discretised structural members to gravity and applied load cases is the predominant source of inspiration for form¹. This principle of form generation has advantages over the two methods mentioned previously. Its advantage over form-finding approaches is that, as the scale of a building becomes larger, a continuous external envelope become less viable as a design option (i.e. discretised grid or grid-like systems are likely to be lighter). Its advantage over the grid or grid-like systems for a predefined surface is that its optimality need not be restricted by the geometry of the predefined surface.

Although some optimisation-driven methods have hitherto been reasonably successful in generating intriguing forms, unfortunately many optimisation-driven methods tend to be capable of either generating small scale building parts or treating ‘academic’ problems only, and fail to tackle the issue of integration inherent in large-scale form generation studies (due to prohibitively large numbers of problem variables and/or inefficient formulations, which make run-time long). It is this field that will be the focus of attention in this thesis.

Thus this thesis proposes that a specific type of structural optimisation, namely (discretised)truss layout optimisation, employing Linear Programming (LP) to

¹c.f. methods such as form-finding (a process of determining form based on the response of material to gravitational force). Also compare with retrofit discretisation of predefined surface into ‘optimised’ grids.

obtain a solution, be employed as a potentially integrative and versatile means of performing generation of early design-stage forms of ‘conventional’ structural configuration, which are comparable to those generated by currently existing methods. The approach will be used to perform form-finding of continuous surfaces and to identify discrete networks of structural members for a predefined envelope¹.

In addition to these conventional structural configurations, as a demonstration of versatility of the optimisation technique employed, an investigation will be undertaken to establish whether the approach can be extended to treat unconventional structural configurations, which most existing form generation techniques cannot address; as an example, ‘tensegrity’ forms will be considered.

A tensegrity is a special class of structural configuration, which has fascinated architects and engineers for over half a century. Although its definition varies from one researcher to another, it is generally agreed that a tensegrity structure requires that compressive members be discontinuous, that there be no transfer of moment at joints and that the structure is pre-stressable. In this highly specialised field, numerous computational approaches exist, which are used for form-finding of the overall geometry of a preconfigured layout of members, typically arranged within a convex polyhedron. However, few methods exist to automatically identify new tensegrity geometries. It is envisaged that the optimisation approach presented in the thesis will be able to achieve this, thereby extending the scope of integrated form-structure conceptual design, while also contributing to our current understanding of tensegrity structures.

1.2 Scope of Research

Section 1.1 includes broad consideration of the scope of the research. However, for sake of clarity, this section presents this in distilled form, also providing fur-

¹Rectilinear envelopes will be employed for ease of demonstration. However, the method can be generalised to treat more complex surface definitions.

ther explanation where necessary.

The scope of this thesis lies within the field of architectural design, focussing on the use of computer-aided form generation at the conceptual design stage. Building designs of all scales are considered (Type 1-4 in Fig. 1.1), although the main focus is on the design of buildings of a ‘substantial’ scale and magnitude, i.e. large enough to warrant the assistance of computer-aided design techniques (predominantly Type 1-2 in Fig. 1.1).

It should be noted that whilst the intention is to take an integrative approach to design, this thesis will not include an investigation of a fully holistic design paradigm, which may for example utilise multidisciplinary optimisation in which multiple design parameters (e.g. services and utilities, spatial layout arrangement) are simultaneously considered, nor will the focus be on refining the design for ease of construction, as has been the focus of some recent studies. Rather, the thesis is concerned with initial stage form conception within the overall design process, which will serve as a guide and inspiration for further development during subsequent phases of the design process. In doing so it is hoped that the study will, albeit in a small way, contribute towards narrowing the gap between the two disciplines of architecture and structural engineering, in the context of conceptual form design.

1.3 Aims

Section 1.1 includes a broad statement of the aims of the thesis. However, for sake of clarity these are presented in distilled form in this section.

The overall aim of this thesis is to investigate the feasibility of applying an existing engineering optimisation (design) tool during the initial¹ conceptual design

¹The focus was on the early stage of design, as early stage decisions tend to have a high impact on the final design adopted in later stages.

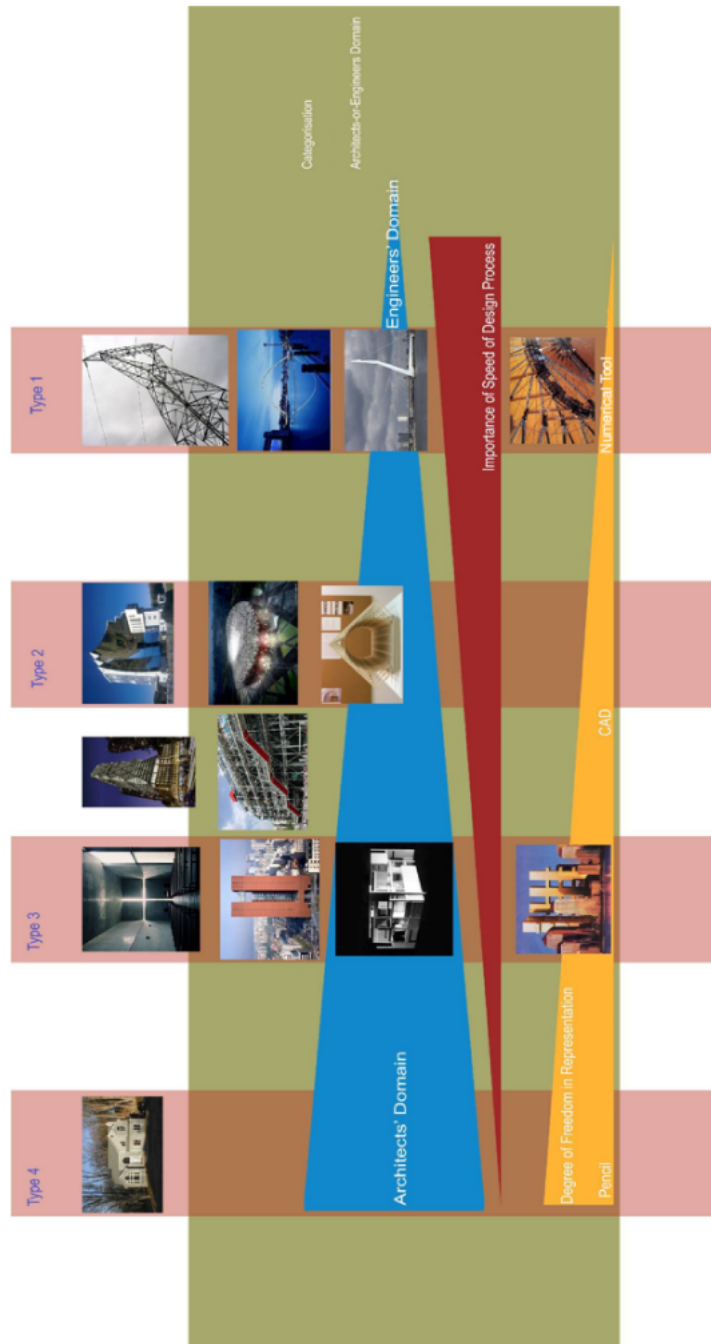


Figure 1.1: Diagram for scope of research

stage, utilising it as an architectural form generation tool. Firstly, larger scale architectural forms with conventional structural configurations are considered, and secondly, a form with unconventional structural configuration, i.e. tensegrity is considered.

To achieve this, the first objective is to generate architectural forms with ‘conventional’¹ structural configurations, comparable to those generated using currently available methods (form-finding of surfaces and discretisation of structural members for a predefined envelope).

The second objective is to extend the capability and versatility of the tool to include form generation of a less conventional structural configuration, specifically tensegrity structures. Existing form generation techniques are not capable of treating such a configuration (notwithstanding specialist tools for tensegrity), despite the significant interest in the field of form design.

1.4 Methodology

In order to achieve the first objective, a particular type of structural optimisation has been chosen: discrete layout optimisation of truss structures. This can involve a linear formulation² and involves the use of mathematical programming solvers³ to obtain solutions. This will be employed as a potentially versatile, integrative, means of generating early design-stage forms of ‘conventional’ structural configuration which are comparable to those generated by currently existing methods.

¹Conventional in contrast with more niche forms which are less widely constructed in practice, e.g. tensegrity structures or reciprocal frames.

²The software under development at the University of Sheffield currently optimises 2D/3D frame structures of scale sufficiently large to be useful to structural engineers. Whilst many other structural optimisation algorithms have been designed to identify mathematically ‘optimum’ solutions, the current Linear Programming (LP) formulations have focused on practicality of the structures generated, with little post-optimisation refinement required.

³Suitability of this decision is discussed in the Literature Review chapters

The approach adopted has been to use conceptual design studies as a vehicle to investigate the applicability of the adopted methodology to different types of construction. This involves the use of differing design constraints, and permits discussion of the generated forms and their validity in the context of other existing form generation methods. The results are presented in *Part II*.

The second objective was achieved by extending the truss layout optimisation design tool to include integer constraints to allow more fine-grained control over the generated structures (leading to a Mixed Integer Linear Programming (MILP) formulation). Parametric studies were then performed to help understand the behaviour of the extended formulation, which was then further extended to permit identification of ‘para-tensegrity’ structures. The resulting para-tensegrity forms were subsequently converted to full tensegrity forms and were extensively analysed in order to check the validity of the generated forms and the findings. The results are presented in *Part III*.

1.5 Structure of the Thesis

The thesis is arranged into four main *Parts*. It commences with *Part I*, which comprises a literature review, divided into three topics relevant to this thesis. The first chapter of *Part I* provides a critical review of the current techniques and methods used for form generation (and, to a lesser extent, optimisation) in architectural design practice. The second chapter serves as an introduction to structural optimisation techniques and presents a concise review of the different techniques available, presenting a justification for using structural layout optimisation and Linear Programming (LP). The third chapter of *Part I* introduces ‘tensegrity’ structures, and provides a critical review of recently developed form-finding techniques for such structures.

The remainder of the thesis is split into three parts; the first two remaining parts, *Part II* and *III* focus respectively on form-structure generation techniques for con-

ventional and unconventional structural configurations.

Part II identifies current issues in computer-aided architectural conceptual design, and critically examines the form-structure relationship. It describes preliminary results obtained using structural layout optimisation technique as a form-generation tool, and proposes ways in which this, originally structurally-oriented, tool can be used as an integrative structure-form design tool, for use at the initial concept design stage. This part also presents the specifications required to accommodate computer-generated conceptual forms for incorporation in design solutions, whilst also listing areas where further work is required.

Part III: Chapter 6 introduces an extension of the same optimisation algorithm employed in *Part II*, in response to the complexity of the ‘optimised’ structures obtained, and presents a method by which the final output of optimised structured can be controlled. In order to control the level of complexity, a mixed integer linear programming (MILP) formulation is presented. As a result, the total number of members in the final optimum structure can be constrained, providing end-users with greater control. Parametric studies are also undertaken to investigate the efficacy of the procedure. This algorithm is then further extended to include a novel method which makes use of MILP to generate para-tensegrity structures, as described in *Part III: Chapter 7*.

Tensegrity structures have attracted the attention of architects (and also engineers) since the 1950s. However, the lack of suitable design tools may have limited development and application of tensegrity structures in architecture, which have to date remained little more than the object of architects’ fascination. Deployable structures are one area of potential application. Unlike the structures commonly used in permanent buildings, where cost-minimisation is typically considered more important than weight-minimisation, in deployable structures (such as foldable radars and emergency shelters) weight-minimisation is typically the governing design consideration. Parametric studies are conducted in order to properly characterise the behaviour of the formulation used. Lastly a discussion

of the optimality of tensegrity structures is presented.

Part IV comprises two chapters which bring together the two strands of work presented in the thesis. The relevance of the findings obtained is considered and the extent to which the original aims and objectives have been achieved is assessed. In *Chapter 8* the scope and context of the investigations undertaken are reviewed, and the implications of the findings are critically appraised; also limitations of the investigations are highlighted. The second chapter within this part, entitled *Conclusions and Recommendations for Further Work*, then summarises the findings and contributions and finally concludes by identifying recommendations for future work.

Appendix A contains complimentary information for *Part II*. *Appendix B* provides additional data omitted for brevity (e.g. zero-area members present in generated solutions). *Appendix C* contains the MATLAB script, which was used to generate the simplified MILP structures in *Part III: Chapter 6*. Finally, *Appendix D* provides an additional explanation for the outcomes obtained in *Chapter 7* (graphical representation of the effect of additional constraints on the optimality of the generated structures).

Part I
Literature Review

Preface

The first chapter in this part, *Chapter 2* consists of a critical review of notable computer-aided architectural design and form-generation techniques, with an emphasis on those which endeavour to synthesise forms for visual expression, shape-driven and sculptural quality and a recent development of techniques which integrate at various stages of design, form and structure. This provides the context for the research contained within this thesis.

The second chapter, *Chapter 3* introduces various types of structural optimisation and their solution techniques and, presents an argument for the use of one particular method of *practical* structural optimisation in order to incorporate a higher degree of realism into form-generation; plastic layout truss optimisation employing linear programming (LP) and an associated technique, mixed integer linear programming (MILP), in comparison with other available methods.

The third chapter, *Chapter 4* introduces architectural form with unconventional structural configuration; a special type of structure, called tensegrity. Its development history is reviewed in order to draw attention to the overall theme of the development of geometry manipulation techniques in architecture, employed independently from that of numerical techniques in engineering despite their mutuality and interdependence, and need for form-structure integration.

A brief history of tensegrity, differing versions of its definitions, common typologies of regular tensegrity and the mainstream researches in a critical area of *form-finding* are summarised, leading to the most recent development of methods

for automatic design or generation of tensegrity.

The structure of the literature review is reflected later, in that of the core parts of the thesis; *Part II* presents form-generation with conventional structural configuration, *Part III: Chapter 6*, proposes further development of the same algorithm, leading to inclusion of form-generation with unconventional structural configuration in *Part III: Chapter 7*.

Chapter 2

Computer-aided Architectural Design and Form-generation

2.1 Computer-aided Design Approaches

Firstly, it should be noted that the term, ‘computer aided design’ in this chapter does not adhere to the conventional usage in design practice as meaning ‘graphical representative techniques by use of computer’ typical in architectural design. Rather, it refers to general involvement of use of computer in generation of forms, mostly in the context of building envelope design¹.

Computer-aided architectural design practice of the last two decades has seen the possibilities of application of freeform via the use of relevant computational tools and techniques such as NURB²-derived forms or parametric modelling techniques. With the advent of these possibilities, there was a period of vigorous experimentation with new techniques, tools and generated forms in the industry, experimenting with shape-driven geometric pattern generation and sculptural quality of form, popularly named; ‘blob’ or curvilinear architecture. Representative example of these include buildings such as Dancing House, Prague (Architect: F. Gehry. Engineer: V. Milunić, 1992-1996), Kunsthaus, Graz (Architects: P. Cook

¹The generation component of design rather than representation [5].

²Non-Uniform Rational B-spline.

2.1 Computer-aided Design Approaches

and C. Fournier, 2003), The Sage Gateshead, Gateshead (Architects: Foster and Partners. Engineer: Buro Happold, 2004) and Burnham Pavillion, Chicago (Architects: Zaha Hadid Architects, 2009).

Whilst being inspiring methods of satisfying aesthetic criteria in design, upon close observation, it is readily noticeable that, for many of the computer-aided form-generation methods of this paradigm, consideration of the complex physical behaviours of forms was neither simultaneous nor highly prioritised. It is hence not untrue to state that the scope for application of computer technology beyond geometric manipulation whether 2D or 3D, was overlooked to a large extent although separate tools were employed to render digitally generated forms structurally possible, thereby partially compensating for their initial lack of adequate structural justification. Often this would mean frequent iteration of design and redesign.

Concurrently, there has been extensive, parallel development in engineering design and analysis methods, such as FEM computational analysis methods, both linear and nonlinear optimisation techniques and powerful computational numerical solvers, primarily concerned with accurate modelling of material physical behaviour, structural stability and economy (and to a lesser extent in relation to this thesis, Computer Numerical Control fabricators in manufacturing).

Influenced by this trend of envisioning form ahead of integrated structural solution to support them, on one hand it posed greater engineering design challenges and propelled the advancement of post-rationalised design solutions (e.g. discipline-specific simulation tools), whilst on the other hand, it served as a beneficial catalyst for engendering a new breed of integrative design solutions; the solutions came in different ways; some were less direct and further away from the immediate issues of form themselves e.g. implementation of more efficient organisational structure or design process within a multidisciplinary design environment whilst other solutions were more direct i.e. improvement or invention of associated form-structure design methodologies and technologies.

2.2 Shape-driven Form-generation Techniques

Having accepted that form and structure are mutually concomitant¹, the importance of which is more acutely experienced when considering the freeform type, currently in the field of form design and form-generation, there are two resulting attitudes. One is shape-driven architectural forms and adoption of creative integrated post-rationalisation (e.g. Helmut Pottman’s ‘architectural geometry’ and discrete meshing). The other is form-structure integration from conception, manifested by a growing number of methods which attempt to integrate at various stages of design, form and structure, some of which have also been developed and realised in built form.

This chapter, hence reviews computer aided design techniques in two main categories. Firstly, predominantly rule or algorithm based pattern or form-generation, i.e. shape-driven techniques, are introduced and remedial yet integrative post-rationalisation techniques (e.g. grid-shell design), which respond to freeform; this is a practical structural design response to predefined freeform, which imposes little on the initially conceived external envelope and thus allows much freedom often desired by architects. Secondly, even more integrated methods of form-structure generation will be introduced. The first subcategory is form-finding, which derives form from resultant material response to gravitational force. In the second subcategory, methods which employ structural optimisation as a definitive source of form-generation, are reviewed.

2.2 Shape-driven Form-generation Techniques

A shape-driven² design approach in computer-aided design, as the name suggests, prioritises the design process according to the chosen aesthetic criteria. It thus

¹There are numerous *architectural* research projects conducted in consideration of materiality (e.g. [6]), physical constraints (e.g. [1]) and practical fabrication issues (e.g. [7])

²A shape-driven design approach is also referred to as form-led or ‘generative’ design approach. This term is widely used in the algorithm based geometry generation and is found to be derived from the term, ‘generative specification’ as appeared in [8], which was intended for shape generation through shape grammars.

2.2 Shape-driven Form-generation Techniques

involves a prescribed set of rules or algorithms through which various potential design solutions can be generated. This type of approach typically relies on variation (e.g. distortion) and repetition of a small number of basic elements. The following subsections will introduce certain rule-based or shape-driven design methods. Note that the presented list of methods is not intended to be exhaustive.

2.2.1 Pattern Generation - Nature Imitation

A typical ‘natural pattern’ generation method employs mathematically expressed, generative algorithms to mimic a physical phenomenon or biological growth pattern.

Cellular Automaton

Cellular Automaton (or CA) is a discrete model of self-replication originally designed to simulate biological growth, by John Von Neumann in the late 1940’s [9]. CA consist of a grid of cells, each of which can be in one of a finite number of states, typically ‘on’ or ‘off’. Each cell is updated by prescribed local interaction rules and the states of its adjacent cells. Architectural designers have taken an interest in CA due to its ability to generate forms (or patterns) from relatively simple rules (c.f. complexity of genetic algorithms).

Its application can range from ornamentation to modelling of spatial structure of urban land use [10]. However due to its discrete nature, application in building form-generation has been limited although recently there have been attempts in complex continuous surface form-generation using this system (e.g. [11] [12]). (See also Fig. 2.1). The possibility of interaction between forms generated by CA and any supporting structural form is unlikely due to the said discrete nature.

Lindenmayer System

Lindenmayer System (or L-system) is a ‘parallel rewriting’ system and has its origin as a system of modelling plant growth [13]. The system is expressed as a formal grammar G [14];

$$G = (V, S, \omega, P) \tag{2.1}$$

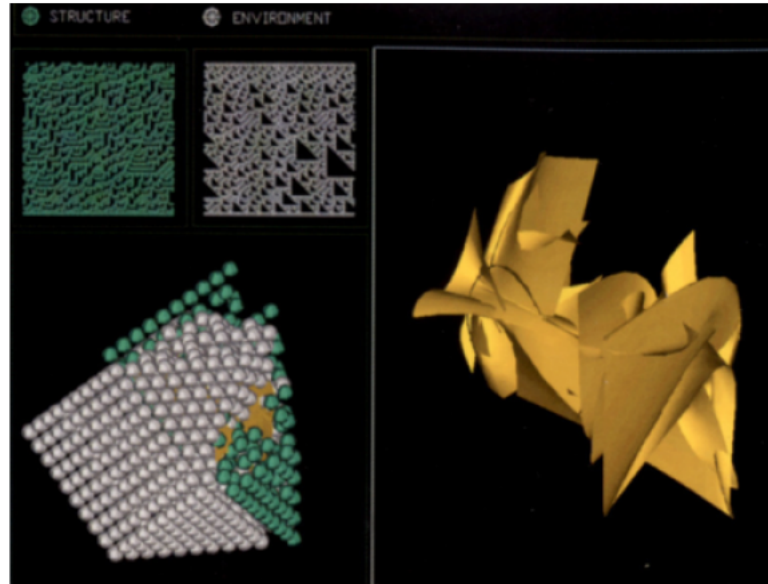


Figure 2.1: Cellular Automata. Manit Rastogi, 1994 as in [11]

where,

V = variables (a set of symbols containing elements that can be replaced)

S = constants (symbols set, containing elements that remain fixed)

ω = initiator (symbols string from V defining the initial state of the system)

P = production rules set

In order to generate forms using the L-system, the rules of grammar are applied iteratively from the initial state, as defined by ω . Each iteration applies a maximum number of rules simultaneously.

An L-system ‘grows’ by repetition of this process. The advantage of this generation system is that it requires relatively simple rules to generate complex forms. Resulting forms can bear resemblance to fractals because of the recursive nature of the process. Representative examples of designers using this method, include Michael Hansmeyer [15] and the Emergent Design Group using HEMLS, a modified version of L-system (See Fig. 2.2). The context-free nature of L-system restricts wider application in architectural design other than for form-generation as a building is designed in a sequence of compartments not a growth-like pro-

2.2 Shape-driven Form-generation Techniques

cess [16].



Figure 2.2: Lindenmayer system-generated free form [17]

Voronoi Diagrams and Weaire-Phelan Geometry

A Voronoi diagram is a ‘decomposition method’ by which a space is decomposed into sub-regions by distances to a discrete number of points. Voronoi diagrams are named after the mathematician Georgy Voronoi, based on his work [18] in 1907 on a class of patterns called *Dirichlet tessellations* [19]. All regions in a Voronoi diagram are convex polygons, each of which has only one ‘generating point’. Application of these diagrams are found in many disciplines including; architecture, urban planning, computational geometry and geophysics. Representative designers in architecture include Chris Lasch [20].

Similarly the Weaire-Phelan structure is a three-dimensional complex structure based on irregular polyhedral geometry simulating the structure of soap bubbles. Most prominently the Beijing National Aquatics Centre designed by PTW Architects and Arup [21] has used irregular Weaire-Phelan geometry as its inspiration (See Fig. 2.3).

2.2.2 Pattern Generation - Abstraction

This type of pattern generation differs from ‘natural pattern’ generation, as it derives its rules for pattern generation from abstract concepts and the associated

2.2 Shape-driven Form-generation Techniques



Figure 2.3: Beijing National Aquatics Center: Weaire-Phelan geometry. © Arup + Ben McMillan [22]

forms are sometimes characterised by ‘emergent’¹ qualities due to its abstract nature.

Research work of Philippe Block is typical of geometry-focused method of form-generation, that

Parametric Modelling

Parametric modelling is a representative and widely used example of a shape-driven design technique. The history of parametric modelling can be traced back to the work of Lin *et al.* [24], on variational geometry². This particular work is considered an important achievement in the development of parametric modelling because it allowed generalisation of models by implicit geometrical representations with mathematical rules [26].

Parametric modelling is a geometric modelling (form-generation) technique where the geometry of a model is not explicitly defined but instead is determined by rules and constraints, which define aspects of the building and their relationships

¹The term ‘*emergent*’ refers to “*the spontaneous occurrence of an organisation or a behaviour that is greater than the sum of its parts*” [23]

²Lin *et al.* in fact cite [24] and [25] as the basis of their own work. However, these papers serve as analyses and proposals rather than direct development work in parametric modelling

2.2 Shape-driven Form-generation Techniques

to each other. Establishment and modification of these relationships is an essential part of the parametric modelling process. Changing a rule or constraint, or modifying a part of the model, usually carries implications for the entire model. In parametric models, the rules are explicit and the geometry is implicit while in conventional building modelling, the geometry is explicit and the rules are implicit. This gives parametric modelling a huge advantage over conventional building modelling, where every aspect of the model must be defined, without referring to other parts of the model.

Examples of parametric modelling tools for architectural design, include; *Digital Project*, an application based on Catia by Dassault Systems, *Generative Components* by Bentley Systems [27] *Grasshopper* and, *ParaCloud*. Fig. 2.4 shows *Kartal Pendik Masterplan*, an urban design example by Zaha Hadid Architects.

These tools and methods typically reflect precise definition of form as their highest priority; however, there have been a growing number of more integrative methods employed in more recent examples and efforts e.g. [28] [29] [30] although an important distinction should be made; these methods employ, albeit efficient, essentially a ‘design-analysis feedback loop’ between the two separate tasks of form-generation and engineering analysis, rather than an integrative, novel approach to form-generation.

A recent example of freeform design through use of parametric modelling is *Metropol Parasol, Seville (2004-2010)* [32] designed by Jürgen Mayer H. and Ove Arup and Partners. It is essentially a large-scale, mushroom-shaped canopy, constructed in a timber lattice-frame structure with joints connected with specialist glue. The geometric configuration of lattice is strictly orthogonal, which alludes to the fact that the aesthetic criteria of form design were prioritised over influence or consideration of engineering solutions during its design process. See Fig. 2.5.

Another notable example, is *Centre Pompidou, Metz, France, (2005-2010)* by Shigeru Ban. As the main inspiration for the design of the roof was of a straw hat, the outer geometry was of the utmost priority [33]. It is this priority, which

2.2 Shape-driven Form-generation Techniques

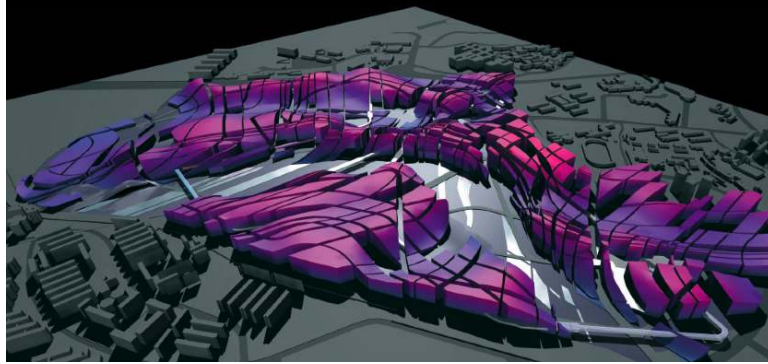


Figure 2.4: Zaha Hadid Architects, Kartal-Pendik Masterplan, Istanbul, Turkey, 2006 as in [31]



Figure 2.5: Metropol Parasol, Seville. Source:[32]

2.2 Shape-driven Form-generation Techniques

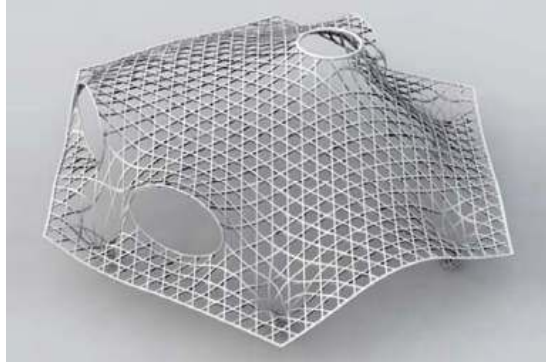


Figure 2.6: Centre Pompidou, Metz, France. Source:[33]

in effect justifies the use of a post-rationalised engineering approach which follows the predefined form. A lattice consisting of triangles and hexagons was projected onto the freeform surface with every curve designed carefully not to be repeated; it was essentially a geometric construct and the structure was post-rationalised at a later stage of design. See Fig. 2.6.

Shape Grammar

Inspired by grammatical rules of language, in 1971, George Stiny and James Gips introduced a rule-based method of form-generation using *shape grammars* [8]. The definition of shape grammar (SG) is expressed as a tuple [8]:

$$SG = (VT, VM, R, I) \quad (2.2)$$

where,

VT = a finite set of shapes

VM = a finite set of shapes (such that $VT^* \cap VM = \phi$)¹

R = a finite set of ordered pairs (u, v) ².

¹where ϕ is an empty set.

²such that u is a shape consisting of an element of VT^* combined with an element of VM and v is a shape consisting of (A) the element of VT^* contained in u or (B) the element of VT^* contained in u combined with an element of VM or (C) the element of VT^* contained in

2.2 Shape-driven Form-generation Techniques

I = a shape consisting of elements of VT^* and VM

Shape grammars generate n -dimensional shapes. In order to generate a shape from a shape grammar, the prescribed shape rules are recursively applied to an initial shape, which determine which shape is to be replaced and how the replacement process (according to geometric transformations, i.e. translation, scale, rotation and mirroring) will be carried out. The generation process is terminated when no rule in the grammar can be applied. Once the process is terminated, another shape is generated, which consists of the given shape with the right hand side of the rule substituted in the shape for an occurrence of the left hand side of the rule.

When using a shape grammar as a form-generation tool, a finite number of rules can generate an infinite number of shapes. The uniqueness and popularity of this particular method of form-generation can be attributed to this potential to generate unexpected ‘emergent’¹ shapes. Applications of this method are found in art [35], architecture [36], either as a form decomposition or form-generation tool, and also in structural engineering as part of structural algorithms [37].

Algorithmic Design

Algorithmic design is an approach which involves the “*designation of computer programs for form-generation from the rule-based logic inherent in architectural programs, typologies, and building design standards*” [38]. It employs scripting languages accessible in many available three-dimensional, geometry manipulation packages to ‘code in’ design intentions [38] [39]. However, it carries the disadvantage of technical difficulty because it requires the user to have a level of competence in computer programming although not to the same degree, compared to direct programming.

u combined with an additional element of VT^* and an element of VM

¹The term ‘emergent’ refers to ‘not predefined’ or ‘unexpected’ [34]

2.2 Shape-driven Form-generation Techniques

While sharing similarities with traditional algorithm-based approaches such as Cellular Automata or L-Systems in that the method of form-generation is based on rule-based logic, this particular design approach draws a distinction; this approach extends beyond the designer-users' passive use of algorithms in a restrictive way and actively engages users to program custom-scripts into the existing programs for form-generations.

2.2.3 Discretisation over Predefined Surface Form

This approach *does not replace* but *compliments* freeform (or form-found geometry). It is a practical structural design response to predefined form, which imposes little on the initially conceived external envelope and thus allows much freedom often desired by architects. It is probably this freedom afforded by this approach, which makes it the most commonly found, which provides post-rationalised supporting structures for forms generated using the tools which exclusively manipulate geometric configuration of forms.

Many methods are geometry-focussed, and due to the fact that discretisation is further along the form design process, following the definition of the outer envelope, some methods tend to be more related to detailing. A noteworthy discretisation method by Cutler and Whiting [40] devised a method of planar remeshing, in which curvilinear freeform is automatically transformed into a series of planar polyhedral panel geometries, rendering the form more economical from the construction standpoint.

A similar method is proposed also by Helmut Pottmann [41], one of the authorities in the research of combining geometry, structure and manufacturing. He explores a research area he calls 'Architectural Geometry at the boundary between applied geometry and architecture'. His approach is comprehensive in that it considers from the initial form-definition to construction. In one of his papers [42], he makes a series of propositions regarding strategies of detailing and discretisation (or geometry processing) using planar polyhedral surfaces whilst

stressing the aesthetic values of mesh configuration.

A recent structure-integrated example is the research by Dimcic [43], which responds to the stringent geometric requirements of freeform with grid shell configuration; it is one of the prevalent methods of configuration and optimisation of the internal members. He makes use of Genetic Algorithms for optimisation with the goal of redistributing stress-concentrated areas.

2.3 Integrated Design

The computer-aided form-generation methods, reviewed in the last section, satisfy sufficiently, aesthetic criteria in design. However, some of these are almost exclusively for geometric form-generation or manipulation, and consideration of the complex physical behaviours of forms do not feature.

This trend of envisioning form ahead of simultaneous, integrated structural solutions, engendered two notable categories of effective methods of integrative engineering form-structure generation, relevant to the thesis. The first is computational form-finding, a numerical process which mimics physical form-finding, i.e. derivation of form from resultant material response to gravitational force. The second subcategory is one which follows the shape-driven form-generation strategy by providing a supporting structure by use of regularised discretisation (e.g. grid-shell design). The third subcategory, is a group of methods which employ structural optimisation as a definitive source of form-generation.

This section introduces these three notable subcategories of integrated design approaches; computational form-finding, regularised discretisation of shape-driven freeform surface, and (structural) optimisation-driven approaches.

2.3.1 Computational Form-finding: from continuous to discrete

Form-finding is a process of deriving a form (or geometry) for a structure which (among other requirements), will need to resist the particular loading to which it will be subjected. Ideally, the process of form finding should identify a geometry that is by some definition, structurally efficient. This approach has a long and distinguished heritage, with, for example, the definition of the form of a cable suspended under its own self-weight being addressed by the likes of Johann Bernoulli, Gottfried Leibniz, and Christiaan Huygens, and the demonstration that the ‘catenary’ was the correct form being one of the early triumphs of differential calculus [44]. It is worthwhile to follow the use of this result into modern form-finding.

At the beginning of 20th century, this catenary shape was extensively explored and creatively exploited by Antonio Gaudi in his architecture, many in 2D planar solid arch designs through a series of complex, direct physical modelling of hanging chains loaded with weights and their inverted forms. See Fig. 2.7



Figure 2.7: Antonio Gaudi’s Sagrada Familia: interior view. Source: [45]

In the more recent past, the mostly 2D usage of catenaries was extended and developed by Heinz Isler into 3D thin membrane shell structures, through physical modelling and rigorous material calibration, which resulted in various novel

forms of concrete shell structures. Whilst such engineers as P. L. Nervi and Eduardo Torroja successfully designed and implemented thin membrane shell forms through their use of spherical dome segments, it was Isler, who in the year of 1959, presented possibilities form-finding of 3D shells, a radically different form-finding method at the time [46]. See Fig. 2.8.

His method, whilst being an undoubtedly innovative and conceptually simple, direct modelling technique, the modelling process was complex and hence difficult to be generalised[47], especially without a parallel numerical modelling technique, which could take advantage of modern computing technology.

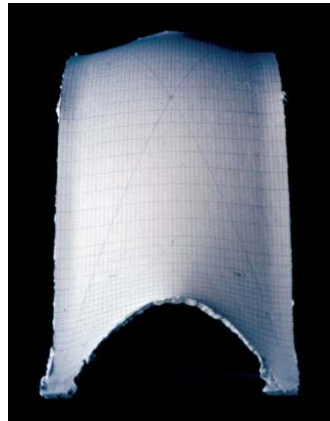


Figure 2.8: Heinz Isler's inverted hanging cloth cast form. Source: [47]

Similar to H. Isler's method, in the design process of Mannheim Multihalle (1975), Frei Otto and his design team made extensive use of hanging models for geometry definition of the double curvature timber roof. The real break-through came, however when for Frei Otto's design of Munich Olympic Park cable-net structures, a novel numerical modelling technique was developed in 1971, namely, force density method, by Schek (and Linkwitz) [48]. It is primarily a search tool for minimal surface solution in cable-net and membrane structures. The strength of the method lies in the assumption that the ratio of tensile force to length of each cable is constant, which makes a set of non-linear equations into a set of linear equations, rendering it directly solvable.

Originally a technique, force-density method which was used for form-finding of tensile nets, with introduction of varied tension factor, Relaxation found its usage in freeform roof definition, one of the most recent examples of which is, MyZiel mall, Frankfurt, jointly designed by Massimiliano Fuksas and Knippers Helbig. In this example, a surface geometry was triangulated in order to form a triangulated mesh and then, the mesh relaxation technique was applied to refine the overall geometry, resulting in a more optimised grid. Still further in development of this technique, was seen the design of Sun Valleys, EXPO Axis Shanghai, by Knippers Helbig; 41.5m high funnel structures of triangulated grid shell configuration [49]. The relaxation technique was applied to refine the triangulate grid; this time additional adjustments were made at the connections which required a higher density of triangulation, due to higher tension forces, through manipulation of tension factors.

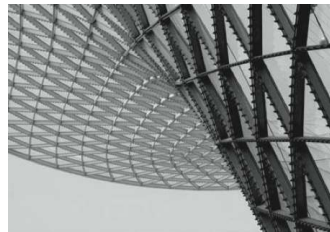


Figure 2.9: Sun Valleys, EXPO Axis Shanghai. Engineered by Knippers Helbig. Source: [49]

A parallel development occurred, in 1970, when Alistair Day formalised a mathematical technique, called Dynamic Relaxation, which he and Bunce applied to analysis of cable network structures[50]. This method could model the behaviour of nonlinear structures by assuming that a structure with a given initial configuration is subject to external forces; its equilibrium can be calculated by integrating a fictitious dynamic equation. In any current configuration of the structure, nodal equations of equilibrium are used to compute out-of-balance forces. In turn, these forces are used in order to obtain the current acceleration. The resulting uncoupled equilibrium equations can then be integrated (see for further explanation).

2.3 Integrated Design

Later, this was extended to modelling of non-tensile structures to meshed, grid shell geometry. Two representative building examples are; the roof grid-shell form-structure over the great court of the British Museum (Architects: Foster + Partners. Engineers: Buro Happold), which employed the process of finding the final geometry through dynamic relaxation from a pure geometric shape [51], and Smithsonian Institution, Washington DC (Architects: Foster + Partners. Engineers: Buro Happold, 2004-2007), which explored the same form-finding technique but with a regularised mesh of quadrangles (Fig. 2.10).



Figure 2.10: Smithsonian Institution, Foster + Partners and Buro Happold. Source: <http://www.fosterandpartners.com/Projects/1276/Default.aspx> Accessed: 20/12/2012

Indeed there are a great number of methods being devised in numerical form-finding besides these. One such example is the work of Xie *et al.* [52], which attempts to replicate, by employing an evolutionary structural optimisation method, Gaudí's experimental design method of employing hanging chains and weights. Also In his work, Kilian [53], uses particle-spring systems, replicating the hanging nets, to regenerate structures comparable to the hanging nets used by Heinz Isler. More recently, the same method which uses particle-spring systems, was

employed in form-finding of Trada plywood double-curvature Shell design Ramboll Computational Design team (Fig. 2.12). It was then discretised into flat panels using a discretisation method (constrained planar re-meshing) used by Culter [40]. Another example which attempts to replicate Isler’s form-finding approach is found in [54], which employs a computational model of freeform shell and mathematical programming combined with the finite element technique. See Fig. 2.11

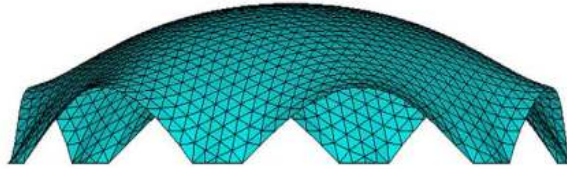


Figure 2.11: Hexagonal freeform shell with six supports. Source: [54]

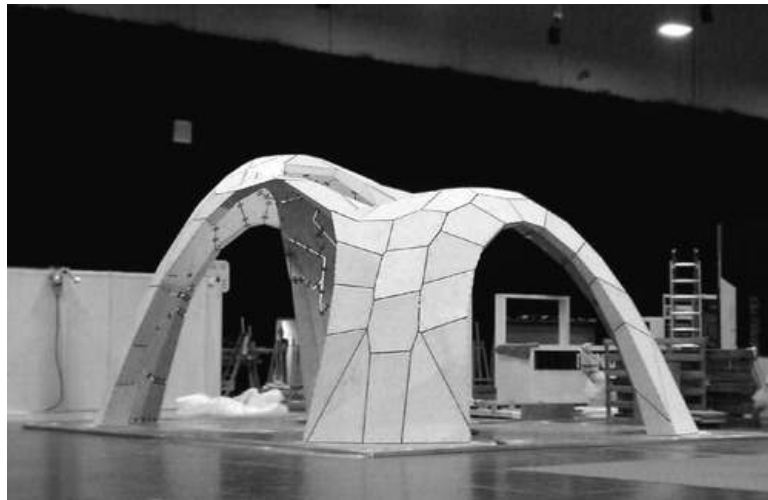


Figure 2.12: Trada plywood shell by Ramboll Computational Design

Most recently, Philippe Block’s research group at ETH Zurich, devised a novel optimisation-based form-finding approach called ‘Thrust Network Analysis’ (or TNA), which aims to find the ‘best fit’, compression-only solution to an arbitrary input surface for given network topologies, i.e. form-finding of 3D freeform funicular structures. [55]. Their method also employs the established form-finding

technique called Force Density Method in order to ensure unique solutions because, since the assigned force densities can be explicitly controlled, the final shape can be explicitly influenced through ‘reciprocal force diagrams’ (which relate form and forces), with the resulting forms extending far beyond forms generated from inverted hanging nets, Fig. 2.13. See also Vouga’s work for related development [56].



Figure 2.13: An example freeform masonry shell. Phillippe Block *et al.*
Source: <http://block.arch.ethz.ch/projects/freeform-masonry-shells> Accessed: 30/11/2012

There are two notable observations, worth mentioning regarding this form-generation approach. The first is that the final outcomes or forms cannot easily be steered toward desired ends without experience; this could be a disadvantage if the design parameters are stringent and the final form needs to be (at least approximately) close to a prescribed shape boundary. On the other hand, it could also be an advantage as this could potentially bear ‘emergent forms’. The second is that currently the approach is rather material-specific as it is confined to homogenous compression only shells and masonry structures, rendering it difficult to apply to common, materials such as steel which have tensile and compressive strength and where flexure as well as compression may therefore be accommodated.

Although there is a wide variety of methods of form-finding with different strengths and weaknesses between them (see [57] for reviews and comparisons), the overall approach of numerical form finding has several advantages. Whether the approach is for continuous surface definition or grid-shell, the resulting form-structure is a very efficient way of resisting load as it tries to eliminate or reduce moments under self-loading (A minor observation worth mentioning is that resulting structures tend to emphasise horizontality rather than verticality). Specifically, for continuous surface definition, the span of the shell is more likely to be subjected to material limitations than grid shells. In the case of discretised surface, grid shell structures, one very important feature is the regularisation of polygon grids; this is its biggest strength for its consideration of manufacturing and constructibility, but it can be its limitation as its structural optimality is constrained by the grid, offering little flexibility outside the grid. Furthermore, when the prescribed geometry is required to be exact, as its highest priority, the method becomes less relevant. In summary, for discrete shell structures (e.g. grid shells), there is a compromise between ‘buildability’ which pushes the designer towards regular polygonal grids, and ‘structural efficiency’ which may lead to a more free-form and less regular discrete structure.

2.3.2 Optimisation-driven approaches

In this subcategory, methods which employ structural optimisation as a definitive source of form-generation, are reviewed. Note that this method does overlap with some methods of form-finding, where optimisation algorithms are extensively used.

Form designers (and/or design tool developers) have been making steady efforts to integrate and co-operate at early project stages and there has been development of more optimisation-driven integrated design tools and methods; for example, a popular graphical manipulation software *Rhino 3D*¹ has a number of plug-in

¹<http://www.rhino3d.com/> Accessed on 10/11/2009

2.3 Integrated Design

software e.g. *MPanel Design*¹ and *ForTen 3000*², for tensile/membrane structure designs, i.e. form-finding design tools which take physical behaviour of designs into consideration.

EifForm, a stochastic optimisation tool has been developed by Kristina Shea [37] and been used for generation of the form used in the construction of a simple canopy [58] (see also 2.14 as in [59]). It generates the overall form of framed structures. The central idea is optimisation of structural efficiency whilst also considering aesthetic criteria, as it combines generative Shape Grammar (or SG) and Simulated Annealing (or SA)³, a heuristic optimisation algorithm. SA was first introduced by Kirkpatrick [60] and developed into a shape generation method by Cagan and Mitchell [61].

EifForm first generates a structural configuration based on SG rules. The performance of this configuration is then tested, after which the most optimal alternative is chosen according to SA. However, it must also be noted that the optimality of designs generated by EifForm is debatable when compared with known optimisation benchmarks.



Figure 2.14: The Hylomorphic Project in the central court of the Schindler House. After [59]

¹<http://www.meliar.com/MPanel.htm> Accessed on 10/11/2009

²<http://www.forten32.com/> Accessed on 10/12/2009

³See Section 3.3.6 for a description in engineering development.

Dominique Perrault's design for the underground station, Piazza Garibaldi, in Naples involved use of Genetic Algorithms¹ in generating possible structural forms; entire populations of structures were evolved and individual structures were selected through predefined architectural and structural fitness criteria [62]. In order to provide a more efficient roof structure, a genetic algorithm was used to assign each node a random z -coordinate. The z -coordinates of all nodes were encoded into a genome, allowing crossover and mutation in the algorithm, and it was found that the performance² of the structure could be improved over the run of 200 generations with 40 individual structures each (See Fig. 2.15).

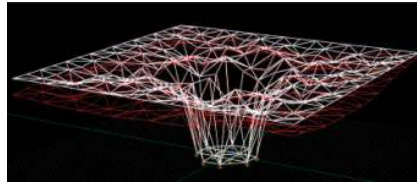


Figure 2.15: Underground Station Roof Structure, Piazza Garibaldi, Naples. After [62]

Many recent examples which employ various levels of optimisation approaches are found in architectural form design field: e.g. application of topology optimisation of building components in prestressed concrete [1], genetic algorithm-based optimisation in conjunction with parametric modelling [63] and evolutionary algorithm-based optimisation of fabric-formed beams and trusses [64]. However, it must be noted that, whilst many of these methods are successful in generating small scale building components and altering initially predefined forms, there are few methods which generate the overall definition of forms using structural optimisation as a main source of inspiration.

Another noteworthy approach is one by Buro Happold SMART design team, who developed a comprehensive optimisation tool, called *SMART Sizer*. it uses a com-

¹See Section 3.3.4 in Chapter 3 for a more thorough description of Genetic Algorithms.

²This refers to the load-bearing capacity of structure per given weight.



Figure 2.16: Optimised loft slab [1]. Source: [1]

combination of direct and iterative algorithms (virtual work, genetic algorithms and topology optimisation), capable of optimising complex 3D forms from concept form designs to detailed sizing of structural members. It has found its use in such projects as Louvre Abu Dhabi for its roof optimisation. In fact, SMART is one among the general optimisation trend (e.g. Arup's in-house optimisation tool [65][66], Abaqus iSight and Bentley Systems SACS Redesign/optimisation feature) in structural design that, regardless of variations in employed algorithms, because of the nature of the engineering design to a regulatory code, whether to British Standards or to Eurocodes, the true optimum generation does not and indeed should not extend further than concept design stage. What they do, however, is that architects/engineers devise a design, which then employs an iterative procedure of input-and-output mostly for code-checking and individual member sizing optimisation. They come with a huge choice of powerful (fast solution convergence rate), proved-and-tested algorithms (e.g. Simplex, Genetic Algorithms, Simulated Annealing etc). Again, the time constraint is the key in any optimisation tool; a real design case will contain a great number of members and complex load combinations and the run-time could be a prohibiting issue in any of these tools.

2.4 Summarising Remarks

In the early stages of the use of CAD in architectural design, the focus was more on shape-driven, form-led approaches, rather than the inclusion of performance-

based drivers. This is perhaps understandable given the historical centrality of form in architectural theories and practice.

The use of CAD in architecture had initially enabled the accuracy of drawings, both two-dimensional and three-dimensional visualisation of initial ideas, efficient exchange of information [67] and relatively easy generation of novel geometry. However, these approaches with their focus on visual form but little practical consideration, have been changing dramatically in the very recent past to adopt a more practical, constructible and ‘possible’ methods of design integration through such means as post-rationalisation, computational form-finding and optimisation.

The attempts to design in a more integrative manner and the associated attempts to devise integrative design systems¹ have been reviewed in this chapter

Nevertheless, it notable that, whilst integration of form and structure (and other performative aspects) has become almost standard through weight-minimisation optimisation and form-finding approaches (e.g. the automotive industry over the last decade or so), the similar development in architectural design has somewhat lagged in its application of similar approaches to form-finding for architectural structures and there is still much to be explored.

This is to some extent due to the scale of the structures; automotive components are typically on the scale of a few centimetres , whereas architectural structures are orders of magnitude larger. This produces challenges for the computational efficiency of structural optimisation approaches; additionally, the often discrete nature of architectural structural forms at the largest scale (thin compression arches/domes or truss structures) means that non-linear aspects such as Euler buckling may become important.

¹Kolarevic suggests that a single modelling system or internalizing the information can be a remedy for some of the present redundancies and inefficiencies in the design industry and, that in order to make possible the transition to digital modes of practice, the technologies based on existing modes of practice should be replaced by tools suitable for new modes of production [68].

2.4 Summarising Remarks

In the subsequent chapter, it will show that these non-linear approaches generally find locally optimal solutions which may be far from the globally optimal form. Perhaps as a consequence, in the limited number of cases of structural optimisation being applied to form-finding of architectural structures the resulting structures have been (from an optimality point of view) disappointing, with the ‘optimised’ forms bearing little resemblance to benchmark optimal structures.

In the light of this, the next two chapters will comprise an investigation of the types of structural optimisation approaches available, setting out their strengths and weaknesses for form-finding of architectural structures, leaving open, a small window of opportunity for truss layout optimisation in a similar effort to generate form by use of computation with considerations to physical reality.

Chapter 3

Structural Optimisation

Structural optimisation is concerned with a search for the optimal configuration of a structure that best satisfies some criterion or criteria of optimality. Pioneering work on this subject was conducted by Maxwell [69] and Michell [70], who set out the basic theoretical framework by which structures of least weight could be found to carry a given system of forces. These approaches typically produce structural forms which are highly complex, almost certainly not practically buildable and often in the form of unstable equilibrium. However, if these practical aspects are set aside momentarily, these they do definitively identify the absolute minimum weight of structure for a given force system, and as such have great potential value in both establishing a benchmark, and giving insights into the features of optimal forms.

In the latter half of the 20th century, computational methods of structural optimisation were developed which could either automate the search for so-called ‘Michell structures’ or take into account more practical issues in the search for an optimal form, such as requiring that the structures should be made from standardised components, that buckling stability be taken into account and that fabrication costs be included.

The field of structural optimisation has thus cleaved to some extent into two groups; a small one developing classical approaches, usually employing linear algorithms to enable identification of Michell structures and a much larger one

3.1 Mathematical Optimisation: Terminology

using heuristic, non-linear computational approaches in an attempt to find more realistic structural forms. We may define these approaches as ‘theoretical’ and ‘practical’

This chapter will firstly present a typical mathematical optimisation problem in order to introduce frequently used terms in optimisation theory. Secondly, it will review various types of optimisation and approaches to the solution of optimisation problems. Thirdly, it will identify limitations of current optimisation methods with emphasis on capability to control over the final form of the optimised structures.

3.1 Mathematical Optimisation: Terminology

A mathematical optimisation problem can be expressed as follows [71]:

$$\text{Minimise or maximise} \quad f(x) \quad (3.1)$$

$$\text{subject to:} \quad g_j(x) \leq b_j \quad \text{where } j = 1, \dots, m \quad (3.2)$$

$$l_i \leq x_i \leq u_i \quad \text{where } i = 1, \dots, n \quad (3.3)$$

3.1.1 Objective Function

In Eqn 3.1, the function $f(x) : \mathbf{R}^n \rightarrow \mathbf{R}$ is the objective function. This represents a numerical value, or specifically a structural characteristic to be optimised. An optimisation problem may either be a single-objective or multi-objective, where multi-objective problem has more than one objective function. For example, the objective function in single-objective structural optimisation might be the total weight of constituent structural members whereas in multi-objective optimisation the objective might be the total weight and total number of members.

3.1.2 Variables

$x = (x_1, \dots, x_n)$ is a vector containing the variables of the optimisation problem. The values of these vectors are to be determined in order to ‘optimise’ (i.e. minimise or maximise) the value of the objective function $f(x)$. Each variable, x_i is restricted to remain within a range of values between *lower bound*, l_i and *upper bound*, u_i . Specifically in structural optimisation, the variables represent characteristics of individual elements within the structural framework (e.g. member cross-sectional area or axial forces). Objective functions and constraint functions are expressed in terms of these variables.

Variables can also be either discrete or continuous [72]; for example, if a variable representing the cross-sectional area of a structural member, is allowed to take any positive value less than the upper bound, then the problem is a continuous optimisation problem. On the other hand, if the variable may only represent the area of a steel section chosen from a predefined set of available sections from manufacturers, the problem is a discrete optimisation problem.

When determining the optimum positions of nodes, the optimisation problem may be either continuous if the nodal positions are to be determined freely within the design domain, or discrete if the positions are to be determined from a predefined grid of nodes. If integer variables are used, the optimisation problem is called an *Integer Programming* problem and if both integer and continuous variables are used, the problem is called *Mixed Integer Linear Programming* problem. Refer to Fig. 3.1.

It must be noted that restricting values to discrete (or integer) variables in the problem formulation can be useful in controlling the complexity of the overall structural layout, e.g. the total number of members in the final optimum solution. However, there are two main disadvantages with discrete problems. Firstly, the optimal discrete solution depends on the predefined discrete layout, which could result in a solution which can only optimise the structure within the constraints of the pre-defined (and probably non-optimal) geometry. Secondly, discrete typically problems require considerably more computation time to solve, compared

3.1 Mathematical Optimisation: Terminology

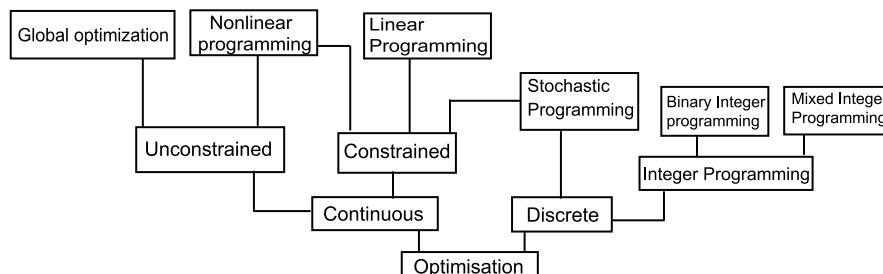


Figure 3.1: Classification of optimisation. After [73]

to continuous problems.

Due to these known disadvantages of including discrete variables, variables are often assumed to be continuous in truss optimisation. In practice, the final solution value from continuous truss optimisation, can be used as a guide when choosing member from a set of readily available specifications of sections.

The use of continuous variables also has a known disadvantage; all potential members may be present in the final optimal form albeit with zero cross-sectional area, i.e. there is no method within the optimisation algorithm itself, of differentiating between members with positive area and members with zero area as the algorithm treats positive and zero area members identically, whereas ‘real’ designers know that an area of zero is a special case i.e., the member does not exist. This can be addressed by the use of binary ‘flag’ variables that take the value 0 if the member has zero area and 1 otherwise.

3.1.3 Constraints

The function(s) in Eqn 3.2, $g_i(x) : \mathbf{R}^n \rightarrow \mathbf{R}, i = 1, \dots, m$ is(are) the *constraint function(s)* and b_j are the (lower or upper) *limits*, which are also called *bounds* of the constraints.

3.1 Mathematical Optimisation: Terminology

In structural optimisation, constraints define the allowable limit(s) on physical behaviour of structures. The inequality governing the maximum stress of an element, $A = F/\sigma$ ¹ is an example of a constraint in structural optimisation.

3.1.4 Feasible Set and Global Optimum

The term *feasible set* describes a set of solutions where the determined variables satisfy all of the stated constraint functions. In global optimisation, algorithms do not immediately produce ‘the’ most optimum solution called *global optimum*; it first produces a number of feasible solutions and then they converge toward the global optimum. In this type of optimisation a global solution will be reached although the efficiency of the search routine can be a problem [71].

3.1.5 Convexity and Local Optima

Optimum solution search algorithms may converge toward *local optima*. Referring to Fig. 3.2, x_{l_1} and x_{l_2} , i.e. x_{l_1} is the local optimum in the sub-domain between $x_l - \delta_1$ and $x_l + \delta_1$, and x_{l_2} , the local optimum in the sub-domain between $x_l - \delta_2$ and $x_l + \delta_2$, despite the global being x_g . Notice the true minimum or global optimum for function $f(x)$ is x_g for all $l_i \leq x \leq u_i$.

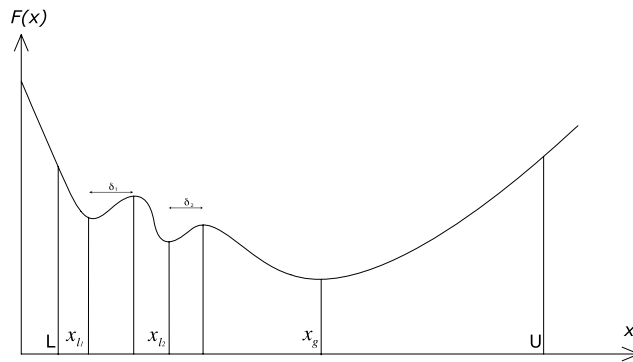


Figure 3.2: Global and local optima. After [73]

¹where A is the cross sectional area of the element of the material stress, σ , to which the force, F is applied.

3.2 Types of Structural Optimisation

An optimisation problem (or, the feasible set, objective function or constraints) is said to be *convex* if any one point can be connected to any other point by a straight line that stays entirely within the solution region, or *non-convex* if this is not the case when plotted. Linear Programming problems are convex by definition while Non-Linear Programming problems may contain both convex and non-convex functions [71].

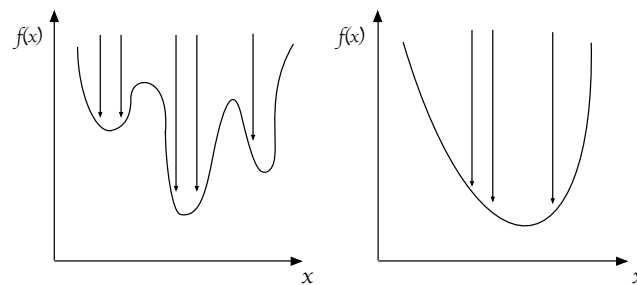


Figure 3.3: Non-convex and convex optimisation: non-convex on left and convex on right

The objective of a local optimisation (cf. global optimisation) is to find the best solution in a specified range within the feasible set. However, this search process is initiated with arbitrarily chosen values of variables to produce an initial feasible solution. The major disadvantage of this type of optimisation is that the successful search for an optimum solution is reliant on the accuracy of the arbitrarily chosen initial values. This point is illustrated in Fig. 3.3; the downward arrows represent the initial arbitrary values. In the figure on the left, there are clearly three separate distinct optimum solutions, which depends on the initial arbitrary values while the figure on the right shows the successful search for the global optimum does not depend on the initial arbitrary values.

3.2 Types of Structural Optimisation

There are a number of different approaches to solving structural optimisation problems. This section introduces a variety of approaches currently used for structural optimisation.

3.2.1 Topology Optimisation

Topology optimisation is concerned with identification of the topology of a structure by optimising (a) specified parameter(s); in truss optimisation, optimising the spatial arrangement of members and nodes. The objective of this type of structural optimisation is to find an optimal distribution of materials to withstand the applied force constraint with the given support constraint, within the design domain. An example topology optimisation problem is shown in Fig. 3.4.

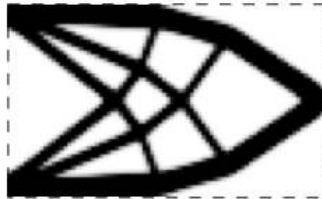


Figure 3.4: Topology optimisation, after [74]. The dotted box denotes design domain

A wide range of applications are found especially in automotive and aeronautical engineering e.g. [75] [76] [77], and [78].

Topology optimisation methods can be subdivided into three approaches; ground structure [79]), homogenisation (e.g. Solid Isotropic Micro-structure with Penalisation - see *Section 3.3.2*), fully-stressed design techniques (e.g. Evolutionary Structural Optimisation [80]). The two main disadvantages of topology optimisation are, over-reliance on arbitrarily chosen refinement values, for optimum solution and, practicality for construction of the solution structures ¹.

3.2.2 Size Optimisation

In size optimisation, the size of elements in a pre-defined structural layout, is optimised, where the problem variables are the member cross-section properties.

¹due to the large number of nodes and discrete nature of the structural elements employed in large structural frames.

The loads, supports and material properties as well as the initial layout, are pre-determined prior to optimisation.

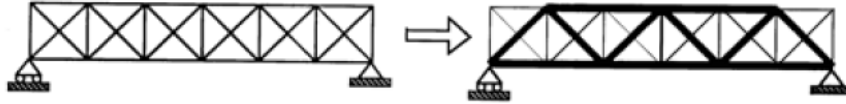


Figure 3.5: Size optimisation. After Bendsøe and Sigmund [81]

3.2.3 Geometry Optimisation

In geometry optimisation, the topology is usually pre-defined and, the nodal coordinates are optimised¹, e.g. Fig. 3.6. The aim of this type of optimisation is refinement of nodal coordinates. Schmit [82] first presented optimisation of three-bar trusses using a non-linear method and provides discussion of possible inclusion of geometry variables in his formulation. Cornell [83] later extended this discussion by including, in his formulation, nodal coordinates and member cross section areas as variables.

Due to the highly non-linear nature of the objective function in geometry op-

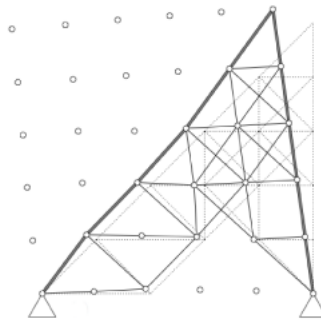


Figure 3.6: Geometry optimisation, after [84]

timisation, an iterative method involving linear steps, can be used, especially if this method is used with size optimisation.

¹Note that some adjacent nodes may merge into each other during search for solution

3.2.4 Shape Optimisation

This type of optimisation is similar to size optimisation, in that the initial layout of the structure is known prior to optimisation. In shape optimisation, the objective is to change the boundary of the material by redistributing the material to reduce high levels of stress and improve the performance of the structure. Until relatively recently, applications with regard to architectural form finding or generation, were rarely found while some use was found at smaller scales e.g. optimisation of individual structural member shapes.

Most recently, Philippe Block's research group at ETH Zurich, devised a novel optimisation-based form-finding approach called 'Thrust Network Analysis' (or TNA), to find the 'best fit', compression-only solution to an arbitrary input surface for given network topologies, i.e. form-finding of 3D freeform funicular structures. [55] with promising results. However, this too is an unsuitable method for discretised truss optimisation, which is to be achieved by this thesis.

3.2.5 Material Optimisation

In material optimisation elements are assumed to be composed of layers of fibre-reinforced materials. The objective is to determine the layer thicknesses and fibre orientation in order to maximise stiffness.

Similar to shape optimisation, it is more suitable for optimisation of small-scale individual members rather than truss designs or practical form-generation for architectural usage.

3.2.6 Layout Optimisation

As in the case of size and topology optimisations, definitions of different types of optimisation, under certain circumstances, can overlap each other. For example, in size optimisation, if only positive finite member constraints are included, and these constraints have a lower limit of zero then members are allowed to vanish, and the size optimisation problem can be considered a topology optimisation

problem [85].

Layout optimisation is an example of combinatorial optimisation; the term first appeared in [86], which was later formally defined by Rozvany *et al.* in [85]. This type of optimisation is concerned with simultaneous determination of member cross-sections (i.e. size optimisation), nodal coordinates (i.e. geometry optimisation) and topology.

With regard to combinatorial optimisation, the terms ‘*layout optimisation*’ and ‘*topology optimisation*’ may be used without distinction if the problem consists of a sufficiently dense grid of elements in the initial ground structure, such that selection of nodes ‘simulates’ determination of nodal coordinates. On the other hand, if the grid is not sufficiently dense, then the topology and geometry are solved iteratively [87]. This iterative form of combinatorial optimisation tends to be highly non-linear¹.

Ground Structures

Michell type structures [70] are effectively continuum structures, with truss-like micro-structures that, in the limit, typically comprise an infinite number of infinitesimal members. This prohibits the application of Michell’s approach to practical structural design, although it gives rigorous benchmarks of optimality for a number of classic problems. An additional problem with the Michell approach is that only a very small class of problems have ever been shown to be tractable by this approach [88].

Consequently, efforts were made to resolve these issues through an approximate formulation of discretisation or use of *ground structure* [79] [89]. The ground structure comprises a grid of nodes, with some initial inter-connectivity by truss members which are candidates for inclusion in the final, “optimal” design. The denser the grid, and the more complete the initial inter-connectivity, the closer the optimal form may approach the ideal optimum for the problem at hand.

¹thus, computationally costly and it may converge toward local optima

3.2 Types of Structural Optimisation

Equally however, a denser grid and high initial connectivity greatly increases the computational effort required to identify the optimal form. See Fig. 3.7 for a basic ground structure.

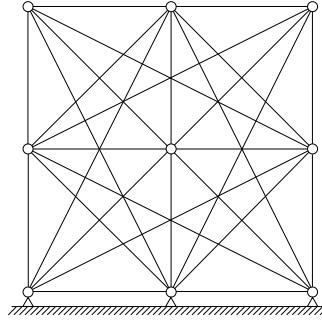


Figure 3.7: Ground structure

The relationship between the number of all potential members m and the total number of nodes n , is expressed as:

$$m = n(n - 1)/2 \quad (3.4)$$

It is note-worthy that variables representing the cross-sectional areas of members can take zero values¹. This can be problematic as members of insignificant, near-zero values, which carry near-zero load, can exist in the final solution.

It is possible that no *unique* optimal form exists for a given problem; several different forms may exist that satisfy all the constraints of the problem and have equal structural volume but different topologies [90]. The ground structure approach produces approximations of analytical optimum solutions of Michell's theoretical optimum as the ground structure is a finite set of potential members and unable to accommodate curved members.

The more dense the ground structure (thus the number of variables), the more computationally expensive the search for an optimum solution while this implies the more accurate approximation to the true optima. The high number of

¹c.f. size optimisation formulations

3.2 Types of Structural Optimisation

problem variables associated with this approach is a major drawback. It is also observed that there is lack of justification for removal of (and/or prohibition of reintroduction of) arbitrarily chosen members in certain ‘ground structure’ approaches, and that there is lack of rigorous method of introducing new members and nodes during optimisation [90].

As a remedy to this problem, *Adaptive Member Adding* approach or AMA [91] has been formulated. Unlike the ground structure with full connectivity such as the one shown in Fig. 3.7, the AMA approach employs a *reduced ground structure* with only adjacent connectivity. During the optimisation process, new members are then introduced to this initial structure according to the pre-set criteria in subsequent iterations. This formulation changes the nonlinear relationship between m and n in Eqn. 3.4 and greatly reduce the number of initial variables.

Optimisation with Elastic theory

Methods based on elastic theory and those based on plastic theory were developed separately. Currently, analysis methods using the plastic theory are less prevalent as those using elastic theory, with the exception of recent development of optimisation methods which combine elastic and plastic constraints [92].

For the past few decades, the research in structural optimisation has been focused on elastic design and plastic methods are not common in design practices¹. Optimisation with elastic theory enables (nonlinear) problems to include such parameters as nodal stability [93], and Euler buckling [94].

However, the basic assumption of elastic theory, that a structure behaves in an elastic manner and fails at the critical stress of materials, is only valid regarding statically determinate structures or structures in brittle materials. In other words, in majority of cases, this assumption fails to be valid as stress redistribution allows the structure to withstand beyond the assumed elastic failure i.e.

¹partly due to the versatility of FEA based methods.

3.2 Types of Structural Optimisation

they fail when a sufficient number of ‘plastic hinges’ are formed [95].

Additionally, elastic structure optimisation is generally more complex than plastic structure optimisation [96], as the elastic relationship between specific stiffness and mass, and between bending and torsion, are highly nonlinear and complex. The high computational expense of non-linear methods and lack of certainty in reaching the global optimum due to non-convexity, also contribute to impracticality, especially in large scale or three dimensions.

Optimisation with Plastic Theory

Michell in his paper in 1904 [70] first established a set of optimality criteria for framework structures. Although this set of optimality criteria preceded the development of plastic analysis theory, Michell’s theory is effectively based on plastic design theory.

Many techniques employing the plastic theory was carried out by Prager [97] and Shield, establishing ‘Prager-Shield’ optimality criteria [98].

Later Dorn and Hemp researched plastic stress constraint layout optimisation problems [79] [99]. Hemp also extended the formulation to include member self-weight and multiple load cases, establishing optimality criteria, known as ‘Hemp optimality criteria’.

The basic truss optimisation algorithm, formulated as a linear programming problem, using the plastic design theory and ground structure approach is relatively simple [99]. Rozvany [85] distinguished two different approaches; *practical engineering approach* i.e. the force equilibrium or lower-bound formulation and *mathematical approach* i.e. the work or upper-bound formulation.

Although the problem formulation, which combines linear programming with plastic layout optimisation, may appear simplistic because it does not allow more realistic highly non-linear efforts (e.g. buckling) to be considered, one advantage is the possibility of inclusion of multiple load cases [88].

3.3 Types of Solution Methodologies

3.3.1 Mathematical Programming: Linear and Nonlinear Programming

This is one of the oldest forms of optimisation [100]. An optimisation problem is said to be a *linear program* if the objective and constraint functions (or $f(x)$ and $g_j(x)$) are linear. In other words if the following is satisfied:

$$g_j(\alpha x + \beta y) = \alpha g_j(x) + \beta g_j(y) \quad (3.5)$$

$$x, y \in \mathbf{R}^n \text{ and } \alpha, \beta \in \mathbf{R} \quad (3.6)$$

If the optimisation problem satisfies the following inequality:

$$g_j(\alpha x + \beta y) \leq \alpha g_j(x) + \beta g_j(y) \quad (3.7)$$

$$x, y \in \mathbf{R}^n \text{ and } \alpha, \beta \in \mathbf{R} \quad (3.8)$$

$$\alpha + \beta = 1 \quad (3.9)$$

$$\alpha \geq 0, \beta \geq 0 \quad (3.10)$$

then the objective and constraint functions are said to be *convex* and the optimisation problem is also said to be a *convex optimisation* problem [71]. Thus, convexity is more general than linearity i.e. any linear program is a convex problem. This point is illustrated in Fig. 3.8¹ Classical optimisation methods can be categorised into two types, according to their search strategies: *direct search* and *gradient-based* methods [101]. The direct search methods employ only the objective function and constraint values in the search process i.e. lack of gradient [102]. These methods require a number of evaluations of the function before obtaining a solution, making the search process relatively slow. However, one advantage of direct search methods is that generalisation is straightforward and thus its application to other classes of problems is possible with minor modification, due to lack of function derivatives.

¹On the other hand nonlinear program may either be a convex or non-convex problem with no certainty of the solution being the global optimum.

3.3 Types of Solution Methodologies

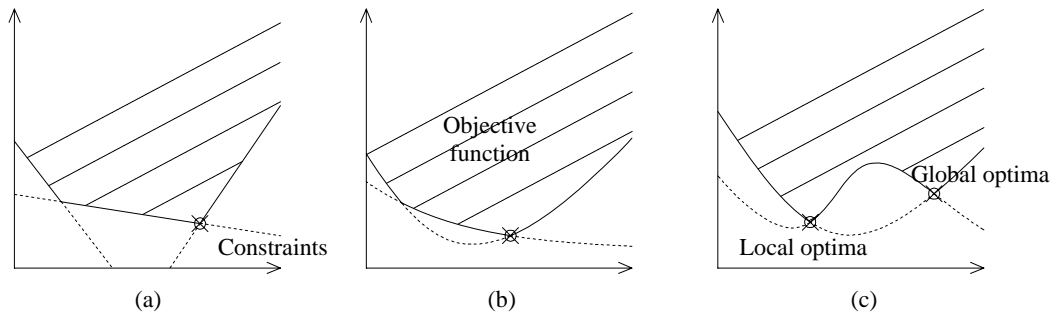


Figure 3.8: Different types of optimisation constraints: (a) Linear, (b) Convex non-linear (c) Non-convex, non-linear.

In contrast, the gradient-based methods [102], employ at least the first-order derivatives and in some cases, also second-order derivatives of the objective function and/or constraints in the search process. The obvious advantage of gradient-based methods is their tendency for quick convergence toward a solution while the disadvantage is the difficulty of applicability for discontinuous problems or the problems where derivatives are not available. The two different groups of methods also share disadvantages. Firstly, the convergence towards an optimal solution depends on the initial solution. The algorithms for most traditional methods tend to converge to local optima in the case of non-convex problems. In addition, the algorithms tend to be problem-specific¹ and most of these algorithms are not efficient for discrete variable problems.

In practice, direct search methods are more widely used. However, constraints are sometimes approximated to linear expressions because the nonlinearity of constraints may result in higher complexity and poor convergence and, in the case of non-convexity, the final solution may be a local optimum.

¹i.e. an efficient algorithm for one type of problem may not have the same level of efficiency in solving a different type of problem.

Linear Plastic Optimisation

Considering a structure containing m members and n nodes and subject to a single load case, the linear programming formulation of the plastic equilibrium approach to truss optimisation can be described as follows:

$$\text{Minimise } \mathbf{V} = \mathbf{l}^T \mathbf{a} \qquad \text{objective function} \qquad (3.11)$$

$$\text{subject to: } \mathbf{B}\mathbf{q} = \mathbf{f} \qquad \text{equilibrium constraint} \qquad (3.12)$$

$$-\sigma_i^- a_i \leq q_i \leq +\sigma_i^+ a_i \qquad \text{stress constraint} \qquad (3.13)$$

$$a_i \geq 0 \qquad \text{area constraint} \qquad (3.14)$$

$$\text{for} \qquad i = 1, \dots, m \qquad (3.15)$$

where \mathbf{V} is the total volume of the structure, \mathbf{l} is a vector of individual member lengths (l_i is the length of member i), \mathbf{a} is a vector of member cross-sectional area (a_i is the area of member i), \mathbf{B} is the direction matrix of members, \mathbf{q} is a vector of internal member forces (q_i is the force in member i), \mathbf{f} is a vector of externally applied nodal forces and finally, σ_i^+ , σ_i^- are the tensile and compressive stresses in member i , respectively.

In this case, the LP problem variables are the internal member forces. These equations are called '*lower-bound*' or '*primal*' formulation, in other words, minimisation. Following is the work formulation, where the virtual work is maximised:

$$\text{Maximise } \mathbf{W} = \mathbf{f}^T \mathbf{u} \qquad \text{objective function} \qquad (3.16)$$

$$\text{subject to: } \mathbf{B}^T \mathbf{u} \leq \mathbf{c} \qquad \text{strain (or compatibility) constraint} \qquad (3.17)$$

$$(3.18)$$

where \mathbf{W} is the total virtual work dissipated by the specified loads, \mathbf{u} is a vector of virtual nodal displacements, which are small, and $\mathbf{c} = \{l_1/\sigma_1^+, -l_1/\sigma_1^-, l_2/\sigma_2^+, -l_2/\sigma_2^-, \dots, l_i/\sigma_i^+, -l_i/\sigma_i^-\}^T$.

3.3 Types of Solution Methodologies

This formulation has the virtual displacements of nodes as its variables. As it is concerned with maximisation of external work, it is called the ‘*upper-bound*’ or ‘*dual*’ formulation. The optimum solutions to both formulations for the same problem, should be the same. This is known as *duality* and is a useful tool in optimisation as problems may be expressed in one form and duality allows an alternative formulation to be found. This permits different sets of data to be determined from one problem (e.g. in this case member forces in the primal and virtual displacements in the dual). Modern LP solvers are capable of simultaneously solving both problems, even if only one formulation has been supplied.

3.3.2 Homogenisation

Homogenisation is a technique in structural optimisation, which originated as a computational analysis tool for analysis of composite materials [103]. In homogenisation, variables relating to the highly heterogeneous parent media are replaced by those of an equivalent, but simplified material model and, the unit ‘cell’ of this new material is analysed in order to determine its properties before the entire structure is examined and the boundary value problem is solved [104]

Bensøe and Kikuchi [105] made use of the FEA based homogenisation method for structural optimisation. Instead of material inclusions in the matrix, the design domain is assumed to comprise of a medium containing a large number of voids [106]. The material properties of each cell are changed by variation of the void dimensions and element orientation. Consequently, elements can then be categorised as being ‘solid’, ‘empty’ or ‘porous’, depending on the size of the void. The optimisation problem becomes a matter of determination of the best material distribution in order to achieve the optimal value of the objective function. Hence, this type of optimisation can be seen as a size optimisation, which can be solved using any (nonlinear) mathematical programming technique. However, as the discretisation of the design domain has a major influence in the proximity of the solution to the absolute optimum, it is desirable to provide a fine grid of elements in the initial problem formulation. With the increased degree of discretisation, mathematical programming methods become computationally

3.3 Types of Solution Methodologies

expensive as a result. In many practical cases, the homogenisation method is used in conjunction with optimality criteria solution methods due to the high computational cost and the need for repeated calculations of the objective and constraint functions.

Solid Isotropic Micro-structure with Penalisation (SIMP)

SIMP is a type of homogenisation and a FEA-based numerical method used in topology optimisation [107]. In SIMP, the design domain is discretised into a set of ground elements. The element thickness to be optimised determines the design, where 0 thickness denotes absence of material, and 1, solid material and the majority of the thicknesses of the elements will be between these two values, resulting in ‘grey’ elements. Such elements are penalised according to a power law proposed in [108], or $\rho = s^{1/p}$ where s is the normalised stiffness and p is a tuning parameter, this penalisation reduces the number of grey elements in each iteration to determine clearer designs, using 0 and 1 thickness.

3.3.3 Evolutionary Structural Optimisation

Evolutionary Structural Optimisation (or ESO) is a heuristic method developed in the 1990s [109], concurrently with homogenisation. It has been used in engineering practice where combinatorial optimisations were sought; e.g. shape and topology optimisations [110], size and topology optimisation [111].

This method seeks to remove material that retains a Von Mises stress below a certain ‘cut-off’ ratio, re-analyse and repeat until a steady state is achieved. Following this, the cut-off level is increased by a set value and the iteration is repeated. With removal of elements, the corresponding number of iterations required to reach a steady state decreases and steps are quickened. The number of iterations required in each step and the number of steps required to reach the optimum, depends on the problems.

One advantage of this approach is that Finite Element Analysis (or FEA) software can be used and it only requires addition of element rejection criteria for

3.3 Types of Solution Methodologies

optimisation. The disadvantages of ESO is that the stresses within the constituent elements may change as a result of members being removed from the structure. In some cases this means the previously removed elements will require reintroduction as to obtain an optimum solution. However, in the primary ESO, this is not possible, leading to higher compliance values than the optimum i.e. non-optimum. Bi-directional ESO (or BESO) [112] improves this as the issue of re-introduction of elements is resolved such that the optimisation needs to be started with a minimum amount of material within the design domain i.e. that needs to carry the applied loads directly to the supports. Optimum topologies ‘grow’ toward the optimum rather than revealing themselves from within an artificially oversized initial design domain. The FE analysis stage thus is shorter and a more realistic optimum solution can be found, although BESO can still provide non-optimal solutions [113].

3.3.4 Genetic Algorithms

The term, Genetic Algorithms (or GA) describes a group of methods, a special class of evolutionary algorithms, for optimisation of complex problems [114]. GAs are stochastic optimisation algorithms and, have been employed in many structural optimisation applications for both discrete and continuous problems [115]. Techniques follow the evolutionary principle of ‘survival of the fittest’ i.e. once the initial population is created, it evolves over a number of generations, individuals’ characteristics, advantageous for survival and breeding pass on to the following generations. Thus, in GA, the operations mimic the principles of survival in evolutionary biology e.g. fitness function for defining efficacy of a solution regarding the objective, crossover for gathering best genes and mutation for preventing premature termination [116]

Initially, in a process called *initialisation*, a population of strings, representing solutions to a specified problem, are generated and ranked according to their closeness to termination condition. Then, reproduction occurs where new populations

3.3 Types of Solution Methodologies

are created by *selection* of the *fittest*¹ strings and through genetic operations such as *crossover* or *mutation*², to produce new strings. The reproduced population should be closer to the optimum solution than the previous one.³ This process is then repeated until solutions are reached.

Like many other stochastic methods, GAs can be used to solve problems with both discrete and continuous domain because GAs use *encodings* of the design variables (cf. variables themselves) and, where the objective function or the constraints lack regularity. GAs does not require the derivatives of objective function.

In comparison to the standard deterministic methods, GAs produce populations of solutions as opposed to a single solution, which does not eliminate but reduces the risk of local optima. and problems with multiple objectives can be solved [118]. The known disadvantages of GAs include; first, their high computational cost renders it unlikely to be practical in optimisation of realistic structural design with the currently available computational capabilities [119], and second, in non-specific problems, an optimum structure is not guaranteed [120].

3.3.5 Dynamic Programming

DP refers to a class of algorithms based on simplification of complex problems into incremental steps of subproblems [121]. It is a strategy suitable for optimisation of multistage decision problems [122] or serial structures⁴ in structural optimisation.

In DP, optimal solutions for individual subproblems can be known at any given stage. When applicable, this condition can be extended incrementally, without altering previous optimal solutions to subproblems. The solution to the initial

¹According to Schema theory [117], in order to ensure ‘population diversity’, less fit strings are sometimes allowed to remain

²This introduces random dataset to prevent idling.

³exceptions exist

⁴the output of one stage is the input of the successive stage

problem is achieved when the condition applies to all of data and nothing remains untreated [122]. DP is useful where the decision sequence is long, and the number of decisions to be considered is large. Some structural optimisation problems can be solved by this approach. However, it should be noted that whether plastic or elastic design, usually only statically determinate structures can be formulated as serial structures. Although for some applications, analytical solutions are possible, in general the solution must be found numerically, leading to high computation time and storage requirements due to what is known as ‘curse of dimensionality’. Hence, conventional DP cannot be used to obtain practical solutions numerically.

3.3.6 Simulated Annealing and Particle Swarm Optimisation

Simulated Annealing (or SA) is a type of optimisation, analogous with annealing process¹ of metal. SA was first introduced by Kirkpatrick [60] and developed into a shape generation method by Cagan and Mitchell [61]. This method was developed in the 1950s [60]. It is a stochastic optimisation procedure, which seeks global optimum solutions by starting with randomised initial solutions. It is suitable for use in all types of optimisation problem including structural topology optimisation. The solution strategy can avoid convergence to local optima by allowing random increase or decrease in values of the variables in each iteration. Consequently, this characteristic makes the procedure slow, especially when restarting from a previous solution [123].

PSO is a similar type of optimisation more efficient than SA, and it can avoid local optima [124]. However, compared to LP, its efficiency is limited in terms of the manageable number of variables.

¹A process for metal to cool into a minimum energy structure.

3.3.7 Tabu Search and Ant Colony Optimisation

Tabu Search refers to a local search technique of heuristic optimisation developed by Glover [125] with the ability to eliminate local minima in nonlinear optimisation problems in search of a global optimum. It typically consists of dynamically generated constraints or *tabus* to guide the search towards an optimum solution, an evaluation function (through the use of memory structures) to determine whether the solution could be improved by a small change in variables at each iteration. It uses a local search procedure to move from one solution to another. It alters the local structure of each solution throughout the search procedure and, each move and the effect it has upon the solution, is stored in tabu list. When the moves result in a more optimal solution, a certain termination condition is satisfied. Regarding truss optimisation, nonlinear, Tabu Search based methods capable of considering multiple load cases, stress, displacement and buckling constraints and multiple objective functions, have been presented [126] [127].

Ant Colony Optimisation is a heuristic optimisation algorithm with a stochastic search procedure that incorporates positive feedback of accumulated information and avoids local optima, developed first by Marco Dorigo [128]. There is a method that combines Ant Colony Optimisation and Tabu Search for truss optimisation [129]. The combined algorithm is used to minimise the weight of a space truss. Though it presents an optimal design the method carries a high computational cost.

3.4 Chapter Conclusion

In search of the most suitable choice of optimisation, various optimal solution search methods and types of optimisation have been reviewed in the previous sections of this chapter. This section provides justification (with comparisons) for the particular choice of the method to be employed for the stated aims and objectives of this thesis.

3.4.1 Justification for Use of Linear Programming: linear vs non-linear approaches

There is a compromise to be made in the choice of structural optimisation approaches, between highly efficient linear approaches, which require some degree of simplification of the problem to retain the linearity, and non-linear methods which are computationally expensive, but which can in principle address non-linear behaviour such as strut buckling. The choice is one of philosophy and practicality; whether to accept the simplification required to enable us to solve large problems, and use a post-optimisation rationalisation of the solution to produce a real design, or to include more realistic problem definitions, but then accept a limitation on the scale of the problem that can be addressed, and to have no certainty that the resulting solution is globally optimal.

In this work, it was decided to use a basically linear approach, primarily because of the certainty of being able to establish globally optimal results albeit for simplified problems, and partly due to the availability at University of Sheffield of world-leading linear programming optimisation software.

3.4.2 Justification for Use of Layout Truss Optimisation

The optimisation method of choice for use in this thesis is layout optimisation; a method which simultaneously optimises member lengths, nodal locations, member cross-sections and members' spatial arrangement i.e. simultaneous size, geometry and topology optimisation, suitable for truss optimisation problems. It

should be noted that shape optimisation and material optimisation are most suitable for optimisation of small-scale individual members or continuous surface structures such as continuous shells, rather than truss designs or practical form-structure generation for large span surface definition, which this thesis aims to achieve.

In addition to the advantage of being able to optimise several aspects of structural members simultaneously, truss optimisation historically has had strong links with linear optimisation techniques, which are, as explained throughout this chapter, computationally very efficient in their search for optimum solution, compared to other search techniques and without the risk of local optima (commonly experienced by nonlinear techniques). Further more trusses find their applications in many large scale and long span roofs and they make an ideal and efficient mode of supporting predefined surface or freeform as well as structural aesthetics, sought after in this thesis.

3.4.3 Limitations of LP plastic layout optimisation

The following subsections introduce common practical issues and limitations of plastic layout optimisation in application in structural engineering and prospects of application as a form-generation method.

Nodal Stability and Euler Buckling

A frequently encountered problem in structural optimisation is that of stability of the optimal form. Stability issues fall into two main areas; member stability (Euler buckling) and overall stability of the structure. A particular form of the latter, overall stability problem can arise where the ground structure comprises pin-jointed nodes. Here, that the optimal ‘structure’ may actually be in unstable equilibrium, and become a mechanism if it is only slightly perturbed. A simple example of this is shown in Fig. 3.9 [130]. This highlights one of the drawbacks of simple optimisation approaches; the algorithm is only as sophisticated as the rules incorporated in it. So, whilst a human engineer would immediately recognise that

the ‘structure’ in Fig. 3.9 is unstable (and therefore not actually a structure at all, but a mechanism) the optimisation algorithm cannot ‘recognise’ this unless it is specifically instructed to do so.

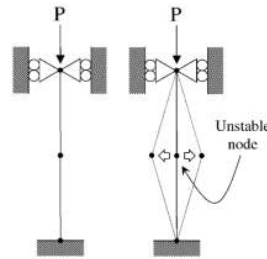


Figure 3.9: Instability of a node within a compression chain, after [130].

Both Euler buckling and overall stability are strictly non-linear problems, the former because the critical buckling stress is a function of the magnitude of the compression force in a member rather than a constant as required for linearity, the latter because overall elastic stiffness of the structure is key in assessing overall stability. This has led to a vigorous area of research in developing non-linear optimisation strategies (e.g. [131] [132] [133]). However, Tyas *et. al.* [130] demonstrated that these issues could be incorporated into an LP approach, using lateral disturbing forces to obviate unstable nodes and iteratively changing allowable compression stresses if Euler buckling were shown to be a problem. Whilst the iterative nature of the analysis meant that the resulting structures could not be proven to be globally optimal, it was shown in [130] that a structurally stable solution could be found that was significantly more efficient than the best form found by non-linear optimisation approaches for a benchmark problem. This suggests that a pragmatic LP approach that uses simplified linear approximations to essentially non-linear phenomena may be a better strategy than an approach that seeks to more correctly model the non-linearity of the problem.

Control Issues and Mixed Integer Linear Programming

In structural engineering, the overcomplexity¹ of optimised structures is a well-known problem [134] and there are a significant number of solution strategies for filtering or standardising the originally optimised forms. The most common approach to achieve this, is to standardise the member cross sections by choosing from a pre-defined set of tabulated data. In particular, an iterative LP method was used [135], in which the problem was defined in terms of existing available steel sections. At each iteration, the stress level in each compression member in the solution is checked against the permissible level of stress as recommended by the design code; if any stress exceeds its permissible level, another value is used for the stress in the member and the iteration continues. When the same section type is chosen for all members in two successive iterations, the search process terminates.

While successfully achieving a degree of realism, the most notable disadvantage of this particular method is that the use of discrete members and cross-reference at each iteration leads to inefficiency, rendering it unlikely to manage the high number of variables in design of realistic structures. Not only is it inefficient but also, in relation to conceptual form-generation, this degree of realism, is less than useful as form-generation concerns user controllability over the *general form* of the structure not *individual member sections*.

Another viable option of control could involve the process of initial optimisation and post-adjustment of arrangement of structural elements. However, this must be also followed by re-optimisation or analysis, as the adjusted arrangement of structural members in the initial solution may no longer be structurally sound. The issue of control still remains to be resolved.

This could be resolved with incorporation of an additional constraint function into the existing LP formulation, which would give the user an additional input variable. The obvious disadvantage of this is however, that the increased number

¹i.e. a high number of nodes and members.

of additional constraints may lead to high computational cost. On the other hand, because it concerns simplification of entire form MILP would, in this case be more suitable.

3.4.4 Concluding remarks

After the discussion on the suitability of a particular choice of optimisation method and its solution search technique, general discussion on the suitability of use of optimisation in the context of architectural form-generation would be appropriate.

The term, *structural optimisation* in a classical sense is associated with either *weight minimisation* or *virtual work maximisation* toward mathematical or numerical optima e.g. minimum numerical value that represents weight. This can be classified as ‘theoretical optimisation’. However, the class of structural optimisation to be employed toward the aims of this thesis, should be distinguished from purely theoretical optimisation as it considers practical issues such as joint costs, design (or solution) run-time, nodal stability and final output control issues (see 3.4.3); hence it is *practical optimisation*.

Unlike theoretical optimisation which presumes no limitation on the performance characteristics, the aim of (any) practical optimisation approach is to achieve *restrained* economy, which can be interpreted by designers, as construction cost minimisation, minimisation of materials, or minimisation of resources, or maximisation of the limited resources for given tasks, coordinated and compromised between different aspects of design, other than structures.

It must be noted, however, concerning form-generation, optimisation and aesthetics of the generated form, terms such as ‘structural efficiency’, ‘structural economy’ and ‘true optimum’ bear minor significance as the outcome of ‘form’ cannot be measured against set numerical values but designers’ subjective judgment of its aesthetic criteria. Thus, in conceptual design practice, the practicality of the optimised structures should be measured in terms of its ability to ‘guide’

3.4 Chapter Conclusion

the form design process. In this regard, the proposed method is deemed appropriate as it considers physical reality and provides a sound structural basis for form at a conceptual stage whilst allowing flexibility for inevitable later changes without premature imposition of detailed design of individual members.

Chapter 4

Tensegrity

4.1 Introduction

“There is a common belief among researchers (and others) - and a belief is all it is, as I have never seen it substantiated - that “tensegrity” structures are lightweight. This is often an argument presented in support of their intended application. In fact, I have seen papers where this claim is made, in conflict with the actual results presented. This is a misconception!” - Ariel Hanaor [136].

Since their beginning as sculptural pieces [137] [138], tensegrity structures have intrigued, both architects and engineers for over half a century. In its very essence, there is a structural principle, which makes this structure able to stand up with a high degree of rigidity. Indeed this structural principle, has engendered research in various fields including, various branches of engineering, robotics, art, architecture, biology and medicine [139] [140].

The discovery began in a period prior to proliferation of computational technology; with the primary emphasis on structural engineering and art/architecture, the two disciplines separately conducted research and developed into various expressions of the same principle. Following this period of preliminary inquiry, great efforts have been made recently to provide feasible form-finding/ form-generation

tools¹ for tensegrity, which would enable tensegrity structures to be computationally configured for physical construction. However, available design tools for automatic *topological configuration* of internal members within a tensegrity are scarce, and perhaps due to this fact (and others), our precise understanding of tensegrity structures and their behaviour, is still to be established [136].

This chapter reviews the history of tensegrity since its ‘invention’, various classifications, and its different definitions. It also introduces different existing techniques for form-finding of tensegrity and finally critically reviews selected existing methods for automatic design or topological configuration for tensegrity structures, highlighting a niche for a novel method for such design, which would help establish a better understanding of tensegrity as a structural principle.

4.2 ‘Invention’ of Tensegrity

Though the word ‘*tensegrity*’ - a contraction of ‘tensile-integrity’ was coined by a polymath, Buckminster Fuller [141], there has been contestation regarding this discovery or ‘invention’ of tensegrity systems, and it is difficult to attribute to any one person.

Despite the discrepancies and omissions amongst authors, claims for the original discovery of tensegrity-principled structures usually involve the following four as far as documented graphic evidences are concerned: Karl Ioganson, Buckminster Fuller, Kenneth Snelson and David G. Emmerich.

It is also interesting to note that Maxwell was also aware of structures, very similar to tensegrity when devising the famous ‘Maxwell’s Rule’. Talking about exceptions to his rule: *“In those cases where stiffness can be produced with a smaller number of lines, certain conditions must be fulfilled, rendering the case one of a maximum or minimum value of one or more of its lines. The stiffness of the frame is of an inferior order, as a small disturbing force may produce a*

¹See Section 4.6.

displacement infinite in comparison with itself”. [69] as in [142].

Thorough examinations of photographs of Karl Ioganson’s sculptural exhibits in Moscow in 1920-21, by Gough, reveal that there was a sculptural object, which appears very similar to a tensegrity prism [137]. Unfortunately the sculptures themselves were destroyed and have had to be reconstructed. Marks [143] attributes it to Fuller’s 4D House, which first appeared in 1928, as its structural design tentatively adheres to a tensegrity principle of separation between tension and compression. However, the formalisation of the constructional principles of tensegrity and the term itself come much later in the form of a patent, submitted in 1959 and published in 1962. There is no mention or evidence to suggest that this is in any way conceptually related to the 4D House.

On Snelson’s own website ¹, he explains the influence of “*Russian Constructivists*” and “*the larger world of geometrical art*”, prior to his encounter with Fuller, though neither Karl Ioganson nor his sculpture is specifically mentioned. It is now a familiar story that in 1948, Snelson as student and Fuller as substitute professor had an encounter at Black Mountain College in North Carolina. The following year Snelson constructed his X-Piece sculpture [138], which in its structural principle was a tensegrity structure. This was then borrowed by Fuller and presumably influenced Fuller’s later formalisation of its principle for his patents. Independently, Emmerich was exploring ‘structures tendues et autotendantes’ (tensile and self-tensioned structures), which were of tensegrity principles, and the patent he submitted to the Institut National de la Propriete Industrielle in 1959 shows of these structures [144] as in [145].

Emmerich cites a structure by Ioganson as a precedent to his own work [146]. The following paragraph by Emmerich has been pointed out by Burkhardt [147]:

“Cette curieuse structure, assemblée de trois barres et de sept tirants, était manipulable à l’aide d’un huitième tirant detendu, l’ensemble étant déformable. Cette

¹<http://www.kennethsnelson.net/icons/bio.htm>

configuration labile est très proche de la protoforme autotendante à trois barres et neuf tirants de notre invention.”, which translates to:

“This curious structure, assembly of three bars and seven ties, was easy to handle using an eighth slackened tie, the unit being deformable. This unstable configuration is very close to the self-tensioning of proto-form with three bars and nine ties of our invention.”

In this, Burkhardt wrongly states the original text “*apparently means*” Emmerich does not recognise Ioganson’s invention of the tensegrity prism. However, this text clearly shows Emmerich did recognise the acute similarity between the two concerned models. Fig. 10 on page 104 of the paper by Gough [137] shows three structures, one of which is recognisably the same as a typical tensegrity prism.

It is worth pointing out that the three, Emmerich, Fuller and Snelson made individual patent claims on various aspects of the principles. The efforts were varied. Fuller’s interest was in line with his lifelong mission of improvement of ‘humanity’s conditions’; in this case, concerning himself with adaptation of this structural principle for the construction of spherical structures for potential uses in housing solutions. It is also possible that he saw tensegrity as an extension of his work on geodesic domes, which for him meant structural optimality. Emmerich had less emphasis on its application than the tensegrity principles and geometric characteristics. Snelson, on the other hand was a purist as he preferred to view tensegrity structures as a use-absent sculptures with structural beauty [138].

In fact, however independent their efforts were, their patents were concerned with the same structural principle of self-stress and tension-compression separation. This inchoate period of development is characterised by physical modelling and experiments by trial and error.

4.3 Definitions

It must be noted that systematic research in tensegrity are on-going and the definitions of tensegrity structures vary from researcher to researcher. Presented in this section is a summary of the various definitions of tensegrity.

Fuller is credited with the portmanteau word, tensegrity by contraction of ‘tensile’ (or tensional) ‘integrity’, which is stated here:

“Tensegrity describes a structural relationship principle in which structural shape is guaranteed by the finitely closed, comprehensively continuous, tensional behaviors of the system and not by the discontinuous and exclusively local compressional member behaviors. Tensegrity provides the ability to yield increasingly without ultimately breaking or coming asunder.” [148]

In the same book, he also claims that tensegrity is inherently an ‘efficient structural system’.

Emmerich on the other hand failed to give this ‘curious’ structural principle any new name as he simply described it ‘tensile and self-tensioned structures’.

Snelson, being a former-student of Fuller, seems to have tried to differentiate his work from Fuller’s [138] by coining deliberately a different term, to describe the same structural principle by calling it a “*continuous tension, discontinuous compression structure*”, which he defined as, “a structural framework whose constituent members are separately placed either in tension or in compression, in which compression members are separated from each other and the tension members are interconnected to form a continuous tension network.” [149]

In his comprehensive book [145], Motro amalgamates and formalises the above three definitions as follows:

“Tensegrity systems are spatial reticulate systems in a state of self-stress. All their elements have a straight middle fibre and are of equivalent size. Tensioned elements have no rigidity in compression and constitute a continuous set. Compressed elements constitute a discontinuous set. Each node receives one and only compressed element.” He calls this version the *“Patent Definition”* as it is derived collectively from the three patents.

The essential conditions in this definition are:

1. No bending elements i.e. separate compression and tension elements
2. Discontinuous compression with one compression member at a node at most and continuous tension members
3. Self-stress provides rigidity for kinematically indeterminate systems and strength for determinate systems
4. Closed and self-supporting system

Pugh on the other hand, gives a different definition yet:

“A tensegrity system is established when a set of discontinuous compression components interacts with a set of continuous tensile components to define a stable volume in space.” [150].

It is worth noting that this definition does not adhere to the first three in that the second and fourth conditions in the previous definition have been eliminated, i.e. more than one compression member meet at a node and/or i.e. external supports can be provided. Motro takes this definition further by calling it *“Extended Definition”*, of which his own version reads:

“A tensegrity system is a system in a stable self-equilibrated state compressing a discontinuous set of compressed components inside a continuum of tensioned components.” [145]

Note the difference between discontinuous compression element or member and ‘a discontinuous set of compression members’.

Now, compare these i.e. both of Motro’s ‘Patent’ and ‘Extended’ definitions, to those of Skelton *et al.*, which classify tensegrity structures into two distinct classes according to only the maximum number of compression members at a node i.e. Class 1 and Class 2 tensegrity systems [151].

“A given configuration of a structure is in a stable equilibrium if, in the absence of external forces, an arbitrarily small initial deformation returns to the given configuration. A tensegrity structure is a stable system of axially loaded-members. A stable structure is said to be a “Class 1 tensegrity structure if the members in tension form a continuous network, and the members in compression form a discontinuous set of members. A stable structure is said to be a “Class 2 tensegrity structure if the members in tension form a continuous set of members, and there are at most two members in compression connected to each node. [151]

Note also that there is no mention of ‘closed continuum’ of tension members, self-supporting ability or presence/absence of external supports. Skelton *et al.* also gave a definition to another distinct class of tensegrity structures as “Class 1 Tensegrity Shell”. These are presented below [151]:

“Class 1 Tensegrity Shell is a 3-dimensional structure in which there exists a set of tensions in all tendons such that the structure is in a stable equilibrium. See Fig. 4.1 It is essentially a ‘tensegrity grid’ as designed by Motro *et al.* In

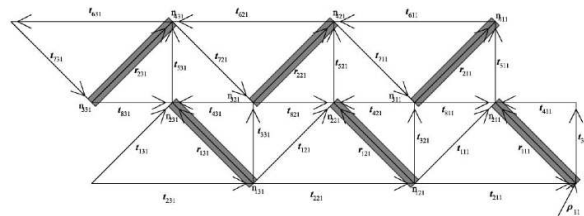


Figure 4.1: Class 1 shell tensegrity, after [151]

4.4 Recent Development in Tensegrity Research in Engineering

summary, most of these definitions coincide and centre around; absence of bending from absolute separation between compression and tension members, varying degrees of separation between each of compression members, and pre/self-stressed equilibrium.

4.4 Recent Development in Tensegrity Research in Engineering

Since the early days of discovery of tensegrity, researchers have carried out extensive analyses of various classes of tensegrity structures in various aspects. In the realm of mathematical and empirical analyses of tensegrity (studying its structural behaviours), Pugh and Kenner presented a practical manual for building tensegrity structures with help of mathematical expressions [150] [152]. Roth and Whiteley [153] established mathematical definitions of rigidity and flexibility for tensegrity frameworks. One crucial aspect of tensegrity, prestress, was extensively defined in varying degrees in [154].

Static and dynamic analyses of tensegrity structures, were covered by Murakami [155]. Tensegrity as part of a general analysis of prestressed mechanisms has been treated by Pellegrino [156].

There have also been developments in modelling methods for tensegrity. For example, a method for modelling and controlling of tensegrity structures [157] was developed using method of constrained particle dynamics, as the basis for the design of a feedback control system which adjusts the lengths of the bars to regulate the shape of the structure with respect to a given equilibrium shape; Nishimura revisited Snelson's cyclic frustum tensegrity modules while considering initial shape-finding and modal analyses of cyclic frustum tensegrity modules; Oppenheim analysed dynamic behaviour of an elastic tensegrity structure and observations of its damping behaviour [158].

A different branch of tensegrity research is application of tensegrity, especially in deployability of tensegrity structures. For example, Sultan and Skelton have proposed a continuous time deployment control strategy for tensegrity structures, based on the existence of an equilibrium manifold [159]; Pinaud [160] presents hardware implementation of a symmetric Class 2 tensegrity structure, analytical geometric reconfiguration and, design and physical construction of tensegrity structures. Research on different classes of tensegrity has also been carried out, e.g. domes [161], tensegrity towers [162] and double layer tensegrity grids [163]

4.5 Classification of Regular Tensegrity

There are three notable researchers regarding typologies of tensegrity; Fuller, Pugh and Motro. Fuller proposed prestressed tensegrity with tensile stress or isometric tension and, geodesic tensegrity with anchorage and triangulation along shortest spherical paths. Pugh [150] provides a series of tensegrity systems, most exclusively of polyhedra; basic 2D and 3D structures are described with the positions of tensile members relative to the centre point of the structure and the complexity of compression members, and the number of layers. He also categorises three basic patterns of tensegrity as diamond, circuit and zig-zag as bases with which to build larger sets of spherical or cylindrical tensegrity structures. Motro's contribution to typologies is the proposal and construction of the double-layer assemblies in single and double curvature.

The following subsections mostly summarises Pugh's [150] and Motro's [145] comprehensive treatment of topological typologies and classification of regular tensegrity structures, inasmuch as it provides visual reference to those not familiar with tensegrity structures.

4.5.1 Spherical Cells

'Spherical cells' as described by Pugh have the following topology; tensile members are mapped on a sphere without intersections between them except the nodes of the system; the tensile members are homeomorphic to a sphere and struts are

4.5 Classification of Regular Tensegrity

contained within the sphere. This category includes ‘diamond-pattern’, ‘circuit cells’, ‘geodesic tensegrity’ and ‘zigzag-pattern’.

The simplest example of ‘diamond-pattern’ tensegrity is a rotated tensegrity prism with a triangular bases called ‘*Simplex*’ 4.2. Tensegrity prisms have n -gonal bases with rotational angles between the top and bottom bases.

Circuit cells can be identified by presence of polygonal circuits of compression

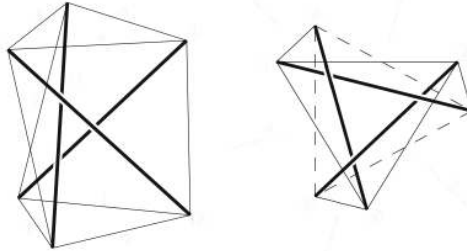


Figure 4.2: Tensegrity:‘Simplex’ configuration in isometric and plan views, after [164]

struts. Circuit cells do not satisfy the ‘patent definition’ as there are two struts at each node. Circuit cells can be derived from tensegrity prisms by completely closing the diamond of cables i.e. the ends of two struts are joined, according to the shortest diagonal of the diamond. Thus, circuit cell tensegrity structures can be a sub-category of Class 2 tensegrity as the strut circuits satisfy Skelton’s definition of Class 2 tensegrity.

Certain regular and semi-regular polyhedra can serve as a geometrical basis to constitute circuit tensegrity systems.

The tensegrity chapter in Fuller’s work, entitled *Synergetics* [148] as well as his patent [165], mostly present geodesic tensegrity dome structures. Configuration of this type of structures relies on the frequency of triangulation of faces (or less commonly, square faces) of the polyhedra which are chosen to generate the dome.

The nodes of the chosen polyhedron are projected onto the circumscribed sphere.

The description of ‘zigzag-tensegrity’ is derived from that of Pugh’s [150]. A ‘Zigzag’-tensegrity is characterised by three non-aligned cables, which ‘zigzag’ between the two ends of each strut. See Fig. 4.3.

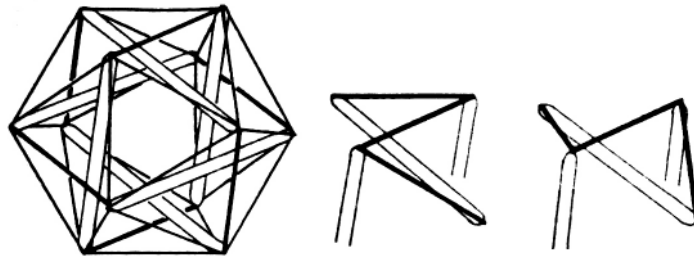


Figure 4.3: Zigzag tensegrity [150].

4.5.2 Star Cell Type

The description of this tensegrity type has been extracted from Motro’s publication [145] on tensegrity as the original publication by Raducanu [166] could not be obtained.

The Star cell type tensegrity structures are derived from the spherical cell type. Raducanu’s designs are extended from four-strut prismatic tensegrity cells. Their diagonals replace upper and/or lower cable squares, without jeopardising equilibrium conditions. Refer to Fig.s 4.4 for the three combinations.

These are structurally stable without one of the requirements of ‘patent definition’ that *three cables are required at each node*. Motro (after Raducanu) [145] makes a slightly controversial claim that tensegrity structures can be constructed with some ‘nodes without struts’. However, this is ‘technical heresy’ because the intermediate nodes between two cables are unnecessary as shown in Fig. 4.24 on p.70 in [145].



Figure 4.4: Three Star cell tensegrity configurations

4.5.3 Assemblies

The previously introduced basic tensegrity types can be arranged into larger assemblies of varying degrees. These arrangements can be subcategorised according to the degree of dimensions of assemblage and/or the degree of dimensions of curvature i.e. 1D single-axis assembly, 2D planar assembly of double-layer of either no curvature, single or double curvature. In general, basic tensegrity types are composed of struts which all share the same length and cables which all share another length. This basic regularity enables them to join into larger systems. In some cases, several lengths of struts and cables may be used. However, ‘topological regularity’ of the basic cells remains unchanged.

4.6 Form-finding and Control of Tensegrity

In (regular) tensegrity systems, *form-finding* is a process of determining the ratio between the uniform length of compression elements, l_s and that of tension elements, l_c in order to ensure rigidity for structural equilibrium. In regular or irregular tensegrity, form-finding is a process of determination of geometrical configuration.

In form-finding of tensegrity, the term ‘*initial state*’ refers to a self-equilibrium state, with unilateral rigidity in the tension members and no ‘*rigidity*’ in com-

pression members ¹. The initial stresses are defined by two parameters: form (i.e. geometry of the members and topology) and force. Shape and geometry are both essential to its structural stability.

Researchers in the field of structural engineering have concentrated their effort on numerical form-finding methods of tensegrity [167] [168] [169], which are essential in designing of tensegrity after defining the structure's topology in order to determine nodal geometries and internal forces. Many of these methods, however, ensure stability provided by self-stress (thus rigidity) but do not propose automatic generation of topologies of tensegric forms.

4.6.1 Experimental Form-finding based on Polyhedral Geometries

Although the term, form-finding is implicitly associated with *numerical* form-finding, The early works by Emmerich, Fuller, Snelson and Pugh *were* form-finding ².

This type of work is primarily concerned with construction of irregular tensegrity structures or regular polyhedra, where structural stability of tensegrity is achieved by heuristic methods based on experimentation. Hence, a general case of mechanical or structural characteristics cannot be derived despite being systematic. A representative example of this approach is Snelson's method of heuristic experimentation. All his works ensure pre-stressibility. Another notable example is Emmerich's geometry-based approach, where he used geometries of polyhedra for configuration of tensegrity [170]; the apices of polyhedra would become nodes of a tensegrity structure. With this approach, static equilibrium was resolved later and the system would have at least one stable self-stress.

¹Motro studied the initial state of tensegrity, the sizing and sensitivity problems and finally mechanical behaviour both static and dynamic.

²This is given the term *form-controlled approach* [145]. However, formal classification of this as an approach may be misleading and misconstrued as a numerical approach.

It is worth noting that the shape of the tensegrity corresponding to a particular basis polyhedron is different from that of the polyhedron [171] and, that some of configurations were incorrect; e.g. some of Emmerich's tensegrity configurations are *geometrical configurations* without necessary self-stress to ensure structural stability [145]. It is emphasised here that much like Emmerich's examples, in architectural form-generation exists a gap between purely geometrical configuration on-paper or on-screen, and physically realisable or realised work.

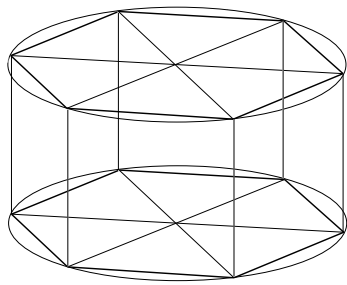
4.6.2 Numerical Approaches

These approaches aim to ensure the mechanical requirements using a theoretical form-finding process. These models take into account, both geometry and internal forces (or pre-stress). As results tend to be general, typically a general case can be derived. According to the review of form-finding methods by Pellegrino and Tibert [171], numerical methods of form-finding of tensegrity can be classified into two main categories; *kinematical* methods and *static* methods.

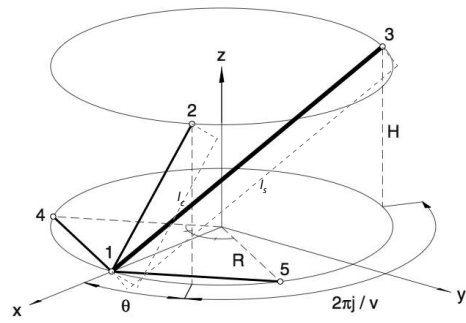
Kinematical Methods

The term, *kinematical method* refers to a method of form-finding which determines the geometry of a given tensegrity structure by increasing the lengths of the compression members while the given lengths of the tension members are kept constant. Alternatively, the lengths of the tension members may be decreased to a minimum while the lengths of compression members are kept constant. In effect these methods process an initially mechanical system into a rigid structure.

Considering a regular tensegrity prism (See Fig. 4.5(a) for base-prism), **analytical approach** seeks the ratio, $r = l_s/l_c$, where l_s is the strut length and l_c is the cable length and, expresses the ratio r in terms of angle θ . This angle, θ describes the relative rotation between the two parallel equilateral triangles and, v the number of vertices of the base polygon, connecting struts to corresponding top polygon (Refer to Fig. 4.5(b)). It was first introduced by Connelly and Terrell [172] [171]. As it concerns regular tensegrity structures, their symmetry simplifies the analysis.



(a) Example base-prism



(b) General polygon-based tensegrity.
Note that j is an integer smaller than v

Figure 4.5: General polygon-based tensegrity, after [171].

4.6 Form-finding and Control of Tensegrity

For the given value of l_c , the value of l_s is maximised for $\theta = \pi(\frac{1}{2} - j)$. For irregular or asymmetric tensegrity systems, the analytical solutions are infeasible due to the large number of variables required to describe a general configuration.

Dynamic relaxation had been used for form-finding of tensile structures such as membrane and cable-net structures [173] [174]. The use of dynamic relaxation (with or without kinetic damping technique) for form-finding of tensegrity was developed by Motro and Belkacem [171].

Assuming a structure with a given initial configuration is subject to external forces, its equilibrium can be calculated by integrating a fictitious dynamic equation. In any current configuration of the structure, nodal equations of equilibrium are used to compute out-of-balance forces. In turn, these forces are used in order to obtain the current acceleration. The resulting uncoupled equilibrium equations can then be integrated.

The same value is usually given to all coefficients of the damping matrix, chosen for quick convergence to the equilibrium state. Detection of a local peak in the total kinetic energy of the structure resets all components in velocity matrix to zero. This process is then repeated, starting from the current configuration, until the peak kinetic energy becomes sufficiently small [173].

Non-linear programming or optimisation approach has been used in for form-finding of tensegrity structures in [175]. The process of form-finding of tensegrity is essentially treated as a constrained optimisation problem. Initially, the connectivity (or element topology) and nodal coordinates are known. Then the length of one or more of the struts is increased, while the ratio, r is fixed, until a configuration is achieved to a maximum. For general expression for a constrained optimisation, refer to Chapter 3.

Referring to the triangular tensegrity prism in Fig. 4.6, initially, the cable length, l_c is set at 1, and it is assumed that either the top or bottom base i.e. three of its six nodes are fixed. The optimisation expression is in the following form:

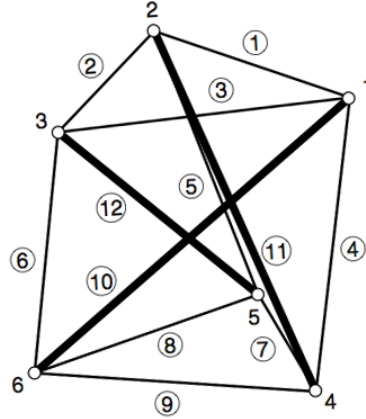


Figure 4.6: Simple tensegrity prism

$$\text{minimise } -l_{s1}^2 = 0 \tag{4.1}$$

$$\text{subject to: } \begin{cases} l_{c1}^2 - 1 = 0 \\ l_{c2}^2 - 1 = 0 \\ l_{c3}^2 - 1 = 0 \\ l_{c4}^2 - 1 = 0 \\ l_{c5}^2 - 1 = 0 \\ l_{c6}^2 - 1 = 0 \\ l_{s3}^2 - l_{s1}^2 = 0 \\ l_{s3}^2 - l_{s1}^2 = 0 \end{cases} \tag{4.2}$$

c_n where $n = (1, \dots, 6)$, denotes the six cables and s_m , where $(m = 1, 2, 3)$ the struts. In this particular case, the ‘optimum’ length of the struts is 1.468 (c.f. the analytical value, $\sqrt{1 + 2/\sqrt{3}}$ or approximately, 1.468).

A notable advantage of the non-linear optimisation approach is that it builds upon its available optimisation technology, while its distinct disadvantages are that, with the increase in the number of variables in constraints, this approach becomes infeasible for larger systems, and that the state of prestress cannot be explicitly controlled, although different geometric configurations of structures with

4.6 Form-finding and Control of Tensegrity

the same topology can be found by varying the ratio between the lengths of struts.

Other more recently developed methods are: genetic algorithms [176] [177], and MILP kanno2011topology for regular tensegrity.

Zhang and Ohsaki [178] presented three optimisation approaches for both shape design and force design. These adapted, for form-finding, the existing energy approach, direct approach and force density approach i.e. minimisation of difference between strain energy in cables and in struts, minimisation of deviation of force components from their target values for the structures modelled as directed graphs in order to determine configurations and member forces at the state of self-equilibrium and, maximisation of stiffness (or minimisation of deviation of member forces from their target values) through optimal distribution of member forces, where configuration of the structure is fixed. In all three approaches, the topology is assumed to be known prior to form-finding.

Similarly Masic *et al.* [179] proposed a method of optimising mass-to-stiffness ratio of both symmetric and asymmetric tensegrity structures. Starting from an initial layout that defines the largest set of allowed element connections, the procedure seeks the topology, geometry and pre-stress of the structure that yields optimal designs for different loading scenarios. The design constraints include strength constraints for all elements of the structure, buckling constraints for bars, and shape constraints. The problem formulation accommodates different symmetry constraints for structure parameters and shape. The static response of the structure is computed by using the nonlinear large displacement model. The problem is solved as a nonlinear program. See *Section 4.7* for a more indepth review of his work.

Statical Equilibrium Approach

The term *statical equilibrium approach* refers to methods of form-finding which determines the possible equilibrium configurations of a tensegrity structure with

4.6 Form-finding and Control of Tensegrity

pre-determined topology¹. The equilibrium conditions for one node determine the resulting shape.

In an **Analytical method**, Kenner [152] used node equilibrium (and symmetry) to determine the configuration of the expandable (regular) octahedron [171].

A different equilibrium approach was used by Connelly and Terrell [172] to find the prestress stable form of ‘rotationally symmetric’ tensegrity structures. A set of linear equilibrium equations were established by use of force density ², as variable for each member.

Williamson *et al.* [180] used the static equilibrium conditions to derive analytical expressions for the equilibrium condition of a tensegrity structure in terms of force density and member connectivity. The novelty of this method is the use of vectors to describe each element, which eliminates the need to use direction cosines and the subsequent functions and that the reduction of the study of a significant portion of the tensegrity equilibria to a series of linear algebra problems. A formulation of loaded tensegrity is also developed.

Force-density method was first proposed by Schek [48] for prestressed net structures. This method is useful because it turns the non-linear equilibrium equations of the nodes into a set of linear equations by introducing the force density for each member. In a purely cable structure, all tension coefficients are positive, and thus a unique solution is guaranteed in the form-finding problem.

A similar principle can be applied to the form-finding of tensegrity, but the self-stressed state of tensegrity structures necessitate neither nodes at support nor external loads, unlike the cable structures.

¹The number of nodes and connecting elements between them are pre-determined prior to form-finding

²force divided by length

4.6 Form-finding and Control of Tensegrity

As this method was originally used for cable nets where all members were under tension. i.e. all coefficients had the same sign, for tensegrity, each element must be defined to be either tension or compression. The advantage of force density method is its generality and possibility to obtain results for irregular systems [145]. There are mainly two methods involving the force-density approach; the iterative method is where self-stress coefficients are evaluated by an increment till the rank of connectivity matrices reaches the required order, requiring much computational power; the analytical method is where matrices are analysed in their symbolic form in order to find the self-stress coefficients that satisfy the required rank condition (i.e. self-stress coefficients are not chosen).

More recently Zhang and Ohsaki [181] presented an extended force density method by using singular value decomposition of the equilibrium matrix with respect to nodal coordinates to find the feasible set of force densities for satisfying the non-degeneracy condition of the structure. A unique configuration of the structure can be obtained by specifying an independent set of nodal coordinates. Estrada [169] proposed a form-finding method that requires only a minimal knowledge of the structure; it only requires the type of each member, i.e. either compression or tension, and the connectivity of the nodes to be known. Then both equilibrium geometry and force densities are iteratively calculated. A condition of a maximal rank of the force density matrix and minimal member length, were included in the form-finding procedure to guide the search of a state of self-stress with minimal elastic potential energy. It is indeed able to calculate novel configurations, with no assumptions on cable lengths or cable-to-strut ratios. This method is purely linear but still starts with known connectivity.

Connelly's **Energy method** [171] shares similarities with force density method in its formulation.

The energy method defines three different types of members within a tensegrity framework; cables, struts and bars ¹. A self-stress state is ensured if the sum of

¹Cables cannot increase in length, struts cannot decrease in length and bars cannot change length

the product of self-stress states and member length (i.e. internal forces) at each node is zero, assuming positive stresses for cable and negative for struts while no condition is set for bars. Besides this equilibrium condition a further condition is required to establish a stable equilibrium configuration; the total potential energy function should be at a local minimum.

A most recent example which introduces multiple self-stress states is found in [182].

4.7 Automatic Generation of Tensegrity

Automatic generation of tensegrity differs from pure ‘form-finding’ in that form-finding requires the topology and designation of compression and tension members to be prescribed prior to the search for equilibrium and stability, as many researchers have developed such as Tran and Lee [183], Pagitz and Tur [184], Estrada [169], and Zhang and Ohsaki [181] amongst others.

Most of the currently available methods of form-finding are limited to the use of heuristic experimentation, hierarchical design based on known components, or mathematical methods for mostly regular tensegrity.

On the other hand, automatic generation of tensegrity requires no such topological configuration as identification of the structure’s topology is one of the objectives. Due to lack of mathematical formulation or computational modelling tools to determine the connectivity pattern of tensegrity structures, Fuller, Emmerich and Snelson all relied on models and experimental constructions for design of their structures, which were largely limited to regular or polyhedral tensegrity structures.

Hence regularised or patterning work were prevalent; there are a number of researchers who proposed different methods of designing tensegrity; e.g. Fu studied the structural behaviour and structural types of tensegrity domes through use of a non-linear software and proposes methods of designing tensegrity geometric grids [185].

4.7 Automatic Generation of Tensegrity

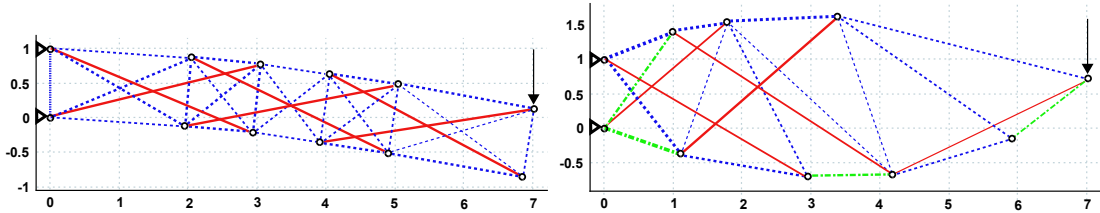


Figure 4.7: Initial and optimised tensegrity beam design, showing deformation under load - green or inconsistent dashes (slack strings), red (compressed bars), blue or consistent dashes (stretched strings). [179]

Relatively recently, Masic *et al.* [179] proposed a method of optimising mass-to-stiffness ratio of both symmetric and asymmetric tensegrity structures. Starting from an initial layout that defines the largest set of allowed element connections, the procedure seeks the topology, geometry and pre-stress of the structure that yields optimal designs for different loading scenarios. The design constraints include strength constraints for all elements of the structure, buckling constraints for bars, and shape constraints. The problem formulation accommodates different symmetry constraints for structure parameters and shape. The static response of the structure is computed by using the nonlinear large displacement model. The problem is solved as a nonlinear program.

Masic's work is significant in that this methodology does not only find feasible tensegrity geometries, but it provides a systematic procedure for analysis and *designing* of optimal tensegrity structures e.g. inclusion of yield and buckling constraints of structural members. However, two notable facts are drawn to attention. The first is that there is no guarantee of global optimal solutions because of the non-convex nature of the non-linear optimisation formulation used. The second should be referred to Fig. 4.7; the optimised tensegrity on the right appears not to have a compressed member connected to the node located at $[x,y]=[6,0]$. This is because there is a compressed bar connected to the node located at $[6,0]$ and to the node at $[3.5, 1.5]$ that overlaps with the visible string depicted in blue

4.7 Automatic Generation of Tensegrity

along its entire length. This is because the nodes in the original configuration, located at $[4, 0.6]$ and $[5, 0.5]$ in the optimal configuration have ‘nearly merged but not merged’, i.e. the string connecting them became very short. Also, the nodes in the original configuration, located at $[3.9, -0.4]$ and $[4.9, -0.5]$ coincide in the optimised configuration. In summary, this method has generated in this particular instance at least, tensegrity structures only *theoretically* without preserving essential structural characteristics of tensegrity. This subsequently also incidentally alludes to a possibility of tensegrity not being optimal in agreement with Hanaor’s assertion ¹ against tensegrity’s optimality, as the optimised tensegrity in this example converged toward a conventional LP structure by eliminating a tensile member.

Masic’s work on optimisation of tensegrity structures is similar to conventional form-finding methods in that the form-finding begins with pre-determined connectivity. However, the notable difference is the use of geometry optimisation, which can allow struts to be reduced and nodes to be merged and, thus can permit change in the initial connectivity, although the instance of this in [179] are not necessarily favourable examples (See the critique on this non-linear optimisation method in 4.6.2).

Paul *et al.* [186] and Rieffel *et al.* [187] used an evolutionary algorithm for generation of irregular tensegrity structures at both small and large scales, which are difficult to design using other methods. In particular, Rieffel *et al.* used an evolutionary algorithm, a generative and grammatical graph-based approach to generate *irregular tensegrity* structures [187]. Similar to Masic’s work, this method differs from the conventional approaches to tensegrity form-finding which tend to be limited to small scale regular tensegrities, in that it is demonstrably capable

¹“The main source of structural inefficiency of strut-tendon systems subjected to flexure is, reduced structural depth, when pretensioned tendons serve as compressive chords. In a cross-section subjected to bending action, the applied bending moment is resisted by an internal couple. In a bar structure (e.g. truss) the internal couple consists primarily of compression in the compression chord and tension in the tension chord.” [136].

of form-finding of large-scale tensegrity structures as well as non-polyhedral irregular tensegrity structures.

The most notable work to date is by Kanno, who formulated form-finding of tensegrity in MILP [188]. His method requires no topological information in order to generate tensegrity structures and his method is generally successful. However, the generated topologies only resemble layer-based polyhedral topologies. See. Fig. 4.8.

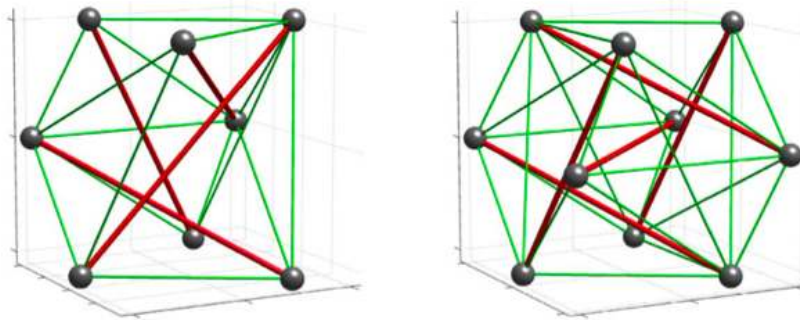


Figure 4.8: Optimised 3D tensegrities. Kanno [188].

4.8 Concluding Remarks

In order to identify new tensegrity forms researchers have applied various methods in both static and kinematical approaches, as summarised in the previous sections. Regardless of approaches or methods, one important condition prior to any form-finding procedure, is that the connectivity of struts and cables be defined, most of which are based on geometry of chosen polyhedra.

Though the task of form-finding is by no means trivial, the regularity of these connectivities based on the known geometry of polyhedra and their derivatives are too restrictive in their approach to design ¹.

¹An exception to this is where the regularity of members provide an advantage.

Hence, instead of mere geometry-configuration for stability of tensegrity (form-finding), which is only one aspect of tensegrity design, a more comprehensive approach to design would be to automate the configuration of connectivity in addition to geometry configuration, for structural stability.

This issue has been addressed, though recently; there have been efforts to generate both regular and irregular tensegrity members without pre-defined connectivity [187] or those which allow change in reconfiguration of the initial connectivity [179] with some success. The most recent example topologies generated by the MILP formulation by Kanno resemble layer-based polyhedral topologies. These methods are still at an inchoate stage of development and variety of techniques for tensegrity form-generation remains to be experimented, including the relatively simple efficient LP layout optimisation techniques.

The task is thus clear; a method of form-generation for non-polyhedra-based tensegrity (in addition to regular tensegrity), should be incorporated into the existing LP layout optimisation formulation.

Part III: Chapter 7 will present a simple mixed integer linear programming (MILP) layout optimisation formulation, which can limit (to one) the number of compressive elements terminating at joints in the structure is described, thereby allowing tensegrity-type structures to be synthesised¹.

¹A relaxed version of the patent-based definition (or Class 1 of Skelton's) will be used as opposed to Motro's extended definition (or Class 2) [145] [189]. Also it is worth noting that the formulation will generate tensegrity-type systems with reactions to external loads with supports as opposed to self-stress unlike the patent-based definition (or Class 1) tensegrity principle assumes.

Part II

Generation of Conceptual Form of Conventional Structural Configuration

Preface

This part comprises essentially two components. The first, and main, component presents an analysis of currently prevalent shape-driven, form-rich architectural designs, a critical appraisal of computer as a design tool and structural layout optimisation techniques, placed in the context of design tools, in addition to design examples. It is based on the manuscript for a paper entitled “*Potential use of structural layout optimisation at the conceptual design stage*”, published in the International Journal of Architectural Computing in March 2012 [190]. However, the work presented here is the candidate’s work in its entirety, and has additional elements and a revised format for presentation here. The précis of this chapter is as follows:

- 1 A review of the relevant literature appears to indicate that the ocularcentric view of the computer simply as a geometry generator by many architectural design professionals may be the root cause of the polarised development that existed between the visual and technical aspects of design in the recent past.
- 2 The role of the computer in the design process is critically appraised.
- 3 The relationship between ‘form’ and ‘structure’ in design is then explored, suggesting the possibility of reducing the degree of polarisation by use of techniques which facilitate a greater degree of form-structure integration.
- 4 There is evidence that design time pressures are leading to traditional early-stage conceptual design activities (e.g. sketching via pencil and paper) being sidelined, or even being actively discouraged. However, while early-stage computer-based conceptual design tools are available, those which consider structural design parameters are scarce. Given that early-stage form-structure integration is likely to be beneficial to a large extent, there would appear to be a need for new computer-based conceptual design tools which also consider structural aspects.

-
- 5 As a potential solution, the use of a structural optimisation-driven form-generation technique is proposed. Several conceptual design studies are presented to evaluate the efficacy of this approach in both 3D and 2D.
 - 6 Finally, the feasibility of adopting such an approach in mainstream architectural design practice is critically evaluated (in the light of the numerous computer-aided, rule-based geometry and parametric modelling techniques which have been developed in recent years). Results from simple conceptual design studies are discussed, potential usage patterns are proposed and areas where improvements are required are highlighted.

The second component of *Part II* is presented in the form of postscript which contains a discussion on the subject of the role of the graphical user interface, in order to provide the reader with a fuller appreciation of the research area.

Chapter 5

Potential Use of Structural Layout Optimisation at the Conceptual Design Stage

Abstract

Despite the recent advancement in computer-aided design in architecture, in areas of form generation techniques, (engineering) performance-based design tools and integrative design tools, there still exists some gap to be closed between the ‘visual’ and the ‘technical’ elements of design. Two causes of this are discussed: long-standing tradition within the discipline and perception of design as a purely visual exercise. Structural layout optimisation is a technique which enables automatic identification of optimal arrangements of structural elements in frames with potential form-generation capabilities. As the technique appears to have the potential to help alleviate the said gap between the visual and the technical aspects of design, it can be considered as an ‘integrative’ form generation tool. Applications of the technique are considered via a set of three-dimensional design studies and an additional set of two-dimensional studies, demonstrating both its potential and areas where refinement is required before it is suitable for application in practice.

5.1 Introduction

Distinct paradigms in architectural design history can be identified according to distinct eras of design and construction tools and materials as much as by the design theories and ideas of those eras [191]. Typically ‘technical’ and ‘visual’ aspects were considered in relative isolation in the recent past, and the limited number of publications in the literature on the interdisciplinary nature of architecture and engineering was further evidence that there are still remnants of a systematic, institutionalised, divide between the ‘visual’ and ‘technical’ aspects of design. This situation is thought to be largely due to the sheer scale, nature and complexity of modern building projects, with the divide apparently concretised by the difference in the very nature of the design tools used by architects and engineers¹.

In this light, recent developments in computer-based tools and techniques (e.g. traditional CAD software) should ideally be ‘integrative’, in the sense that they should help to narrow the divide between the ‘visual’ and ‘technical’ aspects of design. In the recent past, there has been much development in this effort toward integration. However, there is still much to be explored.

While the application of computer-based technology has made numerous large-scale projects possible, it is also true to say that it has led to dendritic sacs of specialist areas of knowledge within the building design sphere. Thus on the one hand there are groups working with highly advanced visual techniques (e.g. form finding and form generation techniques), and on the other hand groups working with highly advanced physical modelling tools (e.g. finite element based tools and other performance-based design approaches). This has arguably resulted in an over-emphasis on certain aspects of the design process, depending on whether the design process has been initiated as a visual or performance-driven exercise.

¹Notwithstanding the apparent ‘integrative’ nature of for example modern ‘Building Information Models’ (BIM) and the most recent, emerging efforts for form-structure integration.

This polarisation, which began from intentional division for design convenience, appears now to be counterproductive and, given the level of development of the seemingly disparate technologies being applied, it seemed anomalous, in the past that few steps appeared to be being taken to provide a bridge between them. However, in the light of a surge of recent advancement with numerous integrated design approaches, his chapter seeks to explore and examine the role of structure in architectural form conceptualisation, and considering the potential role of the structural truss layout optimisation technique in the early design process, and the extent to which this can help bridge the aforementioned divide.

5.2 Form-generation Methods in Context

5.2.1 Background

Form generation involves definition or conception of the external shape of an object or arrangement of its constituent elements. In recent years various methods have been applied to generate highly irregular and/or curvilinear forms (cf. buildings based on simple geometrical shapes, which were common prior to the ubiquitous use of CAD). Ample evidence of this exists in the portfolios of prominent architecture studios (e.g. Gehry & Partners; Future Systems; Foster & Partners), and in the entries to influential architecture competitions (e.g. RIBA Stirling prize; Emporis Skyscrapers Award; AIA Progressive Architecture Award).

Though form may be considered as just one facet of architectural design, it is undeniably a highly important one. Entirely manual form generation techniques can be applied, though computational form generation techniques are likely to find increased use in the future, including [192]:

1. Parametric modelling techniques (using non-Euclidean geometries, NURBS etc)
2. Metamorphosis & evolutionary architecture techniques
3. Performance-based methods (e.g. based on mathematical layout & topology)

5.2 Form-generation Methods in Context

optimisation techniques. See Section 5.2.4 for a more in-depth consideration)

Alternatively, irrespective of whether manual or computational methods are being applied, a number of categories of form generation can be identified: imitation; controlled randomisation; repetition (including mirroring, alignment and segmentation); variation (including misalignment); geometricism (use of simple geometric shapes as primary elements); use of relevant physical principles (other than purely geometric or visual principles); 2D-to-3D extrusion. All the aforementioned can be influenced by internal usage or arrangement requirements, and also by inherent limitations of the available tools and/or structural principles.

Among contemporary design projects (e.g. Fig. 5.1-5.2; References [193], [38]), the form generation methods used typically assume that the structure functions purely according to some visual or ‘geometric’ principles. i.e. a visual representation of ‘form’ is prescribed, with spatial and aesthetic considerations taken into account, but with physical principles largely ignored¹. These physical principles, together with other primarily ‘functional’ or ‘technical’ subsidiary aspects, are usually only accounted for at the subsequent detailed design stage, thus finally allowing the form to be realised ‘off’ the computer screen.

5.2.2 Division between the ‘Visual’ and ‘Technical’ Elements of Design

It is sometimes suggested that the division between the ‘visual’ and ‘technical’ elements of design is a necessary consequence of the dramatic increase in the scale and complexity of modern projects. However, the division can also be partly attributed to long-standing tradition, with historical roots dating back to the time of Bacon [194]. It is also generally accepted that in the 1800s a clear division arose between proponents of the Enlightenment ideology (viewing science as

¹For example, in the case of experimental folding forms (e.g. Fig. 5.1) initial concept models may be constructed using a material very different to that which can feasibly be used in practice, frequently leading to forms which are in practice unrealisable.



Figure 5.1: Garibaldi Exhibition Centre, Grimshaw-Architects, Milan 2006

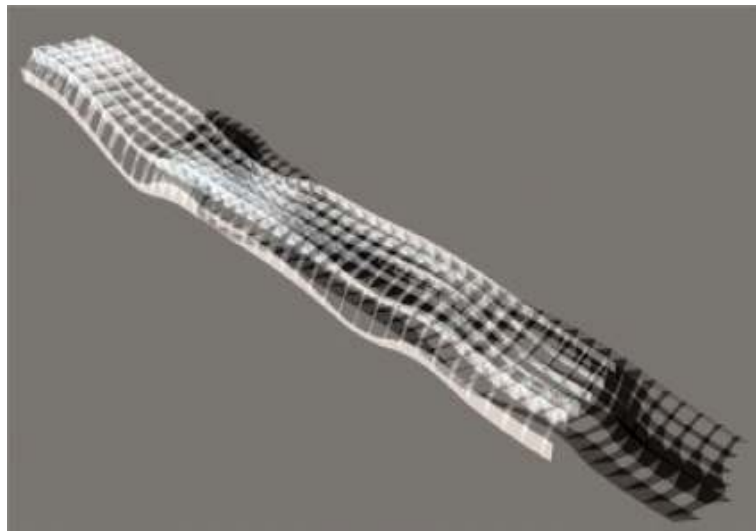


Figure 5.2: Brian Boyer non-structurally initiated



Figure 5.3: Guggenheim Museum Bilbao, Gehry & Partners

the truth) and proponents of the then emerging Romanticism ideology (viewing science as dehumanising, and leading to the destruction of beauty) [195], [196]. These struggles were later reflected in theories of architecture, and subsequently in buildings [197], and continue to influence design practice to the present day.

However it is relevant to consider the following questions: why did a functional, efficient and rational design like the Eiffel Tower not become a definitive aesthetic, considering its harmonious combination of structural efficiency and aesthetic elegance? Why is structural efficiency not viewed as synonymous with beauty? And why are such harmonious combinations not more often the norm in modern-day buildings?

Many prominent contemporary large-scale building designs are ‘form-oriented’ or ‘form-driven’ (that is to say the iconoclastic external envelope or overall form is sought with high priority, at the expense of other aspects of building). Inevitably, this begs the question: what is form in architecture, and why does form seem to govern the design of a building to such a large extent? Loosely ‘form’ can be defined as ‘a visually perceivable pattern or structure with spatial attributes’, and for an object to really take ‘form’, it has to physically exist (i.e. to be ‘realisable’ in practice). However, it is perhaps of more interest to establish the nature of the relationship between form and structure than to identify a single precise definition of form; this inter-relationship will therefore be studied further.

5.2.3 Inter-relationship between Form and Structure

Fig. 5.3 shows The Guggenheim Museum, Bilbao, designed by Gehry & Partners, with truss structures covered in a mesh-type envelope. Fig. 5.4 shows a section through a generic free-form building of a similar type. Fig. 5.4(a) highlights elements that are conventionally perceived to constitute ‘form’ (i.e. surface), whereas Fig. 5.4(b) highlights those that are conventionally perceived to constitute ‘structure’. Fig. 5.4(c) shows both sets of elements. The drawings in Fig. 5.5

clearly highlight ambiguity in the conventional design definitions of ‘form’ and ‘structure’.

Fig. 5.5(a) highlights a part of the building that can be considered to define both ‘form’ and ‘structure’, while Fig. 5.5(b) highlights the structural skeleton taking what appears to be a ‘form’. Unsurprisingly this ambiguity leads us to question the clear-cut division between the two aspects of a building, devised originally for the convenience of designers, fabricators etc. Indeed, the illustrated ambiguity highlights the inevitable interaction between ‘form’ and ‘structure’. Nevertheless, this separation, which was initially developed for practical convenience, is still widely accepted in standard design practice, and dictates the way many designers think and work. How did this happen? Is it because we ultimately perceive design as a primarily visual exercise, with modern computer software applications only serving to reinforce this perception?

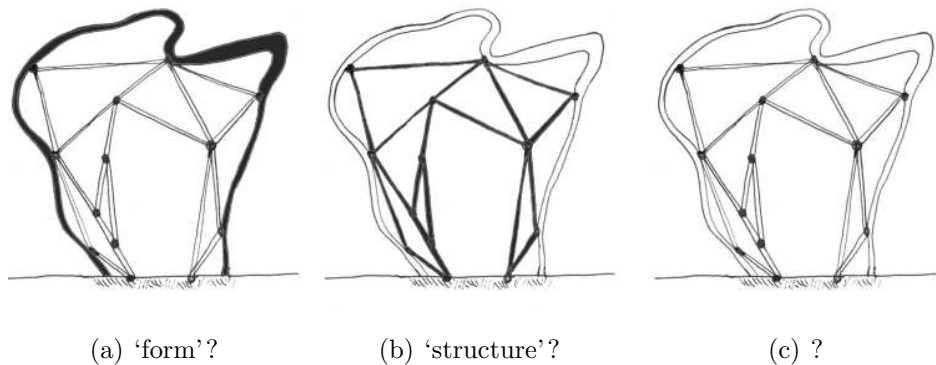
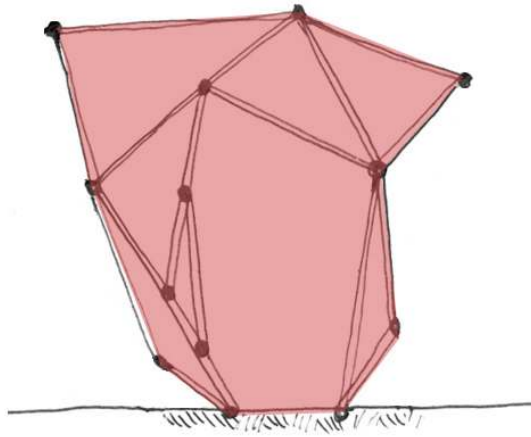


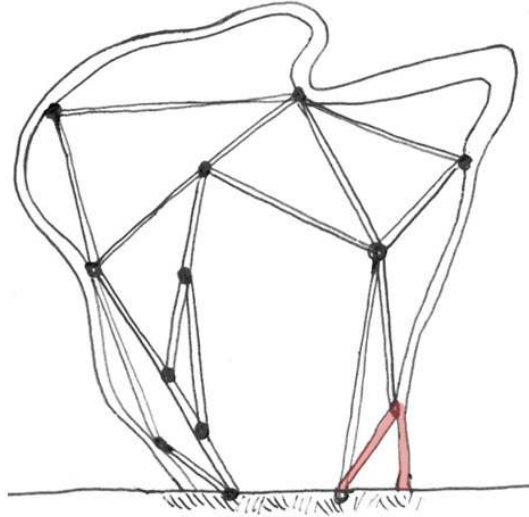
Figure 5.4: Ambiguity in definitions of ‘form’ vs. ‘structure’.

5.2.4 A Critical Appraisal of the Role of Computers in the Design Process

The numerous methods in which a ‘form’ can be generated have been briefly outlined in the previous section. However, given its ever-increasing role in the design process, it is useful in particular to critically appraise the role played by



(a)



(b)

Figure 5.5: Ambiguity between ‘form’ and ‘structure’: (a) a triangular structural element that can be considered to define both form and structure is highlighted; (b) the envelope of elements considered as constituting ‘structure’ is highlighted, showing that this also defines ‘form’.

the computer.

Firstly it can be observed that most common computer interface components are actually unidirectional (there are exceptions e.g. touch screens used in 3D sketching [198]). This necessarily limits the degree of interaction between designer and computer. The most effective machine-to-human interface is currently the computer monitor, where all inputs and outputs are visualised. With the contemporary method of ‘monitor and mouse’ almost all information has to be visually communicated between the media and the designer. This is in common with the conventional method of ‘pen and paper’, indicating that visual communication of information obviously predates computer aided design processes. However, the particular and narrow mode of operation to which designers have become committed when using a computer can be highly restrictive.

Of course if ideas to be communicated are essentially of a visual nature this does not pose a problem. However, upon analysing any building, not even the simplest of objects (e.g. a humble doorknob) is in reality a mere visual entity. For example, surface texture, weight, structure and temperature are other aspects which are essentially filtered out through a simple visual representation. It should also be pointed out that a visual ‘form is still an idea, and visual existence of a design object is virtual; a design object has to be more fully justified in order to physically exist. Transformation of ideas into reality is (or should be) at the heart of the architectural design process.

Nevertheless, designers continue to consider visual representation as the primary means of communication, symptomatic of the current ocular-centric culture in which we live, and which extends into the sphere of computer-aided design process in architecture [199]. This means that simulations, or other means of supporting more abstract ideas or principles (e.g. level of comfort or physical stability), tend to be filtered out through the use of computer visualization, and collation of other information is still separately required. This appears to be a significant missed opportunity, and an aim of the present study is to evaluate the potential for such

simulations to be placed closer to the heart of the conceptual design process.

5.2.5 The Computer as a Truly Integrative Design Tool

Although the computer can never model a building in its complete entirety, it is clearly capable of modelling much more than purely visual aspects. It can be argued that the proliferation of visualization techniques has not necessarily ‘improved or expanded the boundaries of what architecture can be; indeed over-emphasis on the visual can reduce architecture to a mere visual sensation or, in more practical terms, can simply waste time. Although other performance-related aspects of a building can be used to initiate the concept design phase, this is unfortunately not commonplace in standard design practice. This is regrettable as ideally designers should have the freedom to explore other, non ‘visual, aspects of design, be it to identify a physical solution to a social problem or to synthesise a functional sculpture.

Indeed, given the immense capabilities of a modern desktop computer, it should be feasible to ensure that the physical behaviour of any form being designed can be taken into account at the initial conceptual design stage. Incorporation of structural considerations via the use of mathematical optimisation techniques is potentially a step towards achieving this, and hence also to achieving a less misleading representation of reality. With this firmly in mind, a software application originally developed for use by structural engineers to identify the optimal arrangement of structural members in frameworks has recently been re-evaluated by the present authors with a view to using it in the architectural design process. The software is based on the structural layout optimisation technique which will now be briefly described.

The structural layout optimisation technique was first developed in the 1960s in order to automatically identify the optimal arrangement of members in either 2D or 3D frameworks, satisfying predefined constraints and a predefined optimality criteria [79]. Recent advances have meant that very large scale design problems

5.2 Form-generation Methods in Context

can now be tackled [91]. An advantage of using the original layout optimisation formulation, in which all members in the optimal minimum volume (weight) structure are fully stressed, is that highly-developed mathematical optimisation solvers can be used to identify optimal solutions in a short space of time (see Appendix for details of the basic formulation).

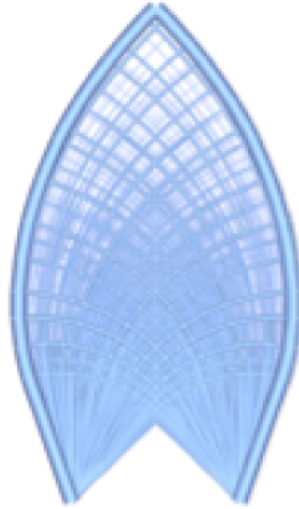
Sample 2D and 3D output is shown in Fig. 5.6; note that in order to generate structurally sound concept designs boundary conditions and applied loading must initially be specified.

Although obtained by specifying relatively simple loading and support conditions, these optimal forms might be considered to exhibit aesthetic characteristics reminiscent of ‘emergent forms (the term *‘emergent’* refers to “*the spontaneous occurrence of an organisation or a behaviour that is greater than the sum of its parts*” [23]). This type of optimisation tool would therefore appear to have the potential to appeal to a wide range of users, including architects and mega-sculptors.

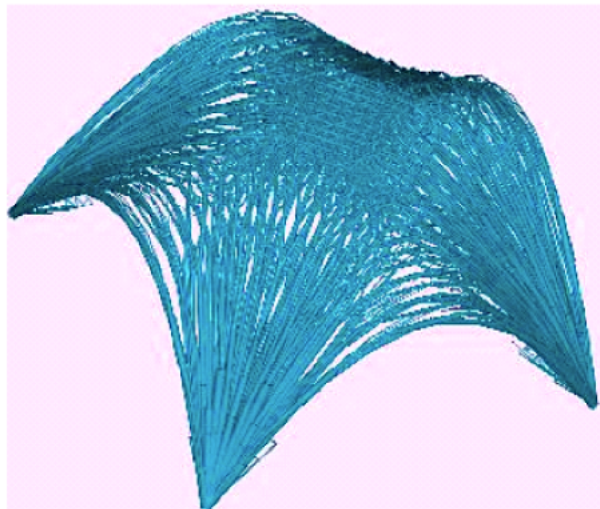
Considering a potential use of the structural layout optimisation technique in an architectural design environment, various questions arise, one of which is, for example, whether the least weight structure would be any appropriate to be sought, unless the weight is of critical importance, as the idea of weight minimisation as a core design concept or motivation in architectural design scenarios is likely be perceived absurd (if not offensive). Furthermore, surely such a technique has the potential to adversely impinge on the creative process at the form conceptualisation stage¹? Whilst both these questions, and no doubt many others, deserve answers in due course, this chapter seeks instead to address a rather simpler question, namely is there potentially a place for structural layout optimisation techniques in the architectural design process?

It is also worth pointing out that we are in a sense here just as interested in the nature of the forms generated (together with the process of identifying them, and

¹Issues of form conception in various branches of architecture-related disciplines have been the subject of much debate, e.g. [192], [193] and [201].



(a) 2D Example structure generated using layout optimisation



(b) 3D Example structure generated using layout optimisation

Figure 5.6: Example structures generated using layout optimisation (after Darwich *et al.* [200]): (a) 2D ‘Michell structure’ (design constraints: two pinned supports at base and a horizontal point load at the top of the domain); (b) 3D roof structure (design constraints: 4 pinned supports at base and uniformly distributed vertical ‘transmissible’ loading).

how this process can be changed to manipulate the forms generated), than in the fact that the forms are structurally ‘optimum. This clearly brings us outside the traditional domain of engineering, where the goal is generally to single-mindedly seek out the most efficient (cost-effective) structural solutions.

Finally, it should be noted that application of optimisation technology in design is by no means new; it is widely used in the automotive and aerospace industries, though has to date found comparatively little application in the construction industry. However, recently some buildings have been designed with the help of this technology (e.g. [201]), and tools such as the EifForm design software developed by Shea [202] have attracted significant interest.

5.3 3D Design Examples

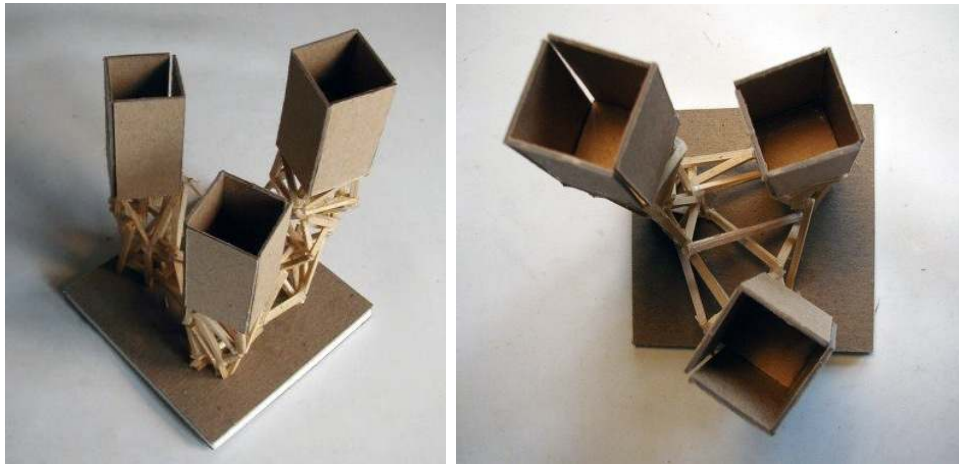
It is now useful to consider a number of examples which illustrate how structural layout optimisation technology might be applied in a realistic design environment. These examples offer a range of opportunities for the software to help designers to identify possible solutions, ranging from an initial relatively unrestricted, unconstrained example (‘Thinking pods’) to a much more highly constrained multi-storey building example with supports prescribed to coincide with existing building frame geometry, and with realistic design loading conditions.

5.3.1 Thinking Pods

Here the brief was to design a multitude of elevated ‘lounge’ spaces for relaxation and cogitation, supported high above the ground on stilts in a wooded area of a University campus. Initial concept design was carried out in collaboration with a student of architecture studying on the campus, with the most promising manually identified design concept shown in Fig. 5.7 It shows individual cuboid-chambers (typical size: 4 x 5 x 5 m) supported on a web of interconnected space

5.3 3D Design Examples

trusses. Though the geometries of these space trusses were not explicitly defined, the plan areas and overall elevations of the chambers were fixed.



(a)

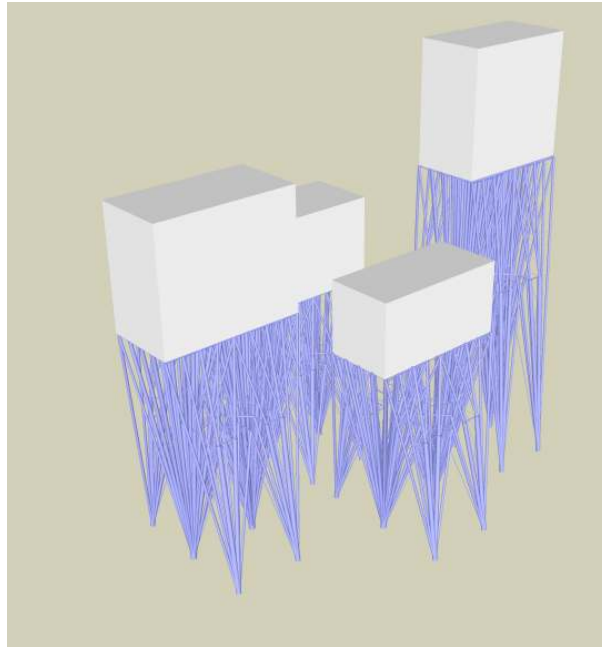
(b)



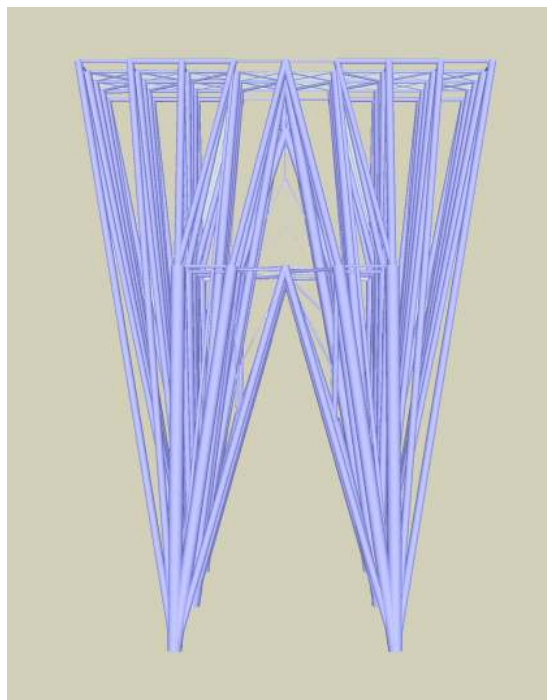
(c)

Figure 5.7: Conceptual design of thinking pods: manually derived.

The same overall design constraints were then fed into the structural layout optimisation tool; the solution obtained is shown in Fig. 5.8 (using simultaneous vertical and horizontal loading as the design load case).



(a)



(b)

Figure 5.8: Conceptual design of thinking pods: obtained using structural layout optimisation.

While the manually derived concept model featured pods supported by trusses which were for reasons of efficiency interlinked (see Fig. 5.7(c)), the design obtained using structural layout optimisation techniques, shown on Fig. 5.8, did not. This was to ensure a rapid run-time, rather than due to an intrinsic shortcoming of the layout optimisation technique itself.

However, the proliferation of structural elements converging on the supports at the base (see Fig. 5.8) does highlight the need to incorporate adequate user-controls when developing a practical software tool based on this approach. For instance, in a real design setting, the ability to specify limits on the number of members converging on a joint, or the positions of individual joints would often be highly desirable. In some case this would necessitate use of a more complex mathematical formulation than the linear formulation used here (e.g. see Appendix A.3 for brief details of a potential MILP-based approach).

In further discussion of the generated form, it is noted that its unrestricted, initial design domain created straight paths for load transfer, resulting in long, straight constituent forms, suggesting use of a more stringent design domain in order to engender less of a generic ‘structure’ but more of a distinct, perceptible aesthetic overall form.

5.3.2 Exhibition Space

A design brief for this project has been arbitrarily devised to demonstrate the capabilities of the software. The conceptual form design guidelines and logical starting point for this conceptual design, are as follows:

- The design is to house an outdoor exhibition space; it aims to provide three separate areas for distinctly different uses.
- These three separate areas should be expressed visually in the resulting external design form.
- The design requires two openings, for the entrance and exit.

- Instead of a simple rectangle for the design domain and assigning the form generation design work to the software algorithm, the design domain space has been actively designed by human designer intuition while allowing generally unrestricted form generation within the specified domains.

The initial, spatial design domain, as shown in Fig. 5.9, was derived with these items in the brief in consideration ¹. Its design scheme was initially, to comprise two main elements; sheltering membranes and three-dimensional dome-type structures from which the membranes were to be hung.

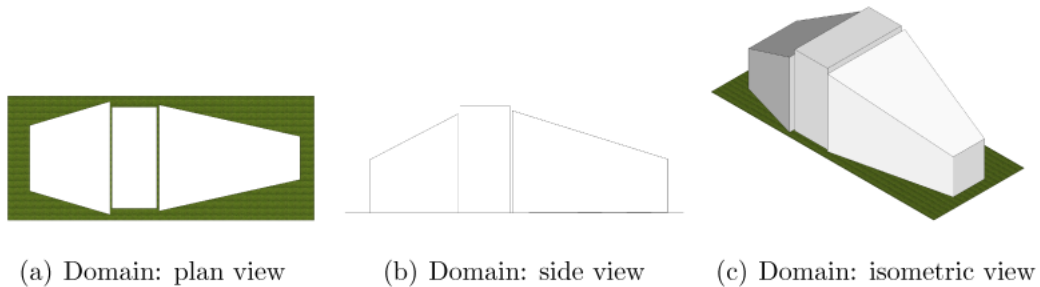
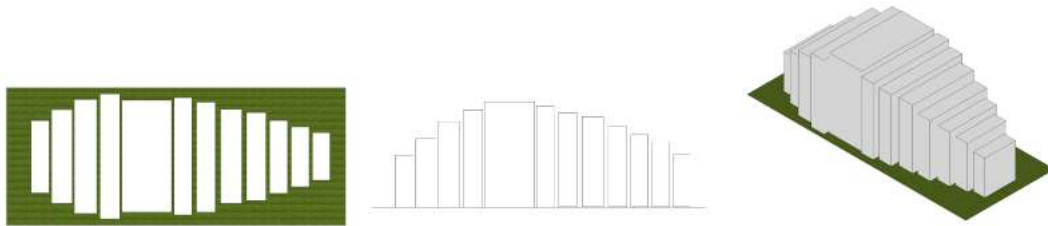


Figure 5.9: Conceptual design of exhibition dome: design domain expressed as 3D masses

However, during the process of ‘one-step’ optimisation with realistic design parameters and constraints, where design domain and constraints were entered and processed, and the output (i.e. optimised structures) was to be generated, it became clear that the problem definition seemed to be computationally inefficient for a computer with generic, standard hardware specifications², readily available to conventional designers. Thus, the problem was broken down into a series of two-dimensional problems, with bracings placed between the optimised structures across the length of the form, for lateral stability - see Fig. 5.10 for the revised

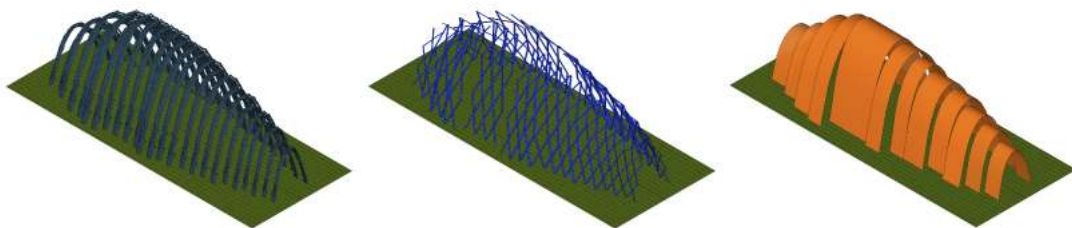
¹Although this process may appear arbitrary, the nature of conceptual design and in particular, that of conceptual form design, in many cases, is not guided by practical or regulatory design requirements but instead derived with ‘creativity and intuition’, and hence inevitably has a degree of arbitrariness.

²the computer to generate the presented forms had one Intel Core 2 Duo processor at processing speed of 2 GHz with two cores with memory of 2 GB



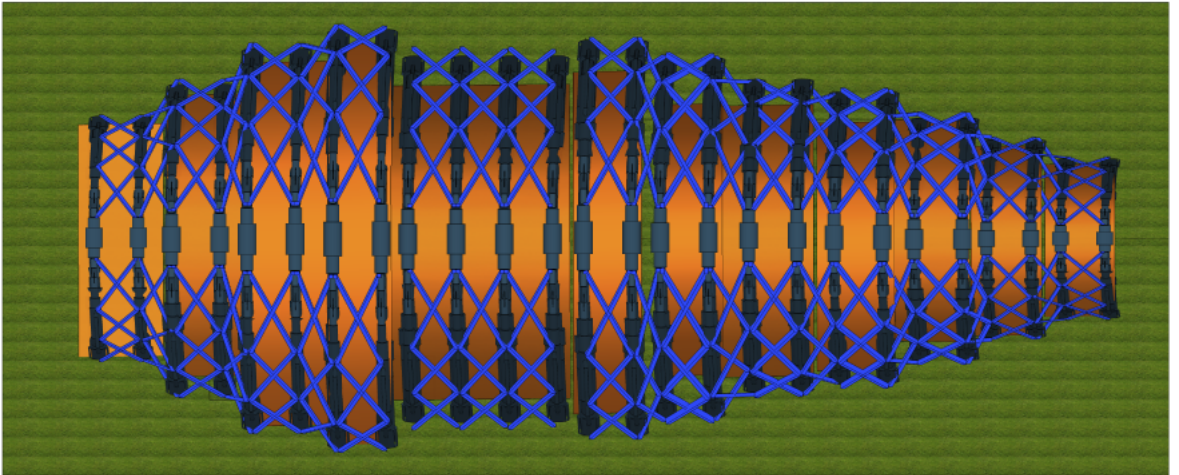
(a) Design domain: plan view (b) Design domain: side view (c) Design domain: isometric view

Figure 5.10: Conceptual design of exhibition dome: further division of design domain for 2D plane structures

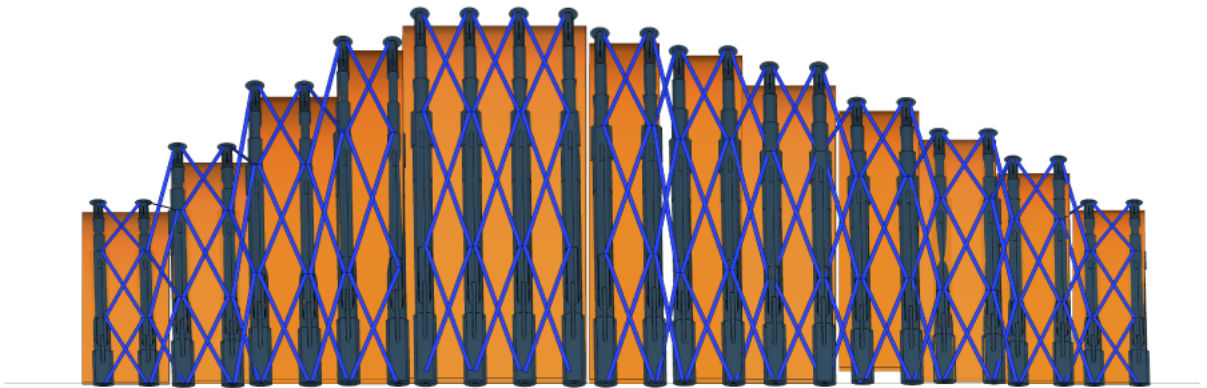


(a) Optimised arches (b) Additional bracings (c) Membrane elements

Figure 5.11: Conceptual design of exhibition dome: assembly

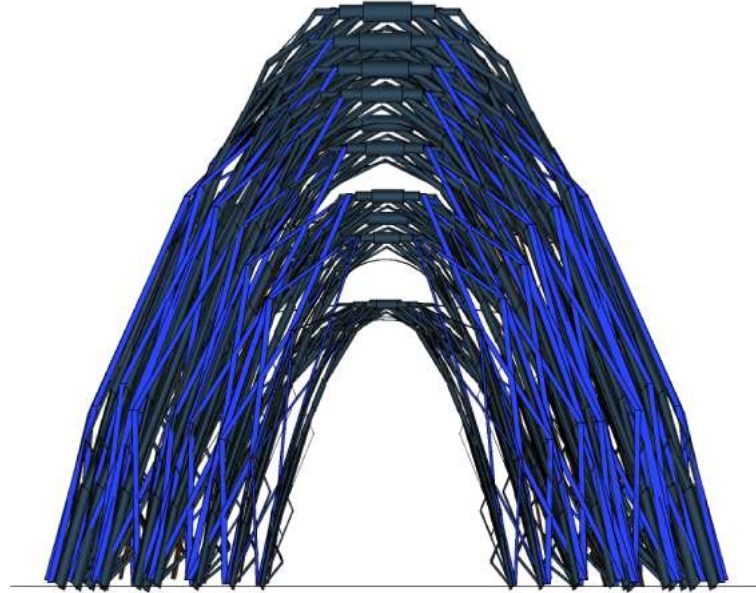


(a) Plan view

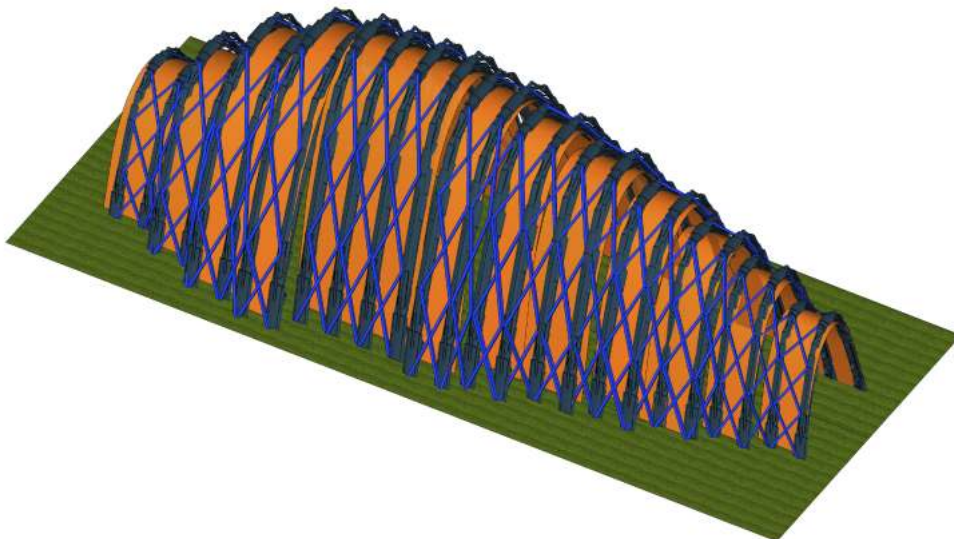


(b) Side view

Figure 5.12: Conceptual design of exhibition dome: optimised catenary arches



(a) Façade



(b) Isometric view

Figure 5.13: Conceptual design of exhibition dome: optimised catenary arches

scheme.

In this particular design scenario, a uniformly distributed load (or UDL) was applied over the horizontal length of the permissible design region, which had varying height. The UDL was in fact applied as a ‘transmissible’ load, i.e. a load of given magnitude and direction to be applied at any potential node along the same line of action of the load - see Appendix A.4.

Referring to Fig. 5.11, the resulting optimised structures are the dark blue-grey, vertical catenary arch structures (Fig. 5.11(a)). In conjunction with the optimised arches, bracing elements (light blue) were retrospectively added for lateral stability (Fig. 5.11(b)). Note that these bracing elements were added manually for demonstration purposes, and would need to be checked later in the design process. The significance of this particular design example lies in the fact that it explores a scenario where an initial form is derived by optimisation, and further, conventionally derived, design elements are added subsequently, by conjunction.

The use of catenary shapes in architectural design, either in 2D or 3D is not new, as they can be seen in arch designs of many of Antonio Gaudi’s buildings and Heinz Isler’s thin concrete shell shelters, derived from inverted hanging chains and hanging nets, respectively [203]. This perhaps calls into question the novelty of these forms and the method used to generate them. However, as it is known, physical modelling entails a very complex process (e.g. issues with scalable dimensions and unscalable material properties) and empirically found forms are difficult to replicate as scale modelling effects and loading conditions will be different in each case. This is one of the reasons why, for example, despite the novelty of his forms, Heinz Isler’s method of physical hanging nets modelling did not become more widespread [204] - computational optimisation is less time-consuming and more comprehensive than physical modelling, with a capability to handle much more complex load cases than uniformly distributed loads and with higher precision¹.

¹It must also be noted that, although for ease of reference the word ‘catenary’ was chosen to describe the form of the arches used in this study, the actual shapes depend on the support

Additionally, discretisation or segmentation of the catenary (or other shapes) into individual members of non-uniform length (as shown in this study) or uniform length (grid structures), is not trivial, and is the subject of much research effort (e.g. 3D freeform discretisation [43][206]).

5.3.3 Pharaonic Village Project

Here the brief was to design a children's games area, covering an area of 20m by 20m located on an Egyptian-themed restaurant complex in the Middle East.

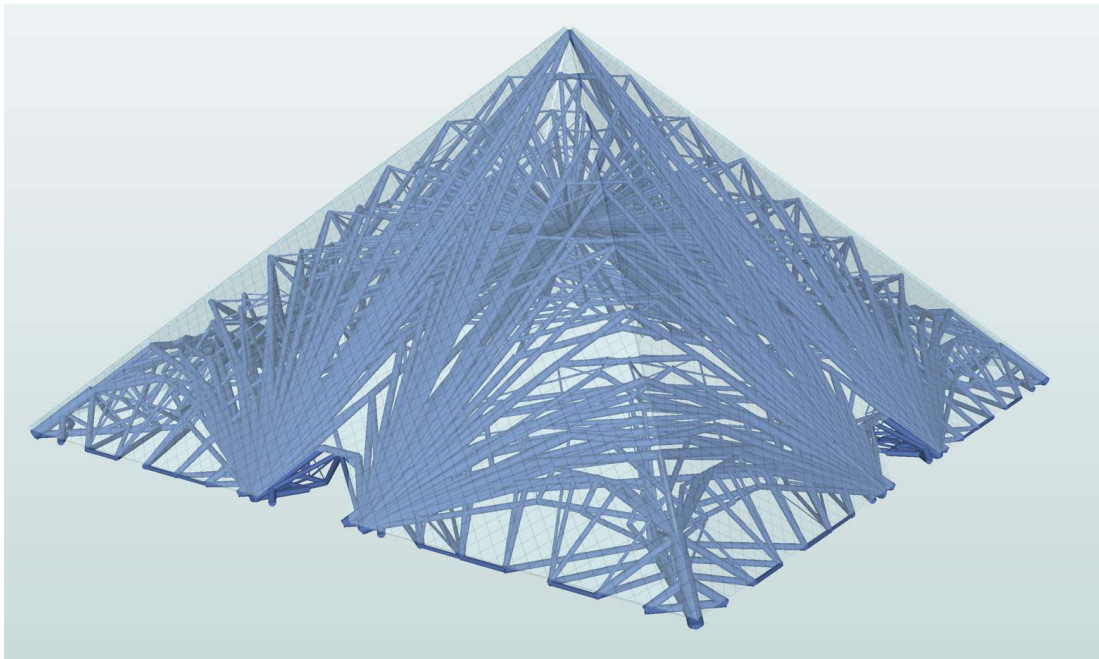


Figure 5.14: Conceptual design of glass pyramid, obtained using structural layout optimisation.

conditions etc. Also the catenary is not an absolute optimum shape of an inverted tensile material when this gains thickness. Further optimised shapes are possible, as shown in Darwich's work [205].

To be in keeping with the Egyptian theme, the requirement was to create a glass-clad pyramid, with its sides inclined at 45-degrees. i.e. the external envelope was prescribed at the start of the design process, but the means of supporting this was left unspecified. It was also required that each face of the pyramid should have a central opening at ground level. To identify a suitable supporting structure the structural layout optimisation tool was used. Assuming symmetrical loading (vertical and horizontal) and geometry, only one eighth of the structure needed to be modelled. Point supports were specified at the corners of the pyramid and to each side of the ground level openings. The permissible design domain was limited to ensure that structural members would not intrude excessively into the internal usable space. Initial results are shown in Figs 5.15 and 5.16.

It appears that the structural solution obtained using the layout optimisation tool is over-complex, especially considering that at the initial stage it is basic design concepts that are usually being sought. However, essential features or design principle of the solution can be extracted for use in later stages of the design process. For example, Fig. 5.16 shows a simplified version of the same basic design (simplification was achieved via a semi-automatic procedure which involved firstly filtering out very small members, then manually removing selected members in congested areas). The simplified version clearly reveals the essential, and apparently novel, structural principle at work (i.e. an elevated central node from which many members radiate), and provides a solution with uninterrupted floor space as required.

5.3.4 Canopy for Roof Terrace in Multi-storey Building

This scenario involves redesign of a sloping canopy roof for a multi-storey office building to be constructed in central London (size: 35 x 40 m in plan). There existed sufficient justification for a redesign of the glass-clad roof terrace canopy on the premise that transparency of glass-cladding should be seen as an opportunity to transfigure the supporting structures into elements which go beyond their designated structural functions, thus, into elements of aesthetic purpose.

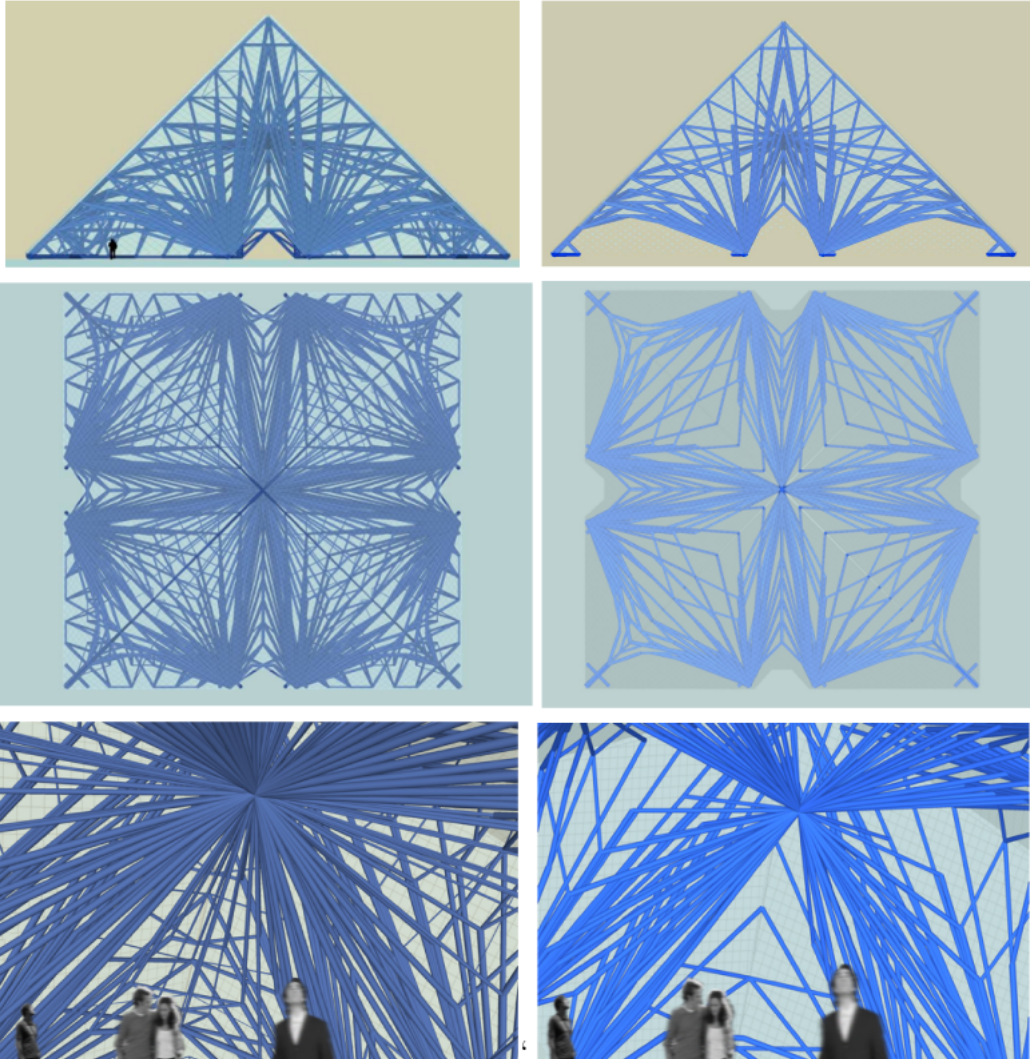


Figure 5.15: Conceptual design of glass pyramid obtained using structural layout optimisation - initial detailed solution: (a) side view; (b) plan view; (c) internal view.

Figure 5.16: Conceptual design of glass pyramid obtained using structural layout optimisation - subsequent simplified solution: (a) side view; (b) plan view; (c) internal view.

In this example real design load data was used, thereby in principle allowing the solution generated to be compared against the more conventional beam-grid design which was arrived in practice; see Fig. 5.17 for the original final design.

The design solution is shown in Fig. 5.18, Fig. 5.19 and Fig. 5.20. The solution has significantly more visual interest than a conventional beam-grid design, provides an uninterrupted floor space and also appears much more structurally efficient ($< 10\%$ of the weight ¹ of the adopted beam-grid design), though care must be taken in comparing the result from a relatively simplistic optimisation with the real design which will inevitably have rationalised the number of different members and required them to fit a more regular grid to simplify glazing details, and in which all members will have been designed to meet the requirements of building codes with adequate factors of safety. Nevertheless, the very large potential weight saving is noteworthy and perhaps gives an indication of how economy of material use is currently highly subordinate to simplicity of construction).

¹The original structure consists of approximately 130 structural members, which measure $16.18m^3$ in volume, whereas the optimised redesigned form consists of approximately 560 members, measuring only $1.037m^3$. However, it is imperative to note that while the design through optimisation considered design load cases of operational live loads, dead loads, environmental loads, and contingencies, the structural design to a regulatory code is much more thorough as it design, to ensure safety, against every imaginable scenario, e.g. joint fatigue design, extreme weather conditions, thermal loading, fire, seismic activities.



Figure 5.17: Original canopy for roof terrace: in context of the main building framing elements

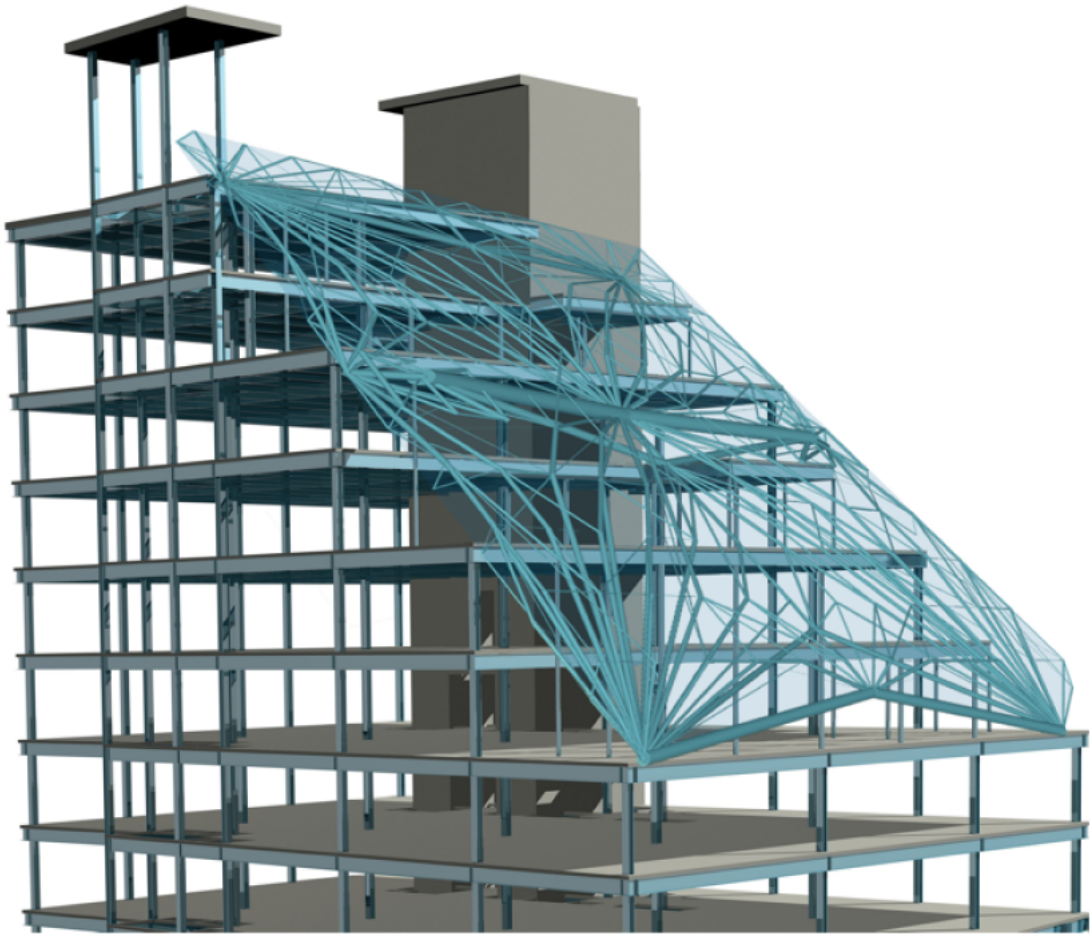


Figure 5.18: New canopy for roof terrace: in context of the main building framing elements

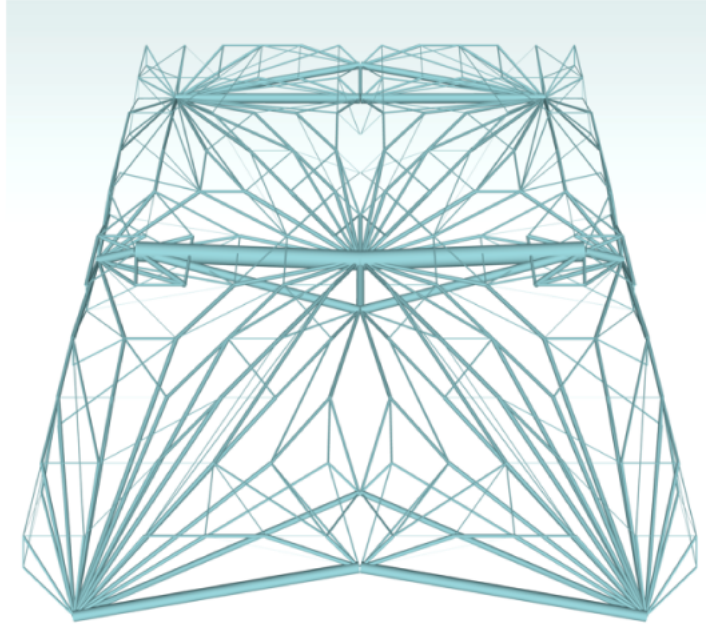


Figure 5.19: New canopy for roof terrace: front view.

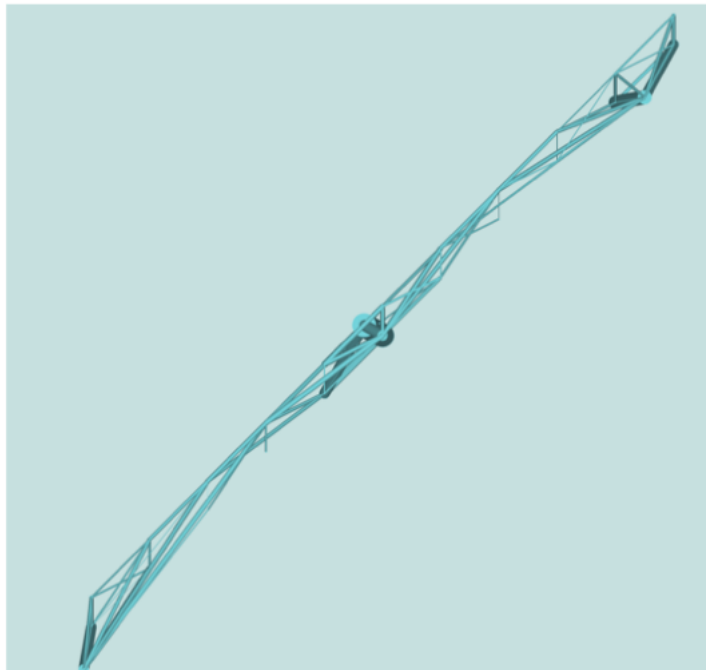


Figure 5.20: New canopy for roof terrace: side view.

5.3.5 Roof Vault

This example is not unlike the catenary arches used in the Exhibition Space example in Section 5.3.2 in that it uses uniformly distributed transmissible loads, although in this example in 3D. Other design constraints are pinned supports at the four corners of the vault and an elevated pinned support at the centre of the vault; see Fig. 5.21 - 5.24

Fig. 5.21 shows a ‘quarter model’, to better show the form. The shape is a discretised near-catenary, reminiscent of Heinz Isler’s concrete shell shelters, derived from inverted hanging nets; note that the flat shape at the top is the result of coarse nodal discretisation employed. This example demonstrates two capabilities of truss layout optimisation, which could be of interest to architectural form designers: form-finding capability and simultaneous discretisation of surface into a visually expressive grid. It is worth noting, however, that the generated grid pattern is different from other methods which generate architectural geometries or which refine a grid mesh (e.g. Helmut Pottmann or Culter’s work).



Figure 5.21: Roof vault design - a quarter model in a discretised, near catenary shape.

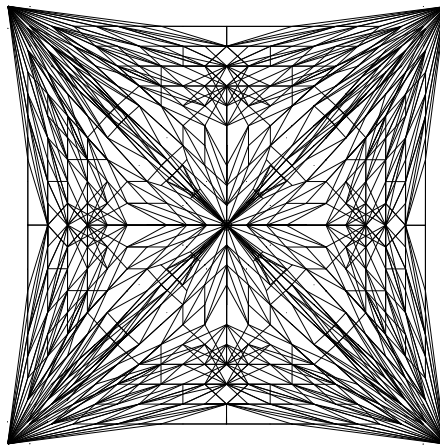


Figure 5.22: Roof vault design: top view in parallel projection

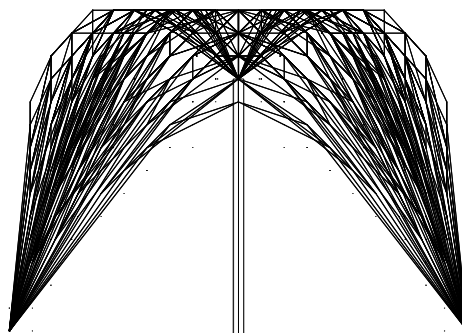


Figure 5.23: Roof vault design: elevation view in parallel projection

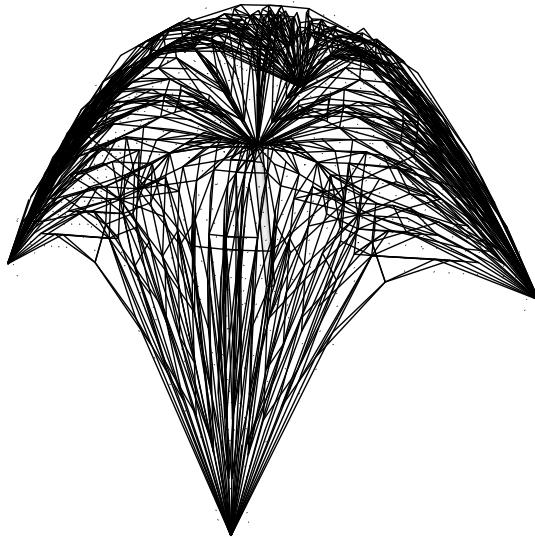


Figure 5.24: Roof vault design: isometric view.

5.4 2D usage Design Examples

5.4.1 Bicycle Canopy

The brief for this project required design of a bicycle-canopy on a site measuring approximately $23m \times 13m$, surrounded by university engineering buildings. Although there was already an existing bicycle parking facility on the site, there were no obvious visual indications that the facility existed and it lacked contextual identity. Thus the aim was to design a canopy with a distinctive structural aesthetic, appropriate for a site surrounded by engineering buildings.

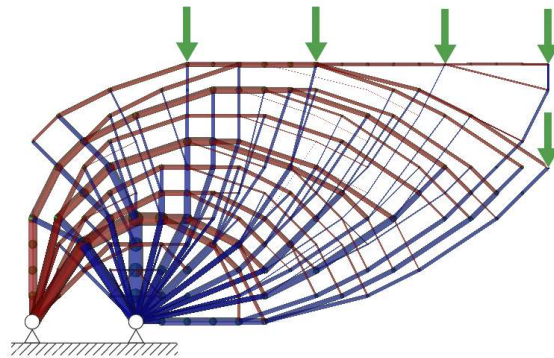
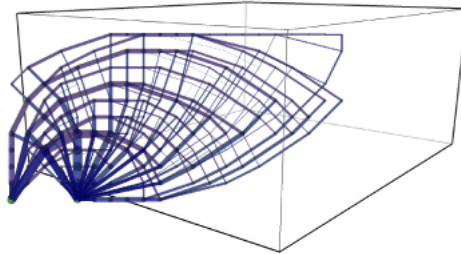
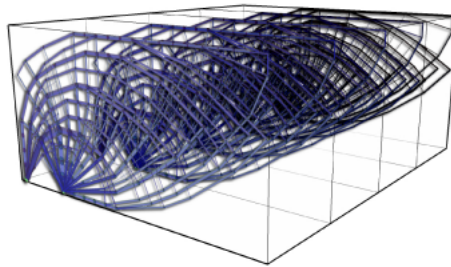


Figure 5.25: 2D original optimised structure with two fixed pinned supports: green arrows represent applied forces, tensile members are denoted in red and compressive members in blue.

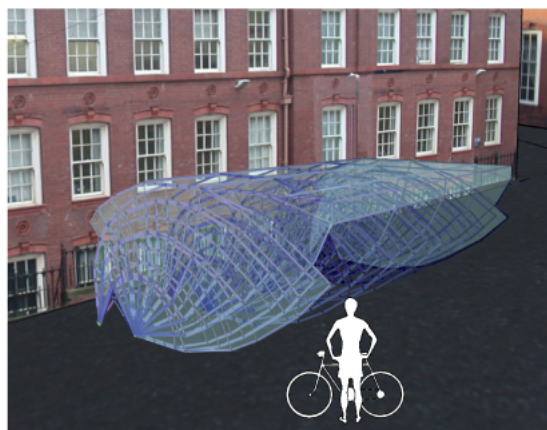
Fig. 5.25 shows the complex truss form generated by the structural layout optimisation procedure. This 2D structure was generated by taking into consideration the supports and appropriate vertical roof loads, together with an effectively unrestricted design domain and sparse distribution of potential nodes. In Fig. 5.26, the structure is duplicated along an axis to form a 3D frame; supplementary elements could be added between them to ensure lateral stability.



(a) The original generated form and the 3D design domain space



(b) Multiple replicated of the original in the 3D design space



(c) The initial concept design in its locational context

Figure 5.26: Bike canopy: 2D planar optimisation and replication approach

5.4.2 Façade Design

Fig. 5.27 shows the initial loading and support conditions and design domain for a simple 2D design problem, and also the resulting ‘tree-like’ optimised structure.

Fig. 5.28 shows application of the optimised structure in a generic façade design, in which a clearly expressed structural form is surrounded by glass-cladding in a building façade. This form is reminiscent of Frei Otto’s hanging models of tree-like branching systems [207] and those of the Stuttgart Airport Passenger Terminals [208], designed by Gerkan, Marg und Partner. Although, both were three-dimensional, their essential orthogonal planar (albeit replicated) qualities make these precedents relevant to this example. Through this benchmarking example, the ability of LP layout optimisation to generate rapidly and without extensive laboratory experiment, structures, similar to those which have already been realised and constructed, further demonstrates its relevance and suggests a potential role in architectural design.

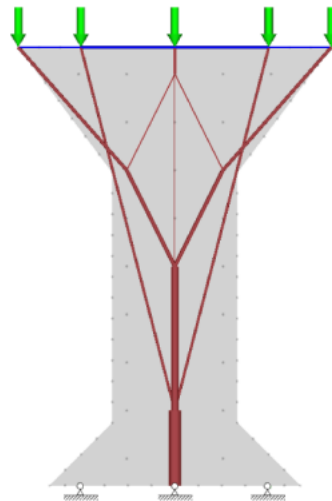


Figure 5.27: 2D original optimised structure for Façade design

It is evident that the generated form is relatively simple, being composed of only 12 compressive members and 4 tensile members per structural unit. This simple

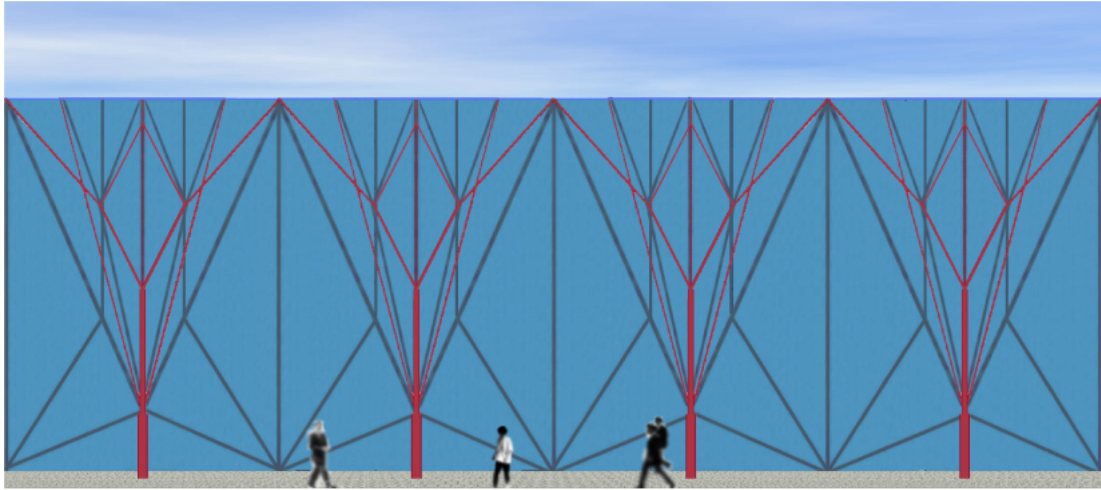


Figure 5.28: Façade design: 2D planar optimisation and replication example



(a) Branching system model by Frei Otto [207]

(b) Stuttgart Airport Passenger Terminals by Gerkan, Marg und Partner (Photograph: James Bowes)

form is therefore in a sharp contrast with the forms shown in Fig. 5.25 and previously in Fig. 5.14. This can be explained by the restrictive outline of the design domain and the sparse spacing of nodes positioned within the design domain. This implies that architectural intuition could usefully be used when defining the design domain and, particularly, the outer geometry. This also highlights the fact that, whilst employing a dense grid of nodes in a design domain may generate forms closer to the true mathematical optimum, a sparse grid may be more

practical when designing architectural forms/structures. Unfortunately the use of sparse grids can also result in failure to produce viable solutions, and thus this is not really a practical remedy for over-complexity i.e. there is clearly a need for a more systematic method of simplifying over-complex ‘optimum’ forms.

5.4.3 Window Frame Design

This particular example is not architectural/structural design in the conventional sense. However, it is provided here in order to demonstrate the feasibility of the engineering tool and its rationale behind it, as a form generation tool in a smaller scale - although the enlargement of design domain and force considerations would easily be applied to such as courtyard roofs. Fig. 5.29 shows the design domain and loads with nodal arrangement for nodal density target number of 100 as an example.

Figs. 5.30 shows 4 window frame patterns, optimised for the same arbitrarily given loads. The final results differ because of the variation in input nodal density. Whilst these solutions are products of a simplified load case considering only uniformly distributed loads and not the products of a detailed structural design code, they present a very useful starting point for form design, especially, if a high degree of integration is sought between structural principles and satisfactory aesthetics in the final product.

A contemporary, existing design, comparable to the generated forms, is the recently constructed Dutch Maritime Museum (designed by Ney and Partners), whose irregular mesh steel-glass structure covering the square courtyard was inspired by a loxidrome map with 16 wind roses before a dynamic relaxation technique was applied to project the 2D mesh onto a 3D shell to find catenary shapes [2]. See Fig. 5.31. A noticeable, aesthetic similarity exists between the roof structure and Fig. 5.31 and Fig. 5.30(a).

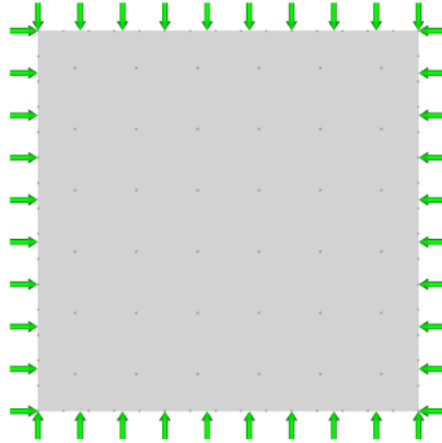
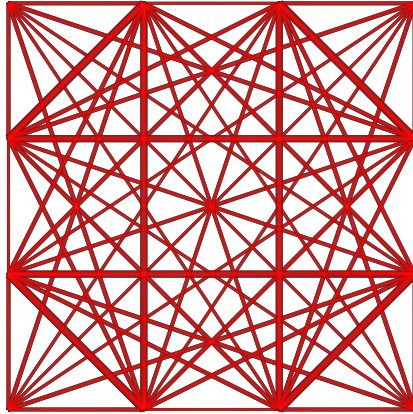


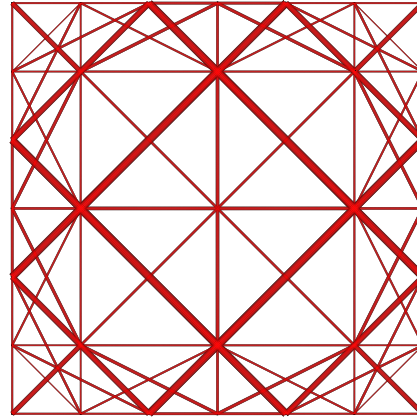
Figure 5.29: Design domain and loads for window frame with nodal density target number of 100

In addition to the high level of design integration between form and structure, another of notable strength of the presented design method is that, by simply varying a pre-settable design parameter, the nodal density in this case, similar but distinct forms or layouts may emerge, making the method flexible. This is particularly useful in design as this is an effective way of responding to frequent changes in design conditions and constraints. Furthermore, assigning different priority levels to different aspects of design can easily be managed. For example, in general, the denser the initial nodal density, the more lightweight the resulting form will be. However, being lightweight may also mean higher fabrication costs due to higher number of member joints. However, in the light of recent advancements in CNC machining and 3D printing technologies¹, the task of regularisation and simplification in order to lower fabrication costs may become less important than the overall weight of the structure. This hence leaves important design decisions to users, in accordance with different needs and requirements.

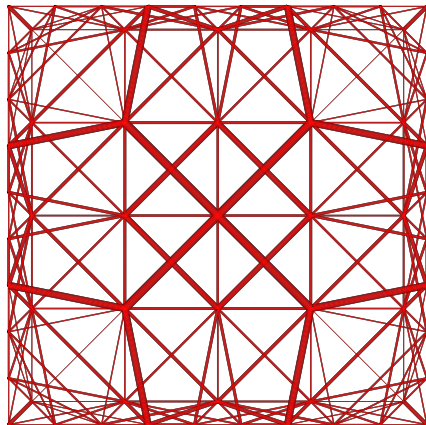
¹Solid freeform fabrication technology or 3D printing builds layer by layer objects of freeform complex geometry, for which commercially available systems exist albeit in small scales. These have the advantage of being able to fabricate any shape by employing various materials including liquid polymers and steel, of either homogenous or multiple composition [209][210][211].



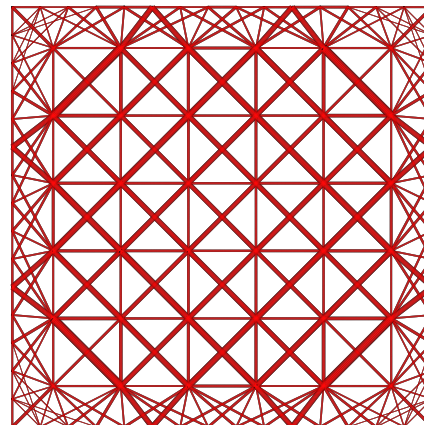
(a) Window frame, generated with target nodal density of 14 nodes



(b) Window frame, generated with target nodal density of 44 nodes



(c) Window frame, generated with target nodal density of 68 nodes



(d) Window frame, generated with target nodal density of 100 nodes

Figure 5.30: Window frame patterns, optimised for given loads, differing in their nodal density

5.5 Discussion

The design examples considered have revealed at least two useful usage patterns for conceptual form generation. The structural layout optimisation tool described could for example be used in the following modes:

- **‘Full Automatic’**: In this mode the user specifies the bare minimum of

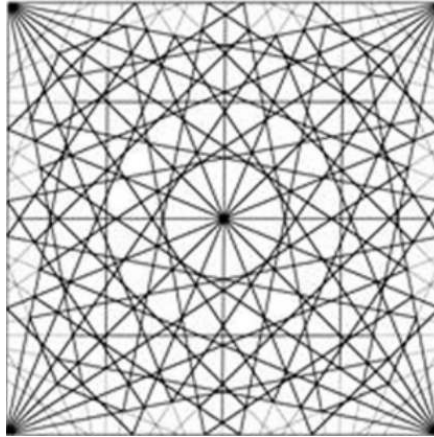


Figure 5.31: The Dutch Maritime Museum: courtyard roof form-structure [2].
Design: Ney and Partners

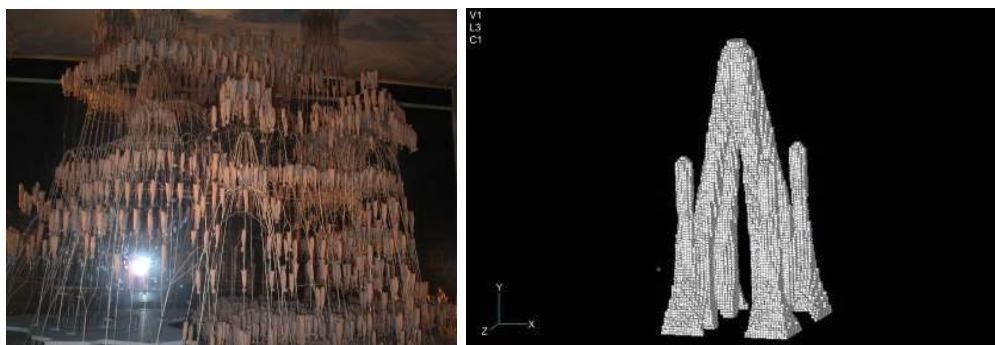
design constraints prior to carrying out an optimisation. This has the potential to yield interesting, possibly ‘emergent’, forms, with no predefined geometry to restrict either the outer envelope or the internal arrangement of the truss members of the final form.

- **‘Optimisation with Prescribed Outer Geometry’:** In this mode the geometry of the outer envelope is fully or partially prescribed by the user prior to carrying out an optimisation. A possible application includes rationalisation of the layout and sizes of internal structural members in a design solution where the outer geometry has already been finalised. Areas where members must avoid can also be specified if required.

It should be noted that the design study described in Sections 5.3.1 (‘Thinking Pods’) and 5.3.5 are essentially an example of the ‘Full Automatic’ method whereas that described in Section 5.3.3 (‘Pharaonic Village Project’) is an example of ‘Optimisation with Prescribed Outer Geometry’. The design study described in Section 5.3.4 (Canopy for roof terrace in multi-storey building) is also an example of ‘Optimisation with Prescribed Outer Geometry’, although the original geometry was adjusted slightly in order to achieve the desired effect. The Exhibition Space in Section 5.3.2 is a combination of the two usage modes, where

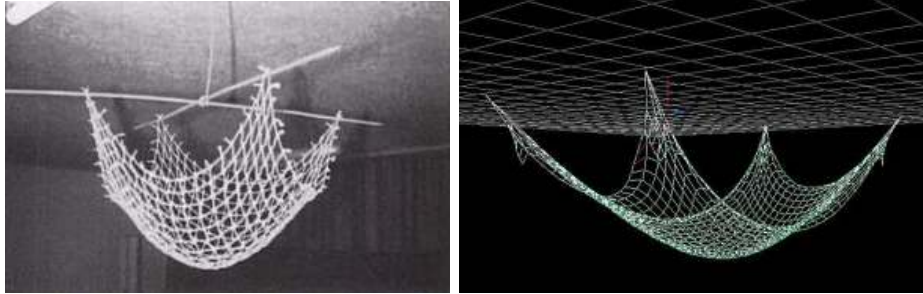
the horizontal geometry in plan is prescribed, but definition of the vertical geometry of the space in elevation is left for the computational optimisation process to determine.

A question may be raised with regard to novelty of some of the generated forms, particularly those considered in *Section 5.3.2* which are in essence a series of simple catenary arches, whose form could be determined by simple inversion of cable elements. Thus on the one hand, it could be stated that the results obtained are merely ‘encouraging’. On the other hand, it could be concluded that the power of a novel method has been demonstrated in this section, which stands as strong as methods which attempt to replicate (or replace) any former iterative physical experimental approaches. One such example is the work of Xie *et al.* [52], which attempts to replicate, by employing an evolutionary structural optimisation method, Gaudí’s experimental design method of employing hanging chains and weights, see Fig. 5.32. This is also analogous to a number of form-finding methods which simulate gravitational response of fabric or cables such as dynamic relaxation and in Kilian’s case [53], particle-spring systems, replicating the said response, to regenerate structures comparable to the hanging nets used by Heinz Isler, see Fig. 5.33.



(a) Inverted image of Gaudí’s physical model. Source: math.upenn.edu. Accessed: 10/11/2012 (b) Computer-based replication. Source: [52]

Figure 5.32: Hanging chain models



(a) Physical model. Source:[203] (b) Computer-based replication. Source:[53]

Figure 5.33: Hanging net models

5.6 Conclusions

1. The longstanding divide between the technical and visual aspects of architecture does not appear to be being bridged by current and emerging computer-based design tools, notwithstanding the apparent integrative nature of some tools (e.g. Building Information Models). Furthermore, because of the visual nature of the interaction between a computer and user, it may be argued that such computer-based tools are even strengthening this divide.
2. Structural layout optimisation is a technology which has the potential to provide the architect with the ability to rapidly identify concept designs which are intrinsically structurally sound. This technology has demonstrated its capability of conceptual form generation, form-finding and simultaneous meshing and therefore has the potential to play a small part in integration between the technical and visual aspects of architecture in design process.
3. In this chapter the structural layout optimisation technique has been applied to a number of conceptual design problems, allowing several potential usage patterns to be identified. For example, when minimal design constraints are imposed the technique can yield interesting emergent forms; when the technology is applied to design problems where the outer envelope has already been fixed, the technique can be used to identify efficient locations for supporting framing elements.
4. Example design studies have highlighted that further work is required to increase the power and flexibility of the structural layout optimisation tool used in this study. Specifically, the issue of impracticality due to complexity is highlighted, to ensure design relevance of the tool in architectural form design. Additionally, whilst the optimisation algorithm is capable of conceptual form generation of conventional structural configuration, form generation of unconventional structural configuration is yet to be investigated. This is fully explored in *Part III*.

Postscript

This subsection includes a brief discussion on the role of the Graphical User Interface (or GUI), a topic beyond the main scope of work in this thesis, though is of interest in relation to the work carried out in this chapter.

5.6.1 Graphical User Interface

One of the findings of this chapter was that the process of form-generation using the particular optimisation formulation employed can be prohibitively stringent, i.e. form-generation was essentially a one-step process from input to output, offering little controllability to designers. Hence, addition of form modification functions is suggested as an area requiring further development.

An optimisation-driven synthesis tool can potentially be a useful tool for architects, who wish to synthesise reference forms which are potentially structurally optimal or guaranteed to be structurally sound and, most likely to be constructible. Upon further analysis of the existing tool¹, it was judged that its user-interface lacked the features which were intuitive to mouse-accustomed users.

Interactive functions such as form modification or generation function, should be incorporated. The findings in the design process of the three projects in *Part II* clearly show the need for more flexible manipulation of initially generated forms.

Fig. 5.34 and 5.35 are simple illustrations of a process in which variations of an initially optimised form can be generated. The four main stages are named as: *Optimised, Extruded, Distorted and Re-facilitated*.

- **Stage 1: Optimised form** represents the initial optimised form, automatically synthesised with given load and support conditions.

¹The existing tool refers to a structural optimisation tool being developed at the University of Sheffield

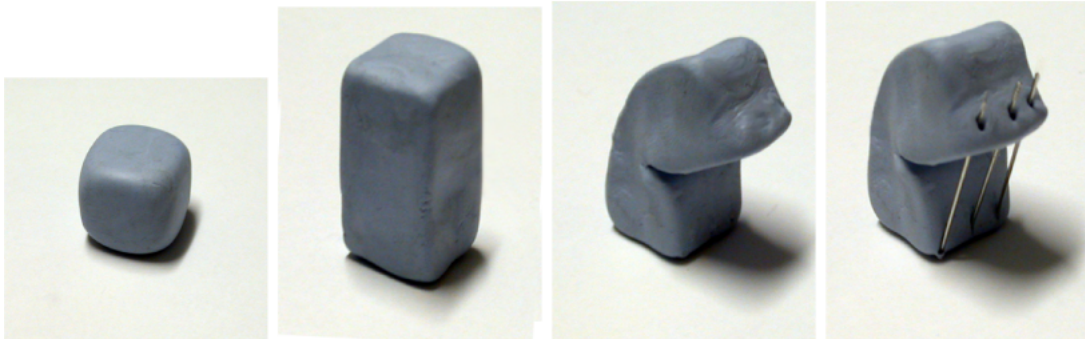


Figure 5.34: ‘Metamorphosis from a cube to a distorted cuboidal shape along a horizontal axis with reinforcement

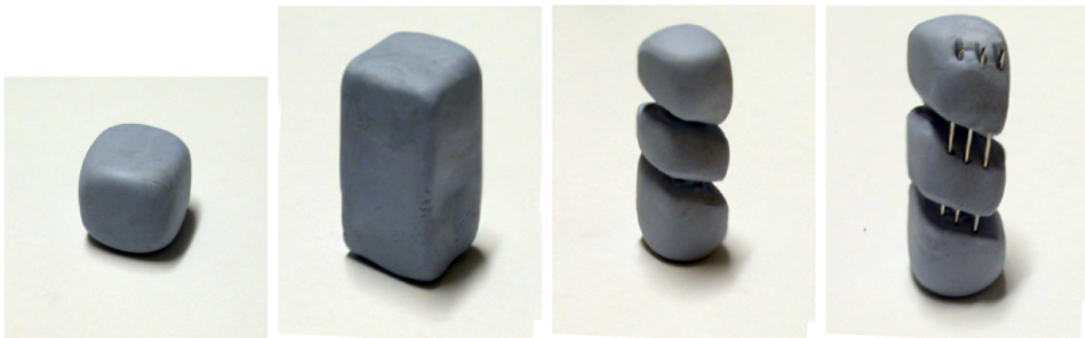


Figure 5.35: ‘Metamorphosis’ from a cube to a rotated cuboidal shape about a vertical axis with reinforcement

- **Stage 2: Extruded form** represents the linear transformation of the initial optimised form. Between Stages 1 and 2 the previous load conditions are temporarily removed.
- **Stage 3: Distorted form** represents the non-linear transformation of the initial optimised form. Between Stages 3 and 4 the previous load conditions under which the optimised form was initially generated, are placed back on the structure.
- **Stage 4: Re-facilitated form** represents the re-facilitated form with possible addition or removal of members.

Fig. 5.36 shows a truss structure example of the same conceptual modification process.

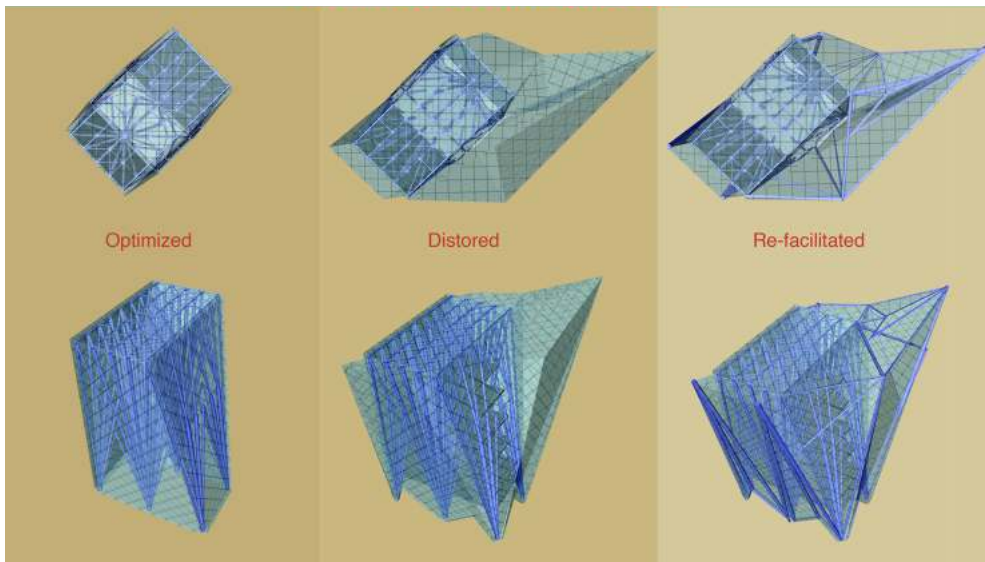


Figure 5.36: 'Metamorphosis': a modification process of a truss structure.

Part III

Generation of Conceptual Form of an Unconventional Structural Configuration: Tensegrity

Preface

The issues found when using form-led design approaches for geometry-generation in architectural design have been critically reviewed in *Part II*. One of the principal issues was the acceptance of ‘geometry-generation’ as ‘form-generation’ whilst overlooking the importance of structural considerations.

Having recognised structure as an inherently integrative aspect of building design, a structural optimisation technique has been proposed to address the issues, amidst a growing development of integrative design methodologies of the recent past. The investigation led to application of the existing linear programming (LP) formulation at an early conceptual, preliminary, phase of design, to conceptual form generation of conventional structural configuration and the results have been presented in *Part II*.

It was found, however, that the forms generated using LP (and hence, use of engineering rationale for conceptual form generation), with such structural aesthetics, exhibited evidence of impracticality and the need for improvement with regard to their complex layout of internal truss members.

The issue of complexity of optimum structures generated using LP, is, in fact, a known issue in engineering applications, for which there are remedial strategies. However, when this issue was identified in engineering, the problems considered, typically included either small-scale simple grillage structures or unrealistic, theoretical loading conditions¹, in contrast to the realistic conditions used for the forms in *Part II*. Moreover, most remedial strategies focused on reduction of complexity through *standardisation of individual members* from a given set of available members, rather than concerning methods of simplification for general form.

In contrast, the use of mixed integer linear programming (or MILP) can be used to affect the general form by applying a constraint on the total number of mem-

¹e.g. single point load at one node in Michell structure

bers in the final structure.

Hence, the first chapter of *Part III*, Chapter 6, presents, a simple implementation of an additional, mixed integer linear programming (MILP) constraint to the existing LP formulation¹. This additional constraint provides an effective method of resolving the issue of over-complex optimal structures in the existing formulation. This same algorithm extends to include a related capability of conceptual form generation of unconventional structural configuration, namely tensegrity in the latter half of this part.

¹which were employed to generate the forms as shown in *Part II*

Chapter 6

Obtaining More Practical Solutions using Mixed Integer Linear Programming

6.1 Abstract

Over-complexity¹ of optimum structures generated using LP, has been a known issue in engineering applications, for which there are remedial strategies. However, most strategies focus on reducing the level of complexity through standardisation of *individual members*, by selecting from a given set of readily available sections, rather than, on devising methods of simplifying the *general form*.

In this study, a method of reducing the level of complexity in the final optimum structures is explored using mixed integer linear programming (or MILP). A simple incorporation of MILP formulation into the existing LP layout optimisation formulation, is presented with a view to providing designers with a capability to control the outcome of final structure. In addition, parametric studies are conducted in order to understand the behaviour of the formulation.

¹i.e. a high number of active nodes and subsequent number of members in the final optimum structure

6.2 Introduction

Optimum form such as Michell structures [70] and their derivatives [99] are only optimal in terms of their total weight or structural volume. In practice, many of this class of structures comprise very many, extremely small structural members. Indeed, in many cases, Michell structures contain regions that have an infinitely rich microstructure; effectively an infinite number of infinitesimally small elements. Clearly, in addition to being practically impossible to construct, such structures would not be remotely ‘optimal’ in terms of overall cost.

This over-complexity in structural optimisation is a well-known problem [134] and there are a significant number of resolution strategies, the most common of which is to standardise the member cross sections by selecting from a pre-defined set of tabulated data. For example, an iterative LP method was used in [135], in which the problem was defined in terms of existing available steel sections. At each iteration, the stress level in each compression member in the solution is checked against the permissible level of stress as recommended by the design code; if any stress exceeds its permissible level, another value is used for the stress in the member and the iteration continues. When the same section type is chosen for all members in two successive iterations, the search process terminates.

Olhoff and Taylor [212] considered a general post-optimisation strategy for modification of design called, ‘*structural remodelling*’, where the objective is to provide an appropriate modification to a given initial design. Structural remodelling is categorised into either ‘reinforcement only’, where the initial design stays the same and ‘compound remodelling’, where members may be added to or taken away from the initial design with a specified total cost.

In a more recent example [213] an FEA-based ESO was used with direct discrete design variables in element size optimisation problems, where solutions were obtained by simple repetitions of analysis and element reduction; element thickness was reduced gradually to the next lower values from the given sets, using ‘sensitivity numbers’. However, the degree of realism achieved for individual members in

the above optimisation methods, is less relevant in relation to conceptual form-generation as the identified issue in architectural concept design concerns user controllability over the *general form* of the structure as opposed to *individual member sections*.

Another common approach involves the inclusion of ‘penalty’ variables in the objective function. For example, Parkes [134] introduced the concept of ‘joint cost’. The approach defines the material penalty involved in fabrication of joints of frame structures. By assuming the material cost of transferring a force from a member to a connection is proportional to the transferred force and, that the force in a member is proportional to its cross-sectional area, it essentially adds a constant length j (joint cost) to each member at a joint. Similarly, Prager [214] included in the objective function, the weight of joints in addition to that of structural members, thereby restricting the level of complexity of general form of optimised structures.

Because of the known issues when using discrete integer variables¹ and due to the computational complexity, (i.e. harder to solve) [216], mixed integer linear programming (or MILP) formulations or ‘member reduction’ approaches using MILP have been used to a lesser degree, than the previously described approaches.

Tyas [217] suggests a number of ways in which integer variables might be used to allow constraints restricting the number of allowable ‘active members’ either in a given region of the structure, or in the structure as a whole. The classical ‘ground-structure’ truss layout optimisation formulation has traditionally been formulated as a size optimisation problem, which can then be conveniently solved using linear programming (LP) algorithms. However, in a conventional size optimisation problem no distinction is made between truss bars with positive area and those with zero area. (i.e. all bars in the original ground structure will be present in the final optimal solution, though some - usually the vast majority will simply

¹, i.e. considerable increase in the solution runtime, and some undesired inevitable weight-increases [215]

have zero area). The traditional LP approach cannot differentiate between active members that are actually present in the final optimum form, and members with zero cross-sectional area, carrying zero ‘load’. Put another way, in an LP formulation, an area of zero carries no special significance, whilst, obviously to a human designer, a member with a cross-sectional area of zero is qualitatively different one with non-zero area. The basic LP formulation is therefore unsuitable when constraints on the numbers of active bars (i.e. bars with non-zero area) in the final structure need to be imposed. Tyas’s suggestion was to introduce a binary variable for each member, to act as a signifier or ‘flag’ as to whether the member had zero (0) or non-zero(1) cross-sectional area. Constraints could then be imposed on the total sum of all these ‘flag’ values in the entire structure, or within a sub-set of the structure.

To the same intention, Ohsaki and Katoh [218] formulated a method of a MILP lower bound and a non-convex non-linear programming (NLP) upper bound, considering member intersection and nodal stability. However, the extent to which MILP variables affect the solution runtime, has not been fully investigated in the context of simplification of overcomplex structures. Most recently, Hagishita and Ohsaki [219] have used a heuristic method called Topology Mining¹ for topology optimisation of framed structures, where the problem is formulated using binary mixed integer non-linear programming.

The following presented work builds on the formulation of restriction of the total number of members in [217], by writing a computer code and conducting parametric studies, to test and observe the ‘behaviour’ of the formulation, and in turn, to provide the user the option of determining the upper limit² to the maximum ‘desired’ number of members in the final structure for simplification and ultimately better constructibility, with the use of MILP.

¹TM is explicitly integrated with non-linear programming and uses a technique of data mining to extract the sets of members that frequently appear in superior solutions and pass them on to generate candidate sets for the next iteration [219].

²inequality constraints

6.3 Formulation

Linear programming (or LP) is concerned with optimisation, where the variables in the objective function and the constraints can be defined linear. However, the optimisation problem is called a mixed integer linear programming (or MILP) problem if some of the unknown variables are required to be integers alongside the non-integer linear variables. Binary mixed integer programming is a special case of MILP where the integer variables are required to be either 0 or 1. The equilibrium LP plastic design formulation to solve for the minimum volume [220] for a ground structure subjected to a single load case and containing m members and n nodes are stated as follows:

Minimise,

$$V = \mathbf{q}^T \mathbf{c} \quad (6.1)$$

subject to:

$$B\mathbf{q} = \mathbf{f} \quad (6.2)$$

$$q_i^+, q_i^-, \geq 0, i=1, \dots, m \quad (6.3)$$

where V is the total volume of the structure, \mathbf{B} is a suitable $(2n \times 2m)$ equilibrium matrix, $\mathbf{q}^T = \{q_1^+, -q_1^-, q_2^+, -q_2^-, \dots, q_m^+, -q_m^-\}$, $\mathbf{c}^T = \{l_1/\sigma_1^+, -l_1/\sigma_1^-, l_2/\sigma_2^+, -l_2/\sigma_2^-, \dots, l_m/\sigma_m^+, -l_m/\sigma_m^-\}$, $\mathbf{f}^T = \{f_1^x, f_1^y, f_2^x, f_2^y, \dots, f_n^x, f_n^y\}$; $l_i, q_i^+, q_i^-, \sigma_i^+, \sigma_i^-$ represent the length, tensile and compressive member forces and stresses in the i^{th} member, respectively. And lastly f_i^x, f_i^y are the x and y direction live load components applied to node j .

6.3.1 Introduction of Binary Variables

The continuous LP problem variables are the member forces, q_i^+, q_i^- and the additional constraints are k_i , a binary variable for every member i either in tension or compression, which indicates whether one of the m number of potential members

in the ground structure, is added in the solution [217] [218].

$$\frac{A_i}{R} \geq k_i, k_i = 1 \text{ or } 0 \quad (6.4)$$

A_i is the area of member i and R is the reduction factor; a constant value chosen arbitrarily to be greater than the maximum expected value of A_i .

Relation 6.4 requires that k_i , the binary flag for member i be > 0 if $A_i > 0$. But the requirement that k_i take only binary values immediately requires that $k_i = 1$ if $A_i > 0$. Thus, we now have a flag that will take the value 1 if the member actually exists with positive cross-sectional area. There is no explicit requirement that the flag take the value 0 if the corresponding cross-sectional area is zero. However, if the value of the objective function will be improved by taking these values to be zero, the optimisation process will be expected to automatically take this option. It is clearly vital that R be sufficiently large in magnitude that the value of A_i/R will always be ≥ 1 , otherwise the constraint in Relation 6.4 cannot be satisfied.

On the other hand, using an unnecessarily large value for R will make the value of $A_i/R \leq 1$. This may lead to problems with the stability and efficiency of the MILP solver. This is because MILP solution strategies generally progress by initially ignoring the integer or binary constraints, solving the relaxed LP problem, then progressively investigating the consequences of forcing the requisite variables to their integer/binary values. Therefore, if A_i/R is non-zero, but very close to zero, the MILP approach may either assume that the value actually is zero (due to numerical round-off) or have difficulty in forcing the variable to the (required) value of 1. Choosing a suitable value of R is therefore of great importance in any given problem context.

Relation 6.4 can be rewritten as:

$$\frac{1}{R} \cdot \mathbf{q} \geq \mathbf{k}^T \boldsymbol{\sigma} \quad (6.5)$$

where $\sigma^T = \{\sigma_1^+, -\sigma_1^-, \sigma_2^+, -\sigma_2^-, \dots, \sigma_m^+, -\sigma_m^-\}$ and $\mathbf{k}^T = \{k_1^+, -k_1^-, k_2^+, -k_2^-, \dots, k_m^+, -k_m^-\}$.

Eqn. 6.6 describes the constraint, which restricts the number of members in the final structure to a predefined maximum value, N_{UB} , the upper bound for the desired number of members in the final structure. The reason for the inequality constraint rather than an equality constraint for an exact number of members is that an exact number of members in the final structure cannot be realistically specified as certain layouts comprising of certain specified numbers of members may not be structurally feasible.

$$\sum_{i=1}^{N_{total}} k_n \leq N_{UB} \quad (6.6)$$

where N_{total} is the total number of members in the ground structure and, N_{final} , the total number of members in the final structure, for ease of reference.

6.4 Effects of Integer Constraints

The examples that follow, are presented to demonstrate that the MATLAB script which was derived from the formulation behaves in a predictable manner. and that the suitable value of for R in each study case is identified, for parametric studies. The results of the parametric studies are presented later, in *Section 6.5*.

6.4.1 3 x 3 Grid Example

Fixed supports in both x and y directions are placed at *Nodes No. 1* and *7*¹ or as shown in Fig. 6.1. The allowable tensile σ^+ and compressive σ^- stresses are, respectively, unit-less 10 and 1. A single point load of 3.0000 in magnitude is placed at *Node No. 6* in positive x -direction horizontally as shown in the same

¹The node numbering convention starts from bottom to top and, from left to right

figure. The number of initial potential members in ground structure is 36.

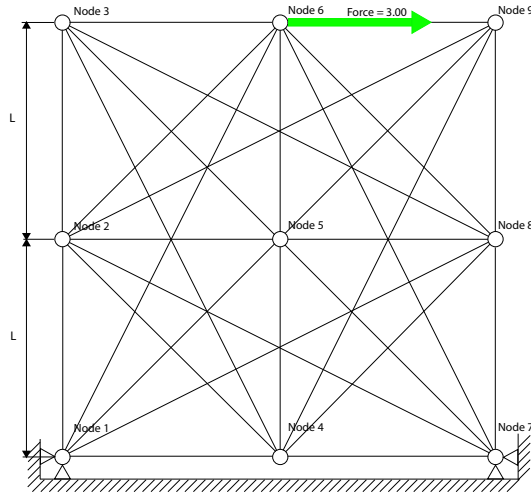


Figure 6.1: Potential members in ground structure and the load. $L = 1$, $F = 3.00$

Without Integer Constraints

A preliminary operation of the existing LP formulation (i.e. without the MILP constraints), is run for two purposes; to study the effect of MILP constraints on CPU time in comparison with the LP formulation and, more importantly to determine the minimum value of the constant, R to be used in the MILP formulation.

Fig. 6.2 shows a final optimised structure without the integer constraints. The total volume optimised by LP is denoted by V_{LP} , and is in this case, 8.0000. The MATLAB script was run 10 times and the average solution CPU time over these runs was 0.092 second ranging from 0.011 to 0.43. N_{final} , the total number of elements in the final structure, is 4.

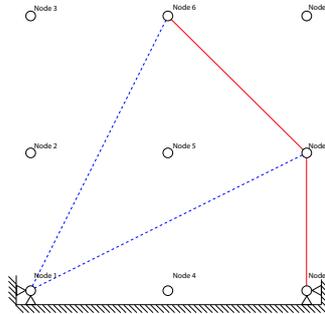


Figure 6.2: Optimised structure without integer constraints - solid red lines represent compression members, and Dashed blue lines, tension members

The maximum force among the members is in the one connecting Nodes *No. 7* and *No. 8*; $q_{34}^- = 3.0000$ in compression. Thus, A_{max} , the maximum area in this layout is 3.0000.

This value stipulates that, with the integer constraints, the value of constant, R to be chosen must be at least 3.0000, such that members whose A_i is smaller than A_{max} , is eliminated from being selected for the final solution, thereby achieving the ‘simplifying effect’ of MILP. In fact, the maximum area, A_{max} amongst all possible layouts under the given conditions will be in the only compressive member in the simplest structure with the fewest number of members; in this case it is a structure with only two members present and A_{max} is 3.3541. This is the reduction factor used for the following example.

With Integer Constraints

The following examples are presented to demonstrate the effects of variables, value of constant, R and, the maximum desired number of members, N_{UB} .

Fig. 6.3(a) and (b) show reduced optimised structures with the constant R set at

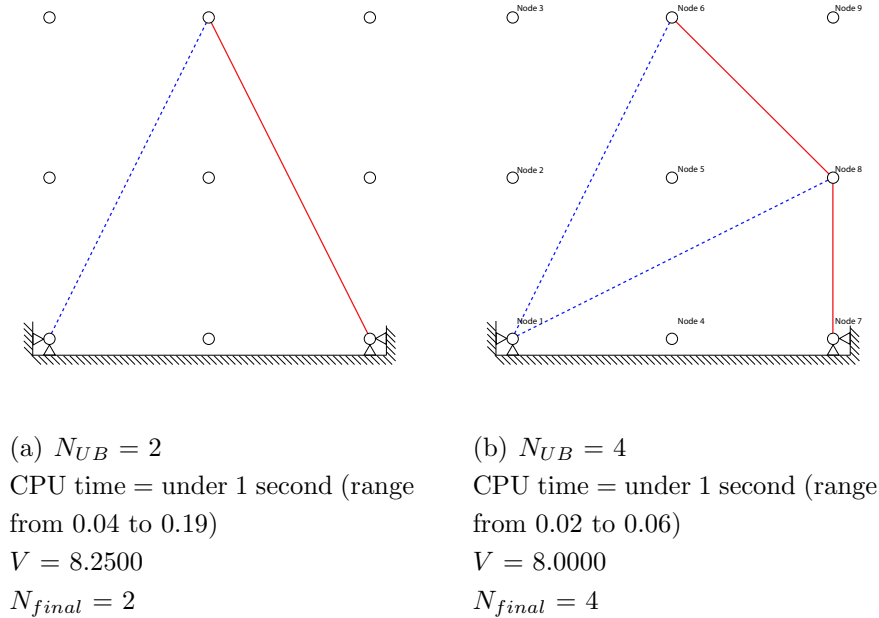


Figure 6.3: Optimised structures with integer constraints

3.3541 ($R > A_{max}$ in LP).

If the value of the constant, R is equal to the maximum area A_{max} in normal LP formulation, then the only MILP solution available will be identical, i.e. $N_{final} = 4$.

One anomaly worth noting is the presence of a member with zero-area when the maximum desired number of members, N_{UB} is 5 (or more). See Fig. 6.4(a). It produces results essentially the same as Fig. 6.3(b) except that there are 5 members which appear to be present in the final solution, with one of them being a ‘zero area’ member, such that the MILP formulation satisfies the integer constraint, numerically (refer to Appendix B for the full description of different arrangements and structures showing zero-area members).

In order to further demonstrate the effect of R , the value is deliberately chosen to be less than that of A_{max} ; in this case, A_{max} (in LP) = 3.0000 and $R=2.0000$.

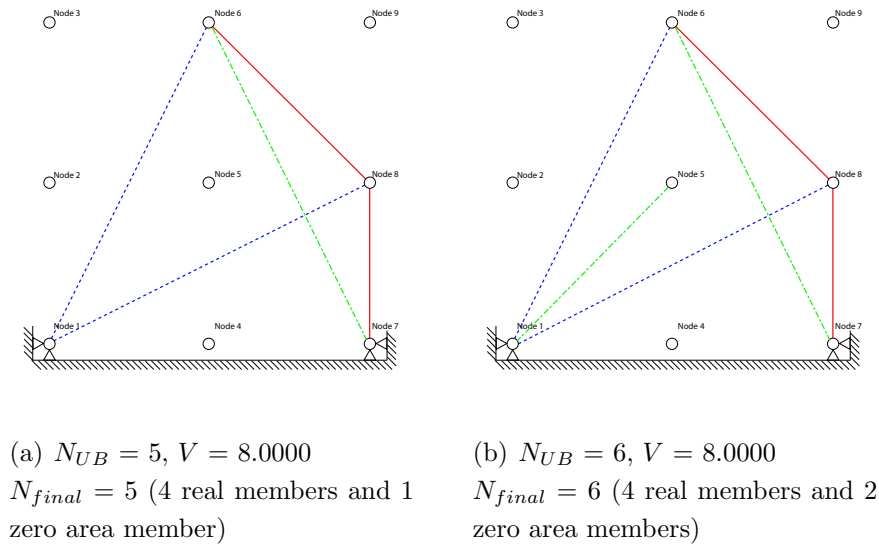


Figure 6.4: Optimised structures with integer constraints

Fig. 6.5 shows optimised structures with the constant R set at 2.0000.

The member with maximum area in this example, is the one connecting Nodes No. 7 and No. 8, with the member force, $q_{34}^- = 2.0000$ in compression and the maximum area, A_{max} of 2.0000. The maximum desired number of members, N_{UB} up to 4, offers no feasible solutions and $N_{UB} = 5$, produces the same results as in Fig. 6.5. The same exception of zero area members, which satisfies the integer constraint, only numerically, is observed when $N_{UB} = 6$. See Fig. 6.4(b)

By having R set to be less than A_{max} , it has been observed that the layout of members were configured to include more members in the final structure, than in the LP solution, as only those which have areas smaller than A_{max} (in LP), were admitted into the solution.

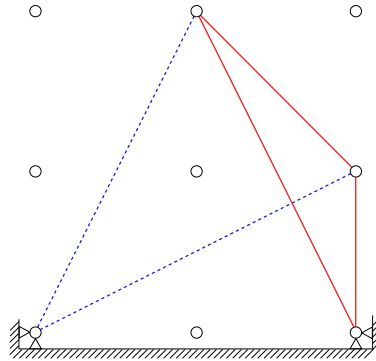


Figure 6.5: Optimised structure with integer constraints, $R=2$

$$N_{UB} = 5$$

CPU time = under 1 second (range from 0.08 to 0.15)

$$V = 8.0833$$

$$N_{final} = 5$$

6.4.2 5 x 3 Truss

Refer to Fig. 6.6 for the problem set-up. The number of initial elements in ground structure is 105. The allowable tensile σ^+ and compressive σ^- stresses are for this case, both unit-less 1. A single point load of 3.0000 in magnitude is placed in negative y-direction horizontally as shown in the same figure.

As in the 3 x 3 truss, the conventional LP solution was found; the structure is shown in Fig. 6.7. The total volume optimised by LP , V_{LP} , in this case, is 18.00. The average solution CPU time over these runs was 0.045 second ranging from 0.031 to 0.078. N_{final} , the total number of elements in the final structure, is 22.

The maximum force among the members is in the one connecting Nodes $No. 1$ and $No. 5$ (or Nodes $No. 11$ and $No. 13$); $q_4^- = 0.9079$ in tension. Thus, initially A_{max} , the maximum area in this layout is 0.9079. Through preliminary integer runs, it was found that the maximum area, A_{max} amongst all possible layouts under the given conditions will be in the simplest structure with the fewest number

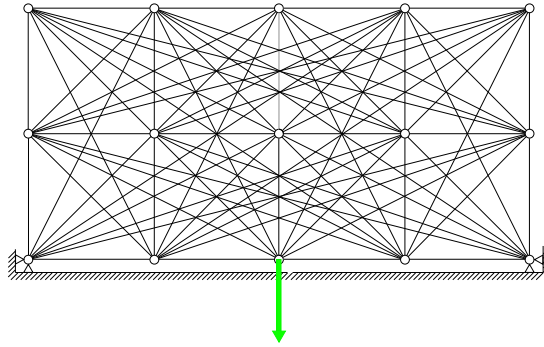


Figure 6.6: Potential members in ground structure and the load. $F = 3.00$

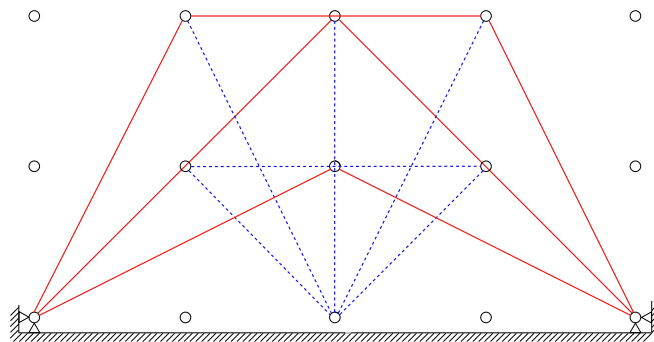


Figure 6.7: Optimised structure without integer constraints - solid red lines represent compression members, and dashed blue lines, tension members

of members; hence, the new $Amax$ is 3.3541. This is the reduction factor used for the parametric studies.

6.4.3 5 x 3 Michell Cantilever

Refer to Fig. 6.8 for the problem set-up. The number of initial elements in ground structure is 105. The allowable tensile σ^+ and compressive σ^- stresses are for this case, both unit-less 1. A single point load of 3.0000 in magnitude is placed in negative y-direction horizontally as shown in the same figure.

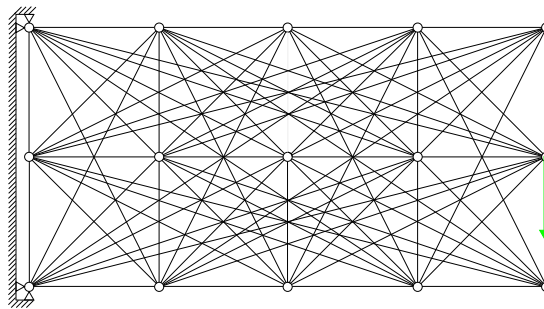


Figure 6.8: Potential members in ground structure and the load. $F = 3.00$

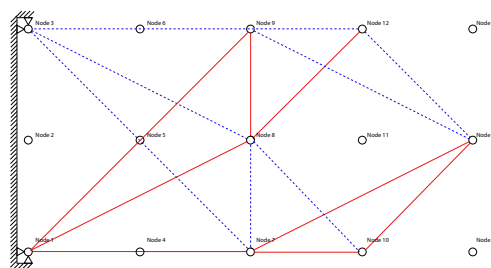


Figure 6.9: Optimised structure without integer constraints - solid red lines represent compression members, and dashed blue lines, tension members

As in the 3 x 3 truss, the conventional LP solution was found; the structure is shown in Fig. 6.9. The total volume optimised by LP , V_{LP} , in this case, is 45.00.

The average solution CPU time over these runs was 0.543 second ranging from 0.5000 to 0.72. N_{final} , the total number of elements in the final structure, is 28. Within the same figure, clarification is required for Node *No. 4*, which appears to be an unrestrained node connecting two compression members i.e. Member *1-4* and Member *4-7*. However, Node 4 is in fact an unused node (as per Nodes *No. 13* and *No. 15* in the same figure), and the member in presence is between Nodes *No. 1* and *No. 7*, going ‘through’ Node *No. 4*.

The maximum force among the members is in the one connecting Nodes *No. 7* and *No. 14* (or Nodes *No. 9* and *No.14*); $q_76^- = 1.9496$ in compression. Thus, initially A_{max} , the maximum area in this layout is 1.9496. Through preliminary integer runs, it was found that the maximum area, A_{max} amongst all possible layouts under the given conditions will be in the simplest structure with the fewest number of members; hence, the new A_{max} is 6.1847. This is the reduction factor used for the parametric studies.

6.5 Parametric Studies

A study was conducted involving parametric analyses with variations in two parameters, in order to find out their effects on the solution CPU time; reduction factor, R and the maximum desired number of members, N_{UB} .

The effects of the variant, R on CPU time is observed over a range of values of N_{UB} while the values of all other variables remain unchanged. In order to obtain a simple set of data, three well-known benchmark type problems with simple loading and support conditions, are chosen. All values of R in each case are above the maximum area, A_{max} found in preliminary operations of LP formulation. Observations are presented in the following subsections. *Simplex* algorithm is used for the linear variables and the *Branch-and-Bound* algorithm is used to handle the integer variables. The solver in MATLAB m-script file (`lp_solve.m`), was acquired through a non-commercial public source.

All operations of MILP optimisation were conducted from a fully connected

ground structure. All studies presented in this section were solved on the following specifications:

O/S: Microsoft Windows Vista (TM) RC 1 (Build 5600)

Intel Pentium 4 CPU at 2.80GHz with 1GB RAM

Platform: MATLAB Version 7.0.1.24704(R14) Service Pack 1

MIP solver: `lp_solve.m`

The three benchmark type problems and the tested, comparable ranges of values for N_{UB} and R , are described in Table 6.1.

6.5.1 N_{UB} and Total Volume in Final Structure

It is well-known but noteworthy that this reduction in the number of members, produces either the same or higher volume (or weight) in the final structure, caused by changes in topology [215].

The effects of N_{UB} are presented in Table 6.2. The general trend has been observed that the reduction in the number of members causes the volume increase, as in the case of 3 x 3 grid and 5 x 3 Michell cantilever structure. However, in the case of 5 x 3 half wheel over the range of R between 1 and 10^8 , the number of members present in the final structure does not appear to have any effect on the volume; different layouts can result in the same volume as in the case of 3 members in the final structure and 5 members in the final structure. Refer to Fig. 6.10. Additionally, in the case where $N_{final} = 10$, the resulting structure is identical as Fig. 6.10(b) albeit with 5 additional zero-area members, which meet the conditions of the MILP constraint, numerically.

6.5.2 Effects of Reduction Factor on CPU time

Fig. 6.11, Fig. 6.13 with 6.12 and, Fig. 6.14 present respectively for the 3 x 3 grid, 5 x 3 half wheel truss, and 5 x 3 Michell cantilever, the average CPU time

6.5 Parametric Studies

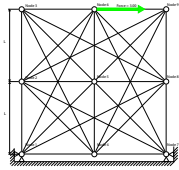
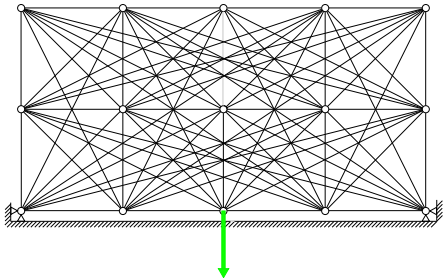
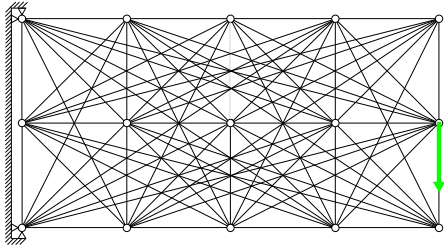
<i>Initial connectivity</i>	<i>Tested range of values</i>		<i>A_{max} (LP)</i>	
	<i>N_{UB}</i>	<i>R</i>	<i>or min. R</i>	<i>m</i>
(a) 3 x 3 Truss	2 to 7	4 to 10 ⁸	3.3541	36
	Results less meaningful above this range			
(b) 5 x 3 Truss	3 to 25	1 to 10 ⁸	3.3541	105
	(Results less meaningful above this range)			
(c) 5 x 3 Michell Cantilever	2 to 18	7 to 10 ¹³	6.1847	105
	(Results, less meaningful above this range) <i>N_{UB}</i> has been tried up to 10 ⁵			

Table 6.1: Ground structures (support conditions and loading positions) and parametric input data

6.5 Parametric Studies

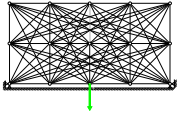
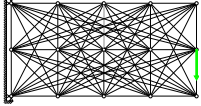
<i>Ground structure</i>	R	N_{UB}	N_{final}	$Vol.$	$Vol./Vol_{LP}$
(a) 3 x 3 Truss	3.3541	2	2	8.25	1.03125
	3.3541	4	4	8.00	1
	3.3541	5	4 (1)	8.00	1
	3.3541	6	4 (2)	8.00	1
(b) 5 x 3 Truss	10.00	3	3	18.00	1
	10.00	5	5	18.00	1
	10.00	10	5	18.00	1
	1.000	10	10	18.00	1
	1.000	11	11 (1)	18.00	1
	1.000	12	12	18.00	1
	1.000	13	13 (1)	18.00	1
	1.000	14	14 (3)	18.00	1
	1.000	15	15(5)	18.00	1
	1.000	16	16(5)	18.00	1
	1.000	17	17(6)	18.00	1
	1.000	18	18(8)	18.00	1
	1.000	19	19(6)	18.00	1
	1.000	20	20(8)	18.00	1
	1.000	21	21(6)	18.00	1
	1.000	22	22(6)	18.00	1
(c) 5 x 3 Michell Cantilever	10.00	2	2	51	1.13333
	10.00	4	4	47.000	1.04444
	10.00	6	6	45.000	1
	10.00	7	7	45.000	1
	10.00	8	8	45.000	1
	10.00	9	9	45.000	1
	10.00	10	10	45	1
	2.000	11	11	48.253	1.07228
	2.000	12	12	47.667	1.05927
	2.000	13	13	46.089	1.02420
	2.000	14	14	45.000	1
	2.000	15	15	45.000	1
	2.000	16	15 (1)	45.000	1

Table 6.2: Increase in volume caused by changes in topology. Values in () brackets, indicate the number of zero-area members - see Appendix B for further details.

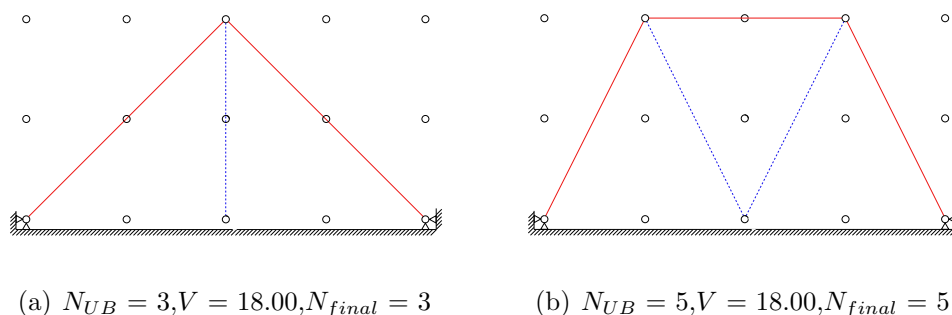


Figure 6.10: Identical volume with 3 members and 5 members in the final structures. ($R=10$)

taken for optimisation in seconds, versus the input value of N_{UB} , desired number of members, varied within the specified range of reduction factors, R . Also the layouts of members in the finalised structures are shown for each value of R .

Fig. 6.11 shows the results for 3 x 3 grid, expectedly that all CPU times with integer constraints are higher than the CPU time without (as it has an extra process of admitting less than or equal to a specified number of members). The notable items are that all constants produced very similar CPU times with each other, not escaping the range between 0.01 and 0.1 and that there appears to be no logical correlation between CPU times and the desired number of members, N_{UB} or the value of R . However, the size of this particular problem is such that the produced CPU times are not suitable for comparative analysis, which leads us to the 5 x 3 half wheel truss.

Fig. 6.13 (5 x 3 half wheel) shows the tendency of CPU time increasing with the increase in the value of the constant, R until R reaches 10^8 , (CPU time under 1 second), at which point all values of N_{UB} produce the same layout for the final structure.

This is because, when a ‘large value’¹ is chosen for R , the numerical round-off to one of the binary values, implies that A_i/R is treated as being effectively zero

¹relative to the value of A_i of members

by the optimisation algorithm, regardless of the actual value of A_i . The distinct exceptions to this tendency are the plots with the values of the constant $R = 10^2$ and 10^7 . This irregularity in the tendency is caused by the different layout of members for these particular values of R despite the same number of members in the final structures. (Refer to the diagrams at top, Fig. 6.13)

Following this, are the results for 5 x 3 Michell cantilever truss as in Fig. 6.14, which shows a similar tendency but without the mentioned exceptions as only one layout is available for a given number of members in the final structure.

In summary, the CPU time increases with the increase in the value of reduction factor, R up to a problem-specific ‘threshold value’ of R , after which point it ceases to produce any meaningful results as the mathematical solver breaks down. Additionally, it must also be noted that the reduction of the number of members in the final structure may not increase the total volume of the structure after a certain point; the LP optimised configuration of 5 x 3 Michell cantilever structure is comprised of 28 members with the total volume of 45.00 while the MILP optimised configurations of the same ground structure, may be comprised of from 6 to 10 members with the same volume of 45.00. Although it remains to be further investigated whether the same holds for large-scale structures, the MILP formulation may be used for simplifying effect without compromising the total volume.

6.5.3 Effects of Desired Number of Members on CPU time

Due to the size of the problem layout, all 3 x 3 grid problems were solved under 0.1 second, rendering any comparison of solution CPU times insignificant, regarding the effects of N_{UB} . The effects of N_{UB} on CPU time are better illustrated in the cases of 5 x 3 half wheel and 5 x 3 Michell cantilever structure.

Fig. 6.12 shows fluctuating CPU times for various values of N_{UB} for a single value of $R = 1$. However, there is an observable tendency; CPU time decreases

with higher values of N_{UB} , with intermittent values of N_{UB} arriving at optimum solutions below 2 seconds, at $N_{UB} = 14, 17-20$ and 22 onwards.

Referring to Fig. 6.13, the peak values of CPU time are all at $N_{UB} = 3$, with the exception of constant $R=5$ and $R=10^2$, the peak values of which are at $N_{UB} = 4$ for both cases. The results can be summarised that in general, CPU time decreases with the increase in N_{UB} toward the number of members in the final optimum structure using the LP formulation without the integer constraints.

A similar trend can be observed in the case of 5 x 3 Michell cantilever structure although Fig. 6.14 shows a more disparate set of results with peak CPU times at various values of N_{UB} ; two peak values at $N_{UB}=7$, two peak values at $N_{UB}=6$, one at $N_{UB}=5$ and one at $N_{UB}=4$. Ignoring $N_{UB}=4$ as marginal, the peak CPU values are between $N_{UB}=5$ and $N_{UB}=7$.

The general trend observed in both cases, is that the CPU time peaks at a value of, or in a small range of values of N_{UB} , which appears to be dependent on the problem.

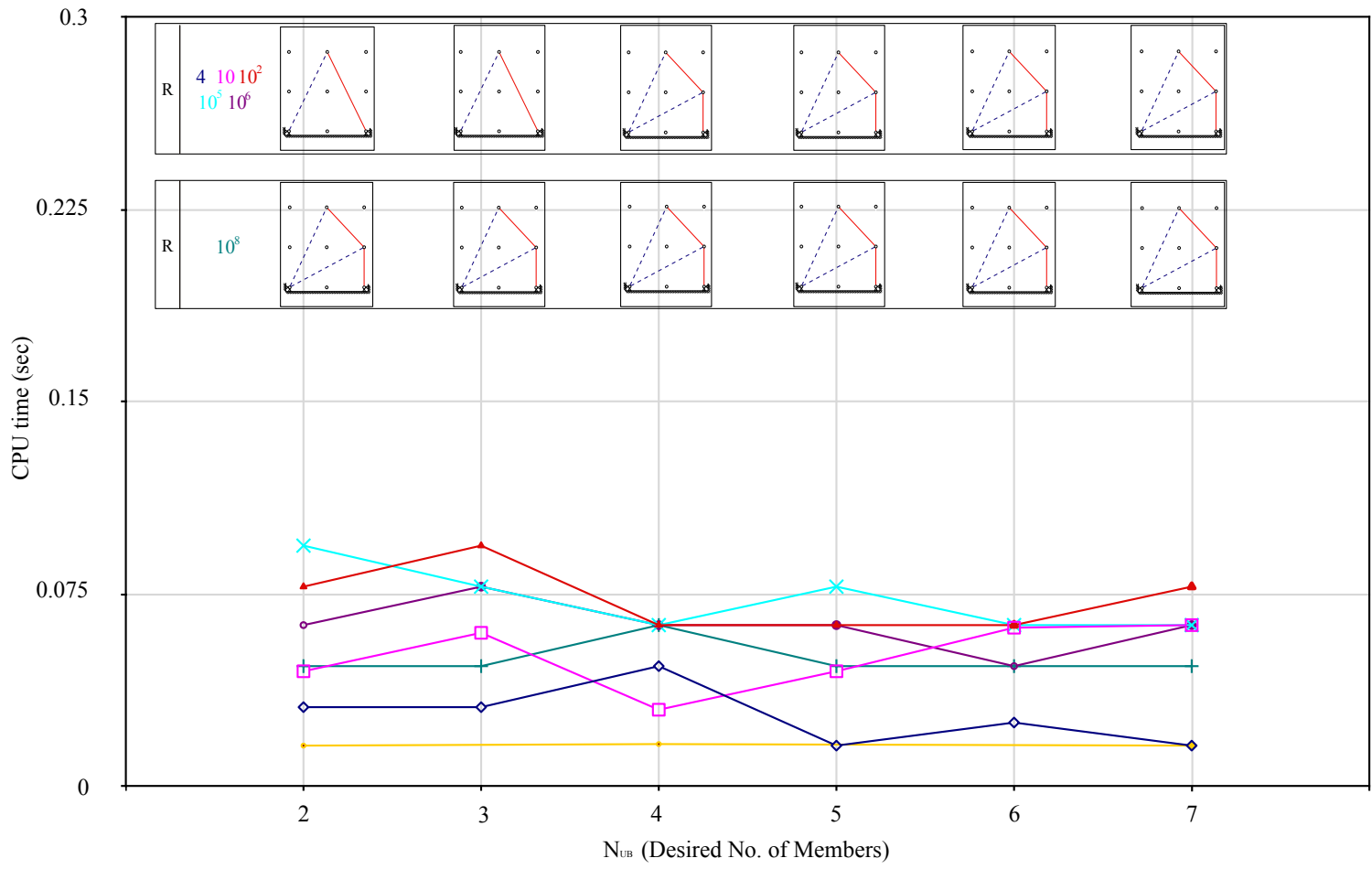


Figure 6.11: Effects of R and N_{UB} on CPU time: 3 x 3 grid

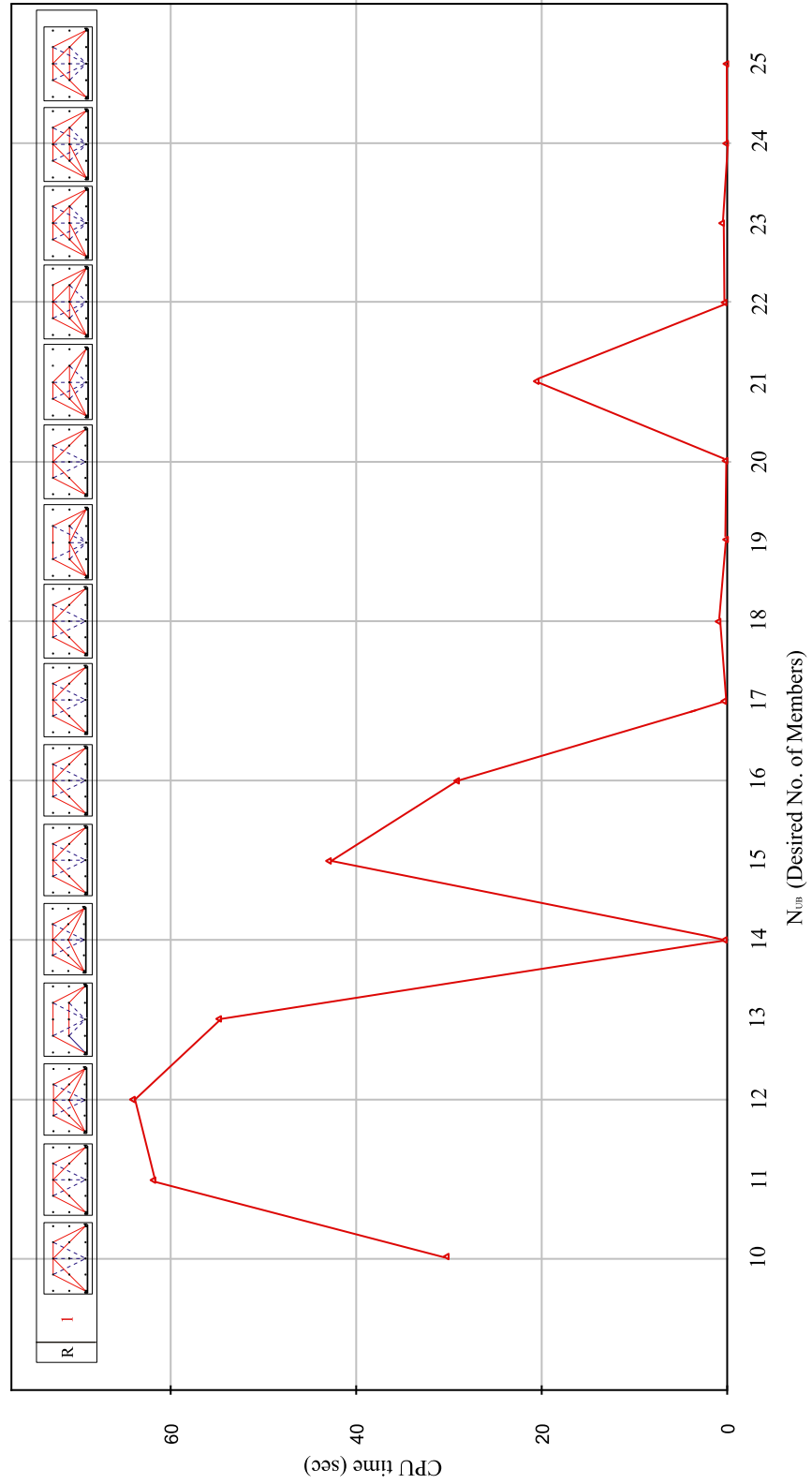


Figure 6.12: Effects of R and N_{UB} on CPU time: 5 x 3 Half Wheel - $R=1$

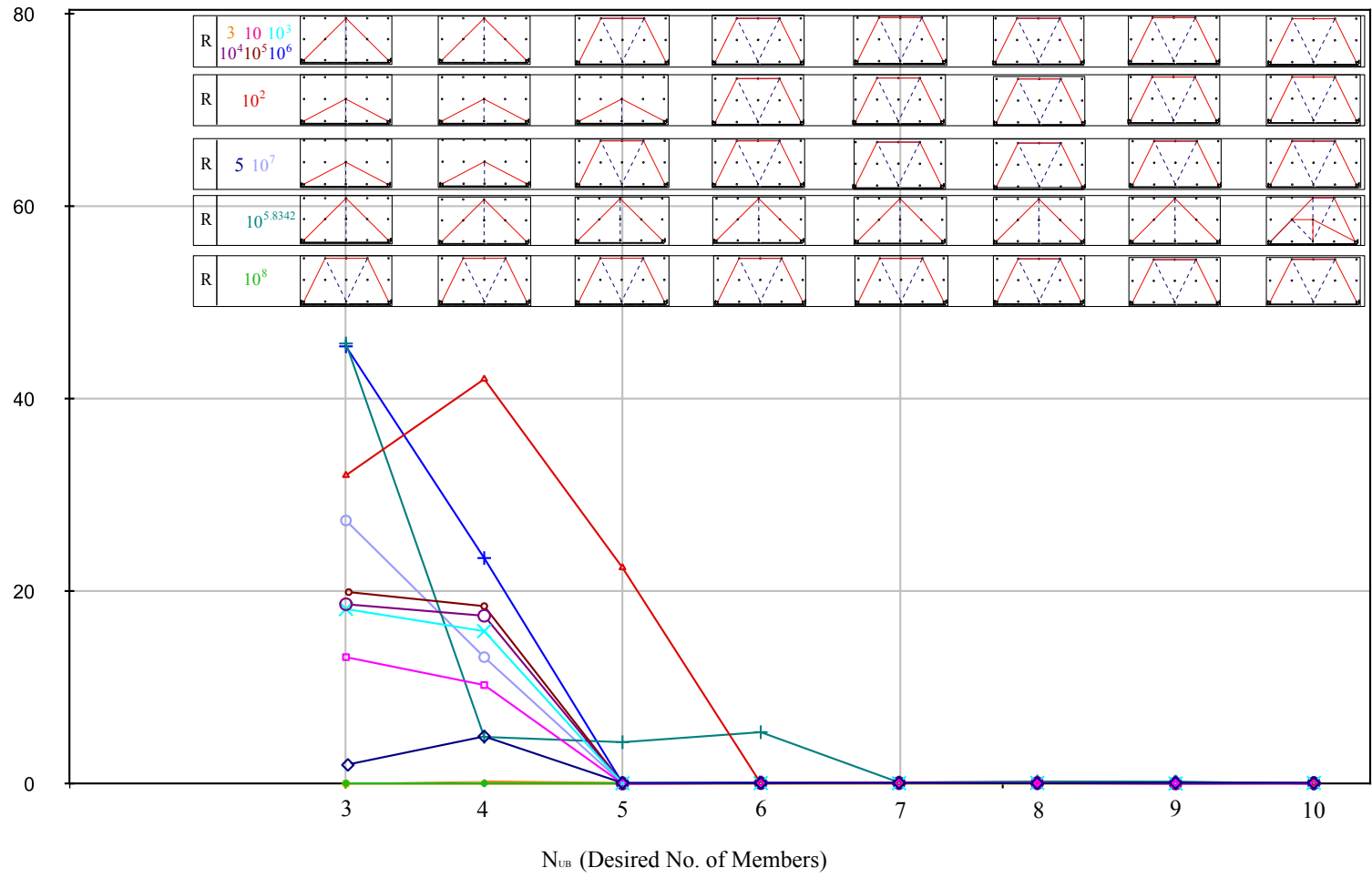


Figure 6.13: Effects of R and N_{UB} on CPU time: 5 x 3 Half Wheel

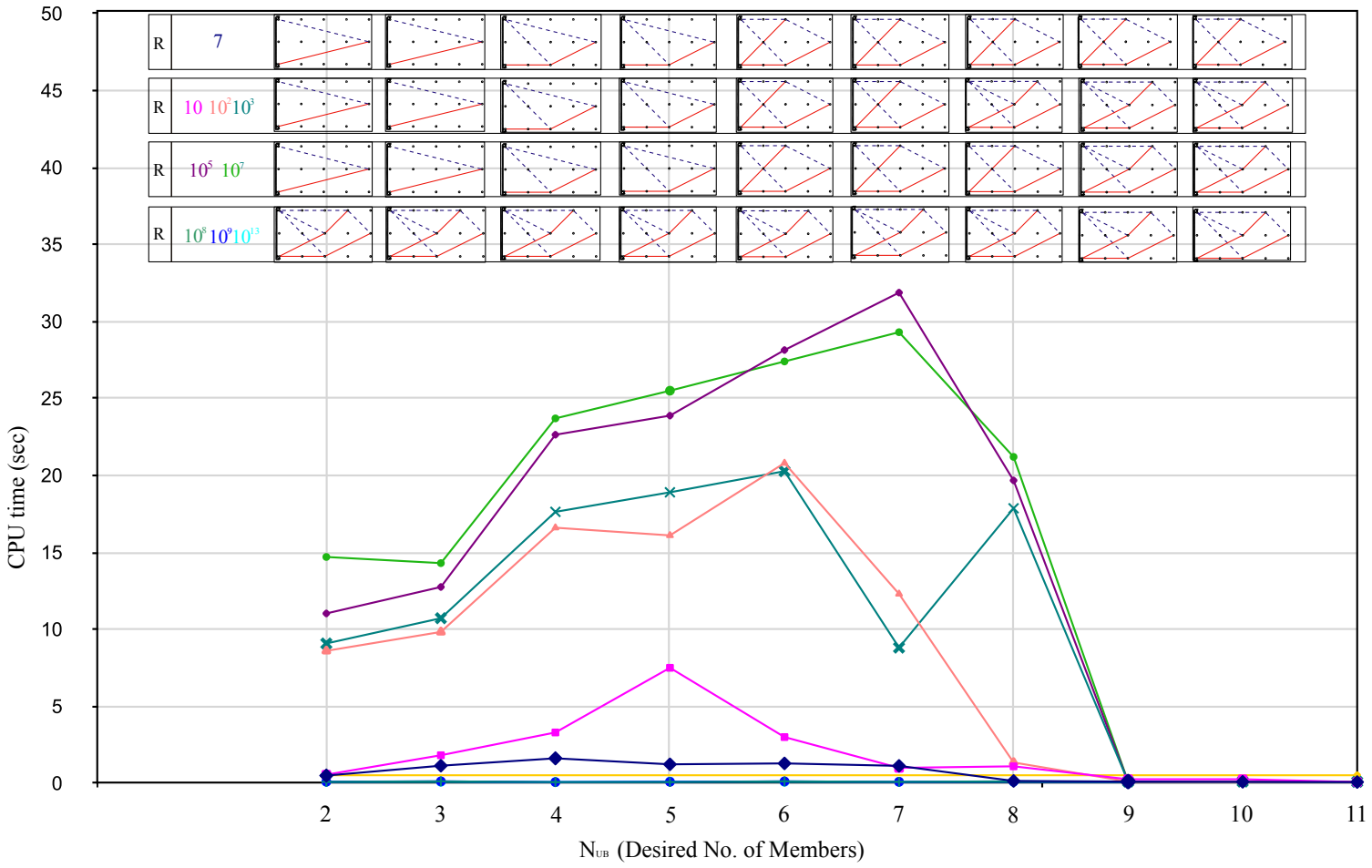


Figure 6.14: Effects of R and N_{ub} on CPU time: 5 x 3 Michell Cantilever Truss

6.6 Discussion and Conclusions

It has been demonstrated that the MILP formulation is capable of achieving reduction of members, which may be desirable for improving the constructibility of the generated optimum structures. Hence, the MILP formulation promises to be a suitable method for reducing the said over-complexity with an appropriate level of realism.

A crucial observation is made, regarding the values of R ; N_{final} , the number of members in the final optimum depends on R , as well as on N_{UB} , i.e. different values of R may generate different sets of combinations of members and, even if the desired number of members is identical, the actual number of members in the final structure, N_{final} may vary according to the value of R .

It is also observed that there is a specific and narrow range of values of N_{UB} , to which R corresponds, e.g. $R = 1$ for N_{UB} between 10 and 16 and, $R = 10$ for N_{UB} between 3 and 5.

For example, in the case of 5 x 3 ‘half wheel’ structure, the MILP formulation with $R = 1$, yields no result when the input value for N_{UB} is below 9, and it only yields results for $N_{UB} = 10$ or above (even if the minimum required number of members, topologically possible is clearly 3 (See Fig. 6.12)). Similarly, when $R = 10$, the formulation only yields meaningful results with N_{UB} up to the value of 5.

This is because the value of R corresponds to the value of A_{max} ; as the presented MILP formulation is design to admit only those members with $A_i > A_{max}$. Thus, the higher the value of R , the lower the N_{final} and the simpler the final structure.

Expectedly the introduction of an additional constraint to the original formulation has increased the CPU time for solving the problems. It was also found that the difference in CPU time between the optimisation procedure with the integer constraint and the one without the constraint widens considerably as the number of members in the initial ground structure becomes larger. Hence a much more

efficient formulation would be required in order to render MILP practical. Adaptation of Member Adding approach developed by Gilbert and Tyas [91], which improves the efficiency of classic LP formulation may present an opportunity for improvement in the efficiency of the MILP formulation. However, in its present form it is unlikely to be compatible with MILP because the constraint, N_{UB} is too stringent to find a feasible solution in a reduced ground structure which is used in Member Adding approach.

One simple strategy to alleviate the computational inefficiency would be to introduce a load tolerance level. As discussed in *Section 6.3.1*, if the cross-sectional area of a potential member is very close to zero but not zero, the binary constraint may either assume that the value actually is zero (due to numerical round-off) or have difficulty in forcing the variable to the (required) value of 1. Thus, if a potential member with small cross-sectional area is filtered out at a predefined ‘load tolerance’ value, before the MILP formulation assigns it 0 or 1, then it would reduce the number of members to be considered by MILP and consequently the computation time would decrease.

Another strategy may be to introduce a minimum desired number of members, $N_{DesiredLB}$ such that the number of members (or variables) is reduced to a smaller set between the two values.

Another factor contributing to increase in the CPU time is the value of the constant, R ; it generally tends to increase with the increase in the value of the constant, until the constant reaches the value which MATLAB considers as a ‘large number (approximately 10^8 with the particular solver and platform in concern and above) .

The last notable finding is that, when N_{UB} , the desired number of members is increased beyond the number of members found in the true optimum without the integer constraint, the CPU time decreases to a minimal level regardless of the chosen value of R .

This leaves much work and further investigation e.g. (1) inclusion of the integer formulation in conjunction with Member Adding Method or introduction of N_{LB} for increased efficiency, (2) further investigation regarding the ‘large number and the exact workings of the formulation and, (3) ways of controlling the final output structure. Furthermore, the use of MILP constraint can lead to a number of other highly useful features and options to the potential users. For example, constraints could be added that would allow the analysis to:

- Place a limit on total number of members in the structure
- Place a limit on total number of members at a given node
- Introduce a penalty based on small angles between members at a node
- Introduce a penalty based on total number of members at a node
- Introduce a penalty to reduce parallel overlapping members

Preface to Chapter 7

In Chapter 6, it was found that the mixed integer linear programming (or MILP) formulation can reduce the level of complexity in the optimum structure effectively, by limiting the total number of members in the final structure and, the behaviour of the formulation is now better understood.

However, the dramatic increase in the run-time of the additional MILP constraint formulation, presents an enormous drawback and suggests further work, required to improve the efficiency¹.

Following the literature survey to form an overview of tensegrity research, two issues were identified; one was that the problem of form-finding of tensegrity, based on *polyhedral geometry*, had been rigorously researched while neither the area of automatic generation of tensegrity topology or connectivity nor irregular tensegrity, had received equal attention and, the other was that among the differing definitions of tensegrity, one description in particular warranted further employment of a MILP formulation:

“A given configuration of a structure is in a stable equilibrium if, in the absence of external forces, an arbitrarily small initial deformation returns to the given configuration. A tensegrity structure is a stable system of axially loaded-members. A stable structure is said to be a “Class 1 tensegrity structure if the members in

¹Despite the need for improvement, it was decided that, in order to explore the fundamental theme of the thesis, it would be more appropriate to investigate further, the same capability of MILP in a smaller, ‘confined’ subtopic, instead of subsequent work of incremental improvement in computational efficiency of the formulation

tension form a continuous network, and the members in compression form a discontinuous set of members. A stable structure is said to be a “Class 2 tensegrity structure if the members in tension form a continuous set of members, and there are at most two members in compression connected to each node. [151]

This description of tensegrity classifies tensegrity structures into two distinct classes according to only the maximum number of compression members at a node i.e. Class 1 and Class 2 tensegrity systems. It was then conceivable that the ability of a MILP constraint, to turn members ‘on’ or ‘off’, can be introduced to the existing LP formulation in order to control the permitted number of compression members at each node, similar to placing a limit on the total number of members in Chapter 6.

As a topic, tensegrity is employed here as a representative example of form generation of unconventional structural configuration; the tensegrity structure began its initial development in the domain of architects’ interest and architectural structures and, are a classic interdisciplinary synthesis of structure and architecture with their essentially indivisible structural aesthetic effecting an architectonic quality. Thus the study of tensegrity is pertinent to the overall investigation, where an engineering tool can produce (or enhance) aesthetics of form, to an architectural intention. The second chapter, Chapter 7 in *Part III* presents this investigation.

Chapter 7

Layout Optimisation of Tensegrity Structures

7.1 Abstract

Tensegrity structures have intrigued and excited engineers for over half a century. In order to identify new tensegrity forms researchers have applied various methods, but perhaps surprisingly layout (or *'topology'*) optimisation techniques appear not to have been employed. In this study a simple mixed integer linear programming (or MILP) layout optimisation formulation which can limit (to one) the number of compressive elements terminating at joints in the structure is described, thereby allowing Class 1 tensegrity type structures to be synthesised. The formulation is first applied to two well-known 2D layout optimisation benchmark problems, demonstrating its efficacy. It is however clear that the volume of a tensegrity type structure identified using the method must always be greater than (or equal to) that of an equivalent structure identified without tensegrity constraints. It is also found that as the numerical discretisation is refined the characteristic features of a tensegrity structure diminish, arguably calling into question Buckminster Fuller's assertion that tensegrity structures are 'lightweight' and inherently 'optimal'.

Work is then extended by modifying an MILP-generated tensegrity type structure to a true tensegrity structure, which is modelled both physically and computa-

tionally, in order to verify the veracity of the generated structure and to further the understanding of its behaviour and structural response to external loading with supports.

7.2 Introduction

A tensegrity is a prestressable structure which consists of only two types of structural members, tensile and compressive, pin-jointed in 2D (or ball-jointed in 3D) at connecting nodes. In particular, a *Class 1* tensegrity structure¹ is one in which no two compressive elements are adjacently connected i.e. compressive elements are connected only to tensile elements [151].

Since its formal documented conception and coinage of the word in 1962 [141], tensegrities have attracted attention not only from structural engineers but also from artists and architects and from as far a field as medical research [221][222].

In structural engineering, previously researchers have carried out extensive analyses of various classes of tensegrity structures, mostly on static properties of tensegrity [223] [224] [145] [142] [151] [150] [225] but also on dynamic properties [155] [151].

Many other researchers, however, focus their effort on form-finding methods of tensegrity [226] [167] [168] [169], which aim to determine nodal geometries and internal forces once the structure's topology has been (typically) manually defined. Whilst these methods successfully deal with determination of self-stress states of tensegrity, they either rely on regular geometries of known polyhedra or assume configured connectivities of compression and tension members prior to form-finding of tensegrity. They therefore do not propose automatic generation or 'design' of topologies of tensegric forms, which is essential in enabling a wider

¹Researches in tensegrity are on-going and definitions of tensegrity structures vary from researcher to researcher. A comprehensive review of definitions can be found in [145]

participation of design in tensegrity.

Recently a geometry optimisation technique in the form of non-linear programming, has been applied to optimise the stiffness of tensegrity structures [179]. The significance of this work is that it provides a procedure for *designing* of optimal tensegrity structures by beginning with pre-determined connectivity but allowing struts to be reduced and nodes to be merged and, so to permit change in the initial connectivity. However, the instance of this in [179] does not necessarily support the effectiveness of this method (see Section 4.6.2 for detailed discussion).

More recently another approach, using evolutionary algorithm has been applied to discover non-load-bearing irregular tensegrities [187]. However, with these few exceptions, most research focuses on the problem of form-finding of tensegrity based on restrictive, regular *polyhedral geometry*, while the area of automatic generation of tensegrity topology or connectivity of irregular tensegrity has drawn less attention.

Furthermore, in his recent paper, Ariel Hanaor, a renowned researcher in tensegrity, prompted to challenge the notion of the perceived optimality of tensegrity as an unsubstantiated belief [136]. Additionally, although not written as a comparative analysis paper, recent work by Gómez-Jáuregui *et al.* regarding generation of double-layer tensegrity grids [227], presents examples of tensegrity grid dome (named ‘floating compression domes’), which are benchmarked against a geodesic dome of conventional configuration. In this example, an inadvertent but useful conclusion is drawn; “...*the floating compression domes designed here resulted heavier than the benchmark structure...*”.

The main objective of this study is thus twofold: firstly to present the novel layout optimisation method to automatically generate irregular 2D tensegrity type structures and, secondly to investigate into the notion of optimality of the load-carrying capacity of these structures.

Thus, in this study a formulation capable of successfully identifying Class 1 tensegrity forms involving conventional *loads* and *supports* is developed, and the efficiency of the structures identified is critically assessed through comparison with structures identified using the standard linear programming layout optimisation formulation.

7.3 MILP Formulation for Tensegrity Structures

7.3.1 Background

The classical ‘*ground-structure*’ truss layout optimisation formulation has traditionally been formulated as a size optimisation problem, which can then be conveniently solved using linear programming (or LP) algorithms. However, in a conventional size optimisation problem no distinction is made between truss bars with positive area and those with zero area. (i.e. all bars in the original ground structure will be present in the final optimal solution, though some - usually the vast majority - will simply have a zero area). This formulation is therefore unsuitable when constraints on the numbers of *active* bars (i.e. bars with a non-zero area) in the final structure need to be imposed. However, constraints of this type are inevitably required when identifying the form of tensegrity structures. *Class 1* tensegrity structures are defined as structures in which the endpoints of compressive elements are only connected to tension members [189]. Thus, when layout optimisation techniques are used to determine efficient tensegrity forms, there is a requirement that the number of struts in compression terminating at any given joint is limited to one.

In order to identify efficient tensegrity forms, here, a variant on the classical LP truss layout optimisation formulation is adopted, in which simple binary variables are added to represent the presence (or otherwise) of particular bars, and additional constraints are added to limit the number of struts at each node point. The resulting mixed integer-linear programming (or MILP) problem can be solved us-

7.3 MILP Formulation for Tensegrity Structures

ing a variety of mathematical programming techniques¹.

The following formulations are divided into two parts; the existing linear programming formulation and additional binary mixed integer formulation.

7.3.2 Plastic LP Layout Optimisation Formulation

The equilibrium LP plastic design formulation to solve for the minimum volume [91] for a ground structure subjected to a single load case and containing m members and n nodes are stated as follows:

Minimise,

$$V = \mathbf{q}^T \mathbf{c} \quad (7.1)$$

subject to:

$$B\mathbf{q} = \mathbf{f} \quad (7.2)$$

$$q_i^+, q_i^-, \geq 0, i=1, \dots, m \quad (7.3)$$

where V is the total volume of the structure, \mathbf{B} is a suitable $(2n \times 2m)$ equilibrium matrix, $\mathbf{q}^T = \{q_1^+, -q_1^-, q_2^+, -q_2^-, \dots, q_m^+, -q_m^-\}$, $\mathbf{c}^T = \{l_1/\sigma_1^+, -l_1/\sigma_1^-, l_2/\sigma_2^+, -l_2/\sigma_2^-, \dots, l_m/\sigma_m^+, -l_m/\sigma_m^-\}$, $\mathbf{f}^T = \{f_1^x, f_1^y, f_2^x, f_2^y, \dots, f_n^x, f_n^y\}$; $l_i, q_i^+, q_i^-, \sigma_i^+, \sigma_i^-$ represent the length, tensile and compressive member forces and stresses in the i^{th} member, respectively. And lastly f_i^x, f_i^y are the x and y direction live load components applied to node j .

7.3.3 Introduction of Binary Variables

The LP problem variables are the member forces, q_i^+, q_i^- and the additional variables are k_i , a binary variable (Eqn 7.4) for every member i , either in tension or

¹This study employed Xpress, a commercial mathematical programming solver

compression, which indicates whether a potential member in the ground structure, m is added in the solution [217] [218].

$$\frac{A_i}{R} \geq k_i, k_i = 1 \text{ or } 0 \quad (7.4)$$

A_i is the area of member i and R is the reduction factor; a constant value chosen arbitrarily to be greater than the area of the member with the greatest value of q_i , A_{max} ¹. The above equation can be rewritten as:

$$\frac{1}{R} \cdot \mathbf{q} \geq \mathbf{k}^T \boldsymbol{\sigma} \quad (7.5)$$

where $\boldsymbol{\sigma}^T = \{\sigma_1^+, -\sigma_1^-, \sigma_2^+, -\sigma_2^-, \dots, \sigma_m^+, -\sigma_m^-\}$ and $\mathbf{k}^T = \{k_1^+, -k_1^-, k_2^+, -k_2^-, \dots, k_m^+, -k_m^-\}$.

Eqn 7.6 describes the constraint, which restricts the number of members at node j to a predefined maximum value of integer, N_{iatj} . As this study is only concerned with *Class 1* tensegrity type structures, this value is set at 1. However, for a possible future work, structures may require that this number be set at different numbers e.g. $N_{iatj} \leq 2$ for *Class 2* tensegrity structures.

$$\sum_{i=1}^{N_{iatj, q^-}} k_i^-, N_{iatj, q^-} \leq 1 \quad (7.6)$$

where N_{iatj} is the total number of members at node j .

7.4 Michell Structure Problems

It is hypothesised that the tensegrity constraint in Eqn 7.6 in the formulation would force the nodes to accommodate not more than one compressive member

¹The value of A_{max} is empirically obtained from a standard operation of LP optimisation (see *Subsection 6.4.1*).

(and any number of tensile members), and thus ‘redirect’ any other adjacent compressive members, by combinations of tensile and compressive members. However, this tensegric property would gradually diminish and the identified minimum volume would converge to the LP solution (or true optimum), if nodal density in the initial design domain is increased. This section presents the investigation of this hypothesis, by employing two well known problems with exact analytical solutions.

7.4.1 Central Point Load between Pin and Pin/Roller Supports

A well-known LP benchmark problem with a known exact analytical solution of π^1 , given that F , the external point load, the distance between the applied load and supports, L , material tensile strength, σ_T and compressive strength σ_C all equal 1, a type first studied by Michell [70], is presented here. With one support translationally fixed in x - and y - directions at lower left-hand corner and a roller, fixed in y -direction but free to move in x -direction at lower right-hand corner, the design domain in x - y ratio of 2:1 rectangle is set up, within which a unit-less point load of 1, is applied vertically downward at the coordinates $(1, 0)$. See Fig. 7.1.

A structure, optimised very close to the theoretical optimum is shown in Fig. 7.2; this is the structure against which the generated tensegrity type structures are compared.

These conditions remain constant as described, with the exception of the nodal density, i.e. the number of nodes within the design domain.

The nodal density is described in terms of either target node number, which is the number of initial connectivity nodes or scale factor, a value corresponding to

¹The general exact analytical is $\min. V = FL \frac{\pi}{2} (\frac{1}{\sigma_T} + \frac{1}{\sigma_C})$, after [70]. In this particular case, $F = 1$, $L = 1$, and $\sigma_C = \sigma_T = 1$.

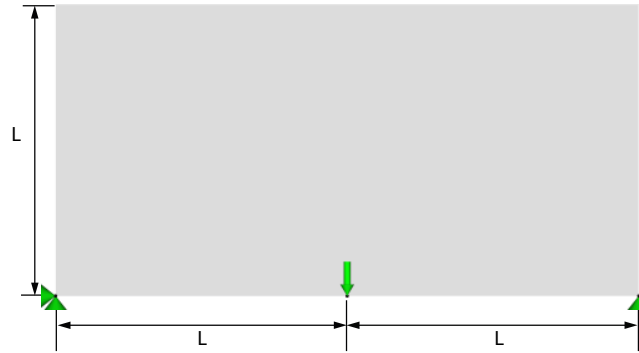


Figure 7.1: Design domain with supports and a central load; $L=1$, $F_y=-1$

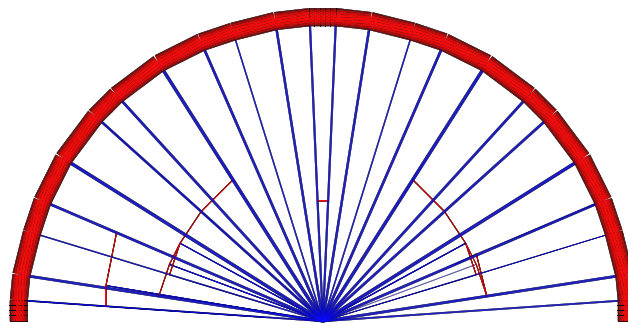


Figure 7.2: Optimised structure: close to Michell's theoretical optimum 'half-wheel' structure; final volume=3.14784, 0.2% heavier than the exact analytical solution of π .

the target node number. It must be noted that nodal density within the design domain is not arranged on a uniform grid. Instead, the target node number (or scale factor) determines the arrangement of the nodes in order to exploit the design domain fully whilst enabling the given standard PC's computational power to identify solutions¹.

The results and corresponding figures are presented in Table 7.1. Note that red denotes that a member is in compression, and blue, that a member is in tension.

In Table 7.1, it is immediately noticeable that the geometric constraints govern the final topology of tensegrity type structures and hence its volume². There is also another noticeable and more significant trend in these figures; as the nodal density within the same design domain increases, the nodal distance between the compression members becomes smaller, with their topology increasingly resembling the conventional LP solution. This trend becomes more apparent when the tensegrity type structures in figures (a)-(d) in Table 7.1 are compared against the LP optimised structures in figures (a)-(d) in Table 7.2, which are of the same layout and parameters except the absence of additional constraints in Eqns 7.4-7.6 do not apply, i.e. The MILP tensegrity type structures increasingly resemble the corresponding LP optimum solution and/or numerically converging closer to LP volume.

In figures (a)-(d) in Table 7.2 the first observation previously made, concerning the tensegrity structures in figures (a)-(d) in Table 7.1, is also present; the increase in nodal density expectedly reduces the overall volume. What is more significant is the volume difference ratio of tensegrity to LP structures. Referring, to Table 7.3, there is an observable trend of the ratio between the two types of structure reducing with the increase of nodal density in the design domain, implying possible convergence. This is more clearly illustrated in Fig. 7.3.

¹The regular design space based on a uniform grid does not support this particular case.

² V_{LP} denotes the volume of LP structure and, V_{Ten} , that of tensegrity type structure.

7.4 Michell Structure Problems

Table 7.1: Optimised tensegrity structures using MILP formulation

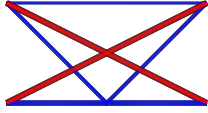
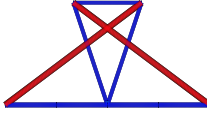
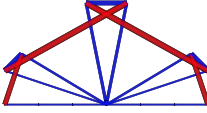
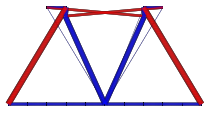
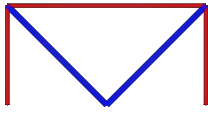
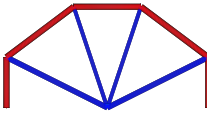
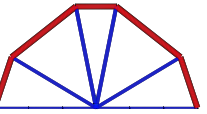
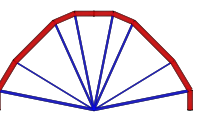
	(a)	(b)	(c)	(d)
<i>Tensegrity Structure</i>				
<i>Target</i>	6	12	22	46
<i>Node No.</i>				
<i>Scale</i>	0.1	0.6	1.2	2.44
<i>Factor</i>				
V_{Ten}	10.00	5.556	4.644	3.796

Table 7.2: Optimised structures using normal LP formulation

	(a)	(b)	(c)	(d)
<i>Optimised Structure</i>				
<i>Target</i>	6	12	22	46
<i>Node No.</i>				
<i>Scale</i>	0.1	0.6	1.2	2.44
<i>Factor</i>				
V_{LP}	4.000	3.333	3.286	3.229

This is because generation of these tensegrity type structures required an introduction of an additional constraint, as a simple introduction of a new constraint in LP usually results in reduced capacity of the classic optimum solutions though it allows more parameter-control mechanisms [228].

Table 7.3: Volume difference ratio of tensegrity to LP structures

	(a)	(b)	(c)	(d)
<i>Tensegrity:LP</i>				
$V_{Ten}:V_{LP}$	2.50:1	1.67:1	1.41:1	1.18:1
<i>Ratio</i>				

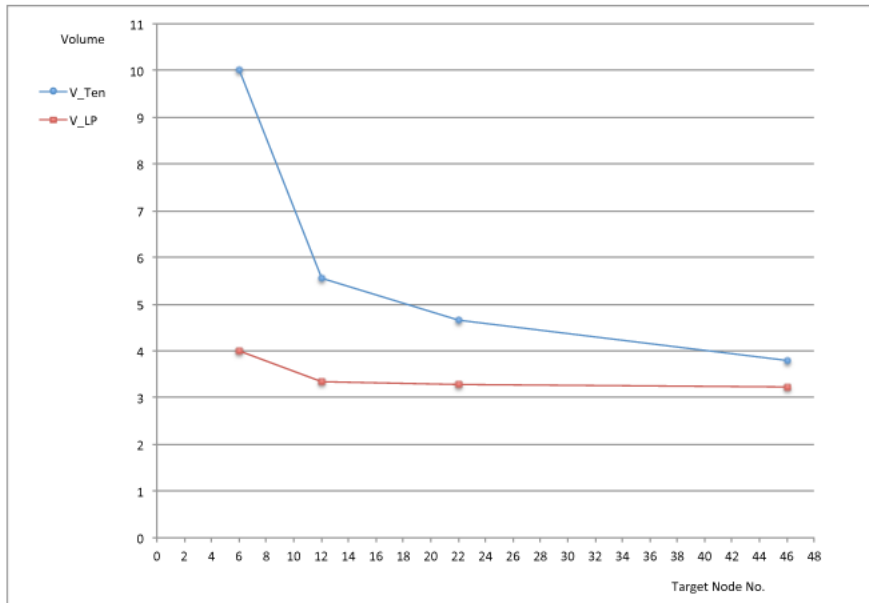


Figure 7.3: Volume convergence between MILP tensegrity and LP for pin and pin/roller support case

7.4.2 Central Point Load between Pin and Pin Supports

Presented here, is another one of well-known Michell structures, with a known exact analytical solution of $(\frac{\pi+2}{2})$ ¹. The design domain and load are shown in Fig. 7.4, which is identical to those in Fig. 7.1, except that this time, both supports are translationally fixed in both x - and y -directions. A structure, optimised very close to the theoretical optimum is shown in Fig. 7.5; this is the structure against which the generated tensegrity type structures are compared.

¹The general exact analytical solution is, $min. V = FL(\frac{1}{2} + \frac{\pi}{4})(\frac{1}{\sigma_T} + \frac{1}{\sigma_C})$, after [70]. In this particular case, $F = 1$, $L = 1$, and $\sigma_C = \sigma_T = 1$.

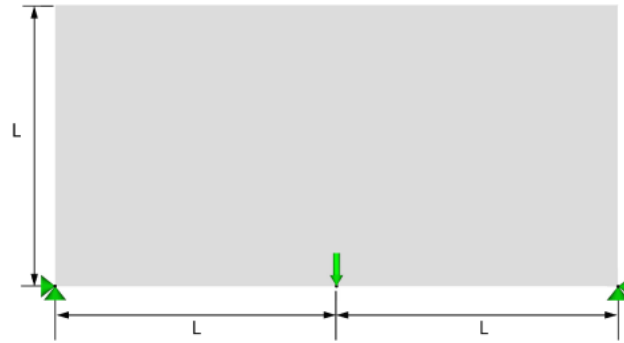


Figure 7.4: Design domain with supports and a central load; $L=1$, $F_y=-1$

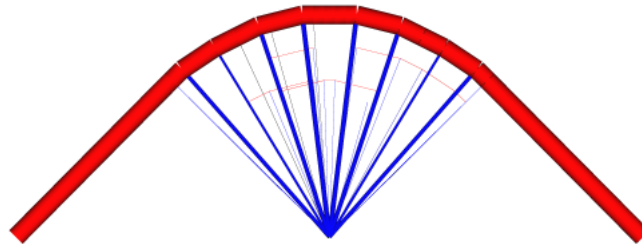


Figure 7.5: Optimised structure, close to Michell's true optimum 'half wheel' structure; final volume=2.57762, 0.2% heavier than the exact analytical solution of $\frac{\pi+2}{2}$.

As in the case of 'pin and pin/roller' supports case in the previous section, these conditions remain the same whilst the nodal density, i.e. the number of nodes within the design domain is varied.

The results and corresponding figures are presented in Table 7.4. These, compared against the figures in Table 7.5, further highlight the same trend observed in Section 7.4.1; the ratio between the MILP-tensegrity and LP structures reduces with the increase of nodal density in the design domain, implying possible convergence to each other, and toward the theoretical optimum volume of $\frac{2+\pi}{2}$.

7.5 Effects of material properties: tensile and compressive strengths

Table 7.4: Optimised tensegrity structures using MILP formulation for pin-pin supports

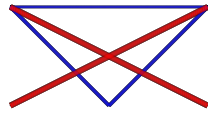
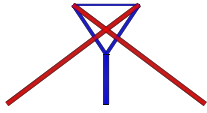
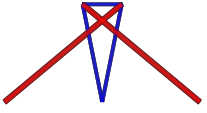
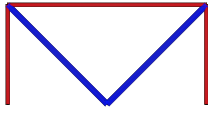
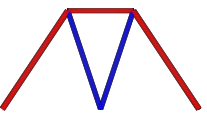
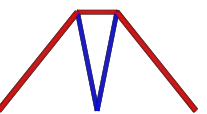
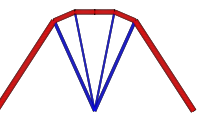
	(a)	(b)	(c)	(d)
<i>Tensegrity Structure</i>				
<i>Target</i>	6	12	22	46
<i>Node No.</i>				
<i>Scale</i>	0.1	0.6	1.2	2.44
<i>Factor</i>				
V_{Ten}	8.00	4.222	3.680	3.196

Table 7.5: Optimised structures using normal LP formulation

	(a)	(b)	(c)	(d)
<i>Optimised Structure</i>				
<i>Target</i>	6	12	22	46
<i>Node No.</i>				
<i>Scale</i>	0.1	0.6	1.2	2.44
<i>Factor</i>				
V_{LP}	4.000	2.889	2.880	2.794

7.5 Effects of material properties: tensile and compressive strengths

This section explores the effects of tensile strength, σ^+ and compressive strength, σ^- (or more precisely the different ratios between σ^+ and σ^-) on the generated MILP and LP optimisation solutions, in an effort to investigate whether a higher values of tensile strength would render MILP tensegrity structure more optimal, in line with the commonly assumed light weight of tensegrity.

7.5 Effects of material properties: tensile and compressive strengths

Table 7.6: Volume difference ratio of tensegrity to LP structures

$Tensegrity:LP$	(a)	(b)	(c)	(d)
$V_{Ten}:V_{LP}$	2.00:1	1.46:1	1.28:1	1.14:1
<i>Ratio</i>				

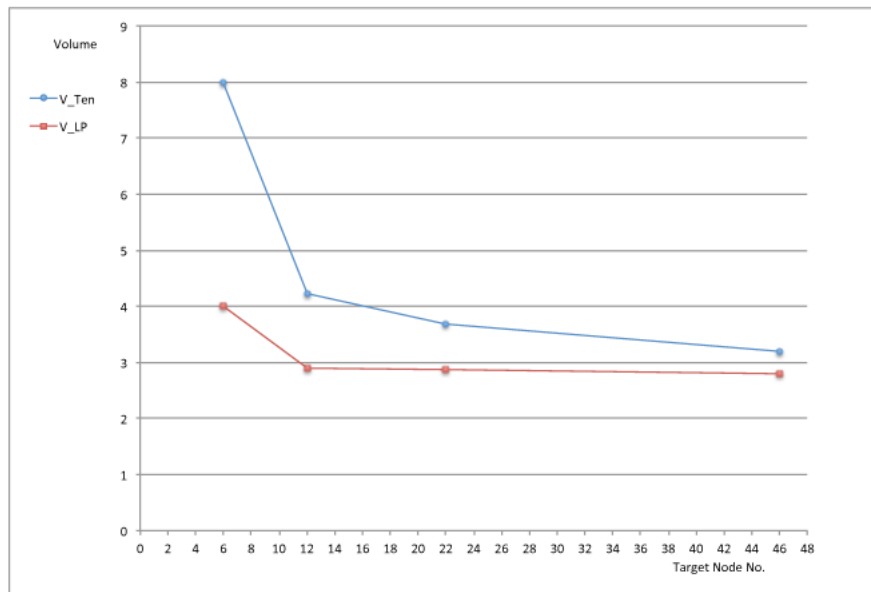


Figure 7.6: Volume convergence between MILP tensegrity and LP for pin and pin support case

7.5 Effects of material properties: tensile and compressive strengths

The results and comparative analyses between LP and MILP structures from the previous section have strongly suggested that tensegrity-type structures, generated using MILP formulation are heavier and thus only converge toward the known analytical optimal LP solutions as the nodal density becomes higher and they cannot be more optimal than conventional LP optimised structures. However, due to the ‘potential of optimality’ from use of more tension members, (nominal and design strengths of which are more favourable in structural steel than those of compression members), a doubt may remain and thus render the conclusion of non-optimality of MILP tensegrity, premature, with presented results so far optimised with the $\sigma^+:\sigma^-$ ratio of 1:1 for simplicity. Presented in this section are, hence, comparisons between MILP and LP structures in their volumes with varied $\sigma^+:\sigma^-$ ratios.

Table 7.7: LP structures with varying $\sigma^+:\sigma^-$ ratios. (σ^- , fixed at 1)

	(a)	(b)	(c)	(d)
$\sigma^+:\sigma^-$ ratio	1:1	2:1	5:1	10:1
V_{LP}	872.5	630.9	484.7	436

Referring to Table 7.7 - in this series of figures, there are two noticeable effects of different $\sigma^+:\sigma^-$ ratios on the optimised structures; firstly, the expectedly decreasing volumes of the final structures with the increasing strength of σ^+ , and secondly (and more significantly), the final configurations or layouts. This second effect on the final configuration is also observable in the MILP structures in Table 7.8 albeit to a lesser extent.

It is shown in Table 7.7, whilst the structure (a) has the equal number of compression and tension members as expected (7 each) and the volumes of compression

7.5 Effects of material properties: tensile and compressive strengths

Table 7.8: MILP tensegrity type structures with varying $\sigma^+:\sigma^-$ ratios. (σ^- , fixed at 1)

	(a)	(b)	(c)	(d)
$\sigma^+:\sigma^-$ ratio	1:1	2:1	5:1	10:1
V_{Ten}	1128	820.6	636.5	575.1

and tension members when $\sigma^+:\sigma^-$ ratio is 1:1, when σ^+ is incremented to 2, there is a noticeable change at the bottom of the structure (b), where the algorithm has attempted to utilise fewer and shorter compression members and more tension members (which is also reflected in the tensegrity structures between (b) and (c) in Table 7.8 but to a lesser and less clear extent). However, there is no change in topological configuration of members in the final solution between (b) and (c) in Table 7.7 with only the volume change (similarly in Table 7.8, there is no topological change between (c) and (d)).

This can be explained by the ‘ratio threshold’ value, above which the final layout would not be affected, firstly due to a low initial nodal density, and secondly and more importantly, because as the σ^+ value becomes much higher than σ^- , tension members are no longer required to extend further for optimality by changing the layout and thirdly due to the initial design domain, loading and support conditions, which would require a minimum number of compression members to transfer the load from the point of load application to the supports. Hence, it follows that, assigning higher values of σ^+ than σ^- , will not result in MILP tensegrity being more optimal than a corresponding LP structure, as shown in this case.

7.6 Tensegrity Columns

The symmetrically loaded tensegrity type structures presented in this section, are without supports and in a stressed condition with the axial loads holding the structure together. These examples also suggest the development to be followed; introduction of self-stressable member-node connectivity.

This section has two motives; one is to further investigate an example tensegrity structure and its structural behaviour, and the other is to investigate the veracity of the (apparently generally accepted) claims for tensegrity's inherent efficiency regarding its load-bearing capacity, and enable discussion of such aspects of tensegrity. As before, red denotes a member is in compression and blue denotes a member is in tension.

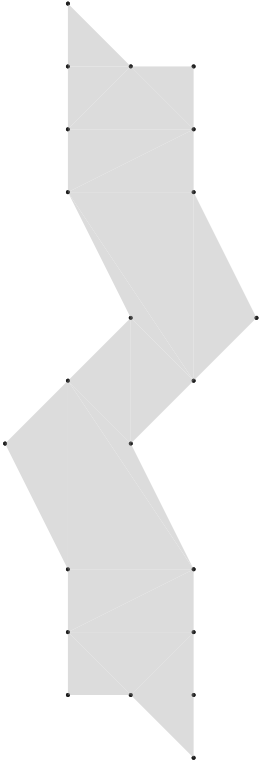
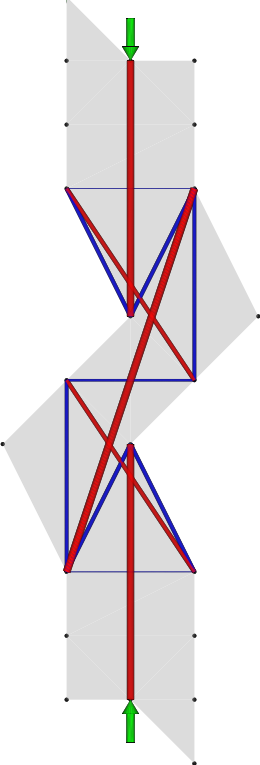
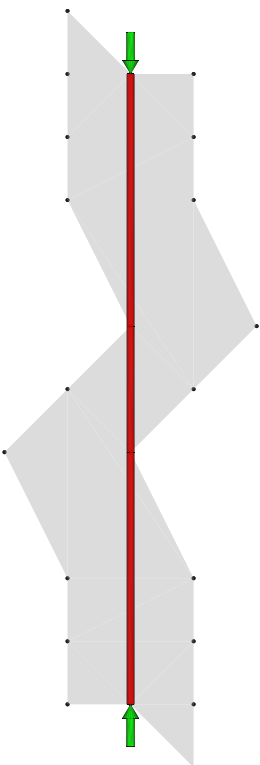
7.6.1 Tensegrity ‘Stayed Column’

Table 7.9 shows: (a) the design domain, (b) the tensegrity type structure and, (c) the corresponding LP structure, optimised using the same design domain and under the same loads as (b) but without the MILP constraint.

Since the structure is loaded along one vertical axis with top and bottom loads of 50 (each), a simple one element structure is obtained when using LP optimisation, with volume, V_{LP} of 50. In comparison, the volume of the tensegrity type structure, V_{Ten} is 700, 14 times the volume of V_{LP} .

The final solution for the design domain and load condition as shown in Table 7.9(a) and (b). Note that this is a ‘para-tensegrity’ structure, which maintains its stability under a very specific loading condition and is neither stable with the load removed nor laterally stable should any joint deflect, not to mention if a lateral load is applied. Hence, for the purpose of this investigation, new members are introduced to the existing para-tensegrity, to triangulate the structure so as to prevent the structure from behaving as a mechanism under certain load conditions, e.g. horizontal point loads. Note that stability was not expressly

Table 7.9: 2D tensegrity structures without supports: axial load along single axis

<i>Design domain</i>	<i>Tensegrity</i>	<i>LP</i>
(a)	(b)	(c)
		
	Data	
<i>Target Node No.=21</i>	V_{Ten}	V_{LP}
<i>Scale Factor=0.001</i>	700	50
<i>Load=50 (each)</i>		

included as a constraint in the initial problem formulation for the purpose of this investigation, i.e. comparative analyses, not practical, detailed design of either tensegrity nor conventional structures; hence the emergence of an unstable solution is neither fundamental nor an unexpected outcome as stability requirements by the method of adding ‘perturbing forces’ at the nodes [130], can remedy this but such requirements were excluded to maintain simplicity and low computational cost.

Fig. 7.7(a) shows the original, existing structure and new members to be added; Fig. 7.7(b) shows the new structure with each joint attached to at least three members, one of which is a compression member.

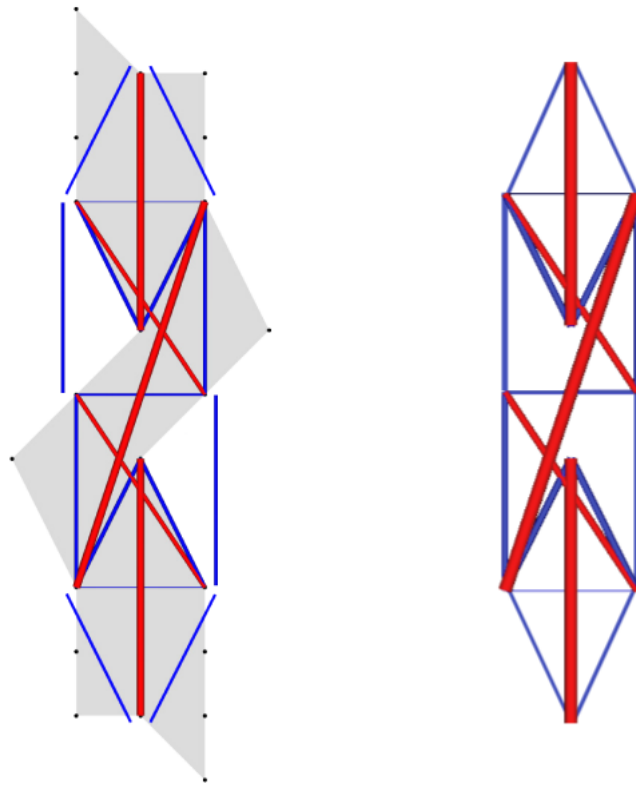
7.6.2 Investigation of Structure and Internal Loads

Two efforts were made in order to verify the structural veracity of this modified structure: construction of a physical model, and a structural analysis, using the commercially available structural analysis software, *SACS*¹.

Firstly, a physical model of the same structure has been constructed as shown in Fig. 7.8. This physical model is identical in its connectivity, and works, in its topological essence, in the same principle as the structures shown in Fig. 7.7, with the same node-to-member connectivity (see *Chapter 8* for further discussion of details of the model with regard to its topology and form-finding).

Secondly, once the physical integrity of the true tensegrity structure, had been verified, the structure was analysed, using SACS under the same joint and load condition. The internal forces resulting from this analysis are displayed in Fig. 7.9 and the internal forces data resulting from the optimisation run for the original

¹SACS by Bentley Systems is an “*integrated finite element structural analysis suite of programmes for the design of offshore structures*”. SACS is the industry standard in offshore engineering as almost all of the world’s energy companies specify SACS software for use by their engineering firms across the lifecycle of offshore platforms [229]



(a) Original 2D tensegrity type structure

(b) Modified tensegrity structure

Figure 7.7: 2D tensegrity type structure, modified with additional tensile members



(a)

Figure 7.8: A physical model of 2D tensegrity structure, based on MILP automatically generated structures in Fig. 8.1

para-tensegrity, are presented in Table E.3. Take note of the fact that they are identical and that the new members in the true tensegrity structure, which were later added to the original para-tensegrity structure, are unloaded under this specific load condition.

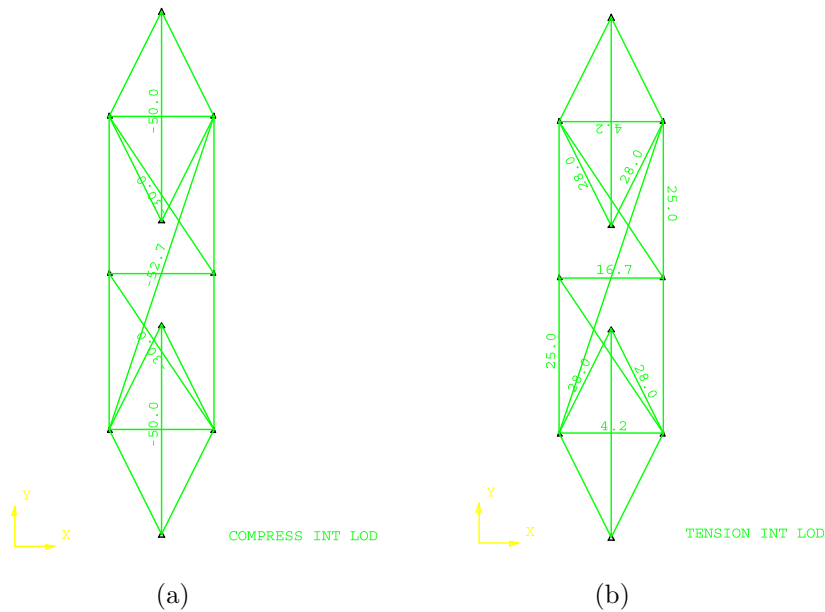
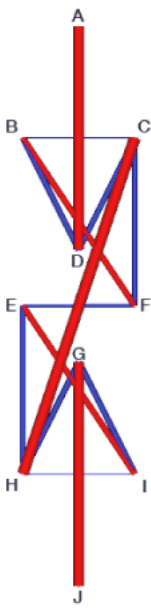


Figure 7.9: Internal member forces, based on SACS analysis; (a) compressive forces; (b) tensile forces

The values in Table E.3 clarifies how the internal loads are distributed within this structure; the equal and opposite external loads are applied vertically at Nodes A and J , putting Members AD and GJ in compression. At Nodes D and G , however, the constraints of tensegrity criteria and domain, force another load path, in order to circumvent any direct route between Nodes D and G . This was done by creating tensile members BD, DC, BC, CF and EF (and IG, HG, HI , and EH), which creates alternative load paths with vertical and horizontal internal forces.

Table 7.10: Para-tensegrity Column: internal loads

<i>Member</i>	q	q_x	q_y	<i>radius</i>	<i>vol.</i>
(a)					
AD	-50.000	0.00	-50.000	3.98942	100.00
BD	27.9508	12.50	25.000	2.98279	31.250
BC	4.16667	4.16667	0.000	1.1516	4.16667
CD	See BD				
EF	16.6667	16.6667	0.000	2.30329	16.6667
BF	-30.0463	-16.6667	-25.000	3.09258	54.1667
HC	-52.7046	-16.6667	-50.000	4.09590	166.667
HG	See CD				
IG	See BD				
JG	See AD				
HI	See BC				
EI	See BF				
CF	25.000	0.000	25.000	2.82095	37.500
EH	See CF				



7.6.3 Load-bearing Capacity of Tensegrity ‘Stayed Column’

It is now of interest to assign physical dimensions to the structure. Please refer to Fig. 7.10 for dimensions of the tensegrity column throughout this section.

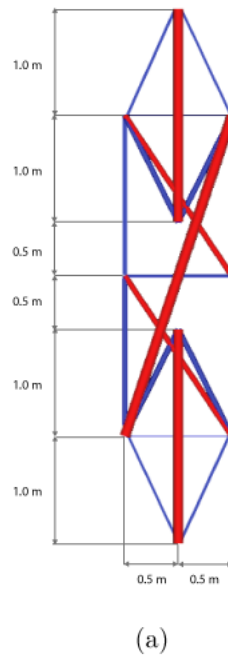


Figure 7.10: Dimensions of tensegrity column

Vertical Load

In order to understand the tensegrity column, its behaviours with a particular emphasis on buckling, are compared to those of the conventional column, maintaining the original cylindrical geometry of the member sections and the load condition; however, this time, realistic steel properties¹ (and dimensional units) are given as follows:

¹Though use of circular hollow sections may be considered more realistic, solid sections are used to simplify analyses as these are the original sections generated by the optimisation runs presented in this chapter.

- Young's Modulus, $E = 205000N/mm^2$
- Yield Stress, $F_y = 355N/mm^2$
- Shear Modulus, $G = 80000N/mm^2$
- Density, $\rho = 7.850 \times 10^{-6}kg/mm^3$ (but self-weight is ignored for force analysis)

Given these properties, Fig. 7.11 shows the expected internal force of -50kN and more interestingly, the utilisation ratio¹, U_c of 0.40 according to Eurocode 3 (EC3, hereafter). The maximum allowable axial load according to EC3 is $25.20N/mm^2$ with the actual value being $10.00N/mm^2$. As the member is not slender, the failure mode is unlikely to be by buckling; the U_c is 0.31 with the max allowable Euler buckling strength at $32.19N/mm^2$, i.e. higher than the maximum design axial load capacity. Based on this maximum axial load capacity and the member cross-section area, the maximum compressive load capacity of this bar, is $125kN$ (or $0.637kN$ per kg of weight)

Given the same properties and load conditions, Table 7.11 shows the tensegrity structure with its individual member utilisation ratios. The highest utilisation ratio, hence the most critical case, belongs to Member HC , for which the maximum allowable axial stress is $66.41N/mm^2$, and the maximum allowable buckling stress is $84.62N/mm^2$. Based on this maximum axial load capacity and the member cross-section area, the maximum compressive load capacity of this critical member, and hence the whole tensegrity column, is $347.9kN$ (or $0.127kN$ per kg of weight, excluding unloaded members). This is much higher than that of the conventional bar, by a factor of 2.78, as a whole. However, the maximum compressive

¹A ratio of 0 denotes no utilisation of the member's structural capacity and the ratio of 1 denotes full utilisation of the structural capacity, where the most critical criterion is presented, e.g. as it is often the case, if the most critical criterion is a combination of axial loading and bending, then the U_c will reflect this as a single value. In the above example, it is a single axial load case which will cause a possible failure

²This is calculated, using; $F_{Euler} = \frac{\pi^2 EI}{(KL)^2}$; $L_{effective} = L_0$ for simply supported columns; $I_{xx} = I_{yy} = \frac{\pi d^4}{64} = \frac{\pi r^4}{4}$ for solid circular sections.

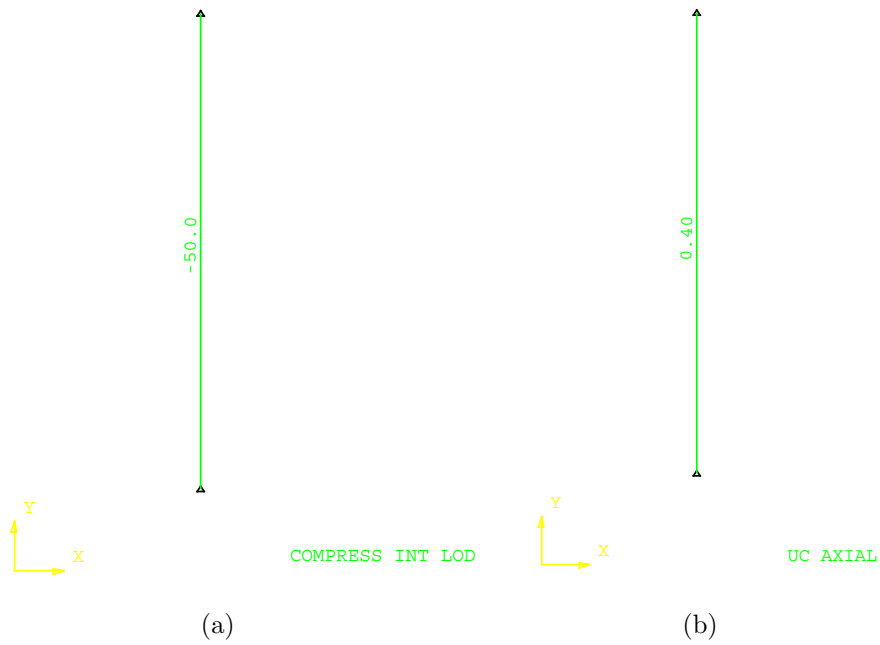


Figure 7.11: One-bar ‘structure’: internal member force and utilisation ratio, U_c based on SACS analysis

load capacity per kg of weight is much lower than that of the one-bar structure; $0.127kN$ compared to $0.637kN/kg$, which gives the ratio of 0.199.

The second noteworthy result is that the U_c for all other compressive members is very low, in comparison to that of the conventional one-bar ‘structure’.

The third noteworthy result is that the U_c for tensile members is particularly low; this is due to the fact that the ultimate tensile strength of steel is higher than the compressive yield strength, according to EC3 (and other design codes).

Unsurprisingly, the utilisation ratios for constituent members in the tensegrity column are low because the ‘tensegrity column’ is composed of a multitude of shorter compressive members; the design compression resistance is dependent on the partial safety factor, which is dependent on the length/cross-section ratio of the member.

In conclusion, it is an interesting finding that, when given realistic steel properties and design criteria, the modified tensegrity structure performs better than the one-bar ‘structure’. However, it is very clear the maximum compressive capacity of the tensegrity structure per weight is much lower by a factor of 5.03, which reinforces the original hypothesis that tensegrity is inherently a non-optimal structure as it contains structural redundancies.

7.6 Tensegrity Columns

Table 7.11: Tensegrity structure: internal member force utilisation ratios, U_c based on SACS analysis

	<i>Member</i>	<i>q</i> (<i>kN</i>)	<i>max. σ_{axial}</i> (<i>N/mm²</i>)	<i>max. σ_{Euler}</i> (<i>N/mm²</i>)	<i>U_{c,Axial}</i>	<i>U_{c,Euler}</i>
	AD	-50.000	156.20	201.22	0.05	0.06
	BD	27.9508	308.70	N/A	0.03	N/A
	BC	4.16667	308.70	N/A	0.03	N/A
	CD	See BD				
	EF	16.6667	308.70	N/A	0.03	N/A
	BF	-30.0463	116.52	148.89	0.09	0.07
	HC	-52.7046	66.41	84.615	0.15	0.12
	HG	See CD				
	IG	See BD				
	JG	See AD				
	HI	See BC				
	EI	See BF				
	CF	25.000	308.70	N/A	0.03	N/A
	EH	See CF				

7.6.4 Tensegrity ‘XIX’ Column

The tensegrity type structure generated in this section is named for ease of reference Tensegrity ‘XIX’ Column, which owes its name to the layout of the compression members.

Table 7.12: ‘XIX’ Tensegrity Column: 2D tensegrity structure with axial load along two parallel axes

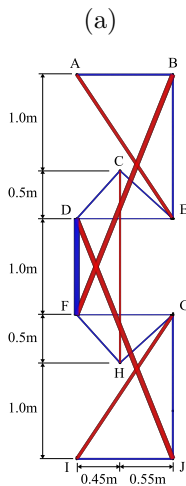
<i>Design domain</i>	<i>Tensegrity</i>	<i>LP</i>
(a)	(b)	(c)
Data		
<i>Target Node No.</i> =21	V_{Ten}	V_{LP}
<i>Scale Factor</i> =0.001	1148	490
<i>Load</i> =50 (each)		

Internal forces and member sizes from optimisation runs are shown in Table 7.13 for Tensegrity ‘XIX’ Column and in Table 7.14 for the corresponding LP structure. As with the design of true tensegrity structure, additional members have been

7.6 Tensegrity Columns

Table 7.13: MILP ‘XIX’ Para-tensegrity column: internal loads

	<i>Member</i>	q	q_x	q_y	<i>radius</i>	<i>vol.</i>
	AB	33.3333	33.3333	0.00	3.25735	33.3333
	AE	-60.0925	-33.3333	-50.00	4.37356	108.333
	BE	33.3333	0.00	33.3333	3.25735	50.00
	BF	-89.7527	-33.3333	-83.3333	5.34502	241.667
	CD	27.4055	18.3333	20.3704	2.95355	18.4352
	CE	24.7768	18.3333	16.6667	2.80833	18.4167
	CH	-37.037	0.00	-37.037	3.43355	74.0741
	DE	15.00	15.00	0.00	2.1851	15.00
	DF	103.704	0.00	103.704	5.74543	103.704
	DJ	See BF				
	FG	See DE				
	FH	See DC				
	GI	See AE				
	GJ	See BE				
	HG	See CE				
	IJ	See AB				



7.6 Tensegrity Columns

Table 7.14: LP ‘XIX’ Column: internal loads

	<i>Member</i>	<i>q</i>	<i>q_x</i>	<i>q_y</i>	<i>radius</i>	<i>vol.</i>	
	AB	22.50	22.50	0.00	2.67619	22.5	
	AC	-54.8293	-22.5 0	-50.00	4.17764	60.125	
	BC	-39.5055	-19.0385	-34.6154	3.54613	45.0865	
	BD	-15.7692	-3.46154	-15.3846	2.24042	32.3269	
	CD	-34.788	-3.46154	-34.6154	3.32767	34.9615	
	CE	-50.00	0.00	-50.00	3.98942	100.00	
	DG	See BD					
	ED	See CD					
	EF	See AC					
	EG	See BC					
	FG	See AB					

introduced to the original MILP tensegrity type structure, rendering it prestressable. See Fig. 7.12 for the final layout and dimensions.

This section contains the same vertical force analysis as in the previous section to reinforce further the results presented in the previous section. All material properties remain the same as in Section 7.6.3. However, it is emphasised here that circular hollow sections (or CHS) are used for compression members to introduce further realism.

Vertical Load: ‘XIX’ Tensegrity and LP columns

In order to understand the tensegrity column, and its behaviours with a particular emphasis on buckling, compared to those of the conventional LP structure, CHSs are employed for compression members as are realistic steel properties (and dimensional units) whilst maintaining the cross-sectional areas of the original members from optimisation. These are found in Table 7.16 for the tensegrity

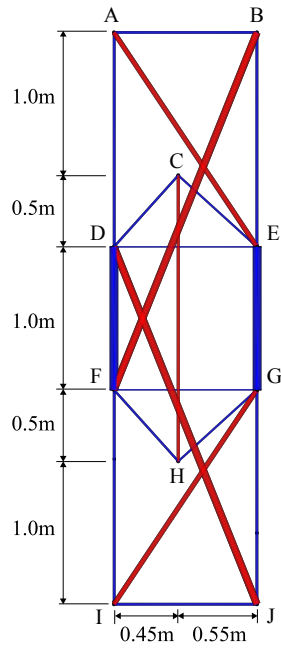


Figure 7.12: Tensegrity 'XIX' column with additional members

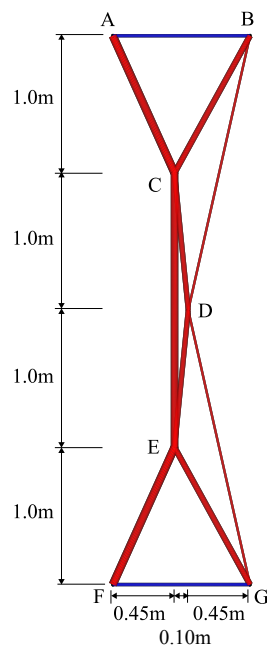


Figure 7.13: LP structure corresponding to Tensegrity 'XIX' Column

7.6 Tensegrity Columns

structure and in Table 7.15 for the corresponding LP structure. Horizontal and vertical pinned supports are located at the bottom two nodes in both the ‘XIX’ Column and the corresponding LP structure; in Nodes *I* and *J* for ‘XIX’ Column and in Nodes *F* and *G* for the corresponding LP structure. Two external loads of equal magnitude are applied in the negative *y*-direction (vertically), to Nodes *A* and *B* in both ‘XIX’ Column and in the corresponding LP structure. These loads are incremented until the most critical member in the structures reaches its full load bearing capacity.

Table 7.15: LP Structure (corresponding to ‘XIX’): CHS sizes

<i>Member</i>	Original Area cm^2	Diameter cm	Thickness cm	Actual Area cm^2
AB	33.33			
AD	33.33			
AE	-60.09	16.83	1.25	61.18
BE	See AD			
BF	-89.75	19.37	1.60	89.33
CD	27.41			
CE	24.78			
CH	-37.04	13.97	1.00	40.75
DE	15.00			
DF	103.70			
DJ	See BF			
EG	See DF			
FG	See DE			
FH	See DC			
FI	See BE			
GI	See AE			
GJ	See BE			
HG	See CE			
IJ	See AB			

In Fig. 7.14, the most critical member is *BD*; its maximum allowable axial load (i.e. $U_c=1.00$) according to EC3 is $200.25N/mm^2$ with the actual value being

7.6 Tensegrity Columns

$199.93N/mm^2$. As the member is not slender, the failure mode is unlikely to be by buckling; the U_c is 0.71 with the max allowable Euler buckling strength at $282.95N/mm^2$, i.e. higher than the maximum design axial load capacity. Based on this maximum axial load capacity and the member cross-section area, the maximum compressive load capacity of this member, is $2170kN$ for a self-weight of $402kg$ (or $5.40kN$ per kg of weight)

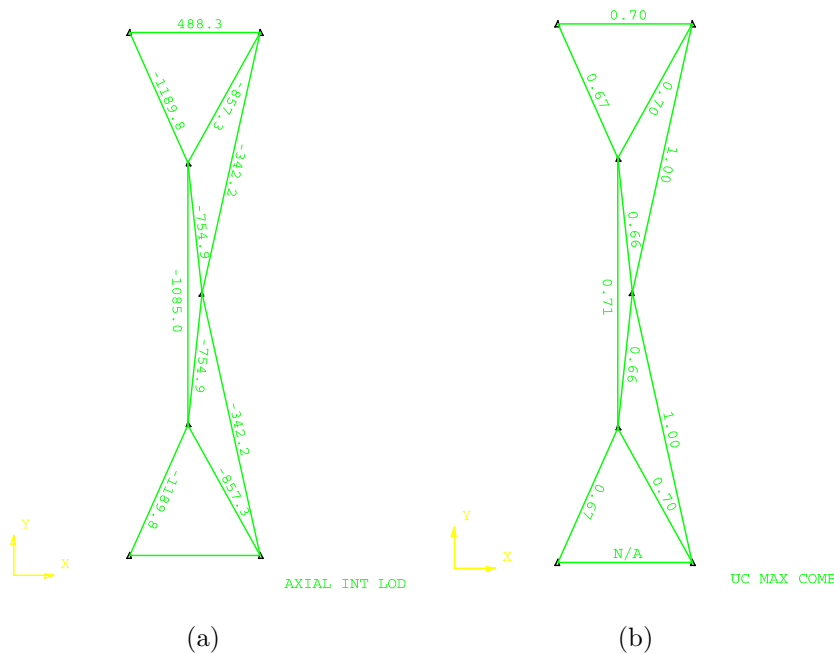


Figure 7.14: LP structure (corresponding to ‘XIX’): internal member forces and utilisation ratios, U_c

Given the same properties and load conditions, Fig. 7.15, shows the tensegrity structure with its individual member utilisation ratios and internal forces. The highest utilisation ratio, and hence the most critical case, belongs to Member BF , for which the maximum allowable axial stress is $281.06N/mm^2$, and the maximum allowable buckling stress is $1110.48N/mm^2$. Based on this maximum axial load capacity and the member cross-section area, the maximum compressive load capacity of this critical member, and hence the whole tensegrity column, is

7.6 Tensegrity Columns

Table 7.16: MILP ‘XIX’ column: CHS sizes

<i>Member</i>	Original Area cm^2	Diameter cm	Thickness cm	Actual Area cm^2
AB	22.50	(cable)		
AC	54.8293	16.83	1.20	58.92
BC	39.5055	13.97	1.00	40.75
BD	15.7692	7.61	0.80	17.12
CD	34.788	11.43	1.2 0	38.57
CE	50.00	17.78	1.00	52.71
DG	See BD			
ED	See CD			
EF	See AC			
EG	See BC			
FG	See AB			

2770kN with a self-weight of 1051kg (or 2.63kN per kg of weight). This is higher than that of the conventional LP structure, by a factor of 1.28, as a whole. However, the maximum compressive load capacity per kg of weight is lower than that of the one-bar structure; 2.63kN/kg compared to 5.40kN/kg, which gives the ratio of 0.49.

Unsurprisingly, that the utilisation ratios for constituent members in tensegrity column is low, is because the ‘tensegrity column’ is composed of a multitude of shorter compressive members; the design compression resistance is dependent on the partial safety factor, which is dependent on the length/cross-section ratio of the member.

In conclusion, this serves as further evidence that, even when given realistic steel properties and design criteria, the modified, tensegrity structure performs better than the corresponding LP structure, purely considering the load resistance. However, it is clear that the maximum compressive capacity of the tensegrity structure per given weight is lower by a factor of 0.49, which reinforces the original hypothesis that tensegrity is inherently a non-optimal structure and it contains

7.6 Tensegrity Columns

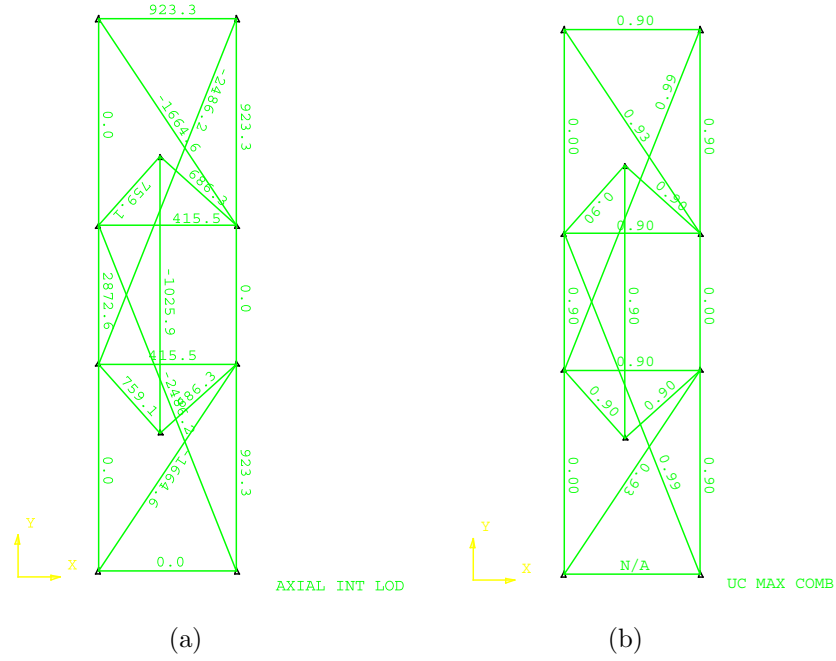


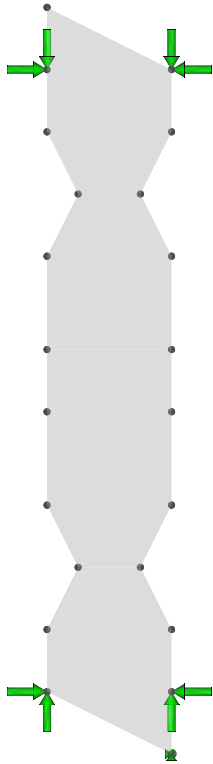
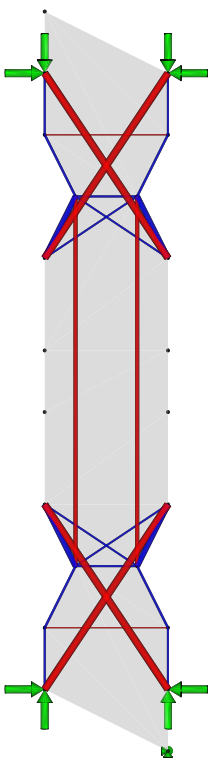
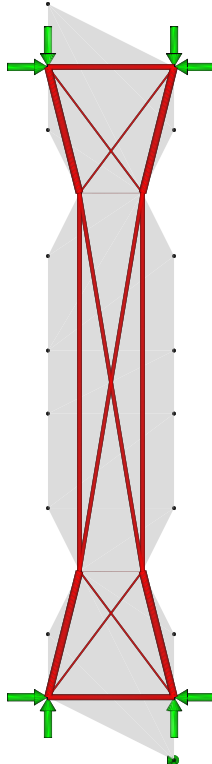
Figure 7.15: LP structure: internal member forces and utilisation ratios, U_c

structural redundancies as in the previous section.

7.6.5 Tensegrity ‘XIIX’ Column

The same vertical force analysis as in the previous section is repeated here. In addition a horizontal analysis is provided.

Table 7.17: 2D tensegrity structures without supports: horizontal and vertical axial loads

<i>Design domain</i>	<i>Tensegrity</i>	<i>LP</i>
(a)	(b)	(c)
		
Data		
<i>Target Node No.=</i> 21	V_{Ten}	V_{LP}
<i>Scale Factor=</i> 0.001	1350	600
<i>Load=</i> 50 (each)		

7.6 Tensegrity Columns

Table 7.18: MILP 'XIIX' Para-tensegrity Column: internal loads

	<i>Member</i>	q	q_x	q_y	<i>radius</i>	<i>vol.</i>	
<p>(a)</p>	AC	25.00	0.00	25.00	2.82095	12.50	
	AH	-90.1388	-50.00	-75.00	5.3565	162.50	
	BD	25.00	0.00	25.00	2.82095	12.5	
	BG	-90.1388	-50.00	-75.00	5.3565	162.5	
	CD	-12.5	-12.5	0	0.00	1.99471	12.5
	CE	27.9508	12.50	25.00	2.98279	15.625	
	DF	See CE					
	EF	25.00	25.00	0.00	2.82095	12.50	
	EG	69.8771	31.25	62.50	4.7162	39.0625	
	EH	22.5347	18.75	12.50	2.67825	20.3125	
	EK	-50.00	0.00	-50.00	3.98942	150.00	
	FG	See EH					
	FH	69.8771	31.25	62.50	4.7162	39.0625	
	IK	See EG					
	IL	See FG					
	IP	See AH					
	JK	See FG					
	JO	See AH					
	JL	See EG					
	KL	See EF					
KM	See CE						
LN	See CE						
MN	See CD						
MO	See AC						
NP	See AC						
OP	See AB						

7.6 Tensegrity Columns

Table 7.19: LP ‘XIIX’ Column: internal loads

	<i>Member</i>	q	q_x	q_y	<i>radius</i>	<i>vol.</i>
<p>(a)</p>	AB	-33.4384	-33.4384	0.00	3.26248	33.4384
	AC	-43.1655	-10.4692	-41.8767	3.70675	44.494
	AD	-10.1541	-6.09245	-8.12327	1.79782	12.6926
	CD	-0.707044	-0.707044	0.00	0.474404	0.35352
	CE	-27.9819	0.00	-27.9819	2.98444	83.9456
	CF	-22.3218	-3.66969	-22.0181	2.66557	67.8892
	DE	See CF				
	DF	See CE				
	EF	See CD				
	EG	See AC				
	EH	See AD				
	FG	See AD				
	FH	See AC				
	GH	See AB				

7.6 Tensegrity Columns

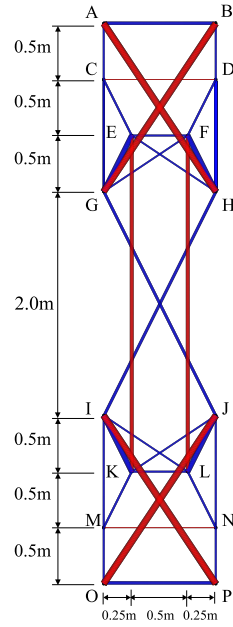


Figure 7.16: Tensegrity 'XIIX' column with additional members

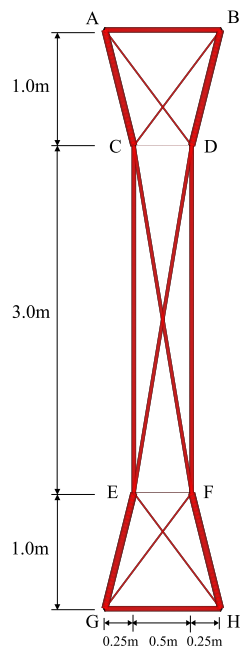


Figure 7.17: LP Structure corresponding to Tensegrity 'XIIX' column

Vertical Load: ‘XIIX’ Column and LP structure

In order to understand the tensegrity ‘column’ structure, its behaviours with a particular emphasis on buckling, are compared to those of the conventional LP structure, utilising commercially available CHSs for compression members and realistic steel properties (and dimensional units) whilst maintaining the section area of the original sections from optimisation. These are found in Table E.5 for the tensegrity structure and in Table E.4 for the corresponding LP structure. Horizontal and vertical pinned supports are located at the bottom two nodes in both ‘XIIX’ Column and the corresponding LP structure; in Nodes *O* and *P* for ‘XIIX’ Column and in Nodes *G* and *H* for the corresponding LP structure. Two external loads of equal magnitude are applied in negative *y*-direction (vertically), to Nodes *A* and *B* in both ‘XIIX’ Column and the corresponding LP structure. These loads are incremented until the most critical member in the structures, reaches its full load carrying capacity. For concision, a summary of results for comparison between tensegrity and corresponding LP structures is provided in Table E.6. For full description of results, see Appendix E.

Horizontal Load: ‘XIIX’ and LP Columns

Maintaining the CHS of the member cross-sections and realistic steel properties, this time, initially a small horizontal load is applied to Node *B* in negative *x*-direction in both ‘XIIX’ tensegrity structure and the corresponding LP structure. This load is incrementally increased until the U_c in the most critical member reaches 1.00 (or 0.99). For concision, a summary of results for comparison between tensegrity and corresponding LP structures is provided in Table E.6. For full description of results, see Appendix E.

Table E.6 is the summary of maximum resisted load per weight comparisons between tensegrity and LP structures in the above analyses.

7.6 Tensegrity Columns

Table 7.21: MILP ‘XIIX’ column: CHS sizes

<i>Member</i>	Original Area	Diameter (<i>cm</i>)	Thickness (<i>cm</i>)	Actual Area (<i>cm</i> ²)
AB	33.44	6.525	3.260	33.44
AC	25.00	5.642	2.820	24.99
AH	90.14	24.45	1.25	91.11
BD	25.00	5.642	2.820	24.99
BG	90.14	24.45	1.25	91.11
CD	12.50	7.61	0.60	13.21
CE	27.95			
DF	See CE			
EF	25.00	5.642	2.820	24.99
EG	69.88			
EH	22.53			
EK	50.00	17.78	1.00	52.71
FG	See EH			
FH	69.877			
GJ	See AC			
HI	See AC			
IK	See EG			
IL	See FG			
IP	See AH			
JK	See FG			
JO	See AH			
JL	See EG			
KL	See EF			
KM	See CE			
LN	See CE			
MN	See CD			
MO	See AC			
NP	See AC			
OP	See AB			

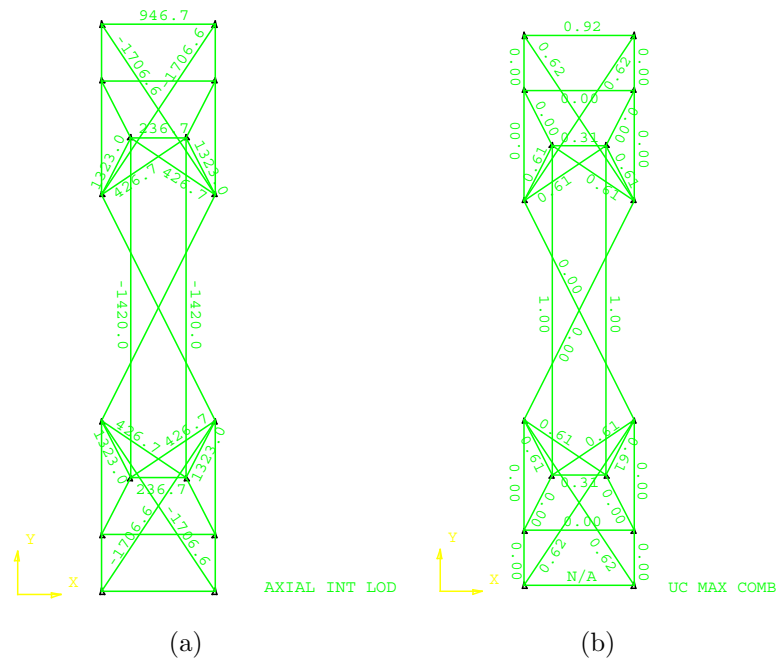


Figure 7.19: MILP-derived 'XIIX' tensegrity structure: internal member forces and utilisation ratios, U_c

7.6 Tensegrity Columns

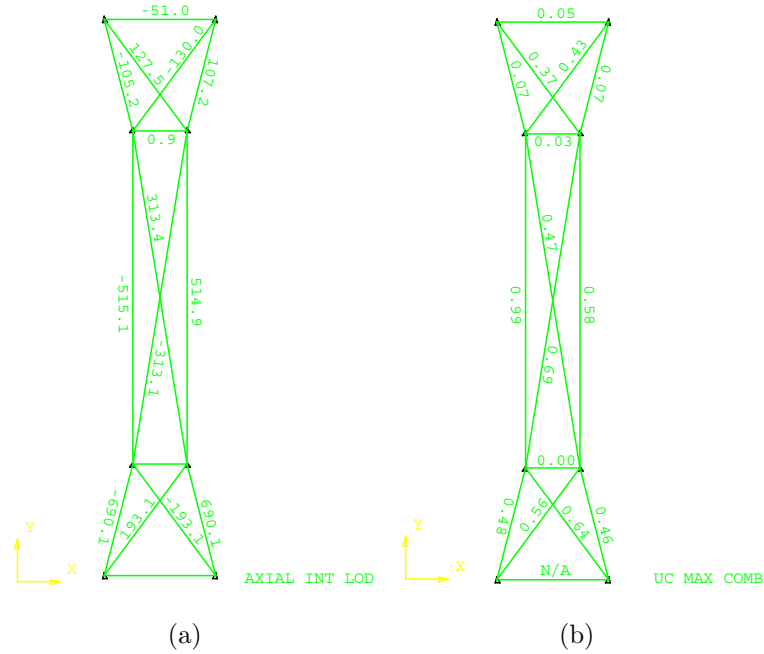


Figure 7.20: LP structure: internal member forces and utilisation ratios, U_c

Table 7.22: Summary of maximum resisted load per weight comparisons between tensegrity and LP structures

	<i>Tensegrity</i> Max. Force (kN)	Weight (kg)	(kN/kg)	<i>Corresponding LP</i>	Max. Force (kN)	Weight (kg)	(kN/kg)
Stayed Column	347.9	2739	0.127	LP	125	196	0.637
‘XIX’ Column	2770	1051	2.63	LP	2170	402	5.40
‘XIIIX’ Column (vertical)	2840	1298	2.19	LP (vertical)	1480	490	3.02
‘XIIIX’ Column (horizontal)	67	1298	0.052	LP(horizontal)	103	490	0.210

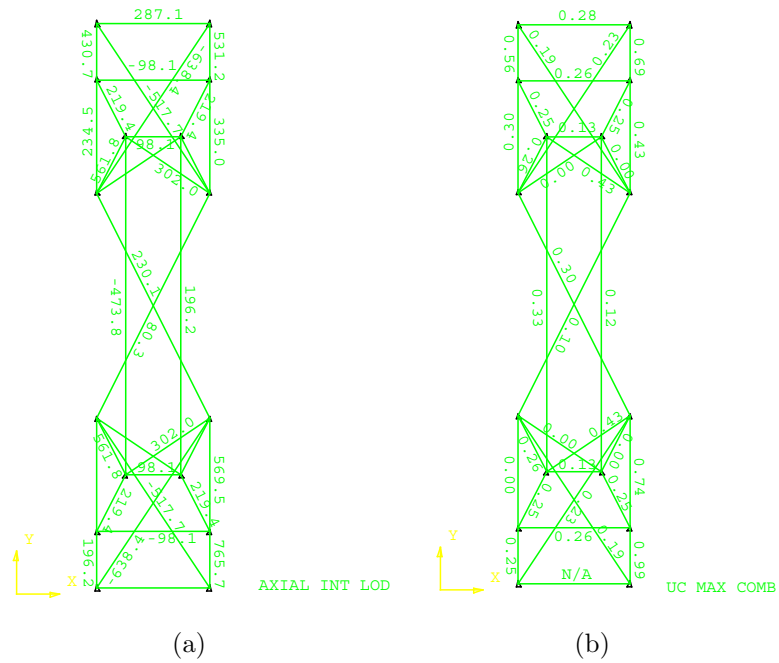
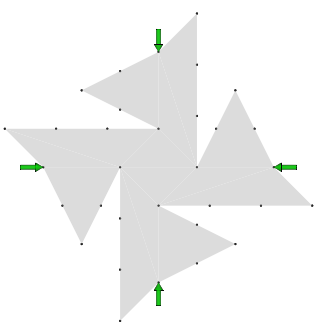
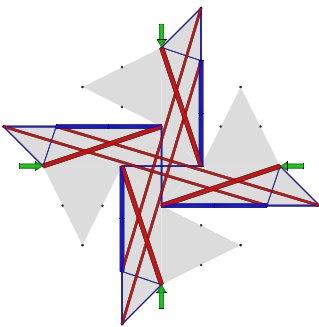
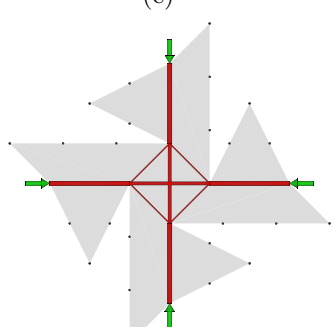


Figure 7.21: MILP structure: internal member forces and utilisation ratios, U_c

7.7 Other Tensegrity-type Structures

This section has one motive; to further demonstrate the capability of the MILP formulation by generating other 2D tensegrity type structures, i.e without supports (c.f. Michell structures with supports in Table 7.1). Two further example structures are presented here.

Table 7.23: 2D tensegrity structures without supports: axial load along two orthogonal axes

<i>Design domain</i>	<i>Tensegrity</i>	<i>LP</i>
(a) 	(b) 	(c) 
	Data	
<i>Target Node No.</i> = 38	V_{Ten}	V_{LP}
<i>Scale Factor</i> = 0.5207	1027	300
<i>Load</i> =50 (each)		

First, Table 7.23 shows, a set of structures; (a) the design domain, (b) tensegrity type structure and, (c) an LP structure, optimised without the MILP constraint.

Because of the shape of the design domain, and the fact that the structure is symmetrically loaded about both vertical and horizontal axes with the loads of 50 (each), the resulting tensegrity type form is reminiscent of a related, reticulate system known as ‘reciprocal frames’¹. Note that the volume ratio between V_{Ten}

¹The term ‘reciprocal frame’ was coined by Graham Brown who applied for a patent regarding this system. It describes a 3D grillage structure constructed of a closed circuit of mutually

7.7 Other Tensegrity-type Structures

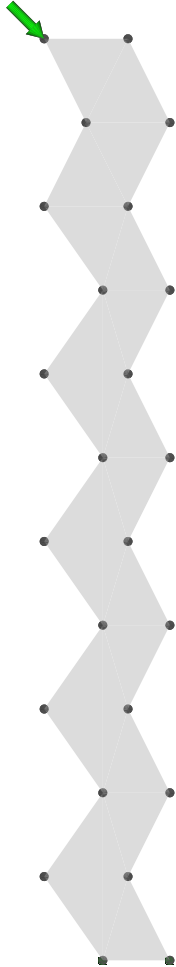
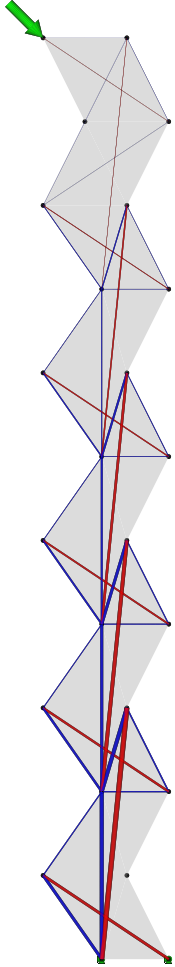
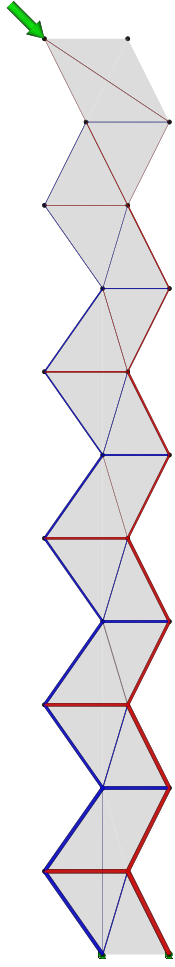
and V_{LP} is 1027:300 or 1:3.423.

Another interesting example of a para-tensegrity structure and a corresponding LP structure, which were generated with a diagonal load being exerted at a node, are presented in Table 7.24. A notable observation is made regarding the deployability of both the para-tensegrity and LP structures (one of the widely accepted advantages of tensegrity structures is their guaranteed deployability due to their reliance on tension members for overall rigidity). Whilst this reliance is a contributing factor to tensegrity's degree of deployability, the corresponding LP structure highlights that it is in fact, regularisation into unit members (in this case aided by design domain), which effects deployability.

supporting beams [230], where “each beam in the grillage is placed tangentially around a central closed curve so that it rests upon the preceding beam and this procedure is continued until the ring is complete. An enclosed polygon is, formed with a set of radiating beams equal in number to the sides of the polygon. The outer end of each beam rests on a perimeter support, such as column or wall, and the inner end rests on the following adjacent beam whilst in turn supporting the inner end of the preceding beam.” [231]

7.7 Other Tensegrity-type Structures

Table 7.24: 2D Tensegrity Tower

<i>Design domain</i>	<i>Tensegrity</i>	<i>LP</i>
(a)	(b)	(c)
		
Data		
<i>Target Node No.</i> =21	V_{Ten}	V_{LP}
<i>Scale Factor</i> =0.001	8.928×10^4	2.306×10^4
<i>Load</i> =100 (each)		

7.8 Discussion

A simple additional formulation on the existing full ground-structure LP formulations, has been devised, in order to generate tensegrity type structures. As illustrated, what would normally be a simple node at which two or more struts coincide are forced to accommodate only one straight strut, creating an indirect path between the two adjacent ends of two struts meeting at a node. In this sense tensegrity can be described as indirect-path-creating method of transferring a force from one end to another, implying its structural inefficiency insofar as its capacity to withstand external loads is concerned.

With regard to the generated forms, it must be stated that whilst fulfilling the main conditions of tensegrity, they do not meet the strictest definition of tensegrity as they have supports and are not self-stressable; thus these may be classified as ‘tensegrity type’ or ‘para-tensegrity’ structures. However, these serve two purposes: firstly, they provide a novel method of configuring connectivity, either regular or irregular, an major initial step in identifying/designing of tensegrity, enabling less restricted and irregular tensegrity topologies and secondly, they provide sufficient evidence to raise questions on the optimality of tensegrity.

As the results show, there is strong evidence that a para-tensegrity structure under a given load is, regardless of topology heavier than the structures identified using LP . It is a notable fact that, since the tensegrity formulation requires definition of an additional constraint in conjunction with LP constraints, it will never be more optimal in terms of weight, for a given applied load.

In order to ensure the relevance of this initial finding of the inefficiency of para-tensegrity structures, the investigation was extended to true tensegrity structures, using modified MILP-generated para-tensegrity structures. Both vertical and horizontal forces were applied, respectively to the structures, and the corresponding results further reinforced that tensegrity structures at least in the presented studies, are inefficient, compared to conventional LP structures, in terms of load

carrying capacity.

One very important topic, which deserves further discussion in relation to the presented results, is that of Euler buckling. In the analyses of tensegrity structures with CHSs, i.e. ‘XIX’ Tensegrity Column and ‘XIIX’ Tensegrity Column (and the respective, corresponding LP structures), it has become apparent that the maximum allowable axial stress was reached, where the most critical members were compressively loaded, before the maximum permissible buckling stress could be reached¹.

This is in line with the finding of Tyas [3], who noticed that commercially available CHSs, behave in a very linear manner, in that unless compressive CHS members are very lightly loaded there is an almost linear correlation between the cross-sectional area of a CHS member and its capacity to resist axial loads and that such nonlinear problems as buckling need not be considered (see Fig. 7.22).

7.9 Conclusions

1. Simple *MILP* formulations were devised to generate 2D tensegrity type structures, in both regular and irregular patterns, away from polyhedral templates.
2. Generating a tensegrity type structure requires the addition of a constraint to the existing *LP* formulation, which means a tensegrity structure cannot ever be lighter than an *LP* structure.
3. As the number of nodes is increased, the *LP* and tensegrity solutions tend to converges to *LP* solutions with the increase in nodal refinement.

¹Euler buckling is a phenomenon in which “a compressively loaded member fails by lateral instability at some load below the plastic crush capacity of the cross-section”[3].

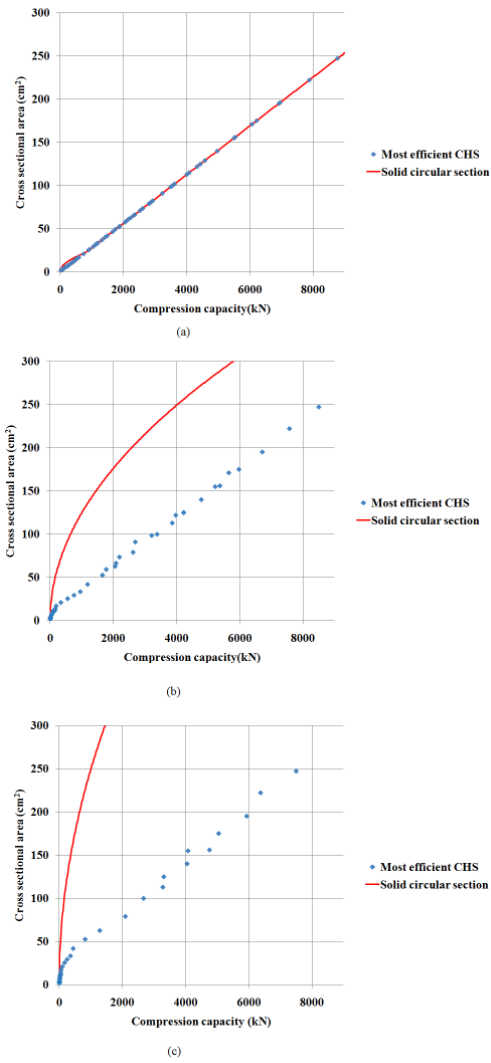


Figure 7.22: Cross-sectional area vs Compressive capacity, for CHS sections available in UK; (a)1m, (b)5m, (c)10m. Source:[3]

4. The example tensegrity structures, have been analysed extensively, regarding their load carrying capacity and structural response to different load conditions, to further reinforce that tensegrity structures may be structurally inefficient, compared to conventional LP optimum structures in terms of the load which they are capable of resisting per given weight, given realistic design properties of both solid and tubular steel sections.
5. The evidence presented in this chapter is an appropriate start to understanding load-carrying capacity and structural efficiency of tensegrity (or ‘strutendon’) in comparison to those of conventional LP structures, indicating that further investigation of Fuller’s suggestion with regard to optimality of tensegrity, is warranted.

Postscript

This part explored the two different but related capabilities of MILP in the context of use of computation-based form-generation methods in architecture design. The first chapter explored its capability to control the level of complexity of structures optimised by LP formulation for potential usage in conceptual form generation. More significantly, in the second chapter, tensegrity and tensegrity type structures, demonstration of generation of form of unconventional structural configuration, have been explored using a novel MILP formulation and it has also proven effective in generating tensegrity type structures dissociated from polyhedral geometry.

In discussion of the latter, it was found that tensegrity type structures are at least structurally less than optimal in comparison to the conventional LP structures, as the crucial requirement for separation between compressive and tensile members, necessitate extra lengths (or weight) of both types of members. Maintaining this logic stance, it was hypothesised that tensegrity structures with self-stress could also be less than optimal. This study has in effect proven its non-optimality with its comparative analyses of tensegrity type and conventional LP-structures as well as extensive tensegrity column analysis. Thus, this also offers a criticism of architectural designers who accept Fuller's assertion that tensegrity structures are 'lightweight' or optimal. The merit in application of tensegrity to foldable/deployable structures, hence, may not be due to tensegrity's lightweight but in its prestress state in relation to foldability. However, further work is required to consolidate proof of this non-optimality.

This analysis of tensegrity structures and development of a synthesis tool which can quickly and accurately generate valid tensegrity-type forms is an example of an integrative method of form design and a contribution toward integration of structural efficiency with architectural merit, which are mutually supportive of each other.

Part IV

**Discussion, Contributions,
Conclusions and
Recommendations for Future
Work**

Preface to Part **IV**

The overall aim of this thesis was to investigate the feasibility of applying an existing engineering optimisation (design) tool during the initial conceptual design stage, utilising it as an architectural form-finding tool.

In *Part II*, the approach adopted was to use conceptual design studies as a vehicle to investigate the applicability of a layout optimisation design tool, applying this to different types of construction. In *Part III*, the same design tool was augmented with MILP constraints to provide greater user-control, which, following testing, was further extended to permit tensegrity form generation.

This Part is designed to bring together the two strands of work described in the thesis, and to consider their relevance in the context of the original aim. The Part comprises two chapters; the first, *Chapter 8* reviews the scope and context of the investigations undertaken, and critically appraises the implications of the findings whilst also discussing limitations of the investigations. The second chapter then summarises the findings and contributions and finally concludes with recommendation for future work.

Chapter 8

Discussion of Research Findings

Numerous design examples were used to assess the feasibility of adopting layout optimisation as a tool for early stage conceptual form-generation. These examples presented in *Part II* revealed various limitations of the numerical technique, one of which was addressed in *Part III*

An essentially ‘one-step’ process of ‘set up and click-solve’ form-generation, with no intermediate designer-computer interaction, presented a major challenge for this particular approach to form-generation.

Three modes of usage were identified: ‘Full Automatic’, ‘Optimisation with Prescribed Outer Geometry’ modes in 3D, and ‘Planar Optimisation and Replication’ mode in 2D. However, all three modes of usage highlighted the need for an integrative (computer-aided) framework of design *and* subsequent manipulation.

Design of any object, regardless of the field, is essentially an iterative process, which requires constant adjustments and manipulation of parameters, and the final decision concerning the form should be placed with the human designer. Hence, any conceptual design tool envisaged to be useful should be, above all else, *flexible*. In this light, the lack of flexible readjustment or intermediate manipulation features seriously impair the feasibility of this approach.

The need for form-generation of a globally optimised building form is useful as a design guide. However, it may be unrealistic in some cases as the actual design elements (and activities) in practice are currently *highly* modularised.

Most notably, although the forms generated by the structural optimisation approach would serve as a good guide to form design, in comparison to the ‘free-flowing’ forms generated by form-led approaches, e.g. [31][27], the forms presented in this thesis tend to be visually less ‘adventurous’.

Many of the generated forms exhibited a high level of (over)complexity, to the point of impracticality, which led to the next phase of research in *Part III*. However, there is an alternative view on this issue. In response to the appraisal of the LP-generated forms as being ‘less adventurous’, there is a paradox relating to the complexity of the LP-generated forms: the parameters used for form-generation could be chosen to ensure the generated arrangement of structural members is yet more complex, to form an enveloping surface or thick web of overlapping members, to be used for surface definition. This ‘super-complexity’ may present visual impact of the sort eagerly sought by architects, whilst still providing structural integrity.

Since the research began and thesis started taking shape, a 2D evolutionary structural optimisation approach has been used to define an exterior of a building [232]. This was achieved by ‘creatively’ manipulating support conditions along the length of the building design, and thereby resulting in optimised structural sections.

Similarly, as a potential followup to the work described in this this thesis, attempts could be made to apply structural optimisation techniques to 3D surface definition problems (via the use of ‘super-complex’ structural forms).

On the other hand, considering the immediate task of improving the practicality of the design solutions obtained using the LP-based formulation, this thesis has

concentrated on the issue of practicality of the generated forms. This crucial issue warranted further investigation, leading to the development of a mixed integer linear programming (MILP) formulation (*Part III: Chapter 6*); a MATLAB script was written in order to investigate the effects and behaviour pattern of the formulation.

It was found that the script was successful in limiting the total number of members in the final optimised structure, demonstrating its capacity to reduce complexity in final optimised design and, more importantly, the behaviour of the MILP formulation is now better understood.

Whilst the member-reduction strategy used in this thesis has proved effective in dealing with the identified issue of over-complexity, the introduction of an additional constraint to the LP formulation has increased the solution CPU time considerably.

This is because the member reduction strategy using the MILP formulation presented in this thesis uses a number of binary variables in the mathematical programming matrix, and MILP is classified as ‘NP-hard’ in computational complexity theory (see [233] for explanation - i.e. computationally very hard to solve). Thus, its success mostly depends on the efficiency of the mathematical programming solver.

`lp_solve`¹, the LP (and MILP) solver used for the parametric studies in *Chapter 6*, is perhaps the most widely used open-source² LP solver, first developed by Michel Berkelaar at Eindhoven University of Technology [234].

Whilst there is no comprehensive academic publication of benchmarks of various available mathematical programming solvers of both commercial and open-source

¹<http://lpsolve.sourceforge.net/5.5/>

²Lesser General Public License

nature, a recent preliminary study by Hans Mittelmann of Arizona State University¹ has published some benchmark results. This study compares 10 widely used mathematical solvers, including `lp_solve`. In this study it was revealed that, compared with commercial solvers (e.g. CPLEX), the performance of `lp_solve` was weak (in terms of the CPU run time to arrive at solutions).

Having said that, MOSEK, the commercial optimiser used in *Chapter 7* for solving for tensegrity type structures with a similar number of binary variables, also struggled to tackle problems bigger than the ones presented in *Chapter 7*. For example, a problem with a design domain with the target number of nodes of 45 or above, struggled to yield a meaningful result, suggesting that even some commercial solvers struggle to solve even medium scale MILP problems.

Hence a much more efficient engineering strategy is required for practical usage of MILP in form design. In this effort², adaptation of ‘Member Adding’ approach developed by Gilbert and Tyas [91], which greatly improves the efficiency of classic LP formulation may present an opportunity for improvement in the efficiency of the MILP formulation. However, in its present form it is unlikely to be compatible with MILP because the binary constraint (i.e. $A_i/R \geq k_i$) used in both *Chapter 6* and *7* means that the ‘dual problem’ used by the ‘Member Adding’ is no longer present.

However, rather than focussing on incrementally improving the computational efficiency of the formulation, it was decided that it would be of more interest to investigate application of MILP to tensegrity design problems. This is in keeping with the fundamental theme of the thesis: versatile use of an engineering tool to

¹<http://plato.asu.edu/ftp/milpf.html>

²On a different note, in light of the relatively recent development of the ‘3D printing’ or rapid prototyping, the overcomplexity of the structures generated by the normal *LP* formulations may not be an issue at all. In fact, given that the complex structures can be rapidly ‘prototyped’, the ‘true’ optimum structures containing numerous nodes and members may even be an advantage as they will use the least amount of material.

provide solutions in the domain of architectural design.

Tensegrity design can also be viewed as a representative example of form generation of unconventional structural configuration. The tensegrity form began its development in the field of architecture and is a classic interdisciplinary synthesis of structure and form, with its essentially indivisible structural aesthetic effecting an architectonic quality. Hence the study of tensegrity is highly relevant to the overall investigation, where an engineering tool can produce (or enhance) aesthetics of form, with an architectural intention.

The most definitive characteristics of tensegrity are separation between compressive and tensile members, complete absence of bending elements, self-stress (with continuous tensile members), and individually isolated compressive members. The existing LP formulation was already capable of generating optimum structures which would present the first two characteristics. Additionally, literature reviews in the field of tensegrity indicated that many researchers had focused on various form-finding methods, often using topological configurations derived from known polyhedra. Thus, the research led to a means of identifying topological configuration of compressive and tensile members in tensegrity structures; *Part III: Chapter 7* demonstrated successfully that MILP is capable of generating tensegrity-type structures with correctly configured tensegrity connectivity.

In that same investigation, it was found that tensegrity type structures are structurally less efficient than structures identified using LP. This is because the crucial requirement for separation between compressive and tensile members, necessitates needless extra lengths (or weight) of members. Further work in this study, on the load capacity of a tensegrity confirmed that self-stressable, ‘true’ tensegrity structures would also be less optimal.

This finding contrasts with Fuller’s early statements about the efficacy of tensegrity structures. Prior to his ‘invention’ of tensegrity, Fuller presented in his 1954 patent [235], novel methods of constructing geodesic structures based on polyhedral geometry; these were to some extent predecessors of his tensegrity structures.

Having judged structural performance by weight per sheltering square foot, his invention of geodesic structures seemed optimal as it provided more square-footage of coverage per given weight than the conventional wall and roof design, while also providing sufficient wind load resistance. In 1962, another of Fuller’s patents, entitled, ‘*Tensile-Integrity Structures*’ [141], he introduced tensegrity domes derived from his geodesic polyhedral domes and makes a clear suggestion that his newly invented structural form is structurally optimal [141].

It is possible to hypothesise that Fuller assumed structural optimality in tensegrity on two grounds: one is its capacity for large coverage with apparently little weight when closely following the geodesic construction method, and the other (perhaps more compelling) reason is the apparent replacement of compression members with tensile members when converting geodesic structures to tensegrity structures.

However, it is perhaps too early to refute Fuller’s claims completely, as the focus of the studies described herein was on ‘tensegrity type’ structures, without self-stress. Self-stress should be included in future work in order to make direct comparisons possible.

Whilst the presented work may lead to criticism of architectural designers who accept Fuller’s assertion that tensegrity structures are ‘lightweight’ or optimal, the method developed also offers a rare computational tool for designing irregular tensegrity structures. The following example illustrates this method.

Designing tensegrity structures using the provided MILP formulation can be initiated by introducing additional tensile members between appropriate nodes as shown in Fig. 8.1. There are six additional tensile members in the design. Fig. 8.1(a) shows the original optimised tensegrity type structure with additional tensile members to be incorporated, and Fig. 8.1(b) shows the post-optimisation, *conjectured design* of tensegrity with the additional members incorporated into the original structure.

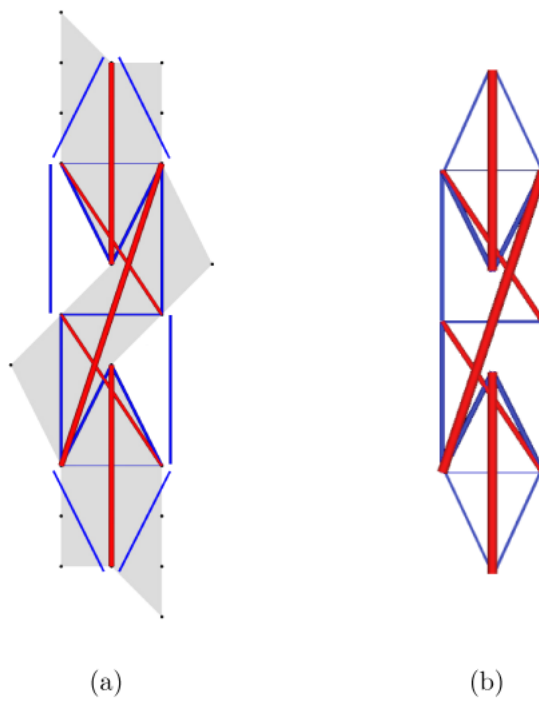


Figure 8.1: 2D tensegrity type structure with conjectured additional tensile members

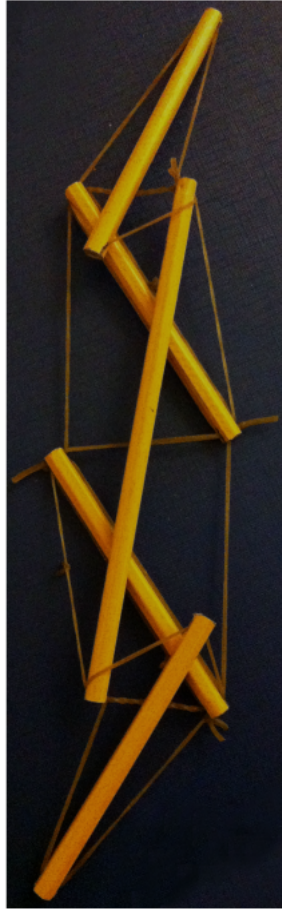
Then, self-stress can be achieved by redistributing any given load¹ amongst all tensile and compressive members including the additional members.

This redistribution of internal forces may be achieved by a number of form-finding methods available (e.g. [167] [168] [169]), although implementation of self-stress into the current MILP formulations should follow.

In the meantime, Fig. 8.2 shows a physical model of 2D tensegrity structure, constructed, with reference to the MILP automatically generated structures in Fig. 8.1. This physical model works in the same way as the structures shown in Fig. 8.1; it should be assumed that any interaction or exertion of forces between the overlapping members are negligible and are thought to pass across each other. It is also worth mentioning that the physical model has the same topology as the generated and designed tensegrity structure in Fig. 8.1(b), but a different geometry. This is because topology is determined by the spatial arrangement of members whilst geometry is determined by the internal member forces, and the introduction of new tensile members in the process of transforming the structure into a true tensegrity structure inevitably altered the shape of the structure without altering its topology.

Whilst the *MILP* formulation is capable of generating regular and irregular tensegrity type structures, and of configuring the topological connectivity of members, it serves only as an initial building block for tensegrity structure design, and a further form-finding process is needed to comply with the strictest definition tensegrity, where self-stress is involved.

¹providing that the load does not exceed the material strengths of the members.



(a)



(b)

Figure 8.2: Physical models of 2D tensegrity structure, based on MILP automatically generated structures in Fig. 8.1

Chapter 9

Contributions and Recommendations for Future Work

9.1 Contributions

1. A linear programming layout optimisation formulation has been applied to the form-generation of conventional structural configurations, with a focus on obtaining qualitative output for use in early stage concept design. Its feasibility has been tested and appropriate modes of usage of the current technology have been classified and discussed, showing the potential for such an engineering optimisation tool to be used in architectural concept design, subject to a number of improvements being made.
2. In response to the apparently impractical, complex, solutions frequently encountered when using layout optimisation, a simple mixed integer linear programming formulation has been devised in order to reduce the total number of members present in the solution, thereby simplifying the form of the output.
3. It has been demonstrated that, in addition to reducing the complexity of the solutions obtained, the inclusion of an additional MILP constraint in

the layout optimisation formulation also offers the user/designer a higher degree of controllability.

4. Parametric studies have been used to help obtain a better understanding of the behaviour of the MILP formulation, and to further demonstrate the capability of the MILP formulation to reduce the degree of complexity in optimised structures if so required.
5. The same extended MILP formulation has successfully been used to generate an unconventional structural configuration, namely an irregular tensegrity (or para-tensegrity) type structure, with special member connectivity configurations.
6. A design method for irregular tensegrity has been developed in which no prior knowledge of nodal connectivity is required, thereby allowing designers to move beyond conventional form-finding or empirical methods, which rely heavily on polyhedral templates.
7. Example tensegrity structures have been analysed extensively, using realistic material and section properties. Specifically, their load carrying capacity and responses to different load conditions have been carefully scrutinised. This served to further reinforce that tensegrity structures may be less structurally efficient than conventional LP generated structures in terms of load resistance for a given weight. The results may call into question Fuller's assertion of tensegrity's intrinsic light weight and inherent 'optimality'.
8. The analyses of tensegrity structures presented have contributed to our overall understanding of this interesting structural form.
9. By extending the layout optimisation tool to provide a method of design for tensegrity structures, the versatility of engineering optimisation as a tool for conventional and unconventional form-generation has been further demonstrated.

9.2 Recommendations for Future Work

9.2.1 Form-generation and Integrated Design Approach

Although the generated forms and designs presented in this thesis were promising, the results obtained in *Part II* indicate the need for two developments.

First is regularisation of the structural member segments, particularly in the form-finding example as fabrication of a multitude of unique individual members is likely to be impractical in present circumstance, although considering the rapid advancement in such technologies as CNC or 3D printing, some practical issues are likely to be alleviated or eliminated.

Second is provision of a robust computer framework or methodology through which both initial form-generation and subsequent design manipulation can be considered and integrated¹.

Improvements in this area may lie not in technical engineering enhancements to be able to model or generate physically viable forms. Rather, a solution may be in the domain of the interface design and organisation of computer design platform, i.e. an overall integrative design platform onto which various aspects of building design can be integrated. There are a number of commercial BIM platforms available. However, provision of an integrated design platform, which incorporates structural optimisation, is rare, although those which incorporate structural analysis capabilities are more common².

Further research should also be undertaken in a more practical environment, with team collaborations involving professionals in various design fields, not necessar-

¹This initial, integrated form (structure) generation/design framework is not to be confused with the likes of Building Information Modelling, which already deal with multiple parameters of building design.

²Some as plug-ins to a major software platforms.

ily confined to consideration of the integration of form and structure but also in manufacturing and fabrication. This would be an addition which could render the tool used in this thesis much more effective and economic. Much work in this area, of holistic approach, from form conception to fabrication is actively being investigated (e.g. [236]).

9.2.2 Structural Optimisation

Due to the mathematical complexity of Michell's optimality theory, until relatively recently, most structural optimisation research dealt mostly with exact solutions and isolated problems with typically simple loading and support conditions. The current capabilities of the optimisation technology developed at the University of Sheffield include the ability to identify optimum solutions with multiple load cases and considerations of buckling, self-weight of members, transmissible loading and joint costs with good computational efficiency.

However, there are a number of issues yet to be resolved. There are two areas of further research required in order to achieve practicality: (i) enhancement in the modelling capability to better represent reality, and (ii) control issues. The work in this thesis briefly explored control issues.

The tested MILP formulation, while having the desired capability to control the final form of the optimised solutions, can be prohibitively slow to solve. The MILP constraints are undoubtedly useful with regard to controllability of the optimised structures. The capability of the MILP formulation may extend to: limiting the number of nodes or the number of members arriving at a node, introduction of penalties on close members at a node and including only members from tabulated sets of commercially available structural member sections. Although this thesis focused on the dichotomous relationship between architecture and engineering, redirecting the thesis from exploring MILP further as a purely engineering investigation, application of MILP to solve larger problems, presents

a compelling area of further research.

9.2.3 Tensegrity

Although it has been possible to prescribe the specialised member connectivity associated with tensegrity type structures, one crucial characteristic of tensegrity, namely self-stress, was not included in the final resulting structures. In order to comply with the orthodox definition of tensegrity no external applied loads should be present, self-stress should be involved and there should be complete separation between compressive and tensile elements. Also, in most tensegrity structures of orthodox definition, tensile members are of one cross-sectional area, whereas the structures generated by the MILP formulation comprise tensile members of various cross-sections. From the perspective of fabricators, this is less than ideal and is an issue which needs to be resolved in order to develop a more versatile design tool.

Lastly the computational efficiency of the MILP formulation needs much improvement if larger scale tensegrity structures are to be generated.

References

- [1] P. Dombernowsky and A. Søndergaard. Three-dimensional topology optimisation in architectural and structural design of concrete structures. In *Symposium of the International Association for Shell and Spatial Structures (50th. 2009. Valencia). Evolution and Trends in Design, Analysis and Construction of Shell and Spatial Structures: Proceedings*. Editorial de la Universitat Politècnica de Valencia., 2010. [xi](#), [16](#), [35](#), [36](#)
- [2] S. Adriaenssens, L. Ney, E. Bodarwe, and C. WILLIAMS. Finding the form of an irregular meshed steel and glass shell based on construction constraints. *Journal of Architectural Engineering*, 18(3):206213, 2012. [xiii](#), [131](#), [134](#)
- [3] Andrew Tyas and Matthew Gilbert. Is euler buckling a significantly non-linear phenomenon in practical structural layout optimisation? *Manuscript for J. of Struct. Multidisc. Optim.*, 2012. [xv](#), [224](#), [225](#)
- [4] E Viollet-le-Duc. *Discourses on architecture*. Grove Press, 1959. [1](#)
- [5] R Oxman. Theory and design in the first digital age. *Design Studies*, 27(3):229–265, 2006. [14](#)
- [6] C. Wu and S. Roe. What a brick wants to become: A design-research project. *AA Files*, (53):8–13, 2006. [16](#)
- [7] C. Hight. Manners of working: Fabricating representation in digital based design. *The SAGE Handbook of Architectural Theory*, page 410, 2012. [16](#)

REFERENCES

- [8] G Stiny and J Gips. Shape grammars and the generative specification of painting and sculpture. *Information processing*, 71:1460–1465, 1972. [16](#), [23](#)
- [9] S Wolfram and M Gad el Hak. A new kind of science. *Applied Mechanics Reviews*, 56:B18, 2003. [17](#)
- [10] R White and G Engelen. Cellular automata and fractal urban form: a cellular modelling approach to the evolution of urban land-use patterns. *Environment and Planning A*, 25(8):1175 – 1199, 1993. [17](#)
- [11] J Frazer. *An evolutionary architecture*. Architectural Association Publications, 1995. [17](#), [18](#)
- [12] M Devetakovic, L Petrusevski, M Dabic, and B Mitrovic. Les folies cellulaires – an exploration in architectural design using cellular automata. In *Proc. 12th Generative Art Conference GA2009*, 2009. [17](#)
- [13] P Prusinkiewicz and A Lindenmayer. *The algorithmic beauty of plants*. Springer New York, 1990. [17](#)
- [14] S Renger and A Traichel. Investigation of the agglomeration and the break-up of isolation material. In *Proc. 17th International Conference on Nuclear Engineering (ICONE17)*. ASME, Jul 2009. [17](#)
- [15] M Hansmeyer. *Distinguishing Digital Architecture*, chapter L-Systems in Architecture, pages 164–168. Birkhäuser, 2007. [18](#)
- [16] P Wonka, M Wimmer, F Sillion, and W Ribarsky. Instant architecture. In *ACM transactions on graphics*, volume 22, pages 669–677, 2003. [19](#)
- [17] M Hemberg, U-M O’Reilly, A Menges, KJM da Costa Goncalves, and SR Fuchs. Exploring generative growth and evolutionary computation in architectural design. *Art of Artificial Evolution*, 2004. [19](#)
- [18] G Voronoi. Nouvelles applications des paramètres continus à la théorie des formes quadratiques. premier mémoire: Sur quelques propriétés des formes quadratiques positives parfaites. *J. Reine Angew. Math.*, (133):97–178, 1907. [19](#)

REFERENCES

- [19] H Edelsbrunner. Triangulations and meshes in computational geometry. *Acta Numerica*, 9:133–213, 2000. [19](#)
- [20] J-R Sack and J Urrutia. *Handbook of computational geometry*. North-Holland, 2000. [19](#)
- [21] T Fischer. Generation of apparently irregular truss structures. *Computer Aided Architectural Design Futures 2005*, pages 229–238, 2005. Voronoi Beijing Swim. [19](#)
- [22] Arup. Total Design. *Arup promotional literature*, 2008. [20](#)
- [23] Ali Rahim. *Catalytic formations: architecture and digital design*. Taylor & Francis Group, 2006. [20](#), [106](#)
- [24] V C Lin, D C Gossard, and R A Light. Variational geometry in computer-aided design. In *Proc. of the 8th annual conference on Computer graphics and interactive techniques*, pages 171–177. ACM, 1981. [20](#)
- [25] RC Hillyard and IC Braid. The analysis of dimensions and tolerances in computer-aided shape design. *Computer Aided Design*, 10(3):161–166, 1978. [20](#)
- [26] J Monedero. Parametric design: a review and some experiences. *Automation in Construction*, 9(4):369 – 377, 2000. [20](#)
- [27] NC Katz. Parametric modeling in AutoCAD. *AECbytes Viewpoints Index*, (32), May 2007. [21](#), [231](#)
- [28] J. Harding, S. Joyce, P. Shepherd, and C. Williams. Thinking topologically at early stage parametric design. *Advances in Architectural Geometry 2012*, 2012. [21](#)
- [29] Í.G. DÍNO. Creative design exploration by parametric generative systems in architecture. *METU JFA*, 1:207, 2012. [21](#)

- [30] P. Sanguinetti, S. Abdelmohsen, J.M. Lee, J.K. Lee, H. Sheward, and C. Eastman. General system architecture for bim: An integrated approach for design and analysis. *Advanced Engineering Informatics*, 2012. [21](#)
- [31] P Schumacher. Parametricism: A new global style for architecture and urban design. *Architectural Design*, 79(4):14 – 23, 2009. [22](#), [231](#)
- [32] J.P. Koppitz, G. Quinn, V. Schmid, and A. Thurik. Metropol parasol-digital timber design. *Computational Design Modelling*, pages 249–257, 2012. [21](#), [22](#)
- [33] A. Menges. Integral computational design: synthesizing computation and materialization in architecture. *Int. J. Archit. Mod. Inf. Technol*, 4(03):2010, 2010. [21](#), [23](#)
- [34] David Blitz. *Studies on Mario Bunge’s Treatise*, chapter Emergent Evolution and the Level Structure of Reality, page 156. Rodopi, 1990. [24](#)
- [35] JL Kirsch and RA Kirsch. The anatomy of painting style: Description with computer rules. *Leonardo*, 21(4):437–444, 1988. [24](#)
- [36] JP Duarte. Towards the mass customization of housing: the grammar of siza’s houses at malagueira. *Environment & Planning B: Planning and Design*, 32(3):347–380, 2005. [24](#)
- [37] K Shea and J Cagan. The design of novel roof trusses with shape annealing: assessing the ability of a computational method in aiding structural designers with varying design intent. *Design Studies*, Jan 1999. [24](#), [34](#)
- [38] K Terzidis. *Algorithmic architecture*. Architectural Press, 2006. [24](#), [98](#)
- [39] M Bessa. Algorithmic design. *Architectural Design*, 79(1):120–123, 2009. [24](#)
- [40] Barbara Cutler and Emily Whiting. Constrained planar remeshing for architecture. In *Proceedings of Graphics Interface 2007*, GI ’07, pages 11–18, New York, NY, USA, 2007. ACM. [25](#), [31](#)

REFERENCES

- [41] Johannes Wallner and Helmut Pottmann. Geometric computing for freeform architecture. *Journal of Mathematics in Industry*, 1(1):4, 2011. [25](#)
- [42] H. Pottmann, S. Brell-Cokcan, and J. Wallner. Discrete surfaces for architectural design. *Curves and Surfaces: Avignon*, pages 213–234, 2006. [25](#)
- [43] M. Dimcic and J. Knippers. Integration of fem, nurbs and genetic algorithms in free-form grid shell design. *Computational Design Modelling*, pages 97–103, 2012. [26](#), [117](#)
- [44] F. Swetz. *Learn from the Masters: International Conference/workshop on the History of Mathematics, Kristiansand, Norway, August 1988*. Classroom Resource Material Series. The Mathematical Assoc. of America, 1995. [27](#)
- [45] George R. Collins. Antonio gaudi: Structure and form. *Perspecta*, 8:pp. 63–90, 1963. [27](#)
- [46] H. Isler. *New shapes for shells*. International Association for Shell Structures, 1960. [28](#)
- [47] J. Chilton. Heinz isler’s infinite spectrum: Form-finding in design. *Architectural Design*, 80(4):64–71, 2010. [28](#)
- [48] H Schek. The force density method for form finding and computation of general networks. *Computer Methods in Applied Mechanics and Engineering*, 3(1):115–134, 1974. [28](#), [85](#)
- [49] M. Dimcic. *Structural optimization of grid shells based on genetic algorithms*. PhD thesis, The University of Stuttgart, 2011. [29](#)
- [50] W.J. Lewis. *Tension Structures: Form and Behaviour*. Inst of Civil Engineers Pub, 2003. [29](#)

-
- [51] C.J.K. Williams. The analytic and numerical definition of the geometry of the british museum great court roof. *Digital tectonics*, Wiley-Academy, United Kingdom, pages 78–85, 2001. [30](#)
- [52] Y.M. Xie, P. Felicetti, J.W. Tang, and M.C. Burry. Form finding for complex structures using evolutionary structural optimization method. *Design Studies*, 26(1):55–72, January 2005. [30](#), [135](#)
- [53] A. Kilian and J. Ochsendorf. Particle-spring systems for structural form finding. *JOURNAL-INTERNATIONAL ASSOCIATION FOR SHELL AND SPATIAL STRUCTURES*, 148:77, 2005. [30](#), [135](#), [136](#)
- [54] I. Vizotto. Computational generation of free-form shells in architectural design and civil engineering. *Automation in Construction*, 19(8):1087–1105, 2010. [31](#)
- [55] T. Van Mele and P. Block. A novel form finding method for fabric formwork for concrete shells. *J. Int. Assoc. Shell and Spatial Structures*, 52:217224, 2011. [31](#), [47](#)
- [56] E. Vouga, M. Höbinger, J. Wallner, and H. Pottmann. Design of self-supporting surfaces. *ACM Transactions on Graphics (TOG)*, 31(4):87, 2012. [32](#)
- [57] D. Veenendaal and P. Block. An overview and comparison of structural form finding methods for general networks. *International Journal of Solids and Structures*, 49(26):3741 – 3753, 2012. [33](#)
- [58] K Shea. Digital canopy: high-end computation/low-tech construction. *arq: Architectural Research Quarterly*, 6(03):230–245, 2003. [34](#)
- [59] J Leuppi and K Shea. The hylomorphic project. *The Arup Journal, Ove Arup and Partner*, (1):28–30, 2004. [34](#)
- [60] S Kirkpatrick. Optimization by simulated annealing: Quantitative studies. *Journal of Statistical Physics*, 34(5):975–986, 1984. [34](#), [59](#)

-
- [61] J Cagan and W Mitchell. Optimally directed shape generation by shape annealing. *Environment & Planning B: Planning and Design*, 20(1):5–12, 1993. [34](#), [59](#)
- [62] K Bollinger, M Grohmann, and O Tessman. Form, force, performance: Multi-parametric structural design. *Architectural Design*, 78(2):20–25, 2008. [35](#)
- [63] P. von Buelow, A. Falk, and M. Turrin. Optimization of structural form using a genetic algorithm to search associative parametric geometry. *Proceedings of Structure and Architecture*, 2010. [35](#)
- [64] D. Veenendaal, J. Coenders, J. Vambersky, and M. West. Design and optimization of fabric-formed beams and trusses: evolutionary algorithms and form-finding. *Structural Concrete*, 12(4):241–254, 2011. [35](#)
- [65] J Bahoric. Aami park, melbourne. *The Arup Journal, Ove Arup and Partner*, (2):16–24, 2010. [36](#)
- [66] Kevin Legenza. Twisting steel and bending the imagination. *Structure Magazine*, pages 47–49, November 2007. [36](#)
- [67] W Jabi. An outline of the requirements for a computer-supported collaborative design system. *Open House International*, 21(1), 1996. [37](#)
- [68] B Kolarevic. *Architecture in the digital age: design and manufacturing*. Taylor & Francis, 2003. [37](#)
- [69] IJC Maxwell. On the calculation of the equilibrium and stiffness of frames. *Philosophical Magazine: Series 4 Vol. 1, (Paper XXVI in Collected Papers, Cambridge*, 27(182):294–299, 1964. [39](#), [69](#)
- [70] AGM Michell. LVIII. the limits of economy of material in frame-structures. *Philosophical Magazine Series 6*, 8(47):589–597, 1904. [39](#), [48](#), [51](#), [145](#), [180](#), [184](#)
- [71] SP Boyd and L Vandenberghe. *Convex optimization*. Cambridge University Press, 2004. [40](#), [43](#), [44](#), [52](#)

-
- [72] P Papalambros. Extending the optimization paradigm in engineering design. *Proc. 3rd Int. Symposium on Tools & Methods of Competitive Engineering, Delft*, 14, 2000. [41](#)
- [73] Y. Collette and P. Siarry. *Multiobjective optimization: principles and case studies*. Springer Verlag, 2003. [42](#), [43](#)
- [74] M Bendsøe and O Sigmund. Material interpolation schemes in topology optimization. *Archive of Applied Mechanics*, 69(9):635–654, 1999. [45](#)
- [75] A Gersborg-Hansen, O Sigmund, and R Haber. Topology optimization of channel flow problems. *Structural & Multidisciplinary Optimization*, 30(3):181–192, 2005. [45](#)
- [76] X Huang, YM Xie, and G Lu. Topology optimization of energy-absorbing structures. *International Journal of Crashworthiness*, 12(6):663–675, 2007. [45](#)
- [77] XY Yang, YM Xie, GP Steven, and OM Querin. Topology optimization for frequencies using an evolutionary method. *Journal of Structural Engineering-ASCE*, 125(12):1432–1438, 1999. [45](#)
- [78] R Yang and A Chahande. Automotive applications of topology optimization. *Structural and Multidisciplinary Optimization*, 1995. [45](#)
- [79] W S Dorn, R E Gomory, and H J Greenberg. Automatic design of optimal structures. *Journal de Mécanique*, 3(1):25–52, 1964. [45](#), [48](#), [51](#), [105](#), [267](#)
- [80] A Lencus, OM Querin, GP Steven, and YM Xie. Aircraft wing design automation with ESO and GESO. *International Journal of Vehicle Design*, 28(4):356–369, 2002. [45](#)
- [81] M Bendsøe and O Sigmund. Topology optimization: theory, methods, and applications. *Springer Verlag*, 2003. [46](#)
- [82] LA Schmit. Structural design by systematic synthesis. In *Proc. 2nd ASCE Conference on Electronic Computation*, pages 105–122. American Society of Civil Engineers, 1960. [46](#)

-
- [83] CA Cornell. Examples of optimization in structural design. Technical Report R65-26, University of Waterloo, Canada, 1968. [46](#)
- [84] M Ohsaki and C Swan. Topology and geometry optimization of trusses and frames. *Recent Advances in Optimal Structural Design*, 2002. [46](#)
- [85] GIN Rozvany and MP Bendsøe. Layout optimization of structures. *Applied Mechanics Reviews*, 48(2):41–119, 1995. [48](#), [51](#)
- [86] P del Torso, P Garibaldi, and U Kitsch. Shape and layout optimization of structural systems. *Structural & Multidisciplinary Optimization*, 2(1):64, 1990. [48](#)
- [87] W Spillers. *Iterative structural design*. North-Holland Amsterdam, 1975. [48](#)
- [88] TJ Pritchard. *Novel Techniques in Structural Layout Optimisation*. PhD thesis, University of Sheffield, 2005. [48](#), [51](#)
- [89] HSY Chan and WS Hemp. Optimum design of pin-jointed frameworks. *Aeronautical Research Council Reports and Memorandum*, 3632, 1970. [48](#)
- [90] B H V Topping. Shape optimization of skeletal structures: A review. *Journal of Structural Engineering*, 109(8):1933–1951, 1983. [49](#), [50](#)
- [91] M Gilbert and A Tyas. Layout optimization of large-scale pin-jointed frames. *Engineering Computations*, 20(8):1044–1064, 2003. [50](#), [106](#), [170](#), [178](#), [233](#), [268](#)
- [92] GIN Rozvany and MZ Cohn. Lower-bound optimal design of concrete structures. *Journal of the Engineering Mechanics Division*, 96(6):1013–1030, 1970. [50](#)
- [93] R Drazumeric and F Kosel. Optimization of geometry for lateral buckling process of a cantilever beam in the elastic region. *Thin-Walled Structures*, 43(3):515–529, 2005. [50](#)

REFERENCES

- [94] M Ohsaki. Design sensitivity analysis and optimization for nonlinear buckling of finite-dimensional elastic conservative structures. *Computer Methods in Applied Mechanics & Engineering*, 194(30-33):3331–3358, 2005. [50](#)
- [95] G Augusti, A Baratta, and F Casciati. Probabilistic methods in structural engineering. *Routledge*, 1984. [51](#)
- [96] N Olhoff and JE Taylor. On structural optimization. *Journal of Applied Mechanics*, 50:1139, 1983. [51](#)
- [97] W Prager. Notes on linear programming: Part XLII. linear programming and structural design. *Rand Research Memorandum KM-2021, ASTIA Document AP150661*, 1957. [51](#)
- [98] W Prager and RT Shield. A general theory of optimal plastic design. *Journal of Applied Mechanics*, 34(1):184–186, 1967. [51](#)
- [99] W Hemp. *Optimum structures*. Clarendon Press, 1973. [51](#), [145](#)
- [100] GB Dantzig. Programming in a linear structure. *Bulletin of the American Mathematical Society*, 54(11):1074–1074, 1948. [52](#)
- [101] J Nocedal and SJ Wright. *Numerical Optimization*. Springer Verlag, 2006. [52](#)
- [102] T Kolda, R Lewis, and V Torczon. Optimization by direct search: New perspectives on some classical and modern methods. *Society for Industrial & Applied Mathematics Review*, 45(3):385–482, 2003. [52](#), [53](#)
- [103] A Bensoussan, J Lions, and G Papanicolaou. *Asymptotic analysis for periodic structures*. North Holland, 1978. [55](#)
- [104] B Hassani and E Hinton. A review of homogenization and topology optimization I-homogenization theory for media with periodic structure. *Computers & Structures*, 69(707):707–717, 1998. [55](#)

- [105] M Bendsøe and N Kikuchi. Generating optimal topologies in optimal design using a homogenization method. *Computer Methods in Applied Mechanics & Engineering*, 71(2):197–224, 1988. [55](#)
- [106] S Nishiwaki, MI Frecker, S Min, and N Kikuchi. Topology optimization of compliant mechanisms using the homogenization method. *International Journal for Numerical Methods in Engineering*, 42(3):535–559, 1998. [55](#)
- [107] GIN Rozvany. A critical review of established methods of structural topology optimization. *Structural & Multidisciplinary Optimization*, 37(3):217–237, 2009. [56](#)
- [108] M Bendsøe. Optimal shape design as a material distribution problem. *Structural & Multidisciplinary Optimization*, 1(4):193–202, 1989. [56](#)
- [109] OM Querin, GP Steven, and YM Xie. Evolutionary structural optimisation using an additive algorithm. *Finite Elements in Analysis and Design*, 34(3-4):291–308, 2000. [56](#)
- [110] DN Chu, YM Xie, A Hira, and GP Steven. On various aspects of evolutionary structural optimization for problems with stiffness constraints. *Finite Elements in Analysis & Design*, 24(4):197–212, 1997. [56](#)
- [111] G Steven, O Querin, and M Xie. Evolutionary structural optimization (eso) for combined topology and size optimisation of discrete structures. *Computer Methods in Applied Mechanics and Engineering*, 188(4):743–754, 2000. [56](#)
- [112] OM Querin, GP Steven, and YM Xie. Evolutionary structural optimisation (ESO) using a bidirectional algorithm. *Engineering Computations*, 15(8):1031–1048, 1998. [57](#)
- [113] M Zhou and GIN Rozvany. On the validity of eso type methods in topology optimization. *Structural and Multidisciplinary Optimization*, 21(1):80–83, 2001. [57](#)

-
- [114] D Goldberg and M Samtani. Engineering optimization via genetic algorithm. In *Proc. of the 9th Conference on Electronic Computation*. ASCE, 1986. 57
- [115] SY Wang, K Tai, and MY Wang. An enhanced genetic algorithm for structural topology optimization. *International Journal for Numerical Methods in Engineering*, 65(1):18–44, 2006. 57
- [116] LM Schmitt. Theory of genetic algorithms. *Theoretical Computer Science*, 269(1-2):1–61, 2001. 57
- [117] Y Xue-xiao and H Song-lin. Schema theory of genetic algorithm. *Journal of Hubei Normal University (Natural Science)*, 2007. 58
- [118] K Deb. Multi-objective genetic algorithms: Problem difficulties and construction of test problems. *Evolutionary computation*, 7(3):205–230, 1999. 58
- [119] H Sakamoto, S Takada, J Itoh, M Miyazaki, and A Hijikata. Investigation of a practical method of structural optimization by genetic algorithms : Proposal of a hybrid GA and application towards the thickness optimization of a CRT. *JSME International Journal. Series A, Solid mechanics and material engineering. The Japan Society of Mechanical Engineers*, 44(3):330–337, 2001. 58
- [120] DE Goldberg. *Genetic Algorithms in Search, Optimization, and Machine Learning*. Addison Wesley, 1989. 58
- [121] R Bellman. *Dynamic Programming*. Harvard University Press, 2003. 58
- [122] SS Rao. *Engineering optimization: theory and practice*. John Wiley & Sons, 1996. 58, 59
- [123] A Das and BK Chakrabarti. *Quantum Annealing and Related Optimization Methods (Lecture Note in Physics 679)*. Berlin Heidelberg: Springer, 2005. 59

-
- [124] TM Blackwell. Particle swarms and population diversity. *Soft Computing - A Fusion of Foundations, Methodologies and Applications*, 9(11):793–802, 2005. [59](#)
- [125] F Glover. Future paths for integer programming and links to artificial-intelligence. *Computers & Operations Research*, 13(5):533–549, 1986. [60](#)
- [126] W Bennage and A Dhingra. Optimization of truss topology using tabu search. *International Journal for Numerical Methods in Engineering*, 38(23):4035–4052, 2005. [60](#)
- [127] K Hamza, H Mahmoud, and K Saitou. Design optimization of N-shaped roof trusses. *Proc. of the Genetic and Evolutionary Computation Conference*, pages 1089–1096, 2002. [60](#)
- [128] M. Dorigo and C. Blum. Ant colony optimization theory: A survey. *Theoretical Computer Science*, 344(2-3):243–278, 2005. [60](#)
- [129] J Bland. Optimal structural design by ant colony optimization. *Engineering Optimization*, 33(4):425 – 443, 2001. [60](#)
- [130] A Tyas, M Gilbert, and TJ Pritchard. Practical plastic layout optimization of trusses incorporating stability considerations. *Computers & Structures*, 84(3-4):115–126, 2006. [62](#), [63](#), [192](#)
- [131] A Ben-Tal and A Nemirovski. Robust truss topology design via semidefinite programming. *SIAM Journal on Optimization*, 7(4):991–1016, 1997. [63](#)
- [132] W Achtziger. Local stability of trusses in the context of topology optimization Part I: Exact modelling. *Structural & Multidisciplinary Optimization*, 17(4):235–246, 1999. [63](#)
- [133] M Kocvara. On the modelling and solving of the truss design problem with global stability constraints. *Structural & Multidisciplinary Optimization*, 23(3):189–203, 2002. [63](#)
- [134] EW Parkes. Joints in optimum frameworks. *International Journal of Solids & Structures*, 11(9), 1975. [64](#), [145](#), [146](#)

REFERENCES

- [135] D Reinschmidt Alan and F Kenneth. Applications of linear programming in structural layout and optimization. *Computers & Structures*, 4(4):855–869, 1974. [64](#), [145](#)
- [136] A. Hanaor. Debunking” tensegrity”-a personal perspective. *International Journal of Space Structures*, 27(2):179–184, 2012. [67](#), [68](#), [89](#), [176](#)
- [137] Maria Gough. In the laboratory of constructivism: Karl Ioganson’s Cold Structures. *October*, 84:90–117, 1998. [67](#), [69](#), [70](#)
- [138] KD Snelson. Letter from Kenneth Snelson to R. Motro, published in November 1990. *International Journal of Space Structures*, 1990. [67](#), [69](#), [70](#), [71](#)
- [139] D Stamenović, JJ Fredberg, N Wang, JP Butler, and DE Ingber. A microstructural approach to cytoskeletal mechanics based on tensegrity. *Journal of theoretical biology*, 181(2):125–136, 1996. [67](#)
- [140] CS Chen and DE Ingber. Tensegrity and mechanoregulation: from skeleton to cytoskeleton. *Osteoarthritis & Cartilage*, 7(1):81–94, 1999. [67](#)
- [141] RB Fuller. Tensile-integrity structures. *US Patent 3,063,521*, 1962. [68](#), [175](#), [235](#)
- [142] CR Calladine. Buckminster fuller’s “tensegrity” structures and Clerk Maxwell’s rules for construction of stiff frames. *International Journal of Solids & Structures*, 14(2):161–172, 1978. [69](#), [175](#)
- [143] RW Marks. *The Dymaxion world of Buckminster Fuller*. Reinhold Publishing, 1960. [69](#)
- [144] DG Emmerich. Charpentes perles (pearl frameworks). *Institut National de la Propriete Industrielle. Reg. No. 59423*, May 1959. [69](#)
- [145] R Motro. Tensegrity: structural systems for the future. *Butterworth-Heinemann*, 2003. [69](#), [71](#), [72](#), [75](#), [77](#), [79](#), [80](#), [86](#), [91](#), [175](#)
- [146] DG Emmerich. *Structures Tendues et Autotendantes*. Ecole d’Architecture de Paris la Villette, 1988. [69](#)

REFERENCES

- [147] RW Jr Burkhardt. A practical guide to tensegrity design: 2nd edition. *Cambridge, Massachusetts: Tensegrity Solutions*, pages 1–216, 2006. [69](#)
- [148] RB Fuller. *Synergetics; explorations in the geometry of thinking*. Macmillan New York, 1975. [71](#), [76](#)
- [149] KD Snelson. Continuous tension, discontinuous compression structures. *US Patent No. 3,169,611*, 1965. [71](#)
- [150] A Pugh. *An introduction to tensegrity*. University of California Press, Jan 1976. [72](#), [74](#), [75](#), [77](#), [175](#)
- [151] RE Skelton, JP Pinaud, and DL Mingori. Dynamics of the shell class of tensegrity structures. *Journal of Franklin Institute*, 338(2-3):255–320, 2001. [73](#), [173](#), [175](#)
- [152] H Kenner. *Geodesic math and how to use it*. University of California Press, 2003. [74](#), [85](#)
- [153] B Roth and W Whiteley. Tensegrity frameworks. *Transactions of the American Mathematical Society*, 265(2):419–446, Jan 1981. [74](#)
- [154] R Connelly. Tensegrity structures: Why are they stable? *Rigidity Theory and Applications*, pages 47–54, 1998. [74](#)
- [155] H Murakami. Static and dynamic analyses of tensegrity structures. part 1. nonlinear equations of motion. *International Journal of Solids & Structures*, 38(20):3599–3613, 2001. [74](#), [175](#)
- [156] S Pellegrino. Analysis of prestressed mechanisms. *International Journal of Solids and Structures*, 26(12):1329–1350, 1990. [74](#)
- [157] N Kanchanasaratool and D Williamson. Modelling and control of class NSP tensegrity structures. *International Journal of Control*, 75(2):123–139, 2002. [74](#)
- [158] IJ Oppenheim and WO Williams. Vibration of an elastic tensegrity structure. *European Journal of Mechanics A-Solid*, 20(6):1023–1031, 2001. [74](#)

REFERENCES

- [159] C Sultan and R Skelton. Deployment of tensegrity structures. *International Journal of Solids and Structures*, 40(18):4637–4657, 2003. [75](#)
- [160] JP Pinaud, S Solari, and RE Skelton. Deployment of a class 2 tensegrity boom. In *SPIE proceedings series*, pages 155–162. Society of Photo-Optical Instrumentation Engineers, 2004. [75](#)
- [161] S Pellegrino. A class of tensegrity domes. *International Journal of Space Structures*, 7:127–142, 1992. [75](#)
- [162] M Masic and R Skelton. Open-loop control of class-2 tensegrity towers. In *Proc. of the 11th Smart Structures & Materials Conference*, volume 5383, pages 298–308, 2004. [75](#)
- [163] A Hanaor and M Liao. Double-layer tensegrity grids: Static load response. Part I: Analytical study. *Journal of Structural Engineering*, 117(6):1660–1674, 1991. [75](#)
- [164] RP Raj and SD Guest. Using symmetry for tensegrity form-finding. *Journal of International Association for Shell & Spatial Structures*, 152:245, 2006. [76](#)
- [165] RB Fuller. Geodesic tent. *US Patent 2,914,074*, 1959. [76](#)
- [166] V Raducanu. Assemblages: conception d’un noeud industriel pour les grilles de tensegrite. *Diplome d’Etudes Approfondies, Universite Montpellier II*, 1997. [77](#)
- [167] JY Zhang, M Ohsaki, and Y Kanno. A direct approach to design of geometry and forces of tensegrity systems. *International Journal of Solids and Structures*, 43(7-8):2260–2278, Jan 2006. [79](#), [175](#), [237](#)
- [168] K Shea, E Fest, and I Smith. Developing intelligent tensegrity structures with stochastic search. *Advanced Engineering Informatics*, 16(1):21–40, 2002. [79](#), [175](#), [237](#)

REFERENCES

- [169] GG Estrada, HJ Bungartz, and C Mohrdieck. Numerical form-finding of tensegrity structures. *International Journal of Solids & Structures*, 43(22-23):6855–6868, 2006. [79](#), [86](#), [87](#), [175](#), [237](#)
- [170] DG Emmerich. Self-tensioning spherical structures: Single and double layer spheroids. *International Journal of Space Structures*, 5(3-4):353–374, 1990. [79](#)
- [171] AG Tibert and S Pellegrino. Review of form-finding methods for tensegrity structures. *International Journal of Space Structures*, 18(4):209–223, 2003. [80](#), [81](#), [82](#), [85](#), [86](#)
- [172] R Connelly and M Terrell. Globally rigid symmetric tensegrities. *Structural Topology*, 21, 1995. [80](#), [85](#)
- [173] M Barnes. Form-finding and analysis of prestressed nets and membranes. *Computers & Structures*, 30(3):685–695, 1988. [82](#)
- [174] M Barnes. Form finding and analysis of tension structures by dynamic relaxation. *International Journal of Space Structures*, 14(2):89–104, 1999. [82](#)
- [175] S Pellegrino. Mechanics of kinematically indeterminate structures. *Ph.D Thesis, University of Cambridge*, Jan 1986. [82](#)
- [176] K. Koohestani. Form-finding of tensegrity structures via genetic algorithm. *International Journal of Solids and Structures*, 2011. [84](#)
- [177] M. Yamamoto, BS Gan, K. Fujita, and J. Kurokawa. A genetic algorithm based form-finding for tensegrity structure. *Procedia Engineering*, 14:2949–2956, 2011. [84](#)
- [178] JY Zhang and M Ohsaki. Optimization methods for force and shape design of tensegrity structures. *Proc. 7th World Congress on Structural and Multidisciplinary Optimization, Seoul, Korea*, 2007. [84](#)

REFERENCES

- [179] M Masic, RE Skelton, and PE Gill. Optimization of tensegrity structures. *International Journal of Solids & Structures*, 43(16):4687–4703, 2006. [84](#), [88](#), [89](#), [91](#), [176](#)
- [180] D Williamson, RE Skelton, and J Han. Equilibrium conditions of a tensegrity structure. *International Journal of Solids and Structures*, 40(23):6347–6367, 2003. [85](#)
- [181] J Zhang and M Ohsaki. Form-finding of self-stressed structures by an extended force density method. *Journal of the International Association for Shell and Spatial Structures*, 46(3):159–166, 2005. [86](#), [87](#)
- [182] H.C. Tran and J. Lee. Form-finding of tensegrity structures with multiple states of self-stress. *Acta mechanica*, 222(1):131–147, 2011. [87](#)
- [183] H. Chi Tran and J. Lee. Advanced form-finding for cable-strut structures. *International Journal of Solids and Structures*, 47(14):1785–1794, 2010. [87](#)
- [184] M. Pagitz and J.M. Mirats Tur. Finite element based form-finding algorithm for tensegrity structures. *International Journal of Solids and Structures*, 46(17):3235–3240, 2009. [87](#)
- [185] F Fu. Structural behavior and design methods of tensegrity domes. *Journal of Constructional Steel Research*, 61(1):23–35, 2005. [87](#)
- [186] C Paul, H Lipson, and FJV Cuevas. Evolutionary form-finding of tensegrity structures. *Proc. of the 2005 conference on Genetic and evolutionary computation*, pages 3–10, 2005. [89](#)
- [187] J Rieffel, F Valero-Cuevas, and H Lipson. Automated discovery and optimization of large irregular tensegrity structures. *Computers & Structures*, 87(5-6):368–379, 2009. [89](#), [91](#), [176](#)
- [188] Y. Kanno. Topology optimization of tensegrity structures under compliance constraint: a mixed integer linear programming approach. *Optimization and Engineering*, pages 1–36, 2011. [90](#)

REFERENCES

- [189] R Skelton Adhikari and WJ Helton. Mechanics of tensegrity beams. *UCSD Structural Systems and Control Lab Report*, 1, 1998. [91](#), [177](#)
- [190] P Park, M Gilbert, A Tyas, and O Popovic-Larsen. Potential use of structural layout optimization at the conceptual design stage. *International Journal of Architectural Computing*, 10(1):13–32, March 2012. [93](#)
- [191] G Sebestyén and C Pollington. *New architecture and technology*. Architectural Press, 2003. [96](#)
- [192] B Kolarevic. *Digital Morphogenesis, Architecture in the Digital Age: design and manufacturing*, chapter 2. Digital Morphogenesis. Taylor & Francis, 2003. [97](#), [106](#)
- [193] K Terzidis. *Expressive Form: a conceptual approach to computational design*. Routledge, 2003. [98](#), [106](#)
- [194] S Woolgar. *Science, the very idea*. Ellis Horwood Chichester, Sussex, 1988. [98](#)
- [195] C Lavin and I Donnachie. *From Enlightenment to Romanticism: Anthology*, volume 1. Manchester University Press, 2003. [101](#)
- [196] I Donnachie and C Lavin. *From Enlightenment to Romanticism: Anthology*, volume 2. Manchester University Press, 2003. [101](#)
- [197] K Frampton. *Modern architecture: a critical history*. Thames & Hudson, 2007. [101](#)
- [198] H Lipson and M Shpitalni. Conceptual design and analysis by sketching. *Artificial Intelligence for Engineering Design, Analysis & Manufacturing*, 14(5):391–401, 2001. [104](#)
- [199] J Pallasmaa. *The eyes of the skin: architecture and the senses*. Wiley-Academy, 2005. [104](#)

REFERENCES

- [200] M Gilbert, W Darwich, A Tyas, and P Shepherd. Application of large-scale layout optimization techniques in structural engineering practice. In *6th World Congress of Structural & Multidisciplinary Optimization*, 2005. [107](#)
- [201] J Reiser and N Umemoto. *Atlas of novel tectonics*. Princeton Architectural Press, 2006. [106](#), [108](#)
- [202] K Shea. *Digital Tectonics.*, chapter Directed randomness, pages 10–23. Wiley-Academy, Chichester, UK, 2004. [108](#)
- [203] John C. Chilton. *Heinz Isler: The Engineer's Contribution to Contemporary Architecture*. Thomas Telford, 2000. [116](#), [136](#)
- [204] John Chilton. Heinz isler's infinite spectrum: Form-finding in design. *Architectural Design*, 80(4):64–71, 2010. [116](#)
- [205] Wael Darwich, Matthew Gilbert, and Andy Tyas. Optimum structure to carry a uniform load between pinned supports. *Structural and Multidisciplinary Optimization*, 42:33–42, 2010. [117](#)
- [206] M. Kuijvenhoven and PCJ Hoogenboom. Particle-spring method for form finding grid shell structures consisting of flexible members. *Journal of the International Association for Shell and Spatial Structures*, 53(1):31–38, 2012. [117](#)
- [207] Frei Otto and Winfried Nerdinger. *Frei Otto: complete works : lightweight construction, natural design*. Birkhäuser, Basel, 2005. [129](#), [130](#)
- [208] Gerhard G Feldmeyer, Manfred Sack, and Casey C. M Mathewson. *The new German architecture*. Rizzoli, New York, 1993. [129](#)
- [209] J. J. Beaman, H. L. Marcus, D. L. Bourell, J. W. Barlow, R. H. Crawford, and K. P. McAlea. *Solid freeform fabrication: a new direction in manufacturing*. Kluwer Academic Publishers, 1997. [132](#)
- [210] E. Malone and H. Lipson. Freeform fabrication of ionomeric polymer-metal composite actuators. *Rapid Prototyping Journal*, 12(5):244253, 2006. [132](#)

REFERENCES

- [211] J. D. Hiller and H. Lipson. Multi material topological optimization of structures and mechanisms. In *Proceedings of the 11th Annual conference on Genetic and evolutionary computation*, page 15211528, 2009. [132](#)
- [212] N. Olhoff and JE Taylor. On optimal structural remodeling. *Journal of Optimization Theory & Applications*, 27(4):571–582, 1979. [145](#)
- [213] C Nha, Y Xie, and G Steven. An evolutionary structural optimization method for sizing problems with discrete design variables. *Computers & Structures*, 68(4):419–431, Jan 1998. [145](#)
- [214] W. Prager. Optimal layout of cantilever trusses. *Journal of Optimization Theory & Applications*, 23(1):111–117, 1977. [146](#)
- [215] GIN Rozvany, OM Querin, Z Gaspar, and V Pomezanski. Weight-increasing effect of topology simplification. *Structural and Multidisciplinary Optimization*, 25(5):459–465, 2003. [146](#), [159](#)
- [216] MG Earl and R D’Andrea. Iterative MILP methods for vehicle-control problems. *IEEE Transactions on Robotics*, 21(6):1158–1167, 2005. [146](#)
- [217] A Tyas. Some thoughts on the use of integer/binary programming for our truss optimisation. *Internal Memorandum, The University of Sheffield*, 2001. [146](#), [147](#), [149](#), [179](#)
- [218] M Ohsaki and N Katoh. Topology optimization of trusses with stress and local constraints on nodal stability and member intersection. *Structural & Multidisciplinary Optimization*, 29(3):190–197, 2005. [147](#), [149](#), [179](#)
- [219] T Hagishita and M Ohsaki. Topology mining for optimization of framed structures. *Journal of Advanced Mechanical Design, Systems, and Manufacturing*, 2(3):417–428, 2008. [147](#)
- [220] M Gilbert, A Tyas, and TJ Pritchard. An efficient linear programming based layout optimization method for pin-jointed frames. In *Proc. 5th World Congress in Structural & Multidisciplinary Optimization*, page 8. ISSMO, 2003. [148](#)

REFERENCES

- [221] DE Ingber. Tensegrity II. How structural networks influence cellular information processing networks. *Journal of Cell Science*, 116(8):1397–1408, 2003. [175](#)
- [222] DE Ingber. Cellular tensegrity: defining new rules of biological design that govern the cytoskeleton. *Journal of Cell Science*, 104(3):613–627, Jan 1993. [175](#)
- [223] R Motro. Tensegrity systems: the state of the art. *International Journal of Space Structures*, 7(2):75–83, 1992. [175](#)
- [224] R Connelly and W Whiteley. Second-order rigidity and prestress stability for tensegrity frameworks. *Siam J Discrete Math*, 9(3):453–491, 1996. [175](#)
- [225] IJ Oppenheim and WO Williams. Vibration and damping in three-bar tensegrity structure. *Journal of Aerospace Engineering*, 14(3):85–91, 2001. [175](#)
- [226] N Vassart and R Motro. Multiparametered formfinding method: Application to tensegrity systems. *International Journal of Space Structures*, 14(2):pp. 147–154(8), Jun 1999. [175](#)
- [227] V. Gómez-Jáuregui, R. Arias, C. Otero, and C. Machado. Novel technique for obtaining double-layer tensegrity grids. *International Journal of Space Structures*, 27(2):155–166, 2012. [176](#)
- [228] EW Parkes. Joints in optimum frameworks. *International Journal of Solids & Structures*, 11:1017–1022, 1974. [183](#)
- [229] Bentley SACS. Bentley sacs, May 2012. [192](#)
- [230] O Popovic-Larsen. *The architectural potential of the reciprocal frame*. PhD thesis, The University of Nottingham, 1996. [221](#)
- [231] J C Chilton. Polygonal living some environmentally friendly buildings with reciprocal frame roofs. In *Proceedings International Seminar on Structural Morphology, Stuttgart, Germany*, pages 21–29, 1994. [221](#)

REFERENCES

- [232] J Burry and A Maher. The other mathematical bridge. *Nexus Network Journal*, 10(1):179–194, 2008. [231](#)
- [233] MR Garey and DS Johnson. *Computers and intractability. A guide to the theory of NP-completeness. A Series of Books in the Mathematical Sciences.* WH Freeman & Company, San Francisco, California, 1979. [232](#)
- [234] M Berkelaar, K Eikland, and P Notebaert. lpsolve: Open source (mixed-integer) linear programming system. *Eindhoven University of Technology*, 1994. [232](#)
- [235] RB Fuller. Building construction. *US Patent 2,682,235*, 1954. [234](#)
- [236] A. Menges. Material computation: Higher integration in morphogenetic design. *Architectural Design*, 82(2):14–21, 2012. [242](#)
- [237] W Darwich, M Gilbert, and A Tyas. Optimum structure to carry a uniform load between pinned supports. *Structural & Multidisciplinary Optimization*, pages 1–10, 2009. [269](#)

Appendix A

Structural Layout Optimization

A.1 Description of structural layout optimization process

The structural layout optimization process involves several steps: (i) the designer defines the extent of the design domain, and also the support and load conditions; (ii) the design domain is populated with n nodes, typically uniformly spaced, which represent the potential end-points of structural members; (iii) the n nodes are inter-connected with m potential structural members, forming a so-called ground structure; (iv) optimization techniques (e.g. linear programming, LP [79]) are used to identify the subset of members present in the structure that best fulfils the required design criteria (e.g. to find the structure which uses the minimum volume of material).

A.2 Linear programming (LP) structural layout optimization formulation

The equilibrium LP plastic design formulation for a 2D ground structure subjected to a single load case and containing m members and n nodes where the design objective is to find the minimum structural volume can be stated as follows [91]:

$$\begin{aligned} &\text{minimise,} \\ &V = \mathbf{q}^T \mathbf{c} \end{aligned} \tag{A.1}$$

$$\begin{aligned} &\text{subject to:} \\ &\mathbf{B}\mathbf{q} = \mathbf{f} \end{aligned} \tag{A.2}$$

$$q_i^+, q_i^-, \geq 0, i=1, \dots, m \tag{A.3}$$

where V is the total volume of the structure, $\mathbf{q}^T = \{q_1^+, -q_1^-, q_2^+, -q_2^-, \dots, q_m^+, -q_m^-\}$, $\mathbf{c}^T = \{l_1/\sigma_1^+, -l_1/\sigma_1^-, l_2/\sigma_2^+, -l_2/\sigma_2^-, \dots, l_m/\sigma_m^+, -l_m/\sigma_m^-\}$, \mathbf{B} is a suitable $(2n \times 2m)$ equilibrium matrix, $\mathbf{f}^T = \{f_1^x, f_1^y, f_2^x, f_2^y, \dots, f_n^x, f_n^y\}$ and where $l_i, q_i^+, q_i^-, \sigma_i^+, \sigma_i^-$ represent the length, tensile and compressive member forces and stresses in member i , respectively. Finally, f_i^x, f_i^y are the x and y direction live load components applied to node j . The LP variables are the tensile and compressive member forces in \mathbf{q} .

A.3 Mixed integer linear programming (MILP) structural layout optimization formulation

As a variation on the formulation given in Eqns (A.1-A.3), it is possible to introduce additional binary and integer variables to indicate for example whether a given member is ‘on’ (present) or ‘off’ (absent) in the final structural solution,

giving rise in mathematical terms to a ‘mixed integer linear programming (MILP) formulation. Such variables make it possible to for example specify the maximum number of members converging on a given joint, increasing the power of layout optimization as far as the designer is concerned, albeit at the expense of computational efficiency. It is also possible to develop MILP formulations which allow more accurate modelling of the behaviour of compression members, which will in reality buckle if overly slender. The usefulness of various MILP formulations are currently being investigated by the authors.

A.4 Transmissible Load

This is a simple illustration of a transmissible load being applied prior to the optimization process, which resulted in the example of Catenary Arches. The load can be applied anywhere along the line of action of the force i.e. either Node A or B as shown in Fig. A.1.

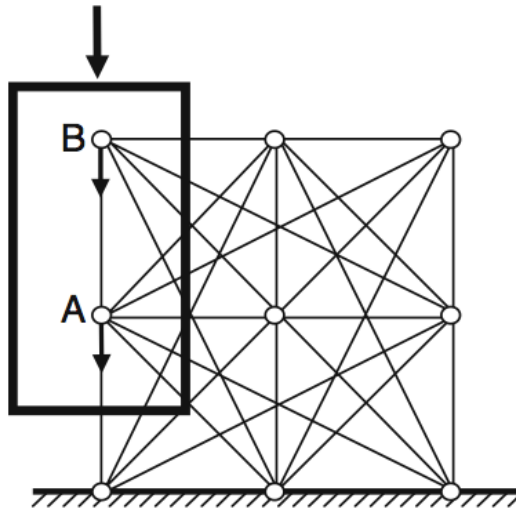


Figure A.1: Illustration of Transmissible Load (after Darwich [237]).

Appendix B

MILP zero area members

In all figures, compression members are represented by red (or solid) lines, tension members, by blue (or regular dashed) lines, and zero-area members, by green (or irregular dashed) lines.

B.0.1 3 x 3 Grid Example

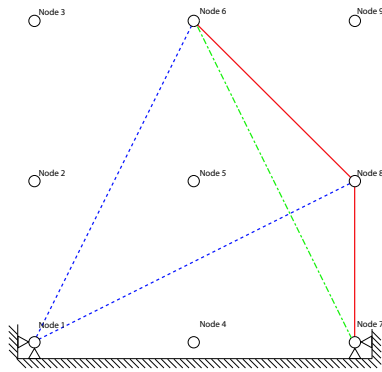
Fig. B.1 shows structures optimized with integer constraints from 3 x 3 grid, which contain zero-area members.

B.0.2 5 x 3 Truss

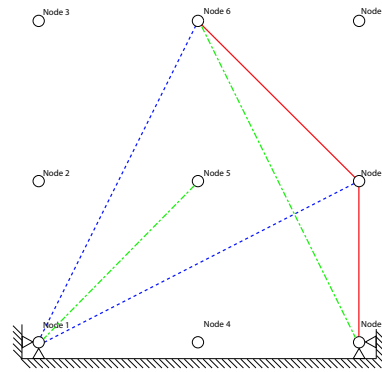
Figs. B.2 - B.3 show various structures optimized with integer constraints from 5 x 3 truss, which contain zero-area members; its N_{UB} ranges from 11 to 22.

B.0.3 5 x 3 Michell Cantilever

Fig. B.4 shows a structure optimized with integer constraints from 5 x 3 Michell cantilever, which contains a zero-area member.

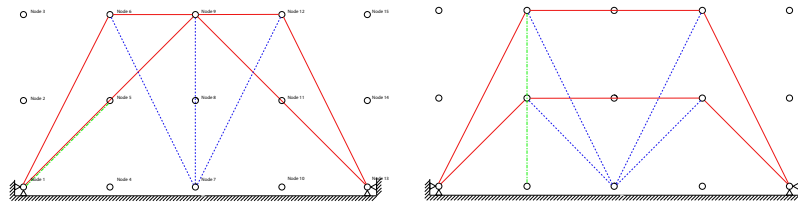


(a) $N_{UB} = 5, V = 8.0000$
 $N_{final} = 5$ (4 real members and 1 zero area member)



(b) $N_{UB} = 6, V = 8.0000$
 $N_{final} = 6$ (4 real members and 2 zero area members)

Figure B.1: 3 x 3 Grid - optimized structures with integer constraints and zero area members

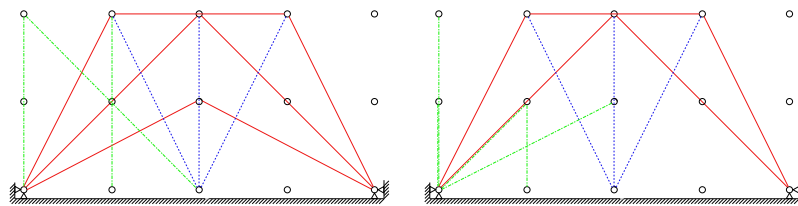


(a) $N_{UB} = 11, V = 18.000$

(b) $N_{UB} = 13, V = 18.000$

$N_{final} = 11$ (10 real members and 1 zero area member)

$N_{final} = 13$ (12 real members and 1 zero area member)

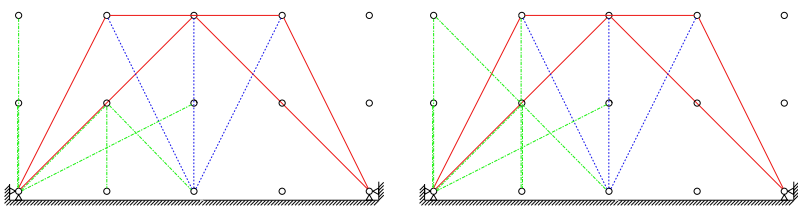


(c) $N_{UB} = 14, V = 18.000$

(d) $N_{UB} = 15, V = 18.000$

$N_{final} = 14$ (11 real members and 3 zero area members)

$N_{final} = 15$ (10 real members and 5 zero area members)



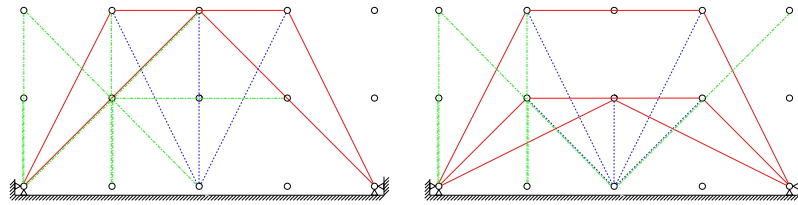
(e) $N_{UB} = 16, V = 18.000$

(f) $N_{UB} = 17, V = 18.000$

$N_{final} = 16$ (11 real members and 5 zero area members)

$N_{final} = 17$ (11 real members and 6 zero area members)

Figure B.2: 5 x 3 Truss - optimized structures with integer constraints and zero area members

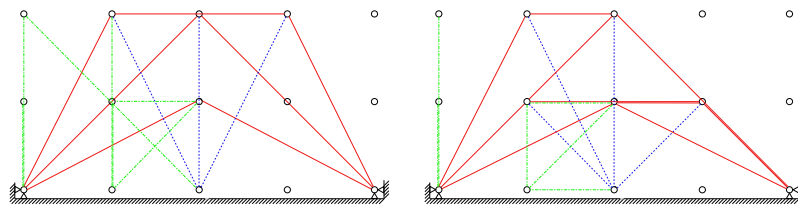


(a) $N_{UB} = 18, V = 18.000$

(b) $N_{UB} = 19, V = 18.000$

$N_{final} = 18$ (10 real members and 8 zero area members)

$N_{final} = 19$ (13 real members and 6 zero area members)

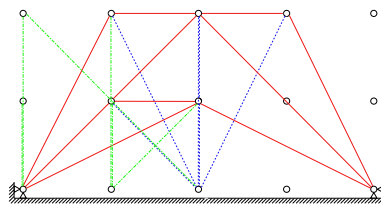


(c) $N_{UB} = 20, V = 18.000$

(d) $N_{UB} = 21, V = 18.000$

$N_{final} = 20$ (12 real members and 8 zero area members)

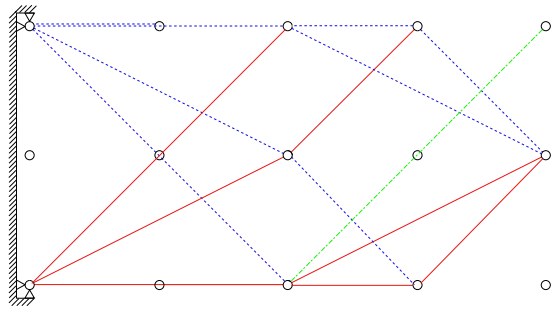
$N_{final} = 21$ (15 real members and 6 zero area members)



(e) $N_{UB} = 22, V = 18.000$

$N_{final} = 22$ (16 real members and 6 zero area members)

Figure B.3: 5 x 3 Truss - optimized structures with integer constraints and zero area members



(a) $N_{UB} = 16, V = 45.000$

$N_{final} = 16$ (15 real members and 1 zero area member)

Figure B.4: 5 x 3 Michell Cantilever - optimized structure with integer constraints and zero area member

Appendix C

MatLab code for MILP

```
001 %% Topology Optimisation - single load case with MILP constraint %%
002 function integer_12_lp_solve, clear
003 %%%%%%%%% variables %%%%%%%%%
004 t0=cputime;
005 Nx=3; Ny=3; N = Nx*Ny ;% No. of nodes in X and Y; %N=total No. of nodes
006 M=N*(N-1)/2; % M = total number of elements
007 Desired_M_LB=1; Desired_M_UB=10; const=1; % Part of Integer Programming
008 supportX=[1 7]; supportY=[1 7]; % supports [X1 X2 ..] % supports [Y1 Y2 ..] in node No.
009 SIG=[10 1]; % allowable stress [tension compression]
010 load_X=[6 3]; load_Y=[1 0]; % load X[node number; value]; %load Y[node number; value]; [1 0] if no load
011 load_tol=10^-2; % load tolerance
012 [nodes] = create_nodes(Nx,Ny,supportX,supportY,load_X,load_Y); % create nodes
013 [elements] = create_elements(nodes,N,SIG); % create elements
014 [minVol,q] = Execute(N,M,elements,supportX,supportY,load_X,
load_Y,load_tol,const,Desired_M_LB,Desired_M_UB);
015 [CPU_TIME] = CALC_CPUTIME(t0);
016 Results(minVol,q,nodes,elements,N,M,load_tol,CPU_TIME);
017 display(minVol); % plot and display
018 disp('No. of initial elements in ground structure'),disp(size(elements,1))
019 %%% nodes = [X Y supportX supportY load_X load_Y] %%%
020 function [nodes]=create_nodes(Nx,Ny,supportX,supportY,load_X,load_Y)
021 X=zeros(Ny,Nx);Y=X;
```

```

022 for i=1:Ny, X(i,:)= [0:(Nx-1)] ; end %X-coord's starting from origin
023 for j=1:Nx, Y(:,j)= [0:(Ny-1)]'; end %Y-coord's
024 nodes(:,1)=X(:); nodes(:,2)=Y(:); nodes(supportX,3)=1;nodes(supportY,4)=1;
025 nodes(load_X(1),5)=load_X(2); nodes(load_Y(1),6)=load_Y(2);
026 %% elements = [Node_a Node_b X_length Y_length L Theta SIG+ SIG- ]%%
027 function [elements]=create_elements(nodes,N,SIG)
028 elemN=0; warning off
029 for node_a=1:N-1
030 for node_b=node_a+1:N
031 elemN=elemN+1;
032 elements(elemN,1)=node_a; % a ----- b
033 elements(elemN,2)=node_b;
034 elements(elemN,3)=nodes(node_b,1)-nodes(node_a,1);% Mem_length in X
035 elements(elemN,4)=nodes(node_b,2)-nodes(node_a,2);% Mem_length in Y
036 elements(elemN,5)=(elements(elemN,3)^2+elements(elemN,4)^2)^.5; % L
037 elements(elemN,6)=atan(elements(elemN,4)/elements(elemN,3)); % Theta
038 end,end, warning on
039 elements(:,7)=SIG(1); elements(:,8)=SIG(2);
040 %%%%%%%%%%% V, feq, Beq matrix set-up %%%%%%%%%%%
041 function [minVol,q]=Execute
042(N,M,elements,supportX,supportY,load_X,load_Y,load_tol,const,Desired_M_LB,Desired_M_UB)
043 V=zeros(1,(M*2+M)); % Part of Integer Programming %
044 V(1:M*2)=[(elements(:,5))./elements(:,7) (elements(:,5))./elements(:,8)]; % V=1/SIG+ and 1/SIG-
045 feq=zeros((N*2+N*2+M*2+2),1); % PoIP %
046 feq(load_X(1))= load_X(2); % placing load in X-direction
047 feq(load_Y(1)+N)= load_Y(2); % placing load in Y-direction
048 feq(load_X(1)+N*2)= -load_X(2); % PoIP %
049 feq(load_Y(1)+N*2+N)= -load_Y(2); % PoIP %
050 feq((N*2+N*2+M*2+2),1)=-Desired_M_LB; % PoIP %
051 feq((N*2+N*2+M*2+1),1)= Desired_M_UB; % PoIP %
052 feq(supportY+N+N*2,:)=[]; feq(supportX+N*2,:)=[]; % PoIP %
053 feq(supportY+N,:)=[]; feq(supportX,:)=[]; % removing 0 force at support
054 Beq=zeros(N*2+N*2+M*2+2,M*2+M); % PoIP %
055 for elemN=1:M
056 c=cos(elements(elemN,6)); s=sin(elements(elemN,6));
057 Beq(elements(elemN,1),elemN)= -c; % Beq(node_a,elemN) = in X
058 Beq(elements(elemN,2),elemN)= c; % Beq(Node_b,elemN) = "

```

```

059 Beq(elements(elemN,1),M+elemN)= c; % Beq(Node_a,elemN) = ""
060 Beq(elements(elemN,2),M+elemN)= -c; % Beq(Node_b,elemN) = ""
061 Beq(elements(elemN,1)+N,elemN)= -s; % Beq(Node_a,elemN) = in Y
062 Beq(elements(elemN,2)+N,elemN)= s; % Beq(Node_b,elemN) = ""
063 Beq(elements(elemN,1)+N,M+elemN)= s; % Beq(Node_a,elemN) = ""
064 Beq(elements(elemN,2)+N,M+elemN)= -s; % Beq(Node_b,elemN) = ""
065 Beq((elements(elemN,1)+N*2),elemN) = c; % PoIP %
066 Beq((elements(elemN,2)+N*2),elemN) = -c; % PoIP %
067 Beq((elements(elemN,1)+N*2),M+elemN)= -c; % PoIP %
068 Beq((elements(elemN,2)+N*2),M+elemN)= c; % PoIP %
069 Beq(elements(elemN,1)+N+N*2,elemN)= s; % PoIP %
070 Beq(elements(elemN,2)+N+N*2,elemN)= -s; % PoIP %
071 Beq(elements(elemN,1)+N+N*2,M+elemN)= -s; % PoIP %
072 Beq(elements(elemN,2)+N+N*2,M+elemN)= s; % PoIP %
073 K_t=(elements(1,7))*const; % PoIP %
074 K_c=(elements(1,8))*const; % PoIP %
075 Beq(elemN+N*2+N*2,elemN)= 1/K_t; % PoIP %
076 Beq(elemN+M+N*2+N*2,elemN+M)=1/K_c; % PoIP %
077 Beq(elemN+N*2+N*2,elemN+M*2)=-1; % PoIP %
078 Beq(elemN+M+N*2+N*2,elemN+M*2)=-1;
079 Beq(N*2+N*2+M*2+2,M*2+elemN)=-1; % PoIP %
080 Beq(N*2+N*2+M*2+1,M*2+elemN)= 1; % PoIP %
081 end
082 Beq((N*2+N+supportY, :)=[]; Beq((N*2+supportX, :)=[]; % PoIP %
083 Beq(N+supportY, :)=[]; Beq(supportX, :)=[];
084 lb=zeros((M*2+M),1);
085 ub=zeros((M*2+M),1);
086 for elemN=1:M; % PoIP %
087 ub(elemN,1)=inf; % PoIP %
088 ub(elemN+M,1)=inf; % PoIP %
089 ub(M*2+elemN,1)=1; % PoIP %
090 end
091 for elemN=1:M; % PoIP %
092 ub(elemN,1)=inf; % PoIP %
093 ub(elemN+M,1)=inf; % PoIP %
094 ub(M*2+elemN,1)=1; % PoIP %
095 end

```

```

096 e=-1;
097 xint=[M*2+1:M*2+M]; options = optimset('largescale','on');
098 [minVol,q] = lp_solve(V',Beq,feq,e,lb,ub,xint);Beq;feq;
099 %[q,minVol,exitflag]=linprog(V',[],[],Beq,feq,lb,ub);
100 %%%%%%%%% counting the number of final elements %%%%%%%%%
101 element_numbers=[1:M 1:M 1:M]';
102 Q=[element_numbers q];
103 disp(Q)
104 counter=0;
105 for i=1:M
106     if Q((i+2*M),2)< 0.01
107         counter=counter+1; % in order to count the final elements
108     end
109 end
110 disp('No. of elements in the final structure'), disp(M-counter)
111 function [CPU_TIME] = CALC_CPUTIME(t0)
112 t_fin=cputime;
113 CPU_TIME=t_fin-t0; a='CPU TIME=';
114 disp(a), disp(CPU_TIME)
115 %%%%%%%%% plot and result %%%%%%%%%
116 function Results(minVol,q,nodes,elements,N,M,load_tol, CPU_TIME),
clf, hold on,axis equal
117 title(['minVol: ' num2str(minVol)])
118 xlabel(['CPU TIME: ' num2str(CPU_TIME)])
119 for node=1:N
120     plot([nodes(node,1) nodes(node,1)],[nodes(node,2) nodes(node,2)],'k.') % nodes
121     h=text(nodes(node,1),nodes(node,2),num2str(node));set(h,'fontsize',8) % node numbers
122     if nodes(node,3)==1, plot([nodes(node,1) nodes(node,1)],[nodes(node,2) nodes(node,2)],'m>'),end %supportX
123     if nodes(node,4)==1, plot([nodes(node,1) nodes(node,1)],[nodes(node,2) nodes(node,2)],'m^'),end %supportY
124     if nodes(node,5)~=0 | nodes(node,6)~=0 % load
125         plot([nodes(node,1) nodes(node,1)+nodes(node,5)],[nodes(node,2) nodes(node,2)+nodes(node,6)],'c--') %barXY
126         plot(nodes(node,1),nodes(node,2),'co'),end % loaded node
127     end
128 for elemN=1:M
129     node_a=elements(elemN,1); node_b=elements(elemN,2);
130     if q(elemN)>load_tol % final tens elements (red)
131         h=text((nodes(node_a,1)+nodes(node_b,1))/2,(nodes(node_a,2)+nodes(node_b,2))/2,num2str(elemN)); %numbers

```

```
132 set(h,'fontsize',7,'color',[1 0 0])
133 plot([nodes(node_a,1) nodes(node_b,1)], [nodes(node_a,2) nodes(node_b,2)], 'r' ),end %members
134 if q(elemN+M)>load_tol % final comp elements (blue)
135 h=text((nodes(node_a,1)+nodes(node_b,1))/2, (nodes(node_a,2)+nodes(node_b,2))/2, num2str(elemN)); %numbers
136 set(h,'fontsize',7,'color',[0 0 1])
137 plot([nodes(node_a,1) nodes(node_b,1)], [nodes(node_a,2) nodes(node_b,2)], 'b' ), end %members
138 end
```

Appendix D

Further Explanation of Effect of Additional Constraints on Optimality

This section provides graphical representation and accompanying explanation, with regard to the effectiveness (or ineffectiveness) of additional constraints in obtaining more optimal solutions to the objective function in linear optimization. It should also be noted that the same principle applies to any nonlinear optimization methods.

Let us consider a constrained optimization problem and say that the objective is, to minimize a simple function, $f(x, y) = (y+x)$. This objective function is subject to three constraints; $x < 2$, $y < 2$, and $x+y > 2$. These are shown in Fig. D.1. In the same figure, the shaded area, enclosed by the constraints, represents the domain of feasible solutions, within which are solutions that should satisfy all three constraints. Since the objective is to minimize $f(x, y) = (y + x)$, non-unique minimum values will be found immediately above the constraint $x + y > 2$.

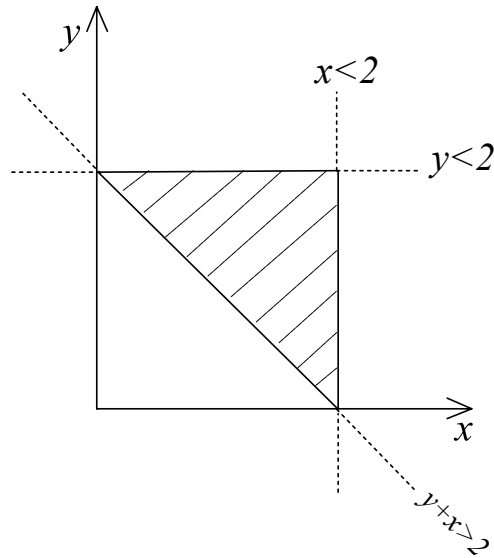
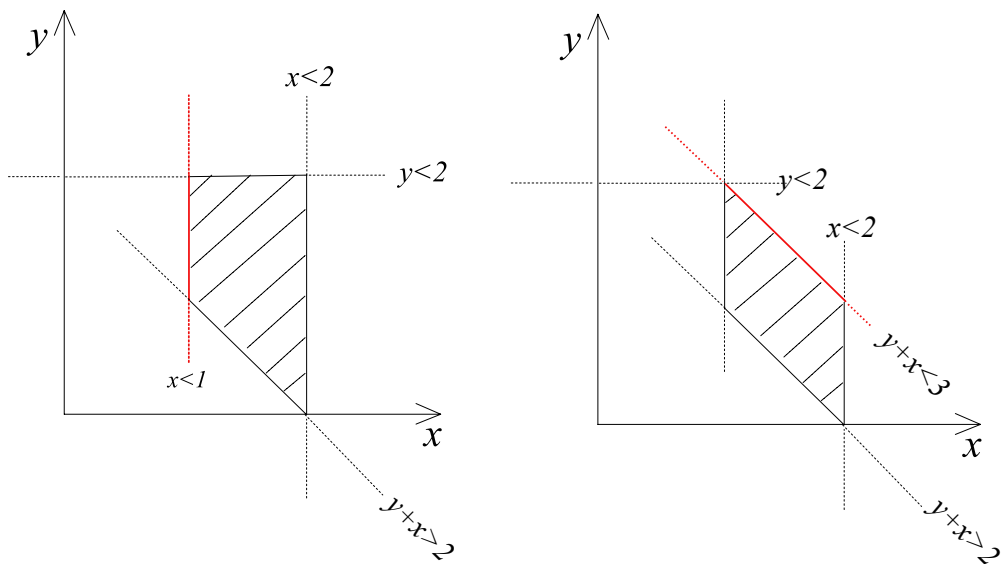


Figure D.1: Original solution domain: enclosed by three constraints

Fig. D.2(a) shows a modified feasible solution domain enclosed by the original three constraints and an additional constraint, $x < 1$. Although the set of available solutions has changed (or reduced in number), it is easy to see that minimum values for x and y , still lie immediately above the constraint, $y + x > 2$. Similarly, Fig. D.2(b) shows a further modification (or reduction) of feasible solution set; whilst this has changed the feasible solution set, the possible minimum values for the objective function remains unchanged, rendering the additional constraint $y + x < 3$ ineffective.

This in effect explains the reason why introduction of additional constraints cannot make the solution more optimal than the original optimization problem, in its definition.



(a) Modified solution domain: enclosed by an additional constraint

(b) Ineffective constraint

Figure D.2: Introduction of additional constraints

Appendix E

Comparisons between Tensegrity and Corresponding LP structures

E.0.4 Tensegrity ‘XIIX’ Column

The same vertical force analysis as in the previous section is repeated here. In addition a horizontal analysis is provided.

Vertical Load: ‘XIIX’ Column and LP structure

In order to understand the tensegrity ‘column’ structure, its behaviours with a particular emphasis on buckling, are compared to those of the conventional LP structure, utilising commercially available CHSs for compression members and realistic steel properties (and dimensional units) whilst maintaining the section area of the original sections from optimisation. These are found in Table E.5 for the tensegrity structure and in Table E.4 for the corresponding LP structure. Horizontal and vertical pinned supports are located at the bottom two nodes in both ‘XIIX’ Column and the corresponding LP structure; in Nodes *O* and *P* for ‘XIIX’ Column and in Nodes *G* and *H* for the corresponding LP structure. Two external loads of equal magnitude are applied in negative *y*-direction (vertically),

Table E.1: 2D tensegrity structures without supports: horizontal and vertical axial loads

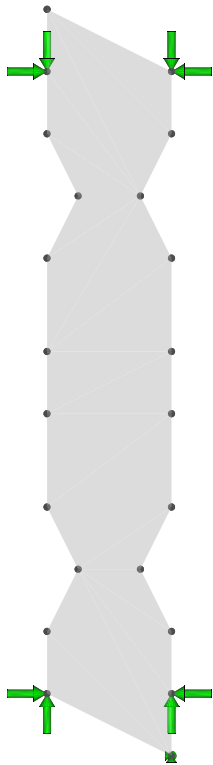
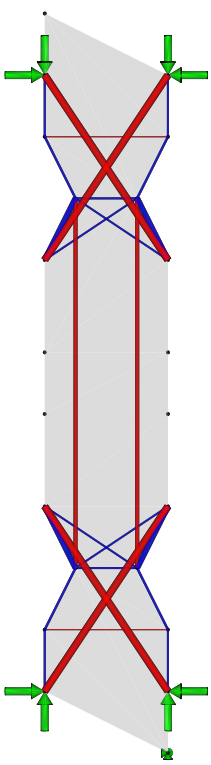
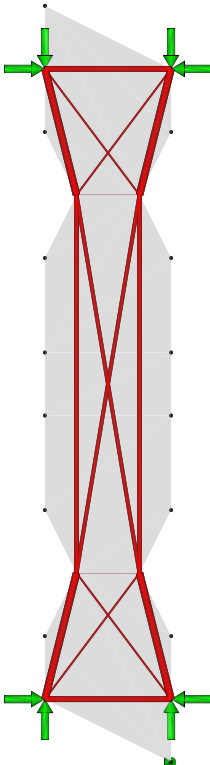
<i>Design domain</i>	<i>Tensegrity</i>	<i>LP</i>
(a)	(b)	(c)
		
Data		
<i>Target Node No.</i> =21	V_{Ten}	V_{LP}
<i>Scale Factor</i> =0.001	1350	600
<i>Load</i> =50 (each)		

Table E.2: MILP ‘XIIX’ Para-tensegrity Column: internal loads

<i>Member</i>	q	q_x	q_y	<i>radius</i>	<i>vol.</i>
AC	25.00	0.00	25.00	2.82095	12.50
AH	-90.1388	-50.00	-75.00	5.3565	162.50
BD	25.00	0.00	25.00	2.82095	12.5
BG	-90.1388	-50.00	-75.00	5.3565	162.5
CD	-12.5	-12.5	0	1.99471	12.5
CE	27.9508	12.50	25.00	2.98279	15.625
DF	See CE				
EF	25.00	25.00	0.00	2.82095	12.50
EG	69.8771	31.25	62.50	4.7162	39.0625
EH	22.5347	18.75	12.50	2.67825	20.3125
EK	-50.00	0.00	-50.00	3.98942	150.00
FG	See EH				
FH	69.8771	31.25	62.50	4.7162	39.0625
IK	See EG				
IL	See FG				
IP	See AH				
JK	See FG				
JO	See AH				
JL	See EG				
KL	See EF				
KM	See CE				
LN	See CE				
MN	See CD				
MO	See AC				
NP	See AC				
OP	See AB				

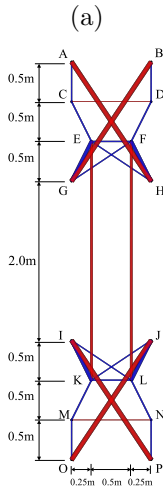
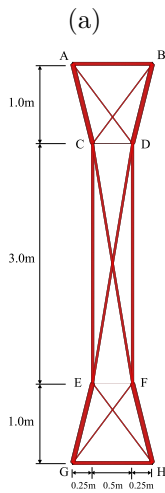


Table E.3: LP 'XIIX' Column: internal loads

<i>Member</i>	q	q_x	q_y	<i>radius</i>	<i>vol.</i>
AB	-33.4384	-33.4384	0.00	3.26248	33.4384
AC	-43.1655	-10.4692	-41.8767	3.70675	44.494
AD	-10.1541	-6.09245	-8.12327	1.79782	12.6926
CD	-0.707044	-0.707044	0.00	0.474404	0.35352
CE	-27.9819	0.00	-27.9819	2.98444	83.9456
CF	-22.3218	-3.66969	-22.0181	2.66557	67.8892
DE	See CF				
DF	See CE				
EF	See CD				
EG	See AC				
EH	See AD				
FG	See AD				
FH	See AC				
GH	See AB				



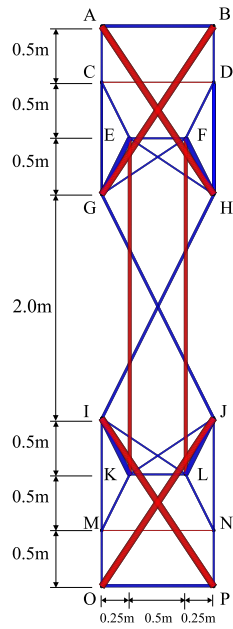


Figure E.1: Tensegrity 'XIIX' column with additional members

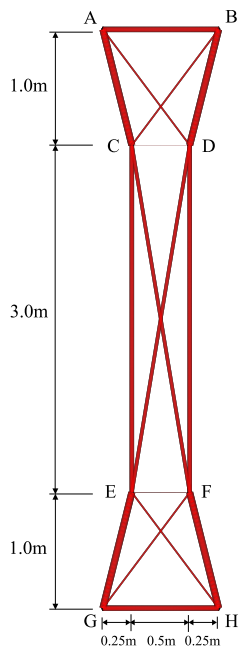


Figure E.2: LP Structure corresponding to Tensegrity 'XIIX' column

to Nodes *A* and *B* in both ‘XIIX’ Column and the corresponding LP structure. These loads are incremented until the most critical member in the structures, reaches its full load bearing capacity.

Table E.4: LP ‘XIIX’ structure: CHS sizes

<i>Member</i>	Original Area	Diameter (<i>cm</i>)	Thickness (<i>cm</i>)	Actual Area (<i>cm</i> ²)
AB	33.44	13.97	0.80	33.10
AC	43.17	13.97	1.20	48.14
AD	10.15	7.61	0.50	11.17
CD	0.71	2.13	0.20	1.21
CE	27.98	10.16	1.00	28.78
CF	22.32	10.16	0.80	23.52
DE	See CF			
DF	See CE			
EF	See CD			
EG	See AC			
EH	See AD			
FG	See AD			
FH	See AC			
GH	See AB			

Fig. E.3, shows the results of the analysis for the LP structure, in which the most critical member is *CD*; its maximum allowable axial load (i.e. $U_c=1.00$) according to EC3 is $228.13N/mm^2$ with the actual value being $227.92N/mm^2$. As the member is not slender, the failure mode is unlikely to be by buckling; the max allowable Euler buckling strength at $380.87N/mm^2$, i.e. higher than the maximum design axial load capacity. Based on this maximum axial load capacity and the member cross-section area, the maximum compressive load capacity of

this member, is $1480kN$ for self-weight of $490kg$ (or $3.02kN$ per kg of weight)

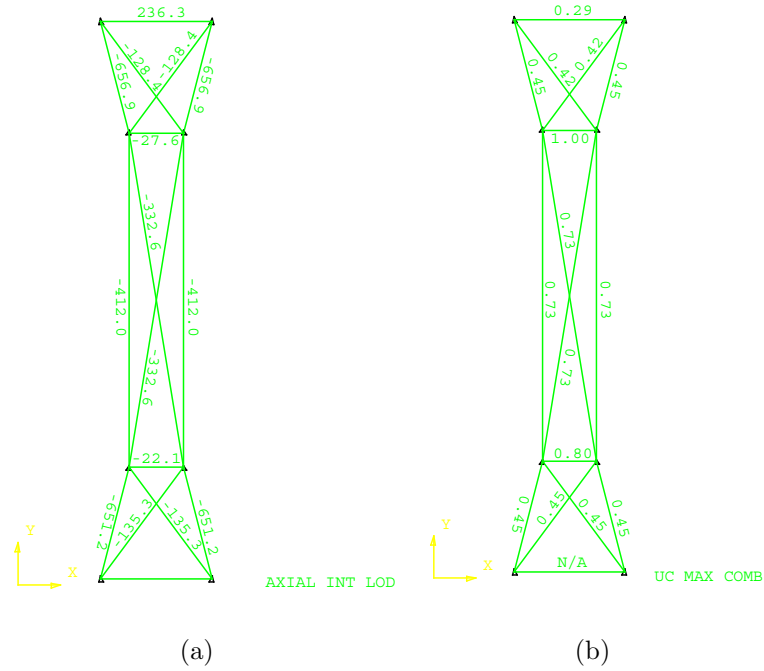


Figure E.3: LP structure: internal member forces and utilisation ratios, U_c

Given the same properties and conditions, Fig. E.4, shows the tensegrity structure with its individual member utilisation ratios and internal forces. The highest utilisation ratio, hence the most critical case, belongs to Member EK , for which the maximum allowable axial stress is $270.05N/mm^2$ (actual: $269.37N/mm^2$), and the maximum allowable buckling stress is $794.05N/mm^2$. Based on this maximum axial load capacity and the member cross-section area, the maximum compressive load capacity of this critical member, and hence the whole tensegrity structure, is $2840kN$ with $1298kg$ of self-weight (or $2.19kN$ per kg of weight). This is higher than that of the conventional LP structure, by a factor of 1.92, as a whole. However, the maximum compressive load capacity per kg of weight is lower than that of the LP structure; $2.19kN/kg$ compared to $3.02kN/kg$, which gives the ratio of 0.73.

Table E.5: MILP ‘XIIX’ column: CHS sizes

<i>Member</i>	Original Area	Diameter (<i>cm</i>)	Thickness (<i>cm</i>)	Actual Area (<i>cm</i> ²)
AB	33.44	6.525	3.260	33.44
AC	25.00	5.642	2.820	24.99
AH	90.14	24.45	1.25	91.11
BD	25.00	5.642	2.820	24.99
BG	90.14	24.45	1.25	91.11
CD	12.50	7.61	0.60	13.21
CE	27.95			
DF	See CE			
EF	25.00	5.642	2.820	24.99
EG	69.88			
EH	22.53			
EK	50.00	17.78	1.00	52.71
FG	See EH			
FH	69.877			
GJ	See AC			
HI	See AC			
IK	See EG			
IL	See FG			
IP	See AH			
JK	See FG			
JO	See AH			
JL	See EG			
KL	See EF			
KM	See CE			
LN	See CE			
MN	See CD			
MO	See AC			
NP	See AC			
OP	See AB			

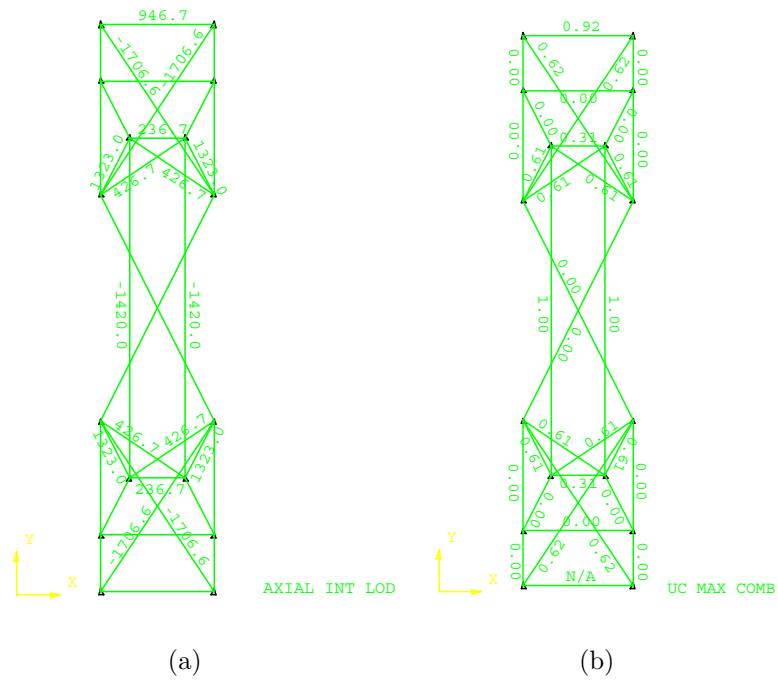


Figure E.4: MILP-derived 'XIIX' tensegrity structure: internal member forces and utilisation ratios, U_c

As before, the utilisation ratios for constituent members in tensegrity column are low; this is because the tensegrity structure is composed of a multitude of shorter compressive members; the design compression resistance is dependent on the partial safety factor, which is dependent on the length/cross-section ratio of the member.

In conclusion, this serves as further evidence that, when given realistic steel properties and design criteria, the modified, tensegrity structure performs better than what it was optimised to perform, i.e. to be able to resist the external force only as much as the conventional LP structure. However, it is very clear that the maximum compressive capacity of the tensegrity structure per given weight is lower by a factor of 0.73, which reinforces the original hypothesis that tensegrity is inherently a non-optimal structure due to its structural redundancies.

Horizontal Load: ‘XIIX’ and LP Columns

Maintaining the CHS of the member cross-sections and realistic steel properties, this time, initially a small horizontal load is applied to Node *B* in negative *x*-direction in both ‘XIIX’ tensegrity structure and the corresponding LP structure. This load is incrementally increased until the U_c in the most critical member reaches 1.00 (or 0.99)

The maximum applicable horizontal load, permissible for the LP structure was found to be $103kN$ with Member *CE* as the critical member. The maximum allowable axial stress for the structure, is $180.09N/mm^2$ and the maximum allowable buckling stress $238.59N/mm^2$. The maximum load capacity per weight is $0.210kN/kg$. Refer to Fig. [E.5](#)

Similarly, the maximum applicable horizontal load, permissible for the ‘XIIX’ tensegrity structure was found to be $67kN$ with a tension member, Member *NP* as the critical member. The maximum allowable axial stress for the structure, is $308.70N/mm^2$. The maximum load capacity per weight is $0.052kN/kg$. Refer to

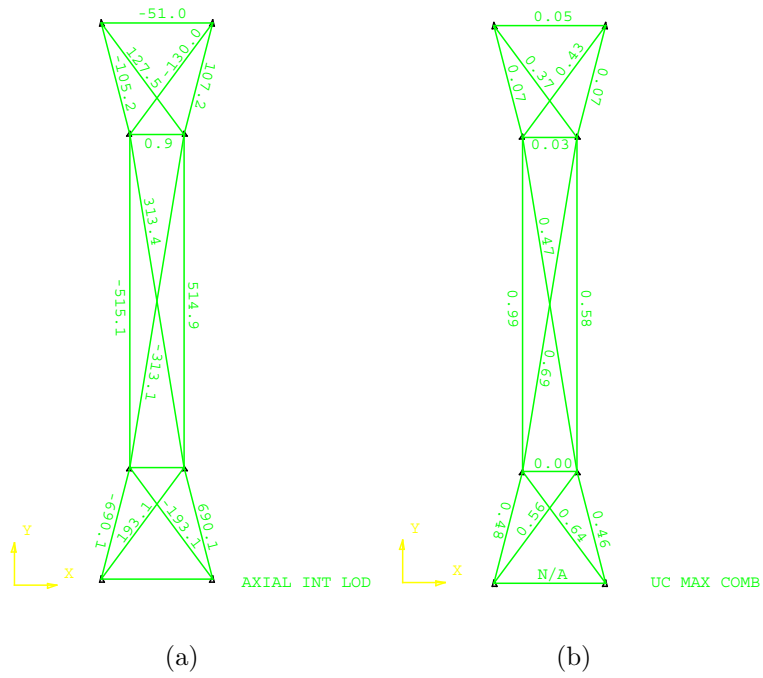


Figure E.5: LP structure: internal member forces and utilisation ratios, U_c

Table E.6 is the summary of maximum resisted load per weight comparisons between tensegrity and LP structures in the above analyses.

Table E.6: Summary of maximum resisted load per weight comparisons between tensegrity and LP structures

	<i>Tensegrity</i> Max. Force (kN)	Weight (kg)	(kN/kg)	<i>Corresponding LP</i>	Max. Force (kN)	Weight (kg)	(kN/kg)
Stayed Column	347.9	2739	0.127	LP	125	196	0.637
‘XIX’ Column	2770	1051	2.63	LP	2170	402	5.40
‘XIIX’ Column (vertical)	2840	1298	2.19	LP (vertical)	1480	490	3.02
‘XIIX’ Column (horizontal)	67	1298	0.052	LP(horizontal)	103	490	0.210